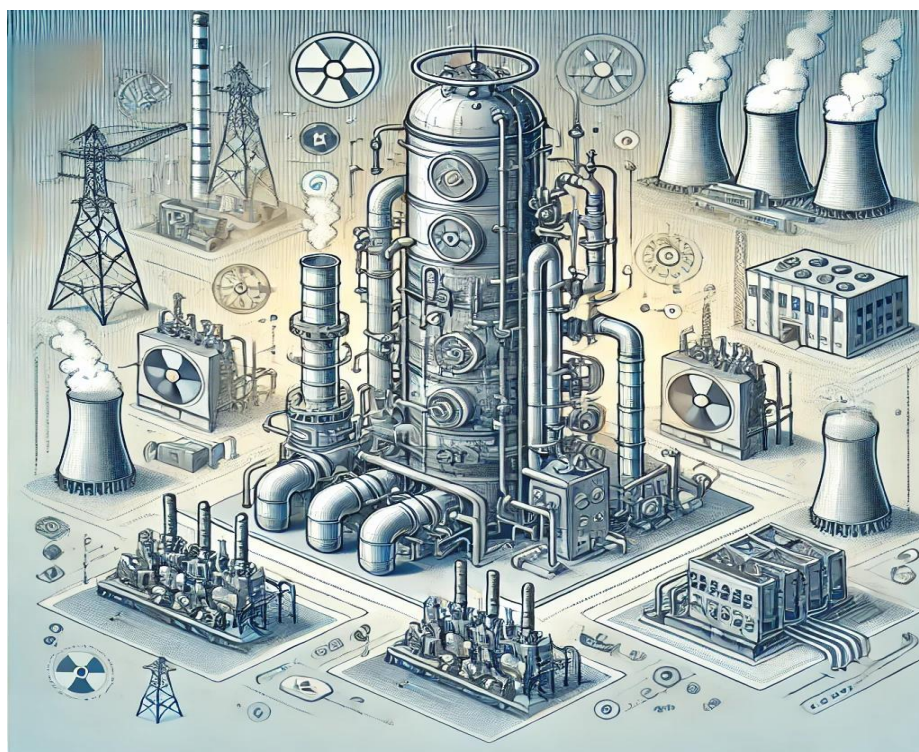


MINISTRY OF EDUCATION AND SCIENCE OF UKRAINE  
NATIONAL TECHNICAL UNIVERSITY  
«KHARKIV POLYTECHNIC INSTITUTE»

A. M. Ganzha, M. P. Kundenko, O. Yu. Iegorova

**STEAM-WATER HEAT EXCHANGERS OF THERMAL POWER PLANTS  
AND NUCLEAR POWER PLANTS**

Monograph



Kharkiv  
NTU «KhPI»  
2024

**Reviewers:**

*G. I. Kaniuk, Doctor of Technical Sciences, Professor, UEPA (Kharkiv)*

*V. V. Starikov, Doctor of Technical Sciences, Professor, NTU "KhPI" (Kharkiv)*

*Recommended by the Academic Council of NTU "KhPI",*

*Protocol No. 8 of November 1, 2024*

**Ganzha A. M.**

**G17** Steam-water heat exchangers of thermal power plants and nuclear power plants : monograph / A. M. Ganzha, M. P. Kundenko, O. Yu. Iegorova – Kharkiv : NTU «KhPI», 2024. – 206 p.

**ISBN 978-617-05-0522-4**

The monograph summarizes the experience of creation, analysis and improvement of steam-water heat exchangers of systems of regenerative heating of feed water of thermal power plants and nuclear power plants. An analysis of the factors that determine the reliability of the devices in operation is provided. The method of estimating the resource of such heat exchangers, caused by erosive and corrosive wear of the inlet sections of the coils and pipes, is given.

For scientists and specialists engaged in the design and operation of energy and heat exchange equipment, as well as students and postgraduates of electrical energy and heat energy engineering specialties.

Fig. 52 Tabl. 20 Bibl. titles: 62

**Ганжа А. М.**

**Г 19** Пароводяні теплообмінники енергоустановок ТЕС та АЕС : монографія / А. М. Ганжа, М. П. Кунденко, О. Ю. Єгорова – Харків : НТУ «ХПІ», 2024. – 206 с. – англійською мовою.

У монографії узагальнено досвід створення, аналізу та вдосконалення пароводяних теплообмінників систем регенеративного підігріву живильної води енергоустановок ТЕС та АЕС. Надається аналіз факторів, що визначають надійність роботи апаратів в експлуатації. Наводиться методика оцінки ресурсу таких теплообмінників, обумовленого ерозійно-корозійним зносом вхідних ділянок змійовиків та труб.

Для науковців та фахівців, які займаються проектуванням та експлуатацією енергетичного та теплообмінного обладнання, а також студентів та аспірантів електроенергетичних та теплоенергетичних спеціальностей.

UDC 621.187.14:66.045.1

ISBN 978-617-05-0522-4

© Ganzha A., Kundenko M., Iegorova O., 2024

© NTU «KhPI», 2024

## CONTENTS

CONTENTS.....	3
INTRODUCTION.....	5
CHAPTER 1 .....	8
STEAM-WATER HEAT EXCHANGERS IN REGENERATIVE SCHEMES OF TES AND NPP POWER PLANTS .....	8
1.1. Regeneration systems for steam turbine units of TPPs and NPPs .....	8
1.2. Design and operational features of surface feedwater heaters.....	15
CHAPTER 2 .....	29
BASIC EQUATIONS DESCRIBING THE PROCESSES OF HEAT AND MASS TRANSFER AND HYDRODYNAMICS IN SURFACE FEEDWATER HEATERS .....	29
2.1. Heat and material balance.....	29
2.2 Thermodynamic and thermophysical properties of water and water vapour.	34
2.3. Coefficients of heat transfer, heat transfer and thermal conductivity of pipe wall materials .....	42
2.4. Temperature characteristics .....	67
2.5. Hydraulic characteristics .....	71
2.6 Design characteristics.....	81
CHAPTER 3 .....	89
EFFICIENCY OF THE SCHEMES OF MUTUAL FLOW OF HEAT CARRIERS IN SURFACE HEAT EXCHANGERS WITH CROSS-CURRENT .....	89
CHAPTER 4 .....	110
THERMAL AND HYDRAULIC CALCULATIONS FOR HIGH AND LOW PRESSURE SURFACE HEATERS AND THEIR GROUP.....	110

4.1 Design thermal and hydraulic calculation .....	110
4.2. Verification thermal-hydraulic calculation .....	125
4.3. Joint verification calculations of heater groups .....	143
CHAPTER 5 .....	145
FLOW DISTRIBUTION IN THE HYDRAULIC NETWORKS OF HIGH- PRESSURE HEATER MANIFOLD SYSTEMS .....	145
5.1. System of equations for the hydraulic network of the collector system of high-pressure heaters.....	146
5.2. Calculation of the hydraulic network of the collector system of high-pressure heaters by the method of contour correction flows .....	151
CHAPTER 6 .....	161
DISTRIBUTION OF THERMAL CHARACTERISTICS IN SURFACE HEAT EXCHANGERS FOR POWER PLANTS .....	161
CHAPTER 7 .....	169
PECULIARITIES OF OPERATION AND MAINTENANCE OF STEAM- WATER HEAT EXCHANGERS OF TES AND NPPS POWER PLANTS .....	169
7.1. Factors Determining the Reliability of Operation of Surface Heat Exchangers for Regeneration Systems of TPP and NPP Turbine Units .....	169
7.2. Erosion and corrosion wear of the inlet sections of coils and tubes of surface heat exchangers of power plants.....	172
CHAPTER 8 .....	187
ESTIMATION OF THE SERVICE LIFE OF SURFACE HEAT EXCHANGERS OF TES AND NPP POWER PLANTS .....	187
REFERENCE LIST .....	201

## INTRODUCTION

The need to reduce energy consumption and energy-saving technologies has increased significantly in recent years. In addition, reducing the cost of electricity production itself is of great importance in energy saving, i.e. - increasing the efficiency of the facilities that produce it. The bulk of electricity, both in Ukraine and abroad, is generated at thermal power plants (TPPs) and nuclear power plants (NPPs) - at power units with powerful steam turbine units (STUs), where the well-known Rankine cycle is used.

As science and practice show, the efficiency of the Rankine cycle, i.e. its efficiency, increases significantly if regenerative heating of the feedwater supplied to the steam generator is used. The main contribution to the regeneration at the STU comes from the heating of feed water and main condensate with steam from the turbine exhaust. It should be noted that this type of regeneration makes good use of heat that is usually discharged in a cold source (condenser), which pollutes the environment. This type of regeneration process at TPPs and NPPs is carried out using groups of steam-water heat exchangers - the so-called low-pressure (IIHT) and high-pressure (IIBT) regenerative feedwater heaters. Regenerative heaters account for a large share of the metal consumption and cost of all turbine equipment at power units, and the requirements for the efficiency and reliability of these heat exchangers are very high.

Regenerative feedwater heaters can be of the surface type (heat exchanger-recuperators) and of the mixing type (contact heat exchangers). Until now, surface heaters have been used in power plant installations mainly. The use of mixing devices is still limited to vacuum extraction from the turbine at a small number of power units due to the low reliability of their operation (high probability of emergency overflow). However, the use of mixing heaters for both vacuum extractions and elevated steam pressures of turbine extractions is one of the promising areas for improving thermal schemes of turbine units at TPPs and NPPs.

Given that surface (recuperative) steam-water heat exchangers have so far made and will continue to make the main contribution to improving the efficiency of the power generation process at power units, this book is dedicated to them.

The first chapter discusses in detail the systems of regenerative heating of high and low pressure feedwater at power plants of thermal power plants and nuclear power plants, as well as various schemes for connecting heaters to them. The most common designs of surface heaters are presented and described. The stages of development and improvement of their design are considered.

The second section presents an in-depth mathematical model of thermal and hydraulic processes in generalised surface heaters. The basic equations describing such processes are given. It provides systematic criterion dependencies of heat transfer coefficients, heat transfer fluid resistances, thermodynamic and thermophysical properties of water and water vapour, thermal conductivity of pipe wall materials, temperature and design characteristics.

The third chapter discusses in detail the problem of determining correction factors for the logarithmic mean temperature head (i.e., the efficiency of the heat transfer scheme) in cross-flow heat exchangers, which are the devices considered in the book. The book provides easy-to-use analytical dependences of such coefficients, which take into account not only the number of cross-flow passes and its scheme, but also the number of parallel elements: pipes, rows of pipes, sections or coils. The application of these dependencies allows us to more accurately determine the heat fluxes transmitted in the devices and to calculate the efficiency of heat exchangers.

The fourth chapter presents generalised and extended methods and algorithms for design and verification calculations of the surface steam-water heat exchangers considered in the book, as well as their groups.

Chapter 5 describes the methodology for calculating the hydraulic networks of collector systems of high-pressure coil heaters. Elements of graph theory are used

here. The methodology makes it possible to determine the hydraulic parameters in all elements of the complex hydraulic network of such devices with a given accuracy.

Chapter 6 describes the methodology for determining local thermal characteristics (temperatures of heat carriers, pipe walls, heat flux density) in cross-flow heat exchangers. The use of this methodology in combination with the methods described in Chapters 4 and 5 allows us to obtain an almost complete picture of the thermal and hydraulic processes at any local point on the heat exchange surface of the studied devices.

The seventh chapter discusses the factors that determine the reliability of the heat exchangers discussed in the book. It analyses the processes of erosion and corrosion wear of the inlet pipe sections of the heating surfaces, the most significant and difficult to correct factor that determines the reliability of operation and service life. The paper presents a methodology for determining the intensity of such wear depending on the thermal, hydraulic and other parameters of the coolants, as well as the actual power unit load schedules.

The last section presents a methodology for assessing the service life of surface heat exchangers of regenerative schemes of TPP and NPP power plants, due to erosion and corrosion wear and the elastic-plastic state of the inlet sections of coils and pipes, taking into account the operating conditions and operating characteristics of power units.

The methodology of presenting the material in the book is structured in such a way that each subsequent chapter is based on the conclusions and previous materials and is their logical continuation.

# CHAPTER 1

## STEAM-WATER HEAT EXCHANGERS IN REGENERATIVE SCHEMES OF TES AND NPP POWER PLANTS

### 1.1. Regeneration systems for steam turbine units of TPPs and NPPs

In the thermal schemes of turbine units of thermal and nuclear power plants, a group of regenerative heaters from the condenser to the deaerator forms a low-pressure regeneration system, and from the feed pump to the steam generator - a high-pressure system, the deaerator and the feed pump make up a deaeration and feeding unit [1]. The entire regenerative scheme consists of a number of cascade and nodal regenerative heaters divided into groups, each of which consists of several cascade heaters, the steam condensate of which is drained into one nodal heater. A more economical scheme is one consisting of only nodal heaters, with either mixing heaters or heaters with pumping of the heating steam condensate into the feed water line directly after the heater. The next most economical scheme is the reverse cascade scheme, in which condensate is pumped to higher heaters (with higher pressure). Such schemes require a lot of drainage pumps (ДН), which reduces their reliability. For high-pressure regenerative feed water heaters, a scheme with cascade condensate drainage (drainage) from the upstream to the downstream unit is currently used (Figures 1.1 - 1.3). For low pressure regenerative feed water heaters, schemes are used where cascade drainage is not carried out in the entire group, but in some parts of it with one or more node heaters and drainage pumps (Figs. 1.4-1.6). As a rule, there is no cascade drainage to the first condenser from the low pressure regenerative feed water heaters (except for some NPP turbine units). The use of mixing heaters, provided that their operation is reliable (emergency overflow), is limited by the steam pressure in the taps below atmospheric pressure, i.e. the scheme is combined. In the accepted terminology, the flow of water heated by regeneration withdrawals from the condenser to the deaerator is called main condensate, and from the deaerator to the steam generator - feed water. In the



following, both of these streams will be referred to as feed water for the sake of generality in this paper.

To increase the efficiency of the cascade drainage scheme, the heating steam condensate is passed through condensate coolers (OK). The condensate cooling of the heater shells by the integrated condensate coolers further improves the operating conditions of the level control system and the drainage system pipework. In low pressure regenerative feed water heaters systems (Fig. 1.4), condensate coolers can be used as separate drainage coolers (OД). In the high pressure feed water, pre-enabled condensate coolers are mainly used, where the feed water flow after the condensate coolers at the inlet to the condensation zone (KII) is combined with the main flow. The flow rate of feed water through the condensate coolers is regulated by throttle washers. Parallel coolers are used in low pressure regenerative feed water heaters and some ПБТ, where a part of the feedwater heating surface pipes of the first pass is contained in a separate casing.

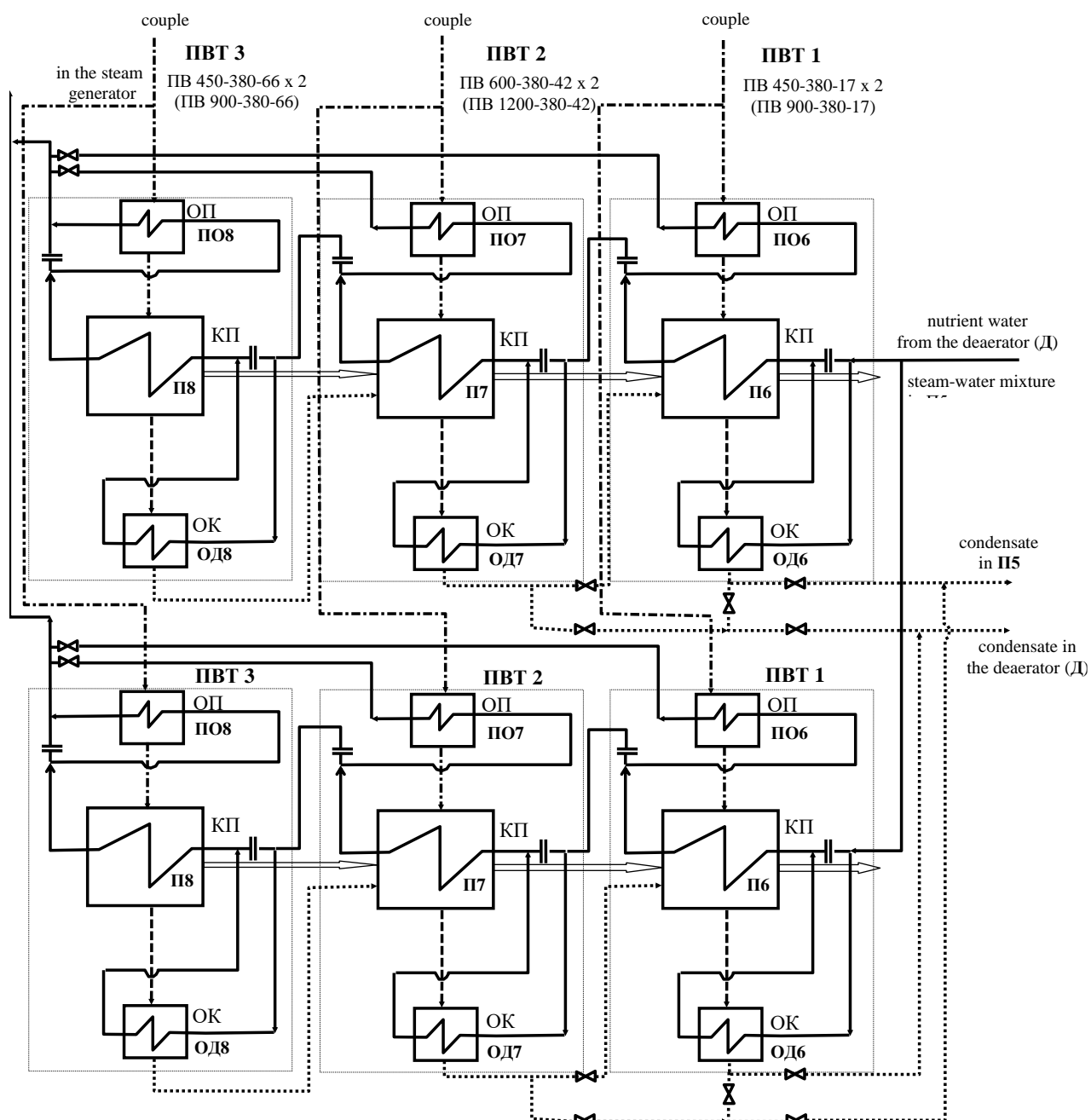


Fig. 1.1 - Two-strand high-pressure regeneration system of the turbine unit

K -300-240 KhTGZ after modernization according to the Ricard-Nekolny scheme with parallel steam cooling

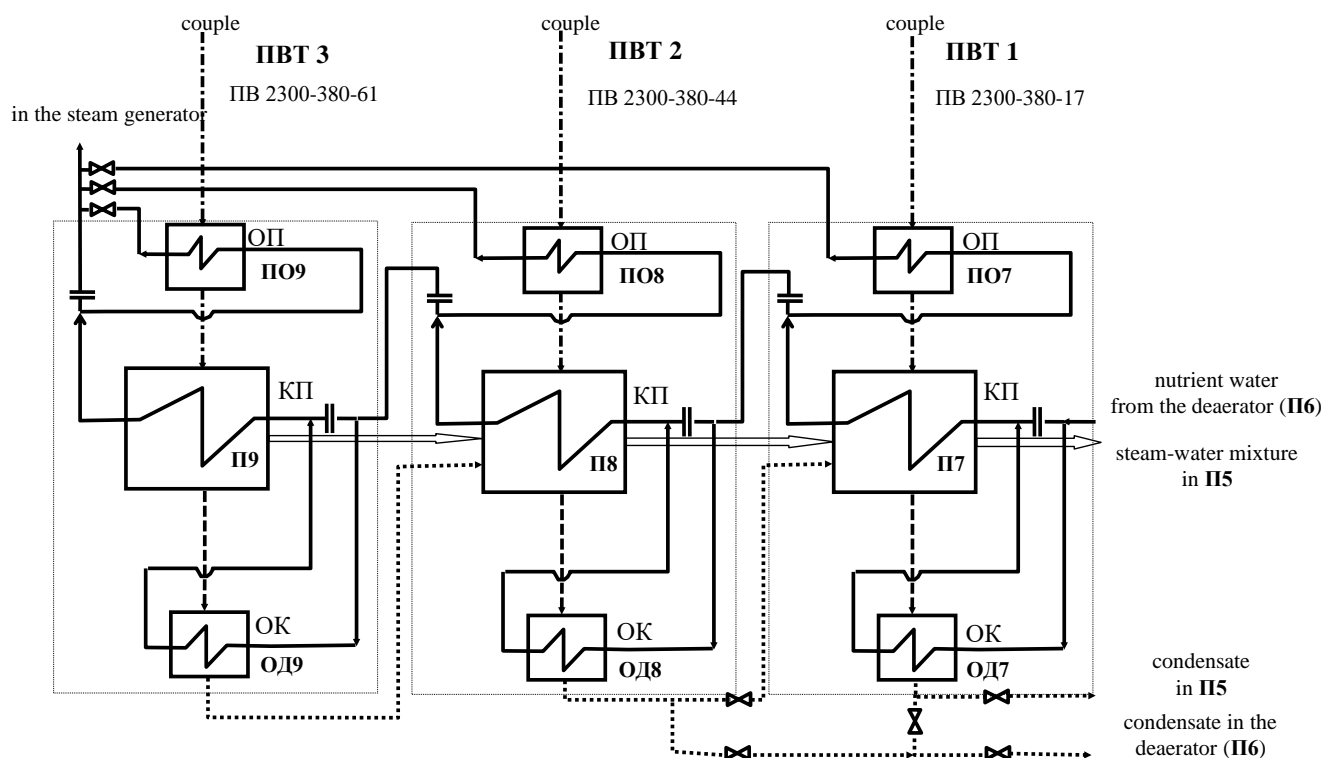


Fig. 1.2 - High-pressure regeneration system of the K-500-240 HTGZ turbine unit with parallel steam cooling

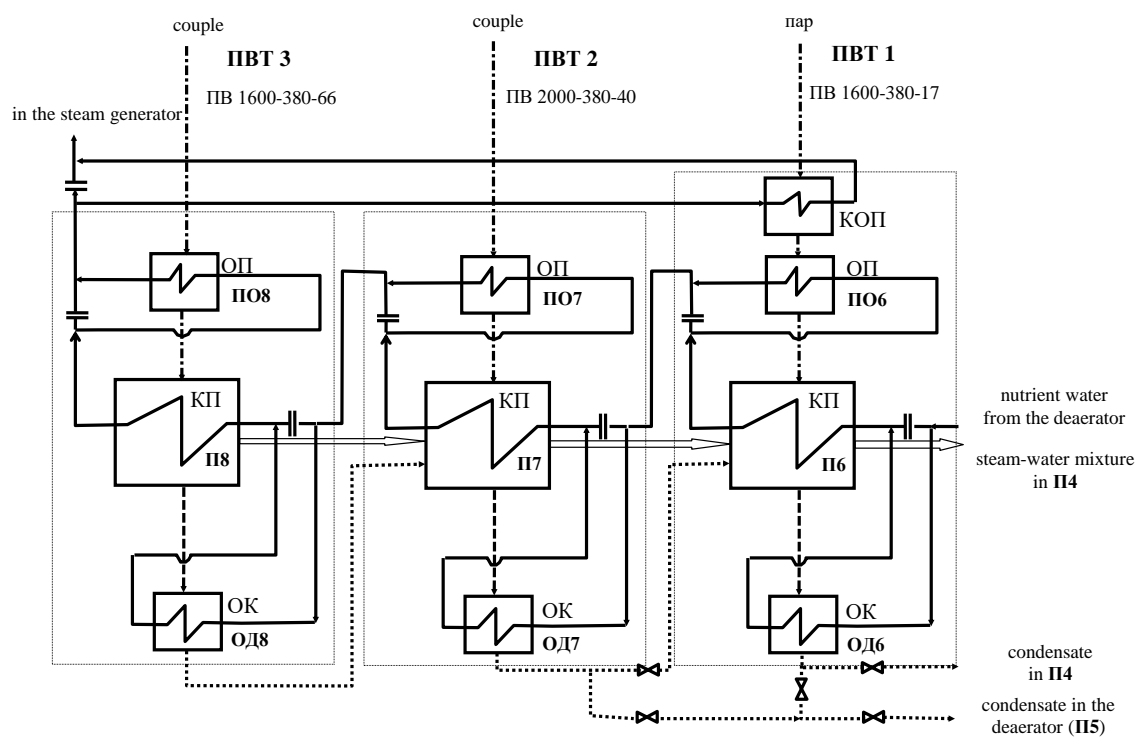


Fig. 1.3 - High-pressure regeneration system of the turbine unit K-800-240 LMZ with serial and final steam cooling (Violin scheme)

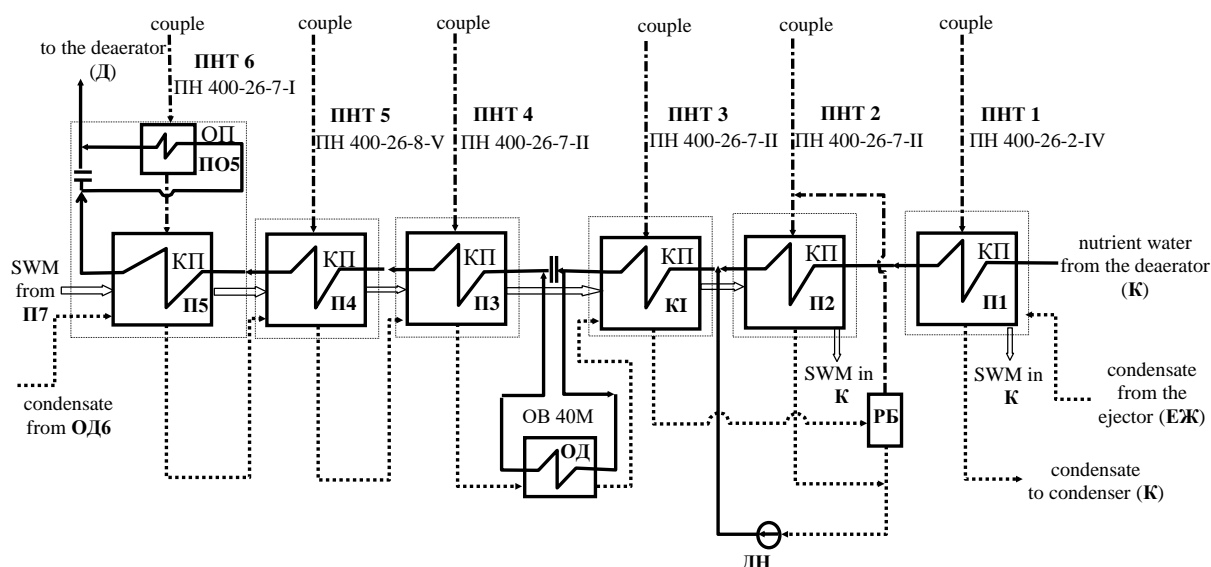


Fig. 1.4 - Low-pressure regeneration system of the turbine unit K-300-240 KhTGZ

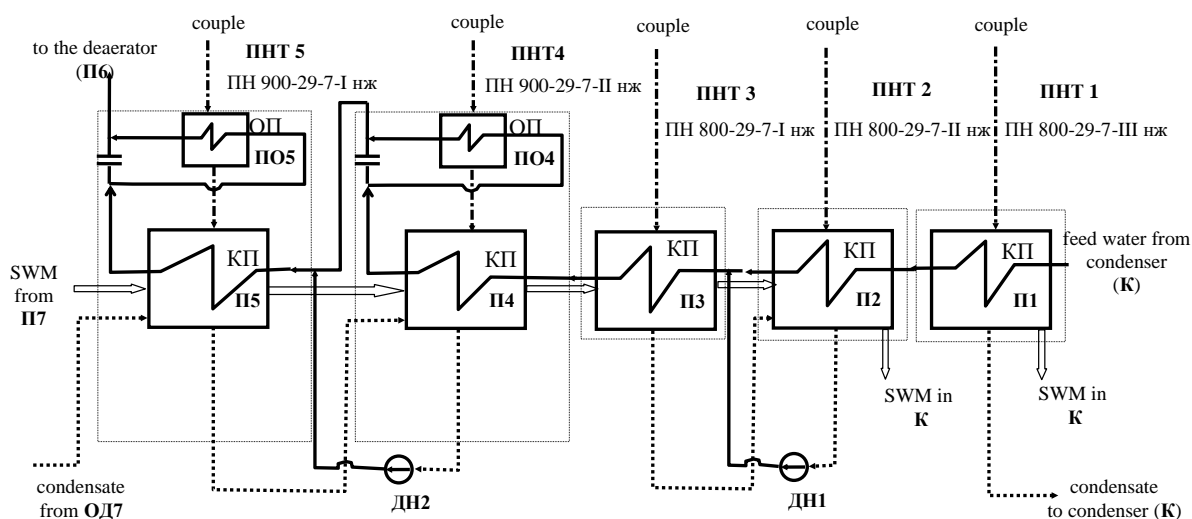


Fig. 1.5 - Low-pressure regeneration system of the turbine unit K-500-240 KhTGZ

In turbine plants with intermediate steam superheating, steam is usually taken from the first feedwater passage of the LWT after the intermediate superheating. When the guarantee mode of operation of the turbine unit approaches the minimum, the temperature pressure between the saturation temperature of this superheated steam at its pressure and the temperature of the feed water after the deaerator (at the inlet) decreases significantly. As a result, the efficiency of superheated steam

utilisation is lost in these modes, and this high-pressure regenerative feed water heaters is usually switched off.

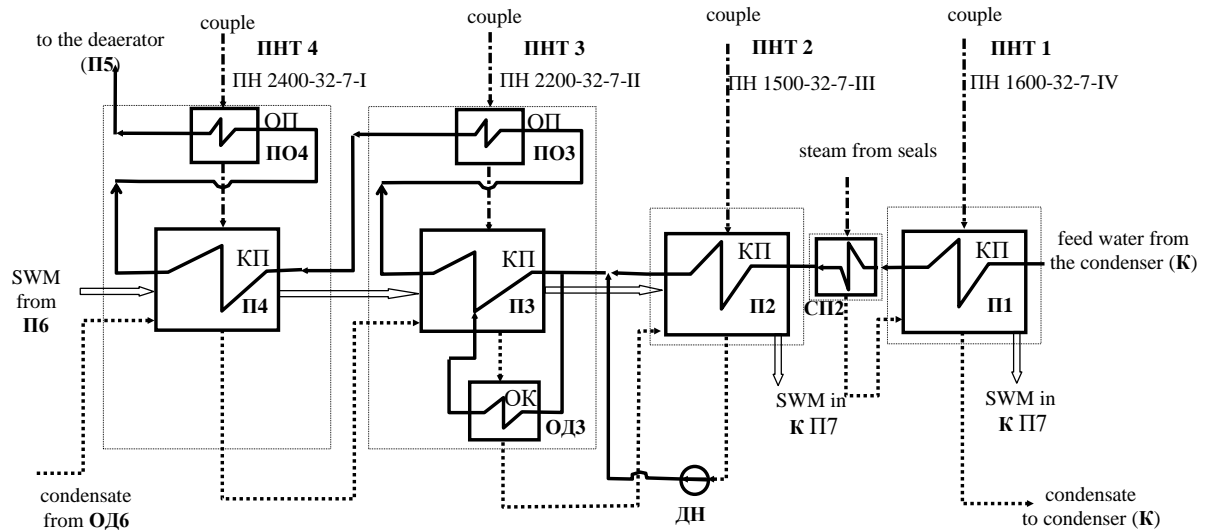


Fig. 1.6 - Low pressure regeneration system of turbine unit K-800-240 LMZ

To increase the efficiency of using superheated steam, steam coolers (ОП) are used in heaters. In low pressure regenerative feed water heaters, the steam cooler can be designed to pass both the entire feed water flow and a part of it that is mixed with the main flow at the outlet, with the flow rate controlled by a throttle washer. In the high-pressure regenerative feed water heaters, the HP is usually designed to pass a part of the feed water flow. At present, there are three main schemes for the inclusion of steam cooling in feedwater high-pressure regenerative feed water heaters systems:

- sequential scheme (Fig. 1.3, excluding the final steam cooling of ПHT 1), which was used in old high-pressure regenerative feed water heaters systems before modernization, where the feedwater flow after the steam cooling in each high-pressure regenerative feed water heaters is combined with the main one and enters the next heater;

- the Ricard-Nekolny scheme (Figs. 1.1, 1.2) with parallel steam cooling, where the feed water flow after the steam cooling is not combined with the main flow after

the heater, but is combined with the water flow after the entire regeneration system. The increased efficiency of the parallel-activated high pressure feed water is due to deeper cooling of the superheated steam and the transfer of this superheat to the hot source with direct fuel savings [1]. The efficiency of the subsequent high-pressure regenerative feed water heaters is reduced due to a decrease in feedwater consumption and steam extraction at them. At the same time, the temperature of the feed water after each steam cooling should not be lower than the temperature of the main flow at the mixing point in the group of high-pressure regenerative feed water heaters [2]. When the guarantee mode of operation of the turbine unit approaches the minimum, the efficiency of some of the steam cooling may decrease, as a result of which these steam cooling can be shut off by a shut-off valve;

- the Violin-Hulz scheme (Fig. 1.3) with end steam cooling, where a part of the feedwater flow after the regeneration system passes through the end steam cooling of the preheaters and returns again. Due to the insufficient cooling depth of superheated steam, this scheme is combined with a sequential scheme, and the final header exists only in the first feedwater heater, where steam is supplied after industrial superheating. As the analysis [1] shows, schemes with parallel and end-stage steam cooling are practically equally economical and surpass the efficiency and reliability of a scheme with exclusively series steam cooling. Therefore, in some 300 MW turbines of the old generation, schemes with series steam cooling were upgraded to Ricard-Nekolny schemes with parallel steam cooling, 500 MW turbines also use a scheme with parallel steam cooling, and 800 MW turbines use a combined scheme with series and one end built-in steam cooler.

High-pressure regeneration systems can be arranged in one (Figures 1.2, 1.3), two (Figure 1.1), and in some cases three parallel lines. The enlargement of high-pressure regenerative feed water heaters may increase the cost of their manufacture and operation, so it is advisable to manufacture some regeneration systems in two- or multi-filament versions.

## 1.2. Design and operational features of surface feedwater heaters

Heat exchangers for regenerative feedwater heating systems of steam turbine power plants with a capacity of 50-300 MW are of vertical design and have a flanged connector on the body. The pipe system consists of U-shaped heating surface pipes with a diameter of 16 mm and a wall thickness of 1 mm, the ends of which are rolled in a pipe board. The main components of the heaters are: a water chamber with connections for supplying and discharging feed water, partitions inside it (to organise a certain number of water passages) and a flange; a pipe system with a pipe board, U-shaped tubes that guide intermediate partitions for the passage of heating steam and condensate collection; a number of frame elements; a housing with connections, support legs and a flange. The peripheral part of the tube board in the assembled heater is fixed by means of studs between the flanges of the body and the water chamber. For heat exchangers with heat exchange surface areas from  $90 \text{ m}^2$  to  $350 \text{ m}^2$  and  $800 \text{ m}^2$ , the plant uses brass tubes of ЛІ-68 and ЛІО70-1 grades. In the ПІН-400 devices (Fig. 1.7, 1.8), which are used in power unit schemes for supercritical steam parameters, in addition to the above, tubes of МНЖ5-1 alloy or stainless steel 08X18N10T are used.

A vapour barrier is installed on the frame channels against the steam inlet to the heater tube bundle. Thanks to the baffles, the heating steam flow makes several passes in the pipe system during the mixed (transverse and longitudinal) flow of the heating surface pipes. After condensation, some of it, along with non-condensable gases (air), is discharged from the heater through a semi-circular perforated pipe to a branch pipe in the lower part of the housing. The condensate from the heating steam and steam from the spontaneous boiling of the injected condensate from the devices with a higher steam pressure in the vessel flows from the guide baffles through the annular holes between the pipes and the pipe passage holes in the guide baffles and enters the condensate level (cavity) in the lower part of the vessel. From there, the condensate is discharged through a spigot. With this disorganised drainage, condensate floods the pipe sections of the heat transfer surface of the lower

part of the bundle. Additional heating steam condensate from the apparatus with a higher pressure in the casing is introduced from the nozzle through a perforated pipe under the condensate level. This makes it difficult to remove the steam-air mixture from the vessel, causes fluctuations in the water (condensate) level in the vessel and complicates the process of regulating this level. The design of the water chamber and the pipe system allows the chamber to be rotated by 180° and the flow of feed water in the pipe system to be reversed from the design flow.

In the heater ПН -400-26-7-I (Fig. 1.7), a built-in steam cooler (ОП) is located in the centre of the pipe bundle in a special casing. After the fourth pass, a part of the feed water flow is directed to the steam cooler pipes. A restrictive diaphragm (throttle washer) is installed on the outlet pipe to ensure the required feed water flow rate through the steam cooling. The steam cooling pipe system has baffles that allow for cross-flow washing of the heating surface by a pair of pipes.



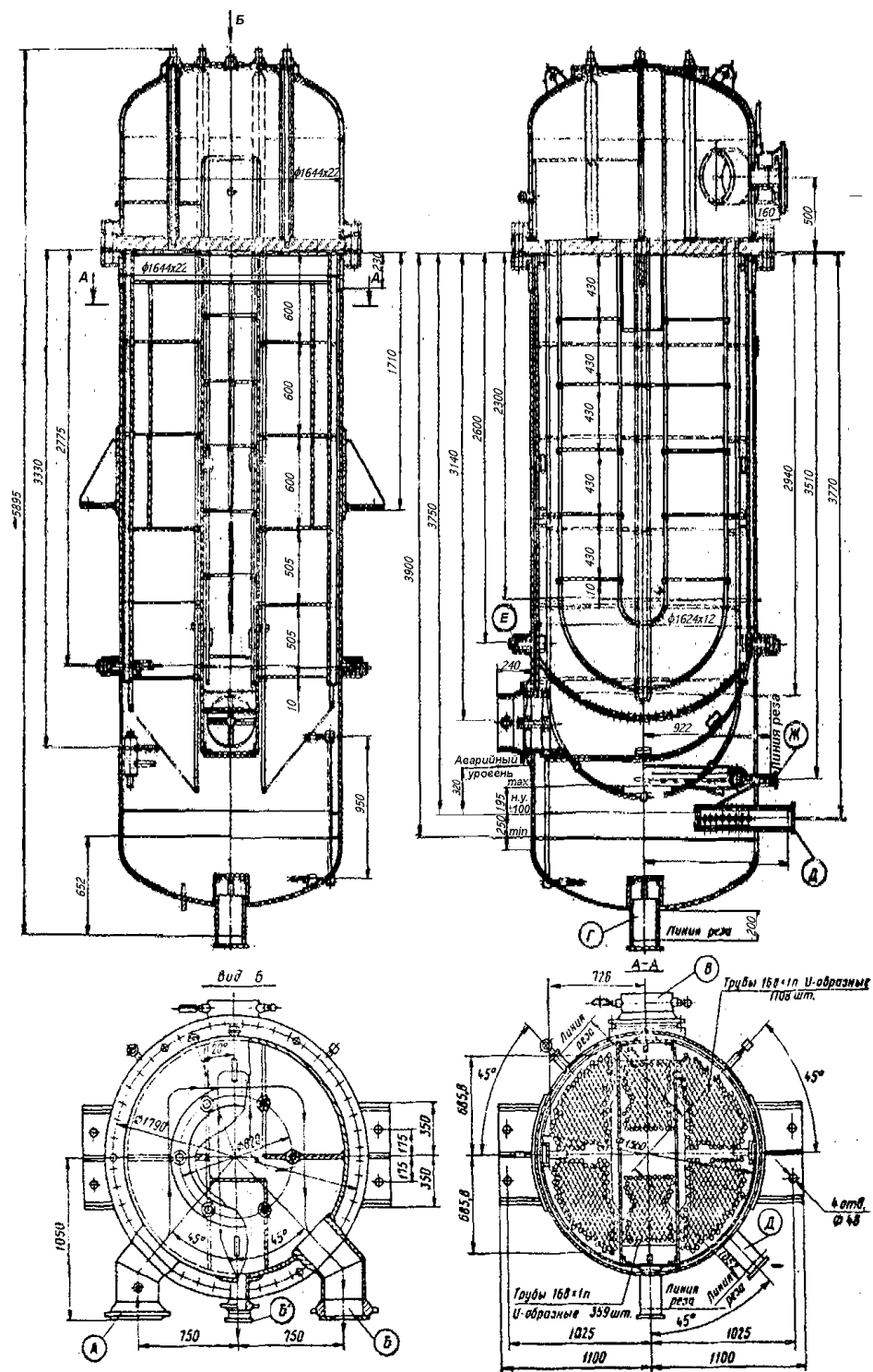


Fig. 1.7 - Design of the heater ПН -400-26-7 -I



Low-pressure heaters for regenerative feedwater heating systems for turbine units with a capacity of 500 MW and above (see example in Fig. 1.9), which are installed at power plants using organic and nuclear fuel. The units are equipped with welded pipe boards. Flange connectors are located on the water chambers. The bends of the pipes of the heating surfaces are U-shaped, and the intermediate partitions of the pipe bundle have devices for collecting condensate flowing down the pipe surfaces, heating steam and its removal to the lower part of the apparatus through the pipes of the pipe system frame. In this group of heaters, tubes with a diameter of 16 mm and a wall thickness of 1 mm or 1.2 mm made of corrosion-resistant steel 08Kh18N10T are mainly used, which are fixed in pipe boards by rolling. Other elements of these heaters are made of carbon steels. Some devices have built-in steam cooling, the design of which is similar to the IIIH -400-26-7-I heater (see Fig. 1.7). The above are the features of the design of the low pressure regenerative feed water heaters that were installed at power plants until the 1970s. During operation, significant shortcomings in their performance and reliability were identified. Subsequently, the high-pressure regenerative feed water heaters were designed to be more structurally advanced and reliable [2]. The steam cooling casing in such devices is located at the end of the fourth feedwater passage and covers the entire tube bundle of this passage (full feedwater flow). The casing is created by vertical partitions, where a horizontal partition is installed 30 mm below the tube board to isolate the board from contact with superheated steam. A part of the first run of feedwater pipes is allocated for the cooling tower (if any). The coolant pipes are the longest and are placed in a rectangular casing, the lower open part of which is below the normal condensate level in the vessel, and the upper part is welded to the tube board and the process cell. The condensate cooling casing has horizontal baffles that provide the necessary stiffness of the pipe bundle and the longitudinal and transverse flow of condensate through the pipes. The baffles in the steam control system are placed at the same distance from each other, the steam sequentially makes one or more passes, the cross-sectional area for its passage in which is consistently reduced.

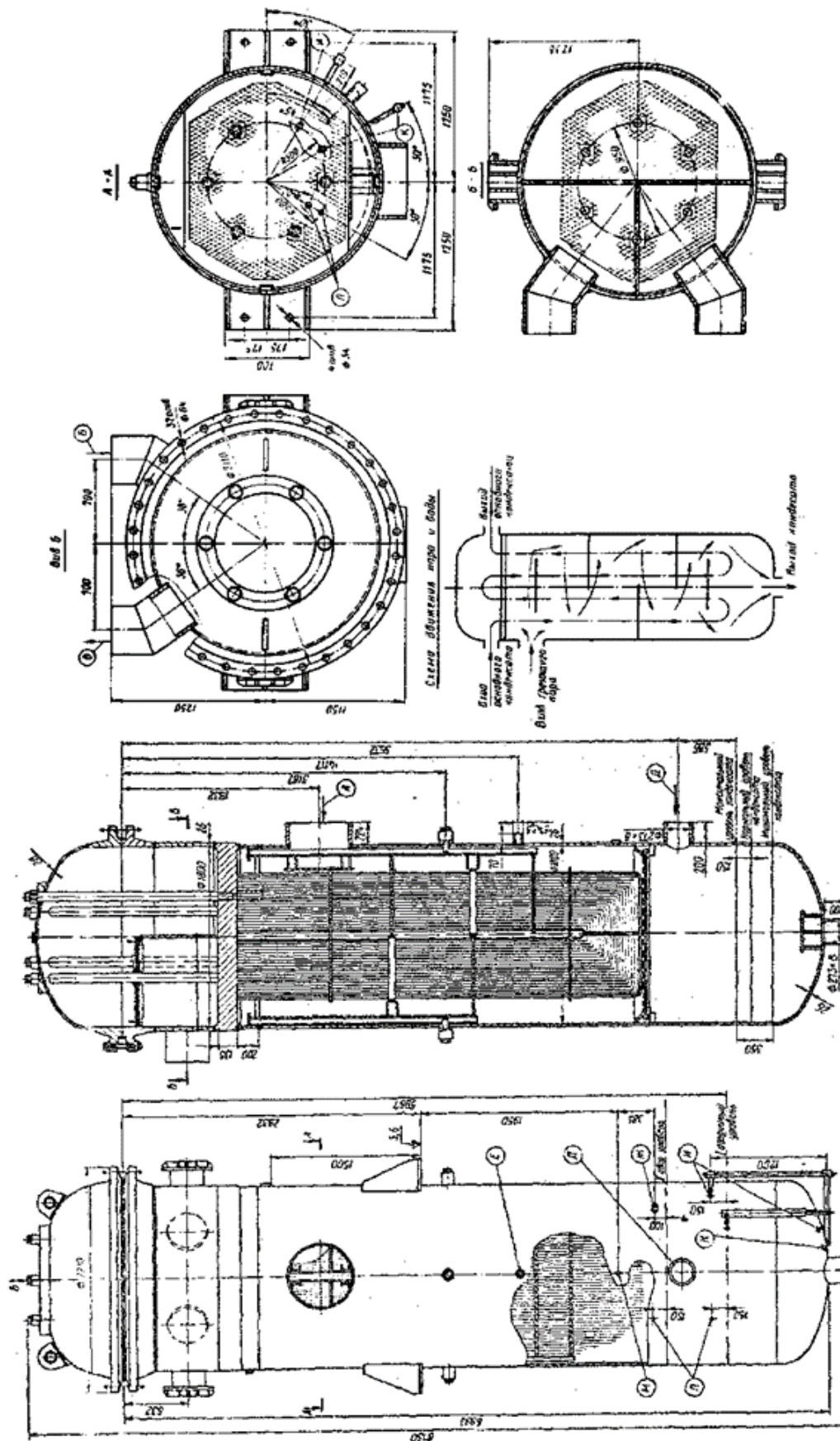


Fig. 1.9 – Construction of the heater ПН 700-29-7 -I (ПН 800-29-7 -I НЖ)

The first two rows of pipes in the bundle on the steam inlet side can have a wall thickness of 2 mm, the rest - 1.2 mm. The accepted location of the condensate inlet pipe from higher-pressure devices prevents steam from being dumped into the air exhaust pipe. In some devices, a steam distribution box is welded to the body, in the lower part of which there is a heating steam inlet pipe, the pipe bundle is located eccentrically and there are special holes for its entry into the inter-pipe space, which ensures minimal hydraulic losses. A 30-50 mm high rim is installed around the outer perimeter of all horizontal bundle partitions to prevent condensate from draining. Horizontal pipe bends are separated by corrugated metal plates. The perforated pipe for the steam-air mixture discharge is vertical and installed in the central part of the pipe bundle. A glass is welded into the lower part of the body, which, together with the lower edge of the casing, forms a water seal that prevents the main steam flow from breaking through to the steam-air mixture discharge pipe if it is installed in the lower part of the heater. To equalise the steam flow rate along the height of the cross-sections between the bundle partitions, two pairs of guide plates are installed in the central part of the steam-air mixture outlet pipe to ensure that the steam is washed mainly transversely along the steam path in the condensation zone. The feedwater velocity in the pipes was reduced to 2 m/s to avoid severe corrosion and erosion wear.

For 200 MW and 300 MW turbine plants in the early 1970s, the ПН 350 and ПН 550 devices were designed in this way again, which were subsequently installed in thermal schemes to replace the outdated ПН 300 and ПН 400 devices, respectively [2].

The main type of high-pressure regenerative feed water heaters used in domestic power units is a vertical collector high-pressure regenerative feed water heaters with a heating surface made of smooth pipes twisted into spirals [1-3]. In spiral-collector high-pressure regenerative feed water heaters, horizontally wound spiral coils are assembled in 4, 6 or 8 vertical columns. The pipe ends of the spiral coils are welded to 4, 6, and 8 vertical collectors (pipes), respectively. The design

features of the high pressure feed waters are determined by the high pressure of the feed water supplied to them after the feed pumps.

The heaters consist of the following main components: a pipe system including spiral coils (heating surfaces), collector pipes, partitions for collecting and draining condensate in the control room, steam cooling and condensate cooling covers, a lower support part of the housing to which the supply and discharge pipes connected to the pipe system are welded, and a removable upper part of the housing connected to the lower flange connector.

All components of typical HDDs are made of low-alloy carbon steels. The pipe system is mainly made of steel 20 with outer diameters of 32 mm and wall thicknesses of 4-6 mm.

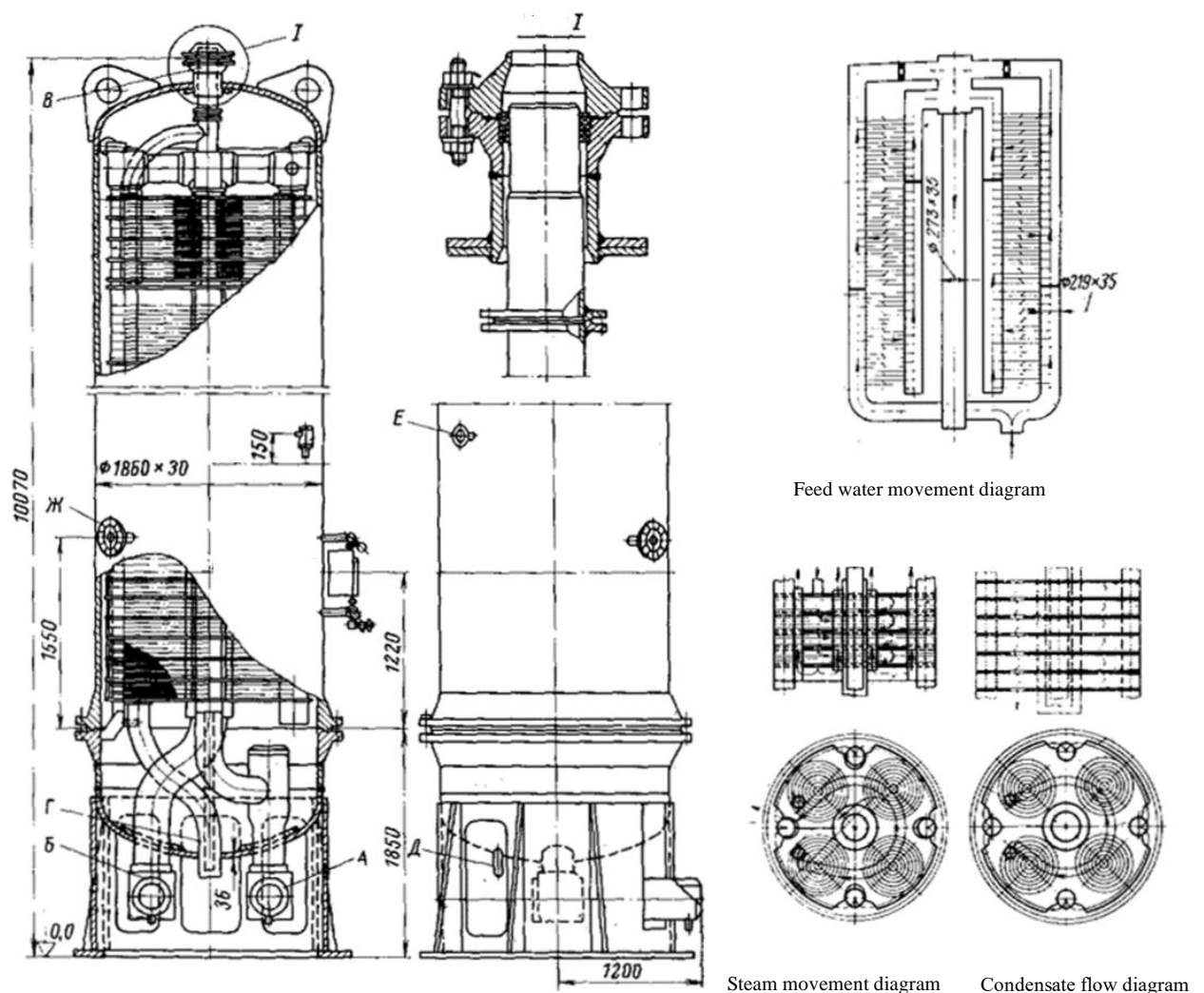
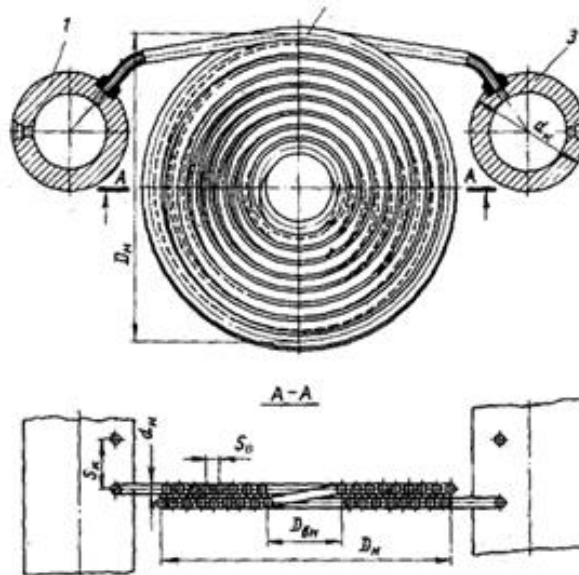
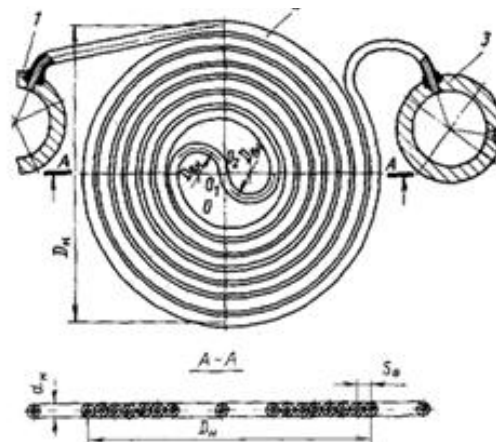


Fig. 1.10 – Design of the IIH 600-380-42 heater before modernization

Fig. 1.10 shows a preheater IIB -600-380-42 (IIBT-2) for 300MW turbine units built before 1972 (before modernisation). The heaters IIB 450-380-17 (IIBT-1) and IIB 450-380-66 (IIBT-3) had a similar design.



a) Double-plane spiral coil



b) Single-shaped spiral coil

Fig. 1.11 - Spiral coils used in high pressure feed water; 1 - distributing manifold; 2 - spiral coil; 3 - collecting manifold;  $D_B$ ,  $D_{BH}$  - outer and inner diameters of the coil;  $d_K$ ,  $d_H$  - diameters of the manifold and the coil pipe;  $S_V$ ,  $S_K$  - steps of coil winding and installation on the manifold



The pipe system of the heaters is a four-collector system with a two-pass feedwater control zone, and the lower part of the coils of the first feedwater passage forms an integrated condensate cooling, connected in a parallel circuit [1]. The pipe system uses two-plane spiral coils (Fig. 1.11 a) with pipe diameters of 32x5 mm. The velocities of the feedwater in them were 3 m/s and more, which led to significant wear at the inlet sections. All feedwater flows are collected through the upper crosspiece into the central pipe, which is used to discharge water from the low pressure regenerative feed water heaters. The connection of the collectors in the upper crosspiece created a rigid frame structure. The multi-pass flow of steam in the steam cooling and condensate in the DC was carried out in the plane of the coil winding with a large number of sharp turns, which led to significant pressure losses. Due to the significant steam resistance in the GP (0.14 and 0.28 MPa in II BT-1 and II BT-2), the saturation temperature in the steam condensation decreased by 4 and 4.6 °C, respectively, and the effect of the steam cooling device was almost completely lost. In addition, steam flow in the plane of the coil winding has a lower heat transfer efficiency than perpendicular to it. In addition to these significant drawbacks, the designs of such heaters before the modernisation had other problems that reduced their efficiency and reliability and led to premature failure.

Starting from 1972-1974, the production of modernised high-pressure regenerative feed water heaters began. In addition, the existing high-pressure regenerative feed water heaters at power units were upgraded. The sequential scheme of steam cooling inclusion in the regeneration system for II BT-1 and II BT-2 was replaced by a more efficient one based on the Rikar Nekolny scheme. In the condensation zones of these high-pressure regenerative feed water heaters, there is a single-pass feedwater flow. The feedwater velocity in the coils does not exceed 2 m/s, the condensate coolers zone is pre-enabled, where the installation of retaining washers and bypass pipelines in the zone ensures the required safe feedwater flow in the condensate coolers coils. The coils are cross-washed with steam (condensate) in the steam cooling and steam condensation, with an unstressed steam supply in the



steam cooling and a lower condensate supply in the steam condensation to prevent its breakthrough into the lower DWP.

The condensate in the condensate coolers and the steam in the steam cooling are sequentially washed through four columns of coils, passing through bypass boxes. The feed water is supplied to the coils of the condensate coolers at the same temperature (all coils operate in parallel). In the steam cooling ПІВТ-1 and ПІВТ-2, two adjacent columns of coils are connected in series from the distributing through the intermediate collector to the collecting collector, from which the feedwater flow from the steam cooling is discharged, the other two columns are connected in parallel to the first two. All coils in the steam cooling of ПІВТ-3 operate in parallel. Thus, in the condensate coolers and steam cooling of ПІВТ-3, the entire condensate or steam flow rate moves according to a single cross-circuit with mixing of the heating medium, and in the steam cooling of ПІВТ-1 and ПІВТ-2, the entire steam flow rate moves according to a double cross-circuit with mixing of the heating medium, where in one stroke the columns are operated in parallel, and the multiplicity is determined by two series-connected columns of coils. The lower bypass boxes of the steam cooling are made of a lower height than the upper ones, which is due to the possibility of changing the previous design. During the modernisation of these UDPs, the rigid connections in the upper crosspiece of the pipe system were also eliminated. However, it is not always possible to implement all the necessary measures and eliminate the shortcomings during the modernisation of existing highway pipelines. Fig. 1.12 shows an enlarged high pressure feed water of the ПІВ-2300 type, which are installed on the K500240 turbine units. All three heaters, ПІВ230038017 (ПІВ1), ПІВ230038044 (ПІВ2) and ПІВ230038061 (ПІВ3), are made in equal-sized housings and have approximately the same heating surface area [1]. The housing of each ПІВТ contains a built-in in-line condensate coolers with the arrangement of choke washers after the zone, a control zone and a built-in steam cooling, which is switched on in a parallel circuit. At the same time, the feed water velocity in the nominal mode of the condensate cooling is 2 m/s, in the control zone

- 1841.67 m/s, and the total hydraulic resistance is 0.65 MPa. The heating surface consists of single-plane spiral coils (see Fig. 1.11 b) made of pipes with a diameter of 32x5 mm in the condensate cooling and steam condensation, and 32x6 mm in the steam cooling. The outer diameter of the coils of the steam condensation and steam cooling is 956 mm, and the condensate cooling is 848 mm. Their deployed length in the steam condensation and condensate coolers is 19.5 m, and in the condensate coolers 15.2 m. The coils of the condensate coolers have a smaller diameter due to the fact that part of the space in the condensate coolers is occupied by bypass pipes (collectors). The level of safe feedwater velocity in 20 steel coils in terms of their erosion and corrosion destruction is 1.52 m/s. To reduce the velocity of feedwater in the zone, it is necessary to increase the flow-through sections. This proved to be possible with the use of single-plane (single-row) spiral coils with a "bifilar" winding (see Fig. 1.11 b). The use of such coils reduces their deployed length and, as a result, the hydraulic resistance.

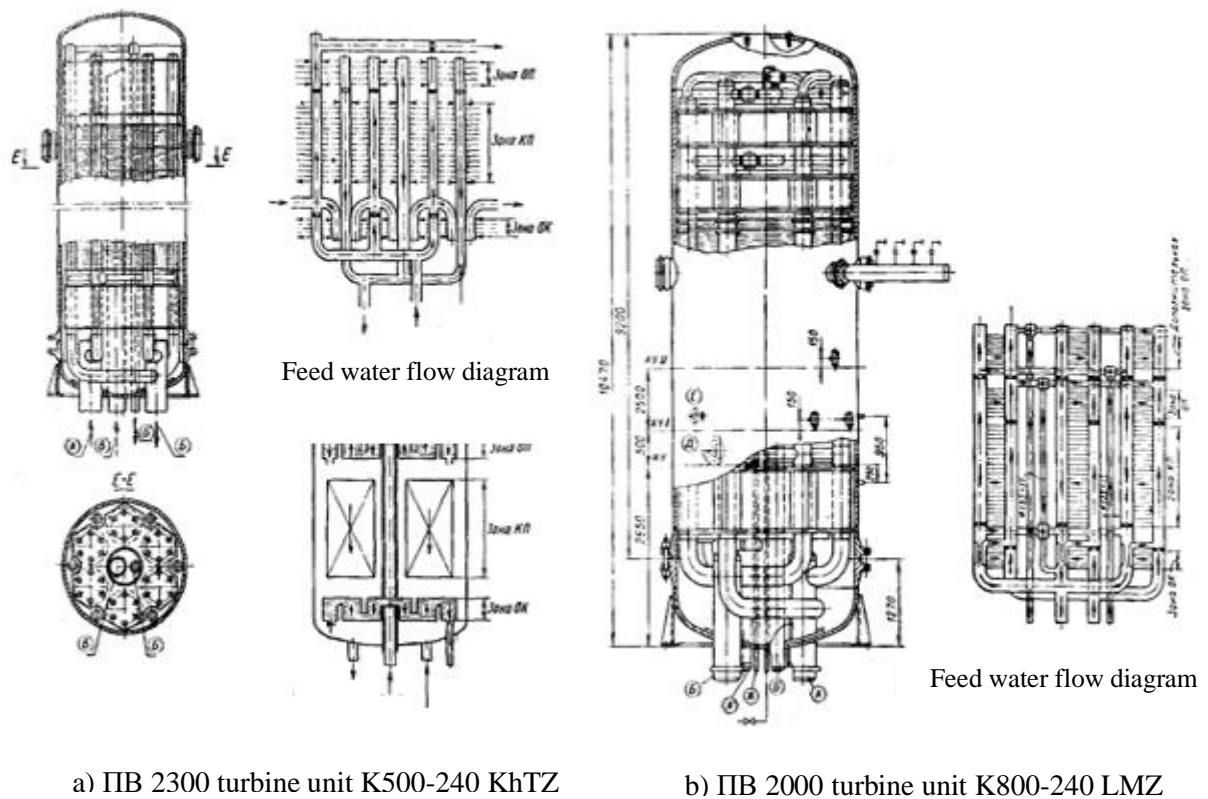


Fig. 1.12 – Design of enlarged high pressure feed water for steam turbine power plants with a capacity of 500 and 800 MW

Since the vertical pitch of the holes in the collectors is reduced by 2 times when switching to single-plane spiral coils, welding of the coil ends to the collectors is staggered, while maintaining the possibility of replacing individual coils without removing neighbouring ones.

Another design advantage of single-plane spiral coils is that their diameter can be changed continuously rather than discretely. This allows for better filling of the casing volume, as the diameters of the casing and the bottom of the low pressure regenerative feed water heaters can be changed discretely every 200 mm. The continuous change in the diameter of such coils is achieved by rotating the line of the half-turn centres. The increase in the number of coils themselves (the height of the high-pressure regenerative feed water heaters casing) is limited by the height of the turbine hall, and an increase in the number of collectors beyond six leads to an increase in the voids inside the casing that are not filled with coils.

The steam in the steam cooling and the condensate in the steam condensation moves perpendicular to the coil winding plane. Condensate enters the condensate coolers from below and moves in a single stream and passes from one column of coils to another via bypass boxes. Feed water is supplied to all columns at the same temperature. In the steam cooling, steam is supplied from above in two streams, which, using bypass boxes, sequentially wash three columns of coils connected in series through intermediate collecting manifolds. Thus, in the condensate coolers, the entire condensate flow rate moves in a single crossflow pattern with mixing of the heating medium, and in the steam cooling, half of the steam flow rate moves in a three-fold crossflow pattern with mixing of the heating medium, and the other half moves in parallel, similarly washing the other three coil columns. The double-stranded PIBT for 1200 MW power units at TPPs and 1000 MW power units at NPPs are based on the above-described ones with the same vessel diameter but a higher height (about 14 m). In contrast to the 500 MW unit, PIBT-2 and PIBT-3 have serial steam cooling, and PIBT-1 has a terminal steam cooling. The control structures use

an 810° inclination of the coils to the horizon. In the 1000 MW NPP unit, there are no steam condensations, horizontal single-plane coils are made of 32x4 mm diameter pipes, and the feedwater supply to the pipe system is lateral, through the cylindrical part of the bottom.

In Fig. 1.12 b shows a PIB heater -2000-380-40 (PIBT-2). Heaters PIB1600-380-17 (PIBT-1) and PIB1600-380-66 (PIBT-3) have a similar design. The heaters are installed in the high pressure regeneration systems of K-800-240 turbine units. The devices have built-in serial heat exchangers consisting of two separate shells - a conventional heat exchanger and an additional heat exchanger located above. In the heater PIB1600-380-17 (PIBT-1), the additional steam cooling serves as the final steam cooling, to which the feed water is supplied separately. In other high pressure feed waters, the conventional and additional feedwater heaters operate in parallel on feedwater. The steam in the steam cooling moves in two parallel streams, sequentially washing the three coil columns of the additional steam cooling, passing through the bypass boxes of its casing, then enters the casing of the conventional steam cooling through the bypass and similarly washes the three coil columns. All the coil columns in the conventional and additional EI operate in parallel. In the steam condensation, a single condensate stream washes all six coil columns, which also operate in parallel. Thus, in both the steam cooling and the steam condensation, steam or condensate moves in a single crossflow pattern with mixing of the heating medium. The diameter of the coils in the condensate coolers is the same as in the steam condensation and steam cooling, since the condensate cooling is made according to the scheme with internal diffusers in the output collectors. Otherwise, the design of the high-pressure regenerative feed water heaters elements is the same as in the PIB2300 turbine plants with a capacity of 500 MW.

## CHAPTER 2

### BASIC EQUATIONS DESCRIBING THE PROCESSES OF HEAT AND MASS TRANSFER AND HYDRODYNAMICS IN SURFACE FEEDWATER HEATERS

#### 2.1. Heat and material balance

A schematic heat diagram of a generalised surface heat exchanger or a heat exchanger consisting of steam cooling (ОП), steam condensation (КП) and condensate cooling (ОК) zones is shown in Fig. 2.1.

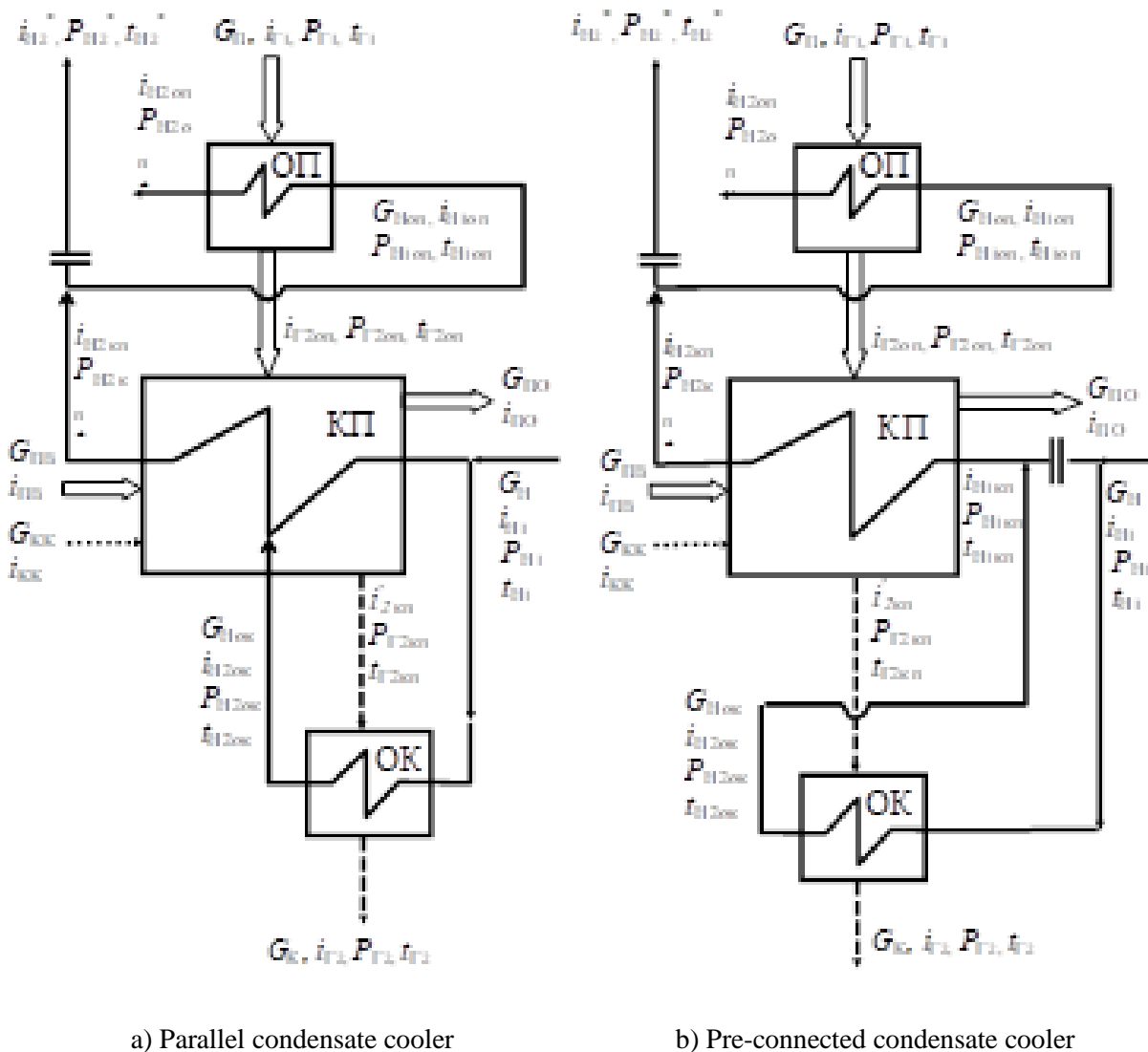


Fig. 2.1 - Schematic thermal diagram of a surface feedwater heater.

The mathematical model of such a steam-water heat exchanger includes the following main dependencies [1, 2, 4-7]:

a) heat balance equation for the entire heat exchanger:

$$Q^T = Q_\Gamma = Q_H \quad (2.1)$$

where  $Q^T$  - is the heat flux transmitted through the pipe walls:

$$Q^T = Q_{o\Pi} + Q_{к\Pi} + Q_{ок} \quad (2.2)$$

$Q_\Gamma$  and  $Q_H$  -are the heat fluxes transferred by the heat transfer media, respectively, given by the heating medium (steam, condensate) and received by the heated medium (feed water):

$$Q_\Gamma = G_n i_n + G_{кк} i_{кк} + G_{\PiБ} i_{\PiБ} - G_{\PiО} i_{\PiО} - G_K i_K - Q_3$$

and

$$Q_H = G_H (i_{H_2} - i_{H_1}) \quad (2.3)$$

$Q_3$  -is the heat flux lost by heat transfer through the insulated heater body;

$G_\Pi$ ,  $G_{\PiБ}$ ,  $G_{\PiО}$ ,  $G_{кк}$ ,  $G_K$  - flow rates: steam from the turbine intake, steam introduced with air from the higher pressure heater, steam removed with air through the air suction device, condensate of the cascade drain from the higher pressure heater, condensate leaving the heater;

$G_H$  - flow rate of the heated medium (feed water);

$i_\Pi$ ,  $i_{\PiБ}$ ,  $i_{\PiО}$ ,  $i_{кк}$  and  $i_K$  - are the enthalpies of: steam from the turbine intake, steam with air from the higher pressure heater, steam with air removed through the air suction device, condensate of the cascade drain from the higher pressure heater and condensate leaving the heater, respectively;

$i_{H_1}$ ,  $i_{H_2}$  - enthalpy of the heated medium (feed water) at the inlet and outlet of the heat exchanger;

b) heat balance equations for individual zones (steam cooling, steam condensation and condensate coolers):

$$Q_{OK} = G_{H_{OK}}(i_{H_{2OK}} - i_{H_{1OK}}) = G_K(i_{\Gamma_{1OK}} - i_{\Gamma_{2OK}}) = Q_{OK}^T \quad (2.4)$$

$$Q_{OK} = G_{H_{OK}} \sum_{j=1}^{n_{OK}} (i_{H_{2OKj}} - i_{H_{1OKj}}) = \sum_{j=1}^{n_{OK}} G_{K_j} (i_{\Gamma_{1OKj}} - i_{\Gamma_{2OKj}}) \quad (2.5)$$

$$Q_{O\Pi} = G_{H_{O\Pi}}(i_{H_{2O\Pi}} - i_{H_{1O\Pi}}) = G_{\Pi}(i_{\Gamma_{1O\Pi}} - i_{\Gamma_{2O\Pi}}) = Q_{O\Pi}^T \quad (2.6)$$

$$Q_{O\Pi} = G_{H_{O\Pi}} \sum_{j=1}^{n_{O\Pi}} (i_{H_{2O\Pi j}} - i_{H_{1O\Pi j}}) = \sum_{j=1}^{n_{O\Pi}} G_{\Pi_j} (i_{\Gamma_{1O\Pi j}} - i_{\Gamma_{2O\Pi j}}) \quad (2.7)$$

$$Q_{K\Pi} = G_{\Pi}i_{\Gamma_{1K\Pi}} + G_{KK}i_{KK} + G_{\Pi B}i_{\Pi B} - G_{\Pi O}i_{\Pi O} - G_Ki_{\Gamma_{2K\Pi}} = Q_{K\Pi}^T \quad (2.8)$$

- if the condensate cooling zone is located parallel to the steam condensation (diagram in Fig. 2.1 a):

$$Q_{K\Pi} = G_H(i_{H_{2K\Pi}} - i_{H_{1K\Pi}}) - Q_{OK} \quad (2.9)$$

- if the condensate cooling zone is enabled before the steam condensation (diagram in Fig. 2.1 b):

$$Q_{K\Pi} = G_H(i_{H_{2K\Pi}} - i_{H_{1K\Pi}}) \quad (2.10)$$

$$Q_{K\Pi} = G_H \sum_{j=1}^{n_{K\Pi}} (i_{H_{2K\Pi j}} - i_{H_{1K\Pi j}}) = \sum_{j=1}^{n_{K\Pi}} G_{K_j} (i_{\Gamma_{1K\Pi j}} - i_{K_j}) \quad (2.11)$$

where  $G_{H_{OK}}, G_{H_{O\Pi}}$  - is the nutrient water consumption in the condensate coolers and condensate coolers zones;

$i_{\Gamma_{1OK}}, i_{\Gamma_{1K\Pi}}, i_{\Gamma_{1O\Pi}}$  - enthalpy of: condensate at the inlet to the condensate cooling zone; superheated, saturated or wet steam at the inlet to the steam condensation zone, superheated steam at the inlet to the steam cooling zone, and

$$i_{\Gamma_{1OK}} = i_{\Gamma_{2K\Pi}} \quad (2.12)$$

$$i_{\Gamma_{1\text{KП}}} = i_{\Gamma_{2\text{ОП}}} \quad (2.13)$$

$$i_{\Gamma_{1\text{ОП}}} = i_{\Gamma_1} = i_{\Pi} \quad (2.14)$$

$i_{H_{1\text{OK}}}$ ,  $i_{H_{1\text{KП}}}$ ,  $i_{H_{1\text{ОП}}}$  - the enthalpy of feed water at the inlet to the condensate coolers, steam condensation and condensate coolers zones, and:

$$i_{H_{1\text{OK}}} = i_{H_1} \quad (2.15)$$

- if the condensate cooling zone is located parallel to the steam condensation (diagram in Fig. 2.1 a):

$$i_{H_{1\text{KП}}} = i_{H_1} \quad (2.16)$$

- if the condensate cooling zone is enabled before the steam condensation (diagram in Fig. 2.1 b):

$$i_{H_{1\text{KП}}} = i_{H_1} + \frac{Q_{\text{OK}}}{G_{\text{H}}} \quad \text{or} \quad i_{H_{1\text{KП}}} = \frac{(G_{\text{H}} - G_{H_{\text{OK}}})i_{H_1} + G_{H_{\text{OK}}}i_{H_{2\text{OK}}}}{G_{\text{H}}} \quad (2.17)$$

$$i_{H_{1\text{ОП}}} = i_{H_{2\text{KП}}} \quad (2.18)$$

$i_{\Gamma_{2\text{OK}}}$ ,  $i_{\Gamma_{2\text{KП}}}$ ,  $i_{\Gamma_{2\text{ОП}}}$  - enthalpies of condensate at the outlet of the condensate cooling zone, wet steam or condensate at the outlet of the KП zone and superheated, saturated or wet steam at the outlet of the low pressure regenerative feed water heaters zone, where

$$i_{\Gamma_{2\text{OK}}} = i_{\Gamma_2} = i_{\text{K}} \quad (2.19)$$

$i_{H_{2\text{OK}}}$ ,  $i_{H_{2\text{KП}}}$ ,  $i_{H_{2\text{ОП}}}$  - the enthalpy of feed water at the outlet of the condensate coolers, steam condensation and condensate coolers zones, and:

$$i_{H_2} = i_{H_{2\text{KП}}} + \frac{Q_{\text{ОП}}}{G_{\text{H}}} \quad \text{or} \quad i_{H_2} = \frac{(G_{\text{H}} - G_{H_{\text{ОП}}})i_{H_{2\text{KП}}} + G_{H_{\text{ОП}}}i_{H_{2\text{ОП}}}}{G_{\text{H}}} \quad (2.20)$$



$H_{OK}, H_{KII}, H_{OII}$  - is the number of sites considered in the condensate coolers, steam condensation and condensate coolers zones;

$j$  - indices of the sections, where in each case the conditions of connection (connection) of the sections on the heating and cooling sides are taken into account;

c) material balance equation for the heat exchanger:

$$G_K = G_{II} + G_{KK} + G_{IIB} - G_{IIO} \quad (2.21)$$

The mathematical model of surface heaters is superimposed on the operating conditions of the steam condensation zone (SCZ\steam condensation ). The condensate of the heating steam is discharged by gravity to the lower part (cavity) of the heater through a system of intermediate condensate drainage partitions, openings (windows) and auxiliary pipelines. If the heat transfer area in the heaters' control zone (steam condensation ) is insufficient, the steam in this zone will not completely condense (i.e. partially). The remaining steam, together with the non-condensable gases, must be discharged from the preheater through an air exhaust device to a downstream preheater, condenser or ejector (depending on the thermal design of the turbine unit). The condensate cooler (OK) or the downstream preheater (if there is no OK) is supplied with condensate minus this residual. If the required heat transfer area for complete condensation of the steam in the control zone steam condensation is excessive, all condensate is fed to the condensate coolers or downstream heater. The saturation pressure and temperature (  $p_s$  and  $t_s$  ) from the control chamber of the preheater must be calculated taking into account the steam resistance of the entire zone or in individual sections;

d) heat transfer equations in the low pressure regenerative feed water heaters, steam condensation and condensate coolers zones:

$$Q_{OK}^T = \sum_{j=1}^{n_{OK}} K_{OK_j} F_{OK_j} \Delta t_{CP\,OK_j}, \quad (2.22)$$

$$Q_{\text{КП}}^T = \sum_{j=1}^{n_{\text{КП}}} K_{\text{КП}_j} F_{\text{КП}_j} \Delta t_{\text{CP КП}_j}, \quad (2.23)$$

$$Q_{\text{ОП}}^T = \sum_{j=1}^{n_{\text{ОП}}} K_{\text{ОП}_j} F_{\text{ОП}_j} \Delta t_{\text{CP ОП}_j}, \quad (2.24)$$

where  $K_{\text{OK}_j}$ ,  $K_{\text{КП}_j}$ ,  $K_{\text{ОП}_j}$ , - heat transfer coefficients of individual sections of the steam cooling (ОП), steam condensation (КП) and condensate coolers (OK) zones;

$F_{\text{OK}_j}$ ,  $F_{\text{КП}_j}$ ,  $F_{\text{ОП}_j}$  - heat transfer areas of individual sections of the steam cooling, steam condensation and condensate coolers zones;

$\Delta t_{\text{CP OK}_j}$ ,  $\Delta t_{\text{CP КП}_j}$ ,  $\Delta t_{\text{CP ОП}_j}$  are the average temperature pressures of individual sections of the steam cooling, steam condensation, and condensate coolers zones;

$j$  - site indices.

The generalised mathematical model is given for heat exchangers with all three zones - condensate coolers, steam condensation and HC. In some heat exchanger designs, one of the zones may actually be missing. This is typical for high-pressure regenerative feed water heaters, which can have both the steam cooling and the steam condensation zones, or only the steam condensation zone. In the thermal schemes of steam turbine plants, condensate coolers are sometimes used as separate devices - drainage coolers (DCs) (see Fig. 1.4). Thus, there is only one characteristic zone in these devices - the DCO. When developing mathematical models of these heaters, the equations and parameters of the missing zones are excluded.

## 2.2 Thermodynamic and thermophysical properties of water and water vapour

Below, we present ready-made approximation polynomial equations from [2, 8-12] for the thermodynamic and thermophysical properties of water and water vapour, the main heat transfer media in steam-water heat exchangers of TPPs and

NPPs. It is convenient to use the dependence in this form in calculations of heat exchangers on a computer.

To calculate the temperature  $t_s$  from the saturation pressure  $p_s$ , the pressure  $p_s$  from the saturation temperature  $t_s$ , the enthalpy  $i'$  and the specific volume of water  $v'$  on the lower, the enthalpy  $i''$  and the specific volume of water vapour  $v''$  on the upper boundary curve from the saturation temperature  $t_s$ , we used the approximation polynomial dependences from [9, 11], which have an error with the tabulated data of no more than 0.001%:

$$t_s = \sum_{j=0}^{11} a_j (\ln(10,197162 p_s))^j ; \quad (2.25)$$

$$\ln(10,197162 p_s) = \sum_{j=0}^9 b_j \left( \frac{t_s}{100} \right)^j ; \quad (2.26)$$

$$i' = 10^3 \cdot \sum_{j=0}^9 c_j \left( \frac{t_s}{100} \right)^j ; \quad (2.27)$$

$$i'' = 10^3 \cdot \sum_{j=0}^7 d_j \left( \frac{t_s}{100} \right)^j ; \quad (2.28)$$

$$v' = \sum_{j=0}^9 f_j \left( \frac{t_s}{100} \right)^j ; \quad (2.29)$$

$$v'' = \frac{100}{P_s} \sum_{j=0}^8 k_j \left( \frac{t_s}{100} \right)^j , \quad (2.30)$$

where  $a_j, b_j, c_j, d_j, f_j$  и  $k_j$  are the coefficients of the polynomials, the values of which are given in Table 2.1.

To calculate the thermal conductivity  $\lambda'$ , kinematic  $\nu'$  or dynamic viscosity  $\mu'$  and Prandtl's number  $Pr'$  of water on the lower boundary curve from the saturation temperature  $t_s$  до 250 °C we used the dependences from [12], and  $t_s$  above 250 °C

from [2, 8], the thermal conductivity  $\lambda''$ , dynamic viscosity  $\mu''$  and Prandtl's number  $Pr''$  of water vapour on the upper boundary curve also from [2, 8]:

$$\lambda' = 0,55758 e^{0,003827t_s - 0,000017t_s^2} \quad \text{with } 10 \leq t_s \leq 60 \text{ }^\circ\text{C}; \delta \leq 0,3\% \quad \_$$

Table 2.1 - Polynomial coefficients

$j$	$a_j$	$b_j$	$c_j$	$d_j$	$f_j$	$k_j$
0	$9,90927 \cdot 10^{-1}$	-5,07871	$-4,16 \cdot 10^{-5}$	2,50096	$1,0001789 \cdot 10^{-3}$	$1,26 \cdot 10^{-2}$
1	$2,785424 \cdot 10^{-1}$	7,27049	$4,2290733 \cdot 10^{-1}$	$1,843054 \cdot 10^{-1}$	$1,390533 \cdot 10^{-7}$	$4,5945234 \cdot 10^{-3}$
2	2,375358	-3,03372	$-2,5507948 \cdot 10^{-2}$	$1,96911 \cdot 10^{-4}$	$2,0639347 \cdot 10^{-5}$	$-3,1913345 \cdot 10^{-5}$
3	$2,107781 \cdot 10^{-1}$	1,256759	$6,222956 \cdot 10^{-2}$	$-1,273775 \cdot 10^{-2}$	$1,4001053 \cdot 10^{-4}$	$-3,168401 \cdot 10^{-4}$
4	$2,129682 \cdot 10^{-2}$	$-5,608659 \cdot 10^{-1}$	$-8,382342 \cdot 10^{-2}$	$9,38497 \cdot 10^{-3}$	$-2,7979589 \cdot 10^{-4}$	$3,3979946 \cdot 10^{-4}$
5	$1,328377 \cdot 10^{-3}$	$2,477563 \cdot 10^{-1}$	$6,921469 \cdot 10^{-2}$	$-8,047757 \cdot 10^{-3}$	$2,7254276 \cdot 10^{-4}$	$-3,4194103 \cdot 10^{-4}$
6	$-3,739348 \cdot 10^{-4}$	$-8,659025 \cdot 10^{-2}$	$-3,453679 \cdot 10^{-2}$	$2,732533 \cdot 10^{-3}$	$-1,5042234 \cdot 10^{-4}$	$1,4519652 \cdot 10^{-4}$
7	$-1,741775 \cdot 10^{-5}$	$2,015339 \cdot 10^{-2}$	$1,0322371 \cdot 10^{-2}$	$-3,471429 \cdot 10^{-4}$	$4,8021276 \cdot 10^{-5}$	$-2,8638253 \cdot 10^{-5}$
8	$2,207171 \cdot 10^{-5}$	$-2,693453 \cdot 10^{-3}$	$-1,699491 \cdot 10^{-3}$		$-8,267041 \cdot 10^{-6}$	$2,0409849 \cdot 10^{-6}$
9	$1,534373 \cdot 10^{-6}$	$1,55318 \cdot 10^{-4}$	$1,1936422 \cdot 10^{-4}$		$5,968357 \cdot 10^{-7}$	
10	$-4,268569 \cdot 10^{-7}$					
11	$-4,29246 \cdot 10^{-8}$					

$$\lambda' = 0,55492 + 0,002367t_s - 0,0000106t_s^2 \quad \text{with } 60 \leq t_s \leq 120 \text{ }^\circ\text{C}; \delta \leq 0,3\%$$

$$\lambda' = 0,604331 + 0,0012582t_s - 0,0000048t_s^2 \quad \text{with } 120 \leq t_s \leq 250 \text{ }^\circ\text{C}; \delta \leq 0,3\%$$

$$\lambda' = 10^{-2} \cdot \left( 68,73 - \frac{0,0006}{(t_s - 140)^2} \right) \quad \text{with } 250 \leq t_s \leq 355 \text{ }^\circ\text{C}; \delta \leq 1\% \quad (2.31)$$

$$\nu' = 10^{-6} \cdot \left( \frac{1688,38}{t_S^3} - \frac{400,36}{t_S^2} + \frac{36,506}{t_S} - 0,029335 \right) \text{ with } 10 \leq t_S \leq 120 \text{ } ^\circ\text{C}$$

$$\nu' = 10^{-6} \cdot 1,3339 e^{-0,00000007 t_S^3 + 0,00006283 t_S^2 - 0,02039 t_S} \text{ with } 120 \leq t_S \leq 250 \text{ } ^\circ\text{C}, \delta \leq 0,59\%;$$

$$\nu' = \mu' \cdot \nu', \quad \mu' = \frac{27950 \cdot 10^{-6}}{t_S} \text{ with } 250 \leq t_S \leq 340 \text{ } ^\circ\text{C}, \delta \leq 5\%; \quad (2.32)$$

$$\text{Pr}' = 13,1487 e^{-0,000000466 t_S^3 + 0,0001934 t_S^2 - 0,03478 t_S} \text{ with } 10 \leq t_S \leq 120 \text{ } ^\circ\text{C}$$

$$\text{Pr}' = 12,1183 e^{-0,0000001 t_S^3 + 0,00009021 t_S^2 - 0,026845 t_S} \text{ with } 120 \leq t_S \leq 250 \text{ } ^\circ\text{C}; \delta \leq 0,48\% \quad \_$$

$$\text{with } 250 \leq t_S \leq 300 \text{ } ^\circ\text{C} \quad \delta \leq 3,5\%; \quad (2.33)$$

$$\lambda'' = 10^{-2} \cdot \left( \frac{698}{400 - t_S} + 0,233 \right) \text{ with } 100 \leq t_S \leq 345 \text{ } ^\circ\text{C}; \delta \leq 5\% \quad \_ \quad (2.34)$$

$$\mu'' = 10^{-6} \cdot (29,23 - 1,079 \sqrt{355 - t_S}) \text{ with } 80 \leq t_S \leq 350 \text{ } ^\circ\text{C}, \delta \leq 7\%; \quad (2.35)$$

$$\text{Pr}'' = \frac{110}{403 - t_S} + 0,64 \text{ with } 100 \leq t_S \leq 330 \text{ } ^\circ\text{C}, \delta \leq 1,5\%. \quad (2.36)$$

As can be seen from the above dependences, the errors in calculating the thermal conductivity  $\lambda_i$  and dynamic viscosity  $\mu$  of water vapour on the upper boundary curve are very large. However, these values are not taken into account in the calculation of heat transfer coefficients in the studied devices. They are given here for a complete description of the thermophysical properties of water and water vapour at the saturation line.

At pressures of unheated water  $p$  up to 2MPa, its parameters differ little from those of water at the saturation line (dependences (2.27)-(2.33) if the temperature of unheated water  $t_S$  is substituted for the saturation temperature  $t$   $^\circ\text{C}$ . For larger values of water pressure, a correction is necessary. The analysis of formulas [2, 8] shows

that the parameters of unheated water consist of the parameters of water on the lower boundary curve at its temperature and corrections for pressure dependence. Therefore, terms [2, 8] are added to the parameters on the saturation line to account for pressure dependence:

$$i_B = i'(t_B) + 1,407 p_B - \frac{183,72 p_B}{390 - t_B}$$

with  $p_B$  up to 40 MPa and  $130 \leq t_B \leq 330$  °C or

$$p_B \text{ up to 1 MPa and } 50 \leq t_B \leq 300 \text{ °C; } \delta \leq 1\% ; \quad (2.37)$$

$$v_B = \frac{1}{\frac{1}{v'(t_B)} + 0,306 p_B (1 + 0,000037 t_B^2)}$$

$$\text{with } p_B \text{ up to 40 MPa and } 5 \leq t_B \leq 300 \text{ °C; } \delta \leq 1\% \text{ _} \quad (2.38)$$

$$\lambda_B = \lambda'(t_B) + 5,93 \cdot 10^{-4} p_B \left(1 + 5 \cdot 10^{-5} (t_B - 115)^2\right)$$

$$\text{with } p_B \text{ up to 40 MPa and } v < 0,002 \frac{m^3}{kg}; \delta \leq 1\% \text{ _} \quad (2.39)$$

$$\mu_B = \mu'(t_B) + 2,55 \cdot 10^{-7} p_B$$

$$\text{with } p_B \text{ up to } p_s \text{ and } 15 \leq t_B \leq 355 \text{ C ; } \delta \leq 1\% \text{ _} \quad (2.40)$$

$$Pr_B = Pr'(t_B) - 3 \cdot 10^{-8} p_B (t_B - 180)^2$$

$$\text{with } p_B \text{ up to 40 MPa and } 27 \leq t_B \leq 330 \text{ °C, } \delta \leq 1\% . \quad (2.41)$$

The specific volume  $T_{II}$  of superheated steam (real gas), depending on the temperature  $T_P$  in degrees Kelvin and pressure  $p_{II} 10^5$  Pa (bars), can be calculated with a given accuracy based on the virial equation of state with interpolation to the third coefficient [9-11]:

$$v_{\Pi} = \frac{R_{\Pi} T_{\Pi}}{100 p_{\Pi}} (1 + b p_{\Pi} + c p_{\Pi}^2 + f p_{\Pi}^3) \quad (2.42)$$

where  $T_{\Pi} = t_{\Pi} + 273,15$ ;

$t_{\Pi}$  – temperature of superheated steam °C;

$R_{\Pi}$  – Constant gas water vapour,  $R_{\Pi} = 0,46151 \left[ \frac{\text{kJ}}{\text{kg K}} \right]$ ;

$b$ ,  $c$  and  $f$  – the first, second, and third temperature-dependent verification coefficients:

$$b = 10^{-4} \cdot \sum_{j=0}^5 b_j \left( \frac{1000}{T_{\Pi}} \right)^j; \quad (2.43)$$

$$c = 10^{-6} \cdot \sum_{j=0}^8 c_j \left( \frac{1000}{T_{\Pi}} \right)^j; \quad (2.44)$$

$$f = 10^{-8} \cdot \sum_{j=0}^8 f_j \left( \frac{1000}{T_{\Pi}} \right)^j, \quad (2.45)$$

where  $b_j$ ,  $c_j$  and  $f_j$  – The coefficients of the polynomials of the approximation of the virial coefficients are shown in Table 2.2:

Table 2.2 - Polynomial coefficients

	$b_j$	$c_j$	$f_j$
0	-5,0114	-29,13316	-34,55136
1	19,6657	129,6571	230,6962
2	-20,9137	-181,95576	-657,2189
3	2,32488	0,704026	1036,187
4	2,67376	247,9672	-977,4513
5	-1,62302	-264,05235	555,889
6		117,60724	-182,0987
7		-21,27667	30,5542
8		0,524802	-1,991713

As is well known from thermodynamics, the enthalpy of a real gas is determined from the state characteristic function:

$$i(p, T) = i_0(p_0, T) + \int_{p_0}^p \left[ v - T \left( \frac{\partial v}{\partial T} \right)_p \right] dp, \quad (2.46)$$

where  $i_0(p_0, T)$  is the enthalpy of a substance in an ideal gas state (in the limit at an initial pressure  $p_0$ ) and a given temperature  $T$ .

The beginning of the enthalpy reference is related to the beginning of the internal energy reference. In accordance with the international agreement, the temperature and pressure at the triple point are taken as zero for water ( $T_0 = 273,16\text{K}$  and  $p_0 = 611,2\text{ Pa}$ ).

Substituting the function of the specific volume of superheated water vapour  $v_{\Pi}$  (virial equation of state (2.42) into the expression under the integral of the characteristic state function for enthalpy (2.46) and the value for water  $i_0(p_0, T)$  (superheated steam), we obtain an expression for the enthalpy of superheated water vapour  $I_{\Pi}$  depending on the temperature  $T_{\Pi}$  in degrees Kelvin and pressure  $p_{\Pi}$  в  $10^5\text{ Pa}$  (bars) [9-11]:

$$i_{\Pi} = 1808,92 + 1,4829T_{\Pi} + 3,7903 \cdot 10^{-4} T_{\Pi}^2 + 46,174 \ln T_{\Pi} - \\ - RT^2 \left( \frac{db}{dT_{\Pi}} p_{\Pi} + \frac{1}{2} \frac{dc}{dT_{\Pi}} p_{\Pi}^2 + \frac{1}{3} \frac{df}{dT_{\Pi}} p_{\Pi}^3 \right) \quad (2.47)$$

where  $\frac{db}{dT_{\Pi}}$ ,  $\frac{dc}{dT_{\Pi}}$  and  $\frac{df}{dT_{\Pi}}$ , and are the temperature derivatives of the first, second, and third verification coefficients (2.43)-(2.45):

$$\frac{db}{dT_{\Pi}} = 10^{-7} \cdot \sum_{j=1}^5 j b_j \left( \frac{1000}{T_{\Pi}} \right)^{j+1}; \quad (2.48)$$



$$\frac{dc}{dT_{\Pi}} = 10^{-9} \cdot \sum_{j=1}^8 j c_j \left( \frac{1000}{T_{\Pi}} \right)^{j+1}; \quad (2.49)$$

$$\frac{df}{dT_{\Pi}} = 10^{-11} \cdot \sum_{j=1}^8 j f_j \left( \frac{1000}{T_{\Pi}} \right)^{j+1}, \quad (2.50)$$

where  $b_j$ ,  $c_j$ ,  $i$ ,  $f_j$  are the coefficients of the polynomials of approximation of the virial coefficients from equation (2.42), which are given in Table 2.2.

The thermal conductivity  $\lambda_{\Pi}$ , dynamic viscosity  $\mu_{\Pi}$  and Prandtl number  $Pr_{\Pi}$  of superheated water vapour are well described by the dependencies [2, 8]:

$$\lambda_{\Pi} = 4,443 \cdot 10^{-6} T_{\Pi}^{1,45} + \frac{1,547 \cdot 10^{-4}}{v_{\Pi}^{1,25}}$$

$$\text{with } p_B \text{ up to 40 MPa and } v < 0,005 \frac{m^3}{kg}; \delta \leq 1\% \quad (2.51)$$

$$\mu_{\Pi} = 9,8 \cdot 10^{-9} \left( T_{\Pi}^{1,2} + \frac{0,431}{v_{\Pi}^{1,48}} \right),$$

$$\text{with } p_1 \leq 40 \text{ MPa, } t_1 < 500^{\circ}\text{C}; \delta \leq 1\% \quad (2.52)$$

$$Pr_{\Pi} = 0,8 + \frac{50}{t_{\Pi} - 325 + \frac{10000}{10,19 p_{\Pi} + 23}}$$

$$\text{with } 0,015 \leq p_1 \leq 8 \text{ MPa, } 50 \leq t_1 \leq 600^{\circ}\text{C}, \delta \leq 1\%, \quad (2.53)$$

where  $T_{\Pi}$  is the temperature of superheated water vapour in degrees Kelvin,  $T_{\Pi} = t_{\Pi} + 273,15$ ;

$t_{\Pi}$  is the temperature of superheated water vapour in  $^{\circ}\text{C}$ ;

$p_{\Pi}$  is the pressure of superheated water vapour in MPa;

$v_{\Pi}$  is the specific volume of superheated water vapour,  $\frac{m^3}{kg}$ ,  $v_{\Pi} = v_{\Pi}(T_{\Pi}, p_{\Pi})$  is calculated according to the equation of state (2.42), where  $p_{\Pi}$  is the pressure in  $10^5 \text{ Pa}$  (bars).

### 2.3. Coefficients of heat transfer, heat transfer and thermal conductivity of pipe wall materials

In this case, the heat transfer coefficient through the cylindrical pipe wall, attributed to the outer surface, is determined as follows [2, 4, 8, 13 -20]:

$$K = \frac{1}{\frac{d_{3OB}}{d_{BH}} \frac{1}{\alpha_1} + \frac{d_{3OB}}{2\lambda_{CT}} \ln \frac{d_{3OB}}{d_{BH}} + \frac{1}{\alpha_2}}, \quad (2.54)$$

where  $d_{BH}$  and  $d_{3OB}$  are the internal and external diameters of the pipes;

$\alpha_1$  and  $\alpha_2$  - heat transfer coefficients of heat carriers washing the pipe from the inside and outside;

$\lambda_{CT}$  - thermal conductivity of the pipe wall material.

When feedwater moves inside straight smooth round pipes, the heat transfer coefficient for turbulent flow ( $Re > 8000$ ) is determined as follows [1, 2, 4, 8, 13-17, 19, 21]:

- for  $0,5 < Pr < 25$ :

$$\alpha = 0,023 \frac{\lambda}{d} Re^{0,8} Pr^{0,4} \varepsilon_l \varepsilon_t, \quad (2.55)$$

- for  $8000 < Re < 5 \cdot 10^6$  and  $0,6 < Pr < 2500$ :

$$\alpha = 0,021 \frac{\lambda}{d} Re^{0,8} Pr^{0,43} \varepsilon_l \varepsilon_t, \quad (2.56)$$

$Re$  – Reynolds number,  $Re = \frac{Wd}{\nu}$  ;

$W$  – average coolant velocity;

$Pr$ ,  $\nu$ ,  $\lambda$  - thermophysical properties of the heat carrier (Prantl's number, kinematic viscosity, thermal conductivity), determined by the average flow temperature;

$d$ ,  $L$  - internal diameter and length of the pipe from the flow inlet;

$\varepsilon_l$  - is the correction for the initial section, at  $\frac{L}{d} \geq 50$   $\varepsilon_l = 1$ , otherwise it is determined according to tables and nomograms [16];

$\varepsilon_t$  - temperature correction  $\varepsilon_t = \left( \frac{\text{Pr}}{\text{Pr}_{\text{CT}}} \right)^{0,06}$  for heating and  $\varepsilon_t = \left( \frac{\text{Pr}}{\text{Pr}_{\text{CT}}} \right)^{0,25}$  for cooling;

where  $\text{Pr}_{\text{CT}}$  is the Prandtl number determined by the wall temperature.

When the medium moves inside curved smooth circular pipes (spiral coils), the heat transfer coefficient is determined as follows:

$$\alpha_3 = \alpha \cdot \varepsilon_3 \quad (2.57)$$

where  $\alpha$  - is for straight pipes;

$\varepsilon_3$  - correction for curvature,  $\varepsilon_3 = 1 + 1,77 \cdot \frac{d}{R}$  [1, 2, 4, 21] or  $\varepsilon_3 = 1 + 11,11d \frac{n_B n_{\text{III}}}{l_P}$  [2];

where  $R$  is the average radius of curvature of the coil,  $R = \frac{l_P}{2\pi n_B n_{\text{III}}}$ ;

$n$  - number of turns in one plane of the coil;

$n_{\text{III}}$  - number of planes in one coil;

$l_P$  is the working length of the spiral coil (formulas (4.8) or (4.9).

When a fluid moves in rough circular pipes, the heat transfer coefficient is calculated taking into account the roughness [1, 2]:

$$\alpha_{\text{III}} = \alpha \varepsilon_{\text{III}}, \quad (2.58)$$

where  $\alpha$  is taken for straight or curved smooth pipes;

$\varepsilon_{\text{III}}$  - correction for roughness,  $\varepsilon_{\text{III}} = \left( \frac{\xi_{\text{II}}}{\xi_{\text{III}}} \right)^{0,5}$  ;

where  $\xi_{\text{II}}$  and  $\xi_{\text{III}}$  are the hydraulic resistances for smooth and rough pipes, the definition of which is described in clause 2.5.

In real high-pressure regenerative feed water heaters and low pressure regenerative feed water heaters, the flow in the tubes or coils is clearly turbulent (determined by flow rates and velocities) and the length of the tubes or coils is much longer than the initial section. In addition, there is no initial section as such due to the high turbulence of the flow at the inlet. Therefore, formulas (2.55)-(2.57) with a temperature correction  $\varepsilon_t$  can be used for high-pressure regenerative feed water heaters and low pressure regenerative feed water heaters. The effect of the surface condition on heat transfer in real heat exchanger operating conditions is given below.

Bundles of pipes with a staggered row arrangement are used in low pressure regenerative feed water heaters. The less efficient corridor arrangement is not used here. In the case of the high-pressure regenerative feed water heaters, the two-plane spiral coils are wound in such a way that a staggered arrangement of turns in different planes of the coils is obtained. In the case of single-plane spiral coils, their ends are welded to the collectors in a staggered manner, which preserves the possibility of replacing the coils without removing the neighbouring ones [1] and ensures a staggered arrangement of turns in separate planes. After the modernisation, only transverse flow of steam or condensate through the spiral coils is provided in the design of the high-pressure regenerative feed water heaters.

The heat transfer coefficients for the cross-flow of staggered tube bundles are as follows [16]:

$$\text{with } \text{Re} \leq 6 \cdot 10^4 \quad \alpha = C \frac{\lambda}{d} \text{Re}^m \text{Pr}^{0,35}, \quad (2.59)$$

where the values of C, m are given in Table 2.3.

Table 2.3 - numbers  $C$  and  $m$  depending on  $Re$

Re		$C$	$m$
from	to		
0,1	4	0,99	0,305
4	50	0,86	0,41
50	$1 \cdot 10^3$	0,59	0,487
$1 \cdot 10^3$	$5 \cdot 10^3$	0,665	0,47
$5 \cdot 10^3$	$5 \cdot 10^4$	0,22	0,6
$5 \cdot 10^4$	$6 \cdot 10^4$	0,026	0,8

$$\text{with } Re > 6 \cdot 10^4 \quad \alpha = 0,334 \frac{\lambda}{d} Re^{0,6} Pr^{0,35} \varepsilon_Z \varepsilon_S, \quad (2.60)$$

where  $Re$  is the Reynolds number,  $Re = \frac{Wd}{\nu}$ ;

$W$ - is the coolant velocity in a narrow cross-section of the bundle;

$Pr$ ,  $\nu$ ,  $\lambda$  - thermophysical properties of the heat carrier (Prandtl number, kinematic viscosity, thermal conductivity) determined by the average flow temperature;

$d$  - outer diameter of one tube;

$\varepsilon_Z$  - correction for the initial section (number of rows or steps  $z$ ), at  $z \geq 30$   $\varepsilon_Z = 1$ , otherwise determined by tables and nomograms [16];

$$\varepsilon_S - \text{correction for steps, } \frac{S_1 - d}{S - d} \geq 0,7 \quad \varepsilon_S = 1 \quad \text{at } \frac{S_1 - d}{S - d} < 0,7 \quad \varepsilon_S = \left( \frac{S_1 - d}{S - d} \right)^{0,25};$$

$S$  - is the diagonal spacing of the partition  $S = \sqrt{0,25S_1^2 + S_2^2}$ , in the case of the triangular partition  $S = S_1$ ;

$S_1, S_2$  - pitches of pipe rows on the pipe board in the transverse and longitudinal directions, with transverse flow of spiral  $S_1 = \frac{S_K}{n_{III}}$  coils;  $S_2 = S_B$

$S_K$  - average installation pitch on collectors in the zones (condensate cooling or steam cooling);

$S_B$  - spiral coil winding pitch.

$n_{III}$  - the number of planes in one coil (single-plane or two-plane).

In some tubing designs, longitudinal washing of pipe bundles can be arranged (in integrated or separate condensate coolers). Such washing of the outermost pipes in the bundle is mainly performed when the condensate flow passes from one pass to another [4, 15, 21]:

- for the laminar flow regime ( $Re \leq 2000$ ):

$$\alpha = 0,15 Re^{0,33} Pr^{0,43} Gr^{0,1} \varepsilon_t \varepsilon_l; \quad (2.61)$$

- for the transient flow regime ( $2000 < Re \leq 8000$ ):

$$\alpha = K_0 Pr^{0,43} \varepsilon_t; \quad (2.62)$$

- for the turbulent flow regime ( $Re > 8000$ ):

$$\alpha = \alpha_0 \varepsilon_{III}; \quad (2.63)$$

where  $Re$  is the Reynolds  $Re = \frac{W \cdot d_E}{\nu}$  number,

$Gr$  - Grasgoff  $Gr = \frac{g \beta (t_{cr} - t) d_E^3}{\nu^2}$  number,

$W$  - is the average velocity of the coolant;

$g$  - is the acceleration of free fall;

$r, \nu, \lambda, \beta$  – thermophysical properties of the heat carrier (Prantl's number, kinematic viscosity, thermal conductivity, isothermal compressibility coefficient) determined by the average flow temperature;

$t_{CT}$  – average wall temperature;

$d_E$  – equivalent thermal diameter, for bundles with a triangular breakdown (staggered bundles) in the zone of the control of the tubing, and in the general case  $d_E = \frac{4f}{\Pi}$  [1, 2];

$d$  – is the outer diameter of one pipe;

$S$  – is the diagonal spacing of the triangular division;

$f$  – flow area (live section);

$W(\Pi)$  – wetted perimeter;

$\varepsilon_t$  – temperature correction, which is determined as for the flow inside smooth pipes (formulas (2.55) and (2.56));

$\varepsilon_l$  – is the correction for the initial section, at  $\frac{L}{d_3} \geq 50$   $\varepsilon_l = 1$ , where  $L$  is the length of the pipe from the inlet, in  $\frac{L}{d_3} < 50$  laminar flow is determined according to Table 2.4 [4, 21]:

Table 2.4 - Correction for the initial section for laminar flow

$L/d_E$	1	2	5	10	15	20	30	40	50
$\varepsilon_l$	1,9	1,7	1,44	1,28	1,18	1,13	1,05	1,02	1

$K_0$  – is a dimensionless complex for the transient flow regime, which is determined according to Table 2.5 [4, 21]:

$\alpha_0$  - is calculated by formulas (2.55) or (2.56) for the flow inside smooth pipes, but with an equivalent diameter  $d_E$ ;

$\varepsilon_{IPP}$  - corrections in the longitudinal flow of pipe bundles for the turbulent flow regime [1],  $\varepsilon_{IPP} = 1 + 0,91 \text{Re}^{-0,1} (1 - 2e^{-\frac{d_2}{d}})$ .

Table 2.5 - dimensionless complex for the transient flow regime

$\text{Re} \cdot 10^{-3}$	2,2	2,3	2,5	3	3,5	4	5	6	7	8
$K_0$	2,2	3,6	4,9	7,5	10	12,2	16,5	20	24	27

As can be seen from the above formulas, some of the coefficients included in them are given in tabular form. Calculations using tables on a computer are difficult. Therefore, the dependencies for  $\varepsilon_l$  i  $K_0$  were interpolated using the least squares method [22, 23]:

$$\varepsilon_l = \sum_{i=1}^5 a_i \left( \frac{L}{d_E} \right)^i, \quad (2.64)$$

$$K_0 = 10^3 \cdot \sum_{i=1}^4 b_i \left( \frac{\text{Re}}{1000} \right)^i \quad 2200 \leq \text{Re} \leq 3500, \quad (2.65)$$

$$K_0 = \sum_{i=1}^2 c_i \left( \frac{\text{Re}}{1000} \right)^i \quad 3500 \leq \text{Re} \leq 8000. \quad (2.66)$$

where  $a_i$ ,  $b_i$  i  $c_i$  are the coefficients of the polynomials given in Table 2.6.

In the case of steam or condensate entering a bundle of smooth pipes with an angle  $\varphi < 90^\circ$  the determination of the heat transfer coefficient with an error of 4% will be as follows [2]:



Table 2.6 - Polynomial coefficients

$i$	$a_i$	$b_i$	$c_i$
0	2,0300504	-1,3283445	-7,5261221
1	$-1,74698297 \cdot 10^{-1}$	1,90784023	5,5443615
2	$1,45988302 \cdot 10^{-2}$	-1,02064144	-1,52679851
3	$-6,0206858 \cdot 10^{-4}$	$2,41442158 \cdot 10^{-1}$	
4	$1,15830753 \cdot 10^{-5}$	$-2,12449557 \cdot 10^{-2}$	
5	$-8,29717478 \cdot 10^{-8}$		

The interpolation error of these formulas is slightly more than 2%.

$$\alpha = \alpha_{\Pi O \Pi} \varepsilon_{\varphi}, \quad (2.67)$$

where  $\alpha_{\Pi O \Pi}$  - is the heat transfer coefficient for the cross-flow ( $\varphi = 90^\circ$ ), which is calculated by formulas (2.59), (2.60);

$\varepsilon_{\varphi}$  - Correction for the angle of attack of the flow,  
 $\varepsilon_{\varphi} = 0,25 \sin(2\varphi - 70) + 0,75$ .

If  $60^\circ < \varphi < 90^\circ$  the nature of the washout is transverse, and if  $0^\circ < \varphi < 10^\circ$ , it is longitudinal. Then, instead of  $\alpha_{\Pi O \Pi}$ , it is necessary to take the heat transfer coefficient for the longitudinal flow (formulas (2.61) - (2.66) and  $\varepsilon_{\varphi} = 1$ ;

In the case when one part of the pipe bundle is washed longitudinally and the other part is washed transversely, the heat transfer coefficient is calculated as follows [2]:

$$\alpha = \alpha_{\Pi O \Pi} \frac{F_{\Pi O \Pi}}{F} + \alpha_{\Pi \Pi} \frac{F_{\Pi \Pi}}{F} \quad \text{or} \quad \alpha = \alpha_{\Pi O \Pi} \frac{N_{\Pi O \Pi}}{N} + \alpha_{\Pi \Pi} \frac{N_{\Pi \Pi}}{N}, \quad (2.68)$$

where  $\alpha_{\Pi O \Pi}$  та  $\alpha_{\Pi \Pi}$  - are the heat transfer coefficients for the transverse (formulas (2.59), (2.60) and longitudinal flow (formulas (2.61)-(2.66));

$F_{\Pi O \Pi}$ ,  $F_{\Pi P}$  and  $F$  - are the areas of heat transfer surfaces of transverse, longitudinal wash and total in the zone;

$N_{\Pi O \Pi}$ ,  $N_{\Pi P}$  and  $N$  - are the number of tubes of transverse, longitudinal washing and total in the zone.

$\frac{F_{\Pi O \Pi}}{F}$  or  $\frac{N_{\Pi O \Pi}}{N} > 85\%$ ., the entire tube bundle is considered to be cross-washed.

In the old designs of the condensate coolers and LW zones of the HCF, mixed steam and condensate washing of the spiral coils was used before the modernisation. With this flow pattern, steam or condensate entered a group of spiral coils through horizontal holes in the casing, then washed the coils parallel to their plane and exited to the next group through the same hole in the other side of the casing. Thus, steam or condensate washed several groups of spiral coils in succession. This movement of steam and condensate is accompanied by large hydraulic losses and is inefficient in terms of heat transfer [1]. The heat transfer coefficient for this case is as follows [1]:

$$\alpha = 0,0165 \cdot \frac{\lambda}{d_E} \cdot Re^{0,8} \cdot Pr^{0,4}, \quad (2.69)$$

where  $Re$  - is the Reynolds  $Re = \frac{W \cdot d_E}{\nu}$  number, ;

$Pr$ ,  $\nu$ ,  $\lambda$  - are the thermophysical properties of the heat carrier (Prandtl number, kinematic viscosity, thermal conductivity) determined by the average flow temperature;

$d_E$  - is the equivalent thermal  $d_E = \frac{4f}{\Pi}$  diameter, ;

$f$  - flow area (live section);

$W (\Pi)$  - wetted perimeter.

In the spiral-collector type heat exchanger control zones, film condensation of steam occurs on horizontal pipes (spiral coil planes), and in the high-pressure regenerative feed water heaters control zones - between condensate separators

(vertical sections of U or U-shaped pipes) and on bends (horizontal sections). The heat transfer coefficient of such a process is determined by the dependencies given in [1, 2, 4, 8, 13-20].

For film condensation of pure steam in vertical sections of pipes and laminar flow of the condensate film, the average heat transfer coefficients are determined from theoretical studies by Nusselt. According to this theory [14-20], the local heat transfer coefficients are as follows:

$$\alpha_x = \frac{\lambda_K}{\delta} = \left( \frac{\lambda_K^3 r g \rho_K (\rho_K - \rho'')}{4 \mu_K \Delta t_{\Pi-CT_{0-x}} x} \right)^{\frac{1}{4}} \quad (2.70)$$

$$\alpha_x = \frac{\lambda_K}{\delta} = \left( \frac{\lambda_K^3 r g \rho_K (\rho_K - \rho'')}{3 \mu_K q_{0-x} x} \right)^{\frac{1}{3}}, \quad (2.71)$$

where  $x$  - is the coordinate along the length of the pipe;

$\delta$  - is the local thickness of the condensate film;

$g$  - is the acceleration of free fall;

$\rho_i r$  - is the vapour density at the film surface and the latent heat of vapour formation, determined by the saturation temperature  $t_s$ ;

$\lambda_K, \rho_K, \mu_K$  - thermal conductivity, density and dynamic viscosity of the condensate film, which are calculated at its average temperature  $t_K$ ;

$\Delta t_{\Pi-CT_{0-x}}$  and  $q_{0-x}$  - are the average private temperature head 'vapour-wall',  $\Delta t_{\Pi-CT} = t_s - t_{CT}$ , and the heat flux density from the beginning of the section (0) to the coordinate  $x$ .

the indices 'Π' and 'CT' refer to the interface and the wall, respectively.

Assuming that the distribution of the condensate temperature across the film thickness is linear from the wall temperature  $t_{CT,x}$  до  $t_s$ , the solution of the Nusselt

equation gives a parabolic distribution of velocities in the film along the thickness [15]. The thickness-averaged value of the condensate film temperature (both local and average along the length), which is used to calculate its properties, in this case is Eq:

$$t_K = t_S - \frac{3}{8}(t_S - t_{CT}) \quad (2.72)$$

The value of the average condensate temperature can be used to calculate the temperature and enthalpy of the condensate at the outlet of the area or zone under consideration.

Given a known distribution of local heat flux densities  $q_x$  or temperature head  $\Delta t_{\Pi-CT,x}$  and heat transfer coefficient  $\alpha_x$  along the length, the heat transfer coefficient is usually averaged using two methods [14]:

$$\bar{\alpha} = \frac{\int_0^L q_x dx}{\int_0^L \frac{q_x}{\alpha_x} dx} \quad (2.73)$$

$$\bar{\alpha} = \frac{1}{L} \int_0^L \alpha_x dx \quad (2.74)$$

It should be noted that the method of averaging according to formula (2.73) is preferable [14], and dependence (2.74) is a special case of averaging when  $\Delta t_{\Pi-CT,x} = \text{const}$  (for this case, formulas (2.73) and (2.74) give similar results). Assuming  $\Delta t_{\Pi-CT,x} = \text{const}$  in formula (2.70) and  $q_x = \text{const}$  in formula (2.71) along the length of the vertical pipe section L under consideration, taking into account the mediation according to (2.73) or (2.74), the dependencies given in the literature [2, 4, 8, 1320 -] are obtained. As a result of the mediation according to formula (2.73), it turns out that at  $\Delta t_{\Pi-CT,x} = \text{const}$  and  $q_x = \text{const}$ , the same results are obtained [14, 24], and according to (2.74), for  $q_x = \text{const}$ , values are obtained that are 13% higher than at

$\Delta t_{\Pi-CT,x} = \text{const}$  [15]. Average heat transfer coefficient from the condensate film to the wall with corrections:

$$\alpha = C \cdot B \cdot \text{Re}_K^{-\frac{1}{3}} (\varepsilon_v \varepsilon_t)^{\frac{4}{3}} \text{ or } \alpha = C_1 \cdot A \cdot (L \Delta t_{\Pi-CT})^{-\frac{1}{4}} \varepsilon_v \varepsilon_t, \quad (2.75)$$

where the coefficients  $C = 0.925$ ,  $C_1 = 0.943$ , regardless of whether  $\Delta t_{\Pi-CT,x} = \text{const}$  or  $q_x = \text{const}$ ;

$\Delta t_{\Pi-CT}$  - is the average temperature head of the vapour-wall in the section,  $\Delta t_{\Pi-CT} = t_s - t_{CT}$ ;

$q$  - is the average heat flux density through the pipe walls in the area;

$\text{Re}_K$  - is the Reynolds number of the condensate film,

$$\text{Re}_K = \frac{qL}{r\mu_K} \quad \text{or} \quad \text{Re}_K = \frac{G_K}{\pi d \mu_K};$$

$G_K$  - is the mass flow rate of condensate condensed in the pipe section;

$L$  - is the distance between the condensate baffles;

$d$  - outer diameter of the pipe;

$\text{Re}_{KP}$  - is the critical Reynolds number of the condensate film during the transition to the turbulent regime of its flow;

$\varepsilon_v$  - is a correction for the wave nature of the film flow, where surface tension forces are taken into account; at  $\text{Re}_K < 4$ , the film flow is only laminar and  $\varepsilon_v = 1$ , otherwise it is laminar-wave and  $\varepsilon_v = \text{Re}_K^{0,04}$ ;

$$\varepsilon_t \text{ - is the temperature correction, } \varepsilon_t = \left( \left( \frac{\lambda_{CT}}{\lambda'} \right)^3 \frac{\mu'}{\mu_{CT}'} \right)^{\frac{1}{8}};$$

$$A \text{ is the parameter, } A = \sqrt[4]{\frac{\lambda_K^3 r g \rho_K (\rho_K - \rho'')}{\mu_K}};$$

$Nu$  - Nusselt number,  $Nu = \frac{\alpha L}{\lambda_K}$ ;

$B$  - Parameter,  $B = Ar^{\frac{1}{3}} \frac{\lambda_K}{L} = \lambda_K \nu_K^{-\frac{2}{3}} \left( g \left( 1 - \frac{\rho''}{\rho_K} \right) \right)^{\frac{1}{3}}$ ;

$Ar$  - Archimedes number,  $Ar = \frac{gL^3 \left( 1 - \frac{\rho''}{\rho_K} \right)}{\nu_K^2}$ ;

$\lambda_{CT}$ ,  $\mu_{CT}$  - thermal conductivity and dynamic viscosity of the condensate film near the pipe wall, determined by the temperature of the outer wall  $t_{CT}$ ;

$\lambda'$ ,  $\mu'$  - thermal conductivity and dynamic viscosity on the surface of the condensate film, determined by the saturation temperature  $t_s$ ;

$\nu_K$ ,  $\mu_K$  - kinematic and dynamic viscosity of the condensate film;

Some authors [2, 4, 15, 16] present formula (2.75) in a form that already takes into account the correction for the wave character of the film. In this case,  $\varepsilon_v=1,2$  is assumed. In this case, the coefficient  $C_1=0,943$  is replaced  $C_1=1,13$ , and the correction  $v$  should be taken into account.

In the case of mixed laminar, laminar-wave and turbulent flow of the condensate film, the heat transfer coefficient is calculated by the specific gravity of the laminar-wave and turbulent regimes at the length  $L$  [15] ( $Re_K \geq Re_{KP}$ ):

$$\bar{\alpha} = \alpha_{\text{л}} \frac{x_{KP}}{L} + \alpha_{\text{т}} \left( 1 - \frac{x_{KP}}{L} \right), \quad (2.76)$$

where  $\alpha_{\text{т}}$  is the heat transfer coefficient in the turbulent section;

$\alpha_{\text{л}}$  - heat transfer coefficient in the laminar (laminar-wave) section;

$x_{KP}$  - is the distance from the point of condensation onset to the point where  $Re_K = Re_{KP}$ .

Taking into account that ,  $\frac{x_{KP}}{L} = \frac{Re_{KP} Pr(k + \varphi)}{Nu_{\text{л}}}$ ,  $Nu_{\text{л}} \cdot Ar^{-\frac{1}{3}} = C \cdot Re_{KP}^{-\frac{1}{3}} (\varepsilon_v \varepsilon_t)^{\frac{4}{3}}$ , or  $Pr(k + \varphi) = \frac{Nu}{Re_K}$ , is a set of similarity criteria and , the expression for the average heat transfer coefficient is obtained in a generalised form:

$$\alpha = \frac{\alpha_T Re_K}{Re_K - Re_{KP} + \frac{\alpha_T}{\alpha_{\text{л}}} Re_{KP}}. \quad (2.77)$$

Thus, the average heat transfer coefficient along the entire length significantly depends on the choice of the value of the critical Reynolds number  $Re_{KP}$  of the transition of the flow film regime to the turbulent one. When water vapour condenses on a vertical surface, it is recommended to take  $Re_{KP}$  equal to 100 [1, 2, 16]. Taking into account the expression of the heat transfer coefficient for turbulent flow, after some transformations, the final dependence is obtained:

$$\alpha = B \frac{0,16 Pr_K^{0,33} Re_K}{Re_K - 100 + 80,287 (\varepsilon_v \varepsilon_t)^{-\frac{4}{3}} Pr_K^{0,33}}, \quad (2.78)$$

where the coefficients  $\varepsilon_v$  та  $\varepsilon_t$  correspond to formula (2.75).

It should be noted that the value of the complex given in references [2, 4, 16]  $80,287 (\varepsilon_v \varepsilon_t)^{-\frac{4}{3}} = 63$  corresponds to  $\varepsilon_v = 1,2$  without temperature correction.

The average heat transfer coefficient, taking into account the velocity of the incoming steam flow, is multiplied by the correction  $\varepsilon_w$ . In the case of laminar (laminar-wave) flow of a condensate film

( $Re_K < Re_{KP}$ ), the correction for the velocity  $\varepsilon_w$  is determined by the dependence shown in Fig. 2.2 [8]:

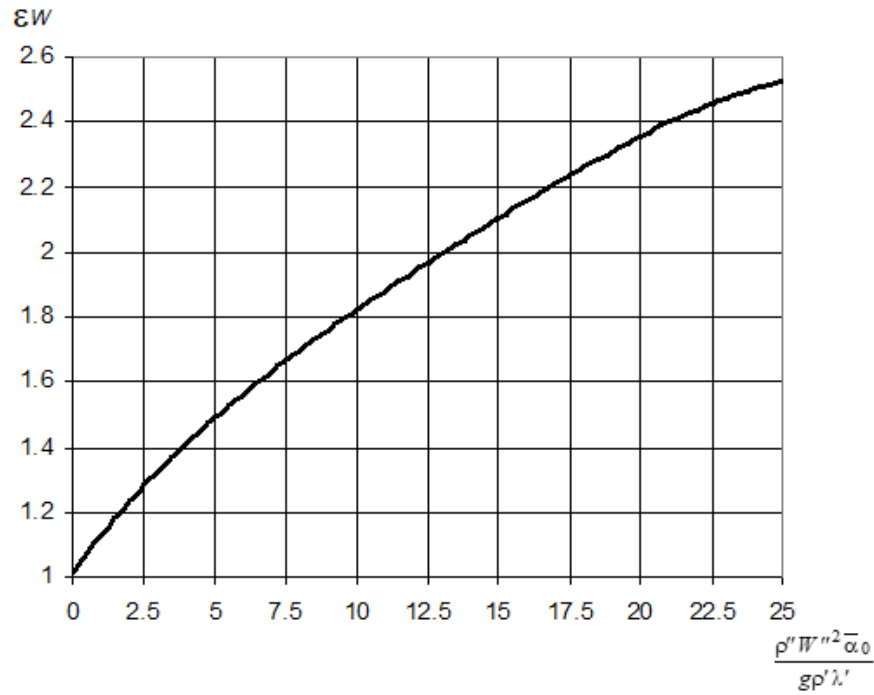


Fig. 2.2 - Correction to the heat transfer coefficient for the velocity of steam flow at laminar flow of a condensate film

To make it possible to calculate on a computer, this dependence was interpolated by the least squares method [22, 23] with an error of no more than 1%, which has the form of a polynomial:

$$\varepsilon_W = 1 + 1,1929964 \cdot 10^{-1} z - 6,104004525 \cdot 10^{-3} z^2 + 2,739704104 \cdot 10^{-4} z^3 - 2,739704104 \cdot 10^{-6} z^4 \quad (2.79)$$

where  $z$  - is the parameter,  $z = \frac{\rho'' W''^2 \bar{\alpha}_0}{100 g \rho' \lambda'}$ ,

$\bar{\alpha}_0$  - It is calculated by formulas (2.75) - (2.78).

When  $Re_K \geq Re_{KP}$  corrected for the steam speed, it will have the form [2, 4, 8, 16]:

$$\varepsilon_W = 1 + 0,013 \left( \frac{\rho''}{\rho_K} \right)^{\frac{1}{2}} \frac{W''}{(g v_K)^{\frac{1}{3}}} \quad (2.80)$$



The defining vapour velocity in formulas (2.79) and (2.80)  $W'$  is the geometric mean:

$$W' = \sqrt{\frac{W_1'^2 + W_1'' W_2'' + W_2'^2}{3}}, \quad (2.81)$$

where  $W_1''$  i  $W_2''$  are the velocities of steam at the inlet and outlet of the condensation zone, if the steam is completely condensed, then  $W_2'' = 0$ .

The heat transfer coefficient for film condensation of practically slow-moving steam on a single horizontal pipe is also determined in accordance with the Nusselt theory. Here, the assumptions are made that the film flow is laminar, condensate flows from the lower forming pipe, the temperature head  $\Delta t_{\Pi-CT}$  is the same along the length of the pipe and the circumference of the cylinder base, and the film thickness on the upper forming pipe is finite (non-zero).

After integration along the circumference of the cylinder base, the heat transfer coefficient of such a process is determined by the Nusselt equation, taking into account the corrections [2, 4, 8, 13 -20]:

$$\alpha_0 = C \cdot B \cdot \text{Re}_{K_0}^{-\frac{1}{3}} \varepsilon_t^{\frac{4}{3}} \quad \alpha_0 = C_1 A (d \Delta t_{\Pi-CT})^{-\frac{1}{4}} \varepsilon_t, \quad (2.82)$$

where at  $\Delta t_{\Pi-CT} = \text{const}$   $C = 0,954$  i  $C_1 = 0,725$ ;

$\text{Re}_{K_0}$  - the average Reynolds number of the condensate film on the upper pipe, calculated along the entire circumference of the cylinder base, or  $\text{Re}_{K_0} = \frac{q\pi d}{r\mu_K}$  or

$$\text{Re}_{K_0} = \frac{G_K}{L\mu_K};$$

$G_K$  - is the mass flow rate of condensate condensed on the pipe;

$L$  - is the length of the pipe;

$d$  - outer diameter of the pipe;

$\varepsilon_t, A, B$  - coefficients given in formula (2.75);

On pipes of small diameter, the wave motion of the film does not have time to form, so the correction  $\varepsilon_{mym}$  is not taken into account.

Nusselt's equation is valid for film condensation of practically slow-moving steam and laminar (laminar-wave) film flow (i.e.  $\rho'' W''^2 < 30$  i  $Re_K \leq 50$ ) for the upper row of a bundle of horizontal pipes or the upper plane of a spiral coil block, where  $W'$  - is the steam velocity at the inlet to the tube bundle or spiral block (in the top row);

$Re_K$  - is the average calculated Reynolds number of the condensate film in the pipe bundle:

$$Re_K = 0,785 \frac{qd}{r \mu_K} + \frac{G_{HK}}{2 \mu_K}, \quad (2.83)$$

where  $G_{HK}$  is the amount of condensate flowing per unit length of pipe from the upstream pipes.

The average heat transfer coefficient for the entire pipe bundle or spiral block enclosed between condensate baffles [2] is as follows:

$$\alpha = \varepsilon_{TP} \alpha_0 \left( \frac{1}{n} \right)^{\frac{1}{4}} \quad (2.84)$$

$\varepsilon_{TP}$  - correction for the appearance of pipes,  $\varepsilon_{TP} = 1$  for straight pipes,  $\varepsilon_{TP} = 0,9$  for spiral coils [2];

$n$  - is the number of pipes vertically,  $n = n_P$  for a corridor bundle,  $n = 0,5 n_P$  for a staggered bundle,  $n = \frac{n_P}{1,5}$  for spiral coils;

$n_p$  - the number of rows of pipes or planes of spirals located vertically between two condensate drainage partitions or in the bends of U- or  $\Pi$ -shaped pipes.

Almost all domestic heaters are designed in such a way that the condensate film flow in them is assumed to be laminar or laminar-wave. Existing theoretical studies for heat transfer during condensation of a slowly moving clean steam in the area of laminar and laminar-wave film flow on a clean smooth surface, based on Nusselt's theory, are in good agreement with experimental data [1].

The formulas are derived in an integral form for two cases of boundary conditions  $\Delta t_{\Pi-CT} = \text{const}$  or  $q = \text{const}$  along the length of the pipe section under consideration. In the process of steam condensation on the outer surface of pipes, where a heated coolant flows inside, in general, these parameters are not constant along the length of the pipe axis. The method of mediating the heat transfer coefficient according to formulas (2.73) or (2.74) does not cover the entire heat transfer equation. In this case, it is necessary to take into account the distribution of all local private temperature heads along the length, and thus the condensation heat transfer coefficient (which includes the private temperature head), heat transfer coefficient and heat flux density. Thus, the average condensation heat transfer coefficient can only be calculated correctly after the entire local heat transfer equation has been integrated over the length (i.e. concentrated). If the average temperature pressure is assumed to be logarithmic, the average condensation heat transfer coefficient can then be expressed from the integral heat transfer coefficient formula (2.54). However, it is possible not to average the condensation heat transfer coefficient, but to conditionally calculate it according to the known relationships (2.75) or (2.82) (i.e., to set  $\Delta t_{\Pi-CT} = \text{const}$  along the length). After integrating the entire local heat transfer equation, taking into account the distribution of private temperature heads along the length, the average temperature head is determined from it, which in this case will no longer be logarithmic. In this case, the conditional average heat transfer coefficient is calculated according to (2.54).

In the studied heat exchangers, the heating steam usually contains dissolved non-condensable gases (air components), the surface of the pipes can be rough and in operation is covered with a significant layer of corrosion and deposits, which significantly affects the heat transfer rate, especially during condensation.

The heat transfer coefficient in the presence of non-condensable gases [13, 14] is conditionally determined by the Newton-Richman formula:

$$\alpha = \frac{q}{t_s - t_{CT}}, \quad (2.85)$$

where  $t_s$  is the saturation temperature at the partial pressure of steam in the mixture  $p_{\Pi}$ , Pa; according to Dalton's law,  $p_{\Pi} = p_{CM} - p_B$ ;

$p_{CM}$  and  $p_B$  are the pressures of the mixture and the partial pressure of air in it, Pa.

The magnitude of the heat load transferred from the vapour-air mixture to the film and the film to the wall must satisfy two equations [13, 14]:

$$q = (r + \Delta i)\beta_P(p_{\Pi} - p_{\Pi GP}); \quad (2.86)$$

$$q = \alpha_{\Pi W}(t_{GP} - t_{CT}), \quad (2.87)$$

where  $\Delta i$  - is the value of steam overheating,  $\Delta i = i_{\Pi} - i''$ , J/kg;

heat of vapour formation  $r$  and  $i''$  are determined by  $p_{\Pi}$ ;

$\beta_P$  - is the mass transfer coefficient, kg/(m<sup>2</sup>·Pa) or s/m;

$p_{\Pi GP}$  and  $t_{GP}$  are the saturation pressure, Pa, and the vapour temperature on the film surface, taking into account its decrease, determined by the method of successive approximations;

$\alpha_{\Pi W}$  - is the heat transfer coefficient from the film to the wall, determined for pure steam at its partial pressure, W/(m<sup>2</sup>·K).

For a steam-air mixture, the partial pressure of steam is:

$$p_{\Pi} = \frac{p_{CM}}{1 + 0,622\varepsilon_M}, \quad (2.88)$$

where  $\varepsilon_M$  is the mass content of air relative to steam,  $\varepsilon_M = \frac{G_B}{G_{\Pi}}$ ;

$G_B$  та  $G_{\Pi}$  are the air and steam flow rates.

The mass transfer coefficient  $\beta_p$  related to the partial pressure gradient is determined by analogy with the heat transfer coefficient:

$$\beta_p = \frac{Nu_D D_p}{d}, \quad (2.89)$$

where  $d$  - is the outer diameter of the pipe;

$D_p$  - is the diffusion coefficient for steam, referred to the partial pressure gradient, (kg/m · Pa) or from:

$$D_p = \frac{D_{1-2} M}{RT_{CM}}, \quad (2.90)$$

where  $M$  - is the molecular weight of the vapour,  $M = 18$  kg/kmol;

$R$  - is the universal gas constant,  $R = 8314$  J/(kmol · K);

$T_{CM}$  - is the temperature of the mixture, K;

$D_{1-2}$  - is the coefficient of mutual diffusion, m<sup>2</sup>/s:

$$D_{1-2} = D_0 \frac{3,648 \cdot 10^4}{p_{CM}} \left( \frac{T_{CM}}{273} \right)^n, \quad (2.91)$$

where  $D_0$  is the coefficient of mutual diffusion m<sup>2</sup>/c at  $p_{CM} = 760$  mm Hg. Art. and  $T_{CM} = 273$ ;

in the temperature range of 273 ÷ 677,5 For a vapour-air mixture,  $D_0 = 2,106 \cdot 10^{-5}$  m<sup>2</sup>/s,  $n = 1,82$  [13]; here  $p_{CM}$  is substituted for Pa.

$Nu_D$  - is the Nusselt diffusion number taking into account the effect of the transverse mass flow [13]:

$$Nu_D = Nu_{D1} \left( \frac{Nu_D}{Nu_{D1}} \right), \quad (2.92)$$

where  $Nu_{D1}$  - is the Nusselt diffusion number without taking into account the influence of the transverse mass flow. Analogy with the Nusselt number for pipe flow by replacing the Prandtl number with the diffusion number [13, 14]:

$$Nu_{D1} = f(Re_{CM}, Pr_D)_{end} \quad Pr_D = \frac{v_{CM}}{D_{1-2}}, \quad (2.93)$$

where  $v_{CM}$  - is the kinematic viscosity of the mixture,;

$$v_{CM} = \frac{\mu_{CM}}{\rho_{CM}}$$

where  $\mu_{CM}$  - is the dynamic viscosity of the vapour-air mixture:

$$\mu_{CM} = \frac{(1 - \varepsilon_V) \mu_{II} + 1,61 \varepsilon_V \mu_B}{1 + 0,61 \varepsilon_V}, \quad (2.94)$$

where  $\varepsilon_V$  is the volume content of air in the mixture:

$$\varepsilon_V = \frac{1}{1 + \frac{1,61}{\varepsilon_M}}, \quad (2.95)$$

$\rho_{CM}$  is the density of the mixture,  $\rho_{CM} = \rho_{II} + \rho_B$ ;

$\rho_{II}$ ,  $\rho_B$ ,  $\mu_{II}$  i  $\mu_B$  are the densities and dynamic viscosities of steam and air calculated from the partial pressure  $p_{II}$ ,  $p$  and the temperature of the mixture  $T_{CM}$ ;

$Re_{CM}$  -is the Reynolds number of the vapour-air mixture:

$$Re_{CM} = \frac{W_{CM} d}{v_{CM}}, \quad (2.96)$$

where  $W_{CM}$  is the average velocity of the vapour-air mixture:

$$W_{CM} = G_{CM} \rho_{CM} f, \quad (2.97)$$

where  $G_{CM}$  - the mass flow rate of the mixture,  $G_{CM} = G_{\Pi} + G_B$ ;

$f$  - is the flow area in the narrow section of the pipe bundle.

The correction factor  $\frac{Nu_D}{Nu_{D1}}$  is equal to [13]:

- for the turbulent mode of the steam-air mixture flow  $Re_{CM} \geq 1000$ :

$$\frac{Nu_D}{Nu_{D1}} = 0,619 \varepsilon_V^{-0,6} \Pi_D^{-0,4} \quad \text{at} \quad 0,1 < \frac{\varepsilon_V}{\Pi_D} < 2,3; \quad (2.98)$$

$$\frac{Nu_D}{Nu_{D1}} = 0,744 \varepsilon_V^{-0,84} \Pi_D^{-0,16} \quad \text{at} \quad 2,3 < \frac{\varepsilon_V}{\Pi_D} < 10, \quad (2.99)$$

- for the laminar regime of the vapour-air mixture flow  $Re_{CM} < 1000$ :

$$\frac{Nu_D}{Nu_{D1}} = 0,782 \varepsilon_V^{-0,7} \Pi_D^{-0,3} \quad \text{at} \quad 0,1 < \frac{\varepsilon_V}{\Pi_D} < 1; \quad (2.100)$$

$$\frac{Nu_D}{Nu_{D1}} = 0,782 \varepsilon_V^{-0,9} \Pi_D^{-0,1} \quad \text{at} \quad 1 < \frac{\varepsilon_V}{\Pi_D} < 10, \quad (2.101)$$

where  $\Pi_D$  - is a dimensionless parameter,  $\Pi_D = \frac{p_{\Pi} - p_{\Pi GP}}{p_{CM}}$ .

Since the parameters of the interface  $t_{GP}$  и  $p_{GP}$  are not known in advance, they are usually calculated by the method of successive approximations. In the process of iterations, the heat load  $q$  from the vapour-air mixture to the film and from the film to the wall is determined (formulas (2.86) and (2.87), and their imbalance is considered. This imbalance should eventually be equal to zero. To speed up the convergence of iterations, it is advisable to use the chord method [22, 23].

The correction factor for the heat transfer coefficient during condensation of steam from the vapour-air mixture will be considered as follows:

$$\alpha = \alpha_{\text{III}} \varepsilon_B$$

and

$$\varepsilon_B = \frac{t_{\text{ГП}} - t_{\text{СТ}}}{t_s - t_{\text{СТ}}} \quad (2.102)$$

The average temperature of the condensate film, which is used to calculate its properties, taking into account the formula (2.72):

$$t_K = t_{\text{ГП}} - \frac{3}{8}(t_{\text{ГП}} - t_{\text{СТ}}) \quad (2.103)$$

According to [1], industrial tests of steam-water heat exchangers, whose tubes are usually covered with a layer of corrosion, show that heat transfer in them often coincides with the data for smooth tubes (except for the condensation process). The effect of natural roughness, which increases heat transfer, and the thermal resistance of rust and deposits, which reduces heat transfer, are mutually compensated.

The film condensation process is strongly influenced by the surface condition of the pipes. Correction factors for the surface condition during condensation are given in Table 2.7. [1, 2, 16]:

Table 2.7 - Correction factor for surface condition

Pure brass pipes	1,0
Stainless steel pipes	1,0
Pipes made of pearlite and carbon steels	0,75 ÷ 0,85
Heavily oxidised, uniformly rough surface of carbon steel pipes	0,7 ÷ 0,75



The thermal conductivity of the main pipe materials used in surface heaters [2] is given in Table 2.8:

Interpolation formulas for thermal conductivity as a function of wall temperature  $t_{CT} \text{ }^{\circ}\text{C}$

The main materials of pipe heating surfaces used in low pressure regenerative feed water heaters and high-pressure regenerative feed water heaters are given in Table 2.9.

Table 2.8 - Thermal conductivity of the main pipe wall materials used in high-pressure regenerative feed water heaters (ПБТ) and high-pressure regenerative feed water heaters (ПНТ)  $\frac{W}{m \cdot K}$

Temperature	Brass			Steel					
$^{\circ}\text{C}$	Л-62	Л-68	ЛЮ70-1	20	X5M	22K	15XM	08X18H10T	08X14MΦ
0	105,8	100,0	105,8	-	37,2	-	-	-	-
100	119,8	107,0	109,3	50,7	35,9	49,4	44,4	16,3	24,7
200	137,2	112,8	110,5	48,6	35,2	47,7	-	17,6	26,0
300	152,4	121,0	114,0	46,0	34,8	45,6	41,4	18,8	26,38
400	168,6	127,9	116,3	42,3	34,4	43,5	-	21,4	-

In accordance with [1, 2], the heat transfer coefficient from the insulation surface to the environment in a closed room, taking into account convective and radiant heat transfer

$$\alpha_3 = 9,77 + 0,07(t_3 - t_B) \quad (2.104)$$

where  $t_3$  - is the external temperature of the insulation, assumed to be 45 °C;

$t_B$  - is the ambient air temperature, assumed to be 25 °C ;

Heat loss through the enclosure insulation is considered to be:

$$Q_3 = \alpha_3 F_3 (t_3 - t_B) \quad (2.105)$$

where  $F_3$  is the area of insulation through which heat is transferred.

Table 2.9 - Thermal conductivity formulas for the main pipe wall materials used in high-pressure regenerative feed water heaters (PIBT) and low pressure regenerative feed water heaters (PIHT)

Material	Error rate	Thermal conductivity,
Brass Л 62	<1% , $0 \leq t_{CT} \leq 400$ °C	$105,4343 + 0,1519 t_{CT} + 1,6 \cdot 10^{-5} t_{CT}^2$
Brass Л 68	<1% , $0 \leq t_{CT} \leq 400$ °C	$100,0943 + 0,0635 t_{CT} + 1,6 \cdot 10^{-5} t_{CT}^2$
Brass ЛО70 -1	<1% , $0 \leq t_{CT} \leq 400$ °C	$106,0257 + 0,025986 t_{CT} + 10^{-6} t_{CT}^2$
Steel 20	< 0,5 % , $100 \leq t_{CT} \leq 400$ °C	$51,85 - 0,078 t_{CT} + 4 \cdot 10^{-5} t_{CT}^2$
Steel X5M	< 0,5 % , $0 \leq t_{CT} \leq 400$ °C	$37,14 - 0,0127 t_{CT} + 1,5 \cdot 10^{-5} t_{CT}^2$
Steel 22K	< 0,15 % , $100 \leq t_{CT} \leq 400$ °C	$51 - 0,0148 t_{CT} - 10^{-5} t_{CT}^2$
Steel 15XM	< 0,01 % , $100 \leq t_{CT} \leq 300$ °C	$45,9 - 0,015 t_{CT}$
Steel 08X18H10T	< 0,15 % , $0 \leq t_{CT} \leq 400$ °C	$16,025 + 2,5 \cdot 10^{-4} t_{CT} + 3,2 \cdot 10^{-5} t_{CT}^2$
Steel 08X14MΦ	< 0,15 % , $100 \leq t_{CT} \leq 300$ °C	$24,133 + 0,0084 t_{CT}$

## 2.4. Temperature characteristics

To calculate the thermodynamic and thermophysical properties, and thus the heat transfer and heat transfer coefficients, and resistances in zones or sections of heat exchangers, it is necessary to determine the average temperatures and pressures of the heat transfer media.

There are several ways to mediate the heat transfer medium temperatures for a zone, section or the entire heat exchanger. All of them can only give approximate results of the averaging, because the derivation of exact dependencies of the average temperatures of the heat transfer fluids encounters certain difficulties.

The mediation of the heat carrier temperature in proportion to the temperature heads is used according to [2, 25, 26]:

$$t_{cp} = t_{ex} + (t_{вх} - t_{ex}) \cdot \frac{\Delta t_{cp} - \Delta t_M}{\Delta t_B - \Delta t_M}, \quad (2.106)$$

where  $\Delta t_B$ ,  $\Delta t_M$  и  $\Delta t_{CP}$  are the temperature heads: higher, lower and average in the zone or section;

$t_{BX}$  and  $t_{ВХ}$  are the temperatures of the heat carrier considered at the inlet and outlet of the zone or section.

It should be noted that this type of proxy cannot be used if  $\Delta t_B \approx \Delta t_M$ .

The temperature of the heat transfer medium in the zone or section is well averaged over the logarithmic mean:

$$t_{CP} = \frac{t_B - t_M}{\ln \frac{t_B}{t_M}}, \quad (2.107)$$

where  $t_B$  и  $t_M$  are the temperatures of the heat carrier in question: the highest and lowest in the zone or section.

The commonly used arithmetic mean of heat transfer fluid temperatures can give quite accurate results in some cases, but it is better to use the logarithmic mean, since in general the distribution of heat transfer fluid temperatures has a pronounced exponential shape.

Average pipe wall temperatures are calculated from the Newton-Richman equation for heat transfer or the equation for heat transfer through a cylindrical wall:

- average outer pipe wall temperature in a zone or section:

$$t_{\text{CT3OBcp}} = t_{\text{3OBcp}} - \frac{Q}{\alpha_2 F} \quad \text{or} \quad (2.108)$$

$$t_{\text{CT3OB cp}} = \frac{t_{\text{BHcp}} + t_{\text{3OBcp}} \left( \frac{d_{\text{3OB}} \alpha_2}{d_{\text{BH}} \alpha_1} + \frac{d_{\text{3OB}} \alpha_2}{2 \lambda_{\text{CT}}} \ln \frac{d_{\text{3OB}}}{d_{\text{BH}}} \right)}{1 + \frac{d_{\text{3OB}} \alpha_2}{d_{\text{BH}} \alpha_1} + \frac{d_{\text{3OB}} \alpha_2}{2 \lambda_{\text{CT}}} \ln \frac{d_{\text{3OB}}}{d_{\text{BH}}}}, \quad (2.109)$$

- average temperature of the pipe inner wall in a zone or area:

$$t_{\text{CTEHcp}} = t_{\text{EHcp}} + \frac{d_{\text{3OB}}}{d_{\text{BH}}} \cdot \frac{Q}{\alpha_1 F} \quad (2.110)$$

$$t_{\text{CTBH cp}} = \frac{t_{\text{3OBcp}} + t_{\text{BHcp}} \left( \frac{d_{\text{BH}} \alpha_1}{d_{\text{HAP}} \alpha_2} - \frac{d_{\text{BH}} \alpha_1}{2 \lambda_{\text{CT}}} \ln \frac{d_{\text{BH}}}{d_{\text{3OB}}} \right)}{1 + \frac{d_{\text{BH}} \alpha_1}{d_{\text{3OB}} \alpha_2} - \frac{d_{\text{BH}} \alpha_1}{2 \lambda_{\text{CT}}} \ln \frac{d_{\text{BH}}}{d_{\text{3OB}}}}, \quad (2.111)$$

where  $t_{\text{HAP CP}}$  and  $t_{\text{BH CP}}$  are the average temperatures of the heat carriers outside and inside the pipe and are determined by formulas (2.106) or (2.107);

$Q$  and  $F$  are heat fluxes transferred in a zone or section through the pipe walls and the heat transfer area on the outer surface of the cylinder;

$d_{\text{HAP Ta}}$   $d_{\text{BH}}$  are the outer and inner diameters of the pipe;

$\alpha_1$ ,  $\alpha_2$  i  $\lambda_{\text{CT}}$  - heat transfer coefficients from the inside and outside of the pipe, thermal conductivity of the pipe wall material.

The average pipe wall temperatures for calculating the heat transfer through the wall  $\lambda_{CT}$  are determined by the arithmetic mean of the temperatures of the outer and inner walls:

$$t_{CTCP} = \frac{t_{CT30BCP} + t_{CTEHCP}}{2} . \quad (2.112)$$

An important temperature characteristic of a separate section or zone of the heat exchanger is the average temperature head, which is the result of solving the system of differential equations of heat balance and heat transfer for elementary intervals. In the case of cross-flow and mixed mutual flow of heat transfer fluids, which are most typical for surface high-pressure regenerative feed water heaters and high-pressure regenerative feed water heaters, the average temperature head is usually determined by the formula [2, 4.13-20, 26, 27, 32-37]:

$$\Delta t_{CP} = \Delta t_{J\text{ ИП}} \cdot \psi . \quad (2.113)$$

where  $\Delta t_{J\text{ ИП}}$  is the logarithmic mean temperature head against the flow, and in general it is considered as follows:

$$\Delta t_{J} = \frac{\Delta t_1 - \Delta t_2}{\ln \frac{\Delta t_1}{\Delta t_2}} , \quad (2.114)$$

where  $\Delta t_1$  - is the temperature head at the inlet of the heating medium into the heat exchanger or zone,  $\Delta t_1 = t_{\Gamma 1} - t_{H1}$  in the forward flow and -  $\Delta t_1 = t_{\Gamma 1} - t_{H2}$  - in the countercurrent;

$\Delta t_2$  - is the temperature head at the outlet of the heating medium from the heat exchanger or  $\Delta t_2 = t_{\Gamma 2} - t_{H2}$  in the forward flow and  $\Delta t_2 = t_{\Gamma 2} - t_{H1}$  - in the countercurrent flow;

$\Psi$ - is a correction factor to the mean logarithmic temperature head against the flow, which takes into account the peculiarities of the mutual flow of heat carriers and depends on dimensionless temperature complexes:

$$P = \frac{t_{H2} - t_{H1}}{t_{\Gamma1} - t_{H1}} , \quad (2.115)$$

$$R = \frac{t_{\Gamma1} - t_{\Gamma2}}{t_{H2} - t_{H1}} . \quad (2.116)$$

The issues of determining the correction factors to the logarithmic mean temperature pressure for various heat transfer fluid flow patterns in heat exchangers are discussed in detail in Section 3. In the case of multi-pass cross-flow of heat transfer fluids in the condensate coolers and VC zones of surface heaters, where the heated heat transfer fluid (feed water) flows in the pipes and is mixed, and the flow of the heating heat transfer fluid (steam, condensate) is close to complete mixing [2], the generalised dependencies (3.48) can be used:

$$\psi = f(P, R, n, z) , \quad (2.117)$$

where  $n$  -is the number of parallel elements (i.e., spiral coils or rows of heating surface tubes) in one pass;

$z$ - is the number of passes of the heating medium.

This generalised universal dependence also takes into account the scheme of inclusion of the heating medium passages: common counterflow or direct flow (described below in Section 3).

In the case of condensation of the heating medium, where  $t_{\Gamma2} = t_{\Gamma1} = t_s$  , i.e.  $R = 0$ , regardless of whether the flow is direct or countercurrent, the coefficient  $\Psi$  is unity.

## 2.5. Hydraulic characteristics

The continuity equation (law of mass conservation) for a one-dimensional flow in the section of the steam condensation, steam cooling, condensate coolers zones or other channel section is as follows:

$$G = \frac{W f}{v}, \quad (2.118)$$

where  $G$  - is the mass flow rate of the medium in the channel section;

$W$  - is the average velocity of the channel section;

$f$  - is the flow area for the medium in the channel;

$v$  - is the average specific volume of the coolant in the channel section.

The equation of pressure losses in the process of heat carrier movement in the section of the steam condensation, steam cooling, condensate cooling zones or other channel section is:

$$\Delta p = \frac{W^2}{2v} \sum \xi + \Delta p_{\text{ГСТ}}, \quad (2.119)$$

where  $\sum \xi$  - is the sum of all hydraulic and local resistances in the channel section;

$\Delta p_{\text{ГСТ}}$  - hydrostatic pressure;

Average heat carrier pressures are determined by the arithmetic mean value:

$$p_{\text{cp}} = \frac{p_{\text{BX}} + p_{\text{ВЫХ}}}{2} \quad \text{or} \quad p_{\text{cp}} = p_{\text{BX}} - \frac{\Delta p}{2}, \quad (2.120)$$

where  $p_{\text{BX}}$ ,  $p_{\text{ВЫХ}}$  and  $\Delta p$  are the pressures at the inlet, outlet of the zone or section and the pressure loss in the zone or section.

The coefficient of hydraulic frictional resistance of the entire pipe section is calculated according to the Darcy-Weisbach law:

$$\xi_{TP} = \lambda_{TP} \frac{L}{d}, \quad (2.121)$$

where  $\lambda_{TP}$  - is the friction coefficient per unit relative length  $\frac{L}{d}$  ;

$d$  - internal diameter of the pipe;

$L$  - is the length of the pipe section.

For turbulent flow in smooth circular pipes, the following dependencies are used  $\lambda_{TP}$  at  $\frac{L}{d} > 30$  [1, 2, 4, 8, 13 -20, 27-31]:

- Blasius formula for  $4 \cdot 10^3 < Re < 10^5$ :

$$\lambda_{TP} = 0,316 Re^{-0,25}, \quad (2.122)$$

- Filonenko formula for  $4 \cdot 10^3 < Re < 10^{12}$ :

$$\lambda_{TP} = (0,79085 \ln Re - 1,64)^{-2}, \quad (2.123)$$

where  $Re$  - is the Reynolds number,  $Re = \frac{Wd}{\nu}$  ;

$W$  - is the average velocity of the coolant;

$\nu$  - is the kinematic viscosity of the coolant determined by the average flow temperature.

For turbulent flow in rough circular pipes, the following dependencies are used [17, 31]:

- in the domain of the quadratic law of drag Eq:

$$\lambda_{TP} = \left( 0,868 \ln \left( 3,7 \frac{d}{\Delta} \right) \right)^{-2}, \quad (2.124)$$

- For all turbulent regimes, the formula is applicable:

$$\lambda_{TP} = 0,11 \left( \frac{\Delta}{d} + \frac{68}{Re} \right)^{0,25}, \quad (2.125)$$



where  $\Delta$ - is the absolute surface roughness.

The coefficient of resistance to transverse flow of bundles of high-pressure regenerative feed water heaters pipes and low pressure regenerative feed water heaters spiral coils in the condensate coolers and steam cooling zones at a staggered arrangement [13, 17]:

$$\xi = \xi_0(z+1), \quad (2.126)$$

where  $\xi_0$  - is the drag coefficient of one step,  $\xi_0 = CRe^{-0,27}$ ;

$$Re - \text{Reynolds number, } Re = \frac{Wd}{\nu};$$

$W$  - is the average velocity of the coolant in a narrow section;

$\nu$  - is the kinematic viscosity of the heat carrier determined by the average flow temperature;

$d$  - is the outer diameter of the pipe;

$C$  - coefficient, the value of which is given in Table 2.10.

where  $\psi = \frac{x_1 - 1}{x'_2 - 1}$ ,  $x'_2 = \sqrt{0,25x_1^2 + x_2^2}$ , is the relative diagonal pitch;

$$x_1 = \frac{S_1}{d} \text{ and } x_2 = \frac{S_2}{d};$$

Table 2.10 - Values of the coefficient  $C$

$\psi$	$x_1$	$C$
0,1 ÷ 1,7	$\geq 1,44$	$C = 3,2 + 0,66(1,7 - \psi)^{1,5}$
0,1 ÷ 1,7	$< 1,44$	$C = 3,2 + 0,66(1,7 - \psi)^{1,5} + \frac{1,44 - x_1}{0,11}(0,8 + 0,2(1,7 - \psi)^{1,5})$
1,7 ÷ 6,5	1,44 ÷ 3	$C = 0,44(\psi + 1)^2$
1,7 ÷ 6,5	$< 1,44$	$C = (0,44 + (1,44 - x_1))(\psi + 1)^2$
$\geq 1,7$	3 ÷ 10	$C = 0,062 + 0,21(10 - x_1)^{-0,24}$

$S_1, S_2$  - are the transverse and longitudinal pipe row spacing.

Drag coefficients in the transverse flow of spiral coils for  $1,02 < \frac{S_B}{d} < 10$   
 $2 \cdot 10^4 < Re < 5 \cdot 10^5$  [1]:

$$\xi_{CH} = \xi \varepsilon_{CH}, \quad (2.127)$$

where  $\varepsilon_{CH}$  - is the correction for spiral coils in a staggered arrangement

$$\varepsilon_{CH} = 0,57 + 0,18 \left( \frac{S_B}{d} - 1 \right) + 0,53 \left( 1 - e^{-0,58 - 9,2 \left( \frac{S_B}{d} - 1 \right)} \right);$$

(triangular lattice),

$S_1, S_2$  - are the pitches of the pipe rows in the transverse and longitudinal directions,  
 $S_1 = \frac{S_K}{n_{\Pi\Pi}}, S_2 = S_B;$

$S_K$  - is the average installation pitch on collectors in the zones (condensate coolers or steam cooling),

$S_B$  - is the spiral coil winding pitch.

At longitudinal washing of pipe bundles in the tubing, the drag coefficient is determined as follows [1] ( $2 \cdot 10^4 < Re < 5 \cdot 10^5$ ):

$$\xi_{\Pi\Pi} = \xi \varepsilon_{\Pi\Pi}, \quad (2.128)$$

where  $\varepsilon_{\Pi\Pi}$  - is the correction for the longitudinal washing of pipe bundles

$$\varepsilon_{\Pi\Pi} = 0,57 + 0,18 \left( \frac{S_B}{d} - 1 \right)$$

$\xi$  - is the drag coefficient calculated similarly to the flow in pipes (formulas (2.121)-(2.125), but for the equivalent diameter  $d_E$ ,  $d_E = \frac{4f}{\Pi}$  ;

$d$  - is the outer diameter of one pipe;

$f$  - flow area (live section);

$P$  - wetted perimeter.

In the case of steam or condensate entering a bundle of smooth pipes with an angle of  $20^\circ < \varphi < 90$  the definition of the drag coefficient will be as follows [17]:

$$\xi = \xi_{\Pi O \Pi} \varepsilon_{\varphi}, \quad (2.129)$$

where  $\xi_{\Pi O \Pi}$  - is the drag coefficient for the cross-flow ( $\varphi = 90^\circ$ ), which is calculated by formulas (2.126), (2.127);

$\varepsilon_{\varphi}$  - is the correction for the angle of attack of the flow,  
 $\varepsilon_{\varphi} = \sin^2 \varphi + 0,16 \cos^2 \varphi$ .

If  $0^\circ < \varphi < 20^\circ$  – the nature of the washout is considered to be longitudinal, where instead of  $\alpha_{\Pi O \Pi}$ , the drag coefficient for longitudinal flow should be taken (formula (2.128) and  $\varepsilon_{\varphi} = 1$ ).

In the case when one part of the pipe bundle is washed longitudinally and the other part is washed transversely, the drag coefficient can be considered as follows:

$$\xi = \xi_{\Pi O \Pi} \frac{F_{\Pi O \Pi}}{F} + \xi_{\Pi P} \frac{F_{\Pi P}}{F} \quad \text{or} \quad \xi = \xi_{\Pi O \Pi} \frac{N_{\Pi O \Pi}}{N} + \xi_{\Pi P} \frac{N_{\Pi P}}{N}, \quad (2.130)$$

where  $\xi_{\Pi O \Pi}$  and  $\xi_{\Pi P}$  are the drag coefficients for the transverse (formulae (2.126), (2.127) and longitudinal flow (formula (2.128)).

$F_{\Pi O \Pi}$ ,  $F_{\Pi P}$  and  $F$  - are the surface areas of the transverse, longitudinal and total flows in the zone;

$N_{\Pi O \Pi}$ ,  $N_{\Pi P}$  and  $N$  - are the number of tubes of transverse, longitudinal wash and total in the zone.

If  $\frac{F_{\Pi O \Pi}}{F}$  or  $\frac{N_{\Pi O \Pi}}{N} > 85\%$ , the entire tube bundle is usually considered to be cross-washed.

In the case of mixed washing of spiral coils in the condensate coolers and LW zones of the LLD, steam or condensate is washed sequentially over several groups of coils in their plane. This movement of steam and condensate is accompanied by large hydraulic losses and is inefficient in terms of heat transfer [1]. The drag coefficient for such a flow is as follows [1]:

$$\xi = 3,4 n_{\text{CEKII}}, \quad (2.131)$$

where  $n_{\text{CEKII}}$  - is the number of sections (groups) of spiral coils that are washed in series.

In the steam condensation zone, the hydraulic resistance coefficient (steam resistance) is determined according to formulas (2.126)-(2.128) by the average velocity of pure steam or steam-air mixture  $W$ , taking into account the velocities at the inlet and outlet of the chamber (if any) [2].  $W$  - is determined according to formula (2.81). The coefficients of local resistances depend on the perfection of the design of the heater units and are mostly determined by experiment. Here are the values of local resistances that are most commonly found in surface heaters [2, 4, 13, 17, 28, 31]. Some of them have been converted for convenient use in further calculations. The coefficients of local resistances at sharp sudden flow constrictions and expansions, inlets and outlets are given in Table 2.11. The coefficients of local resistances  $\xi_M$  at flow turns in pipes are given in Tables 2.12 and 2.13.

Table 2.11 - Local resistance coefficients

Type of local resistance	$\xi_M$
1. Sudden narrowing	
a) the determining velocity in the narrow section of the ultrasonic conduit $f_{y3K}$	$0,5 \left(1 - \frac{f_{y3K}}{f}\right)$
б) determining velocity in the outlet section $f$	$0,5 \left(1 - \frac{f_{y3K}}{f}\right) \left(\frac{f}{f_{y3K}}\right)^2$
2. Sudden expansion	
a) determining velocity in the exit section $f$	$1,1 \left(1 - \frac{f}{f_{\text{шир}}}\right)^2$
б) determining velocity in the wide section $f_{\text{шир}}$	$1,1 \left(1 - \frac{f}{f_{\text{шир}}}\right)^2 \left(\frac{f_{\text{шир}}}{f}\right)^2$
3. Flow inlet to the pipe from a sufficiently large chamber (п.1 $f \rightarrow \infty$ ), relative to the velocity in the pipe	0,5
4. Flow outlet from the pipe into a sufficiently large chamber (п.2 $f_{\text{шир}} \rightarrow \infty$ ), relative to the velocity in the pipe	1,1

Table 2.11 continued

5. Flow inlet from the pipe to the distributing manifold with side supply	1,3
6. Angular flow outlet from the collecting manifold $D_{\text{КОЛ}}$ to the pipe of smaller diameter $D_{\text{БН}}$ , relative to the velocity in the pipe	$0,7 + \frac{D_{\text{БН}}}{D_{\text{КОЛ}}}$
7. Turn of the flow with a shock in the inlet or outlet water chamber relative to the inlet velocity	1,5
8. Turning the flow by an angle of $180^\circ$ through an intermediate water chamber relative to the velocity at the pipe outlet	2,5
9. Flow entry into the inter-pipe space from the nozzle at an angle of $90^\circ$ to the pipe axes relative to the velocity at the outlet of the nozzle	1,5
10. Flow outlet from the inter-pipe space through the nozzle at an angle of $90^\circ$ to the pipe axes, relative to the velocity in the nozzle	1
11. Turn of the flow by an angle of $180^\circ$ through the baffle in the inter-pipe space (transition from one passage to another) relative to the velocity in the section between the baffle and the casing	1,5

Table 2.12 - Resistance coefficients of smooth bends with  $\frac{R}{d} \geq 3,5$ 

The angle of rotation	$20^\circ$	$20^\circ \div 60^\circ$	$60^\circ \div 140^\circ$	$140^\circ \div 180^\circ$	$180^\circ$
$\xi_M$	0	0,1	0,2	0,3	0,5

where  $R$  - is the turning radius,  $d$  - is the internal diameter of the pipe

Table 2.13 - Resistance coefficients for sharp turns

The angle of rotation	$30^\circ$	$45^\circ$	$60^\circ$	$75^\circ$	$90^\circ$
$\xi_M$	0,25	0,5	0,8	1,2	1,75

Local resistance coefficients in spiral coils:

$$\xi_M = \xi_{\text{вх}} + \xi_{\text{пов}} + \xi_{\text{вых}}, \quad (2.132)$$

where  $\xi_{BX}$  - is the resistance of the coil inlet from the distributing collector,

$$\xi_{BX} = (0,56 \frac{d}{D_{КОЛ}} - 0,039)(n - i + 1) - 8,05 \frac{d}{D_{КОЛ}} + 1,84 ;$$

$\xi_{ПОВ}$  is the resistance to flow turns in the coil turns,  $\xi_{ПОВ} = 0,5n_B n_{ПЛ}$ ;

$\xi_{ВИХ}$  is the resistance of the coil outlet to the collecting collector,

$$\xi_{ВИХ} = 1,1 + 0,9i^2 \left( \frac{d}{D_{КОЛ}} \right)^4$$

$n$  - the number of coils from the beginning of the collector section to the blind end or outlet pipe;

$i$  - is the serial number of the coil along the flow in the distributing or collecting section of the collector to the blind end or outlet pipe;

$n_B$  и  $n_{ПЛ}$  - number of turns in one plane and planes of one coil, respectively;

$d$  и  $D_{КОЛ}$  - internal diameters of the coil and collector, respectively.

Pressure loss from flow acceleration in non-isothermal flow [2, 30]:

$$\Delta P_{уск} = (\rho_{CP} W)^2 \left( \frac{1}{\rho_{ВИХ}} - \frac{1}{\rho_{ВХ}} \right) , \quad (2.133)$$

where  $\rho_{ВХ}$ ,  $\rho_{ВИХ}$  and  $\rho_{CP}$  - are the inlet, outlet, and average flow densities in the section.

In the flow of superheated steam in the steam cooling zone, pressure and drag losses from the acceleration of the flow at non-isothermal flow can occur due to a sharp change in its temperature and the drag coefficient can be determined depending on [1]:

$$\xi_{уск} = \frac{2(t_{ВХ} - t_{ВИХ})}{273 + t_{CP}} , \quad (2.134)$$

where  $t_{BX}$ ,  $t_{BHX}$  and  $t_{CP}$  - are the flow temperatures at the inlet, outlet, and average in the section, °C.

When condensate flows in the condensate coolers zone, the pressure and resistance losses due to flow acceleration in a non-isothermal flow are very small, since the properties of water change slightly with temperature and these losses can be ignored.

The decrease or increase in pressure due to the difference in elevation at the beginning and end of the section when water moves in the channels (hydrostatic head) is determined by:

$$\Delta P_{гст} = \rho_{cp} g (h_{BHX} - h_{BX}) , \quad (2.135)$$

where  $h_{BX}$  i  $h_{BHX}$  - are the heights of the channel at the inlet and outlet relative to a certain zero level;

$\rho_{CP}$  - is the average water flow density.

In the surface tubing low pressure regenerative feed water heaters end high-pressure regenerative feed water heaters, constriction devices (choke washers) are used to ensure the specified flow rates of feed water through the condensate coolers or condensate coolers zones.

In accordance with the algorithm for selecting choke washers for a given flow rate  $G_{III}$  and pressure drop across the washer  $\Delta P_{III}$ :

$$\frac{d_{III}}{D_{BH}} = f(x) , \quad (2.136)$$

$$x = \frac{G_{III}}{D_{BH}^2 \sqrt{\Delta P_{CУЖ} \rho}} , \quad (2.137)$$

$$\Delta P_{CУЖ} = \Delta P_{III} \left( 1 - 1,03 \left( \frac{d_{III}}{D_{BH}} \right)^2 \right) , \quad (2.138)$$

where  $d_{\text{III}}$  and  $D_{\text{BH}}$  - are the smaller inner diameter of the washer and the inner diameter of the pipeline or collector where the washer is installed;

$p$  - density of the medium;

$f(x)$  - a function of the auxiliary parameter  $x$ , which is given in [2] in the form of a graph;

$\Delta P_{\text{ЗВУЖ}}$  - pressure drop directly on the constricting device (choke washer) without taking into account the pressure recovery behind it. The pressure will be restored if the washer is installed in an area greater than or equal to three internal diameters [31].

Coefficient of local resistance of the throttle washer, taking into account the pressure recovery:

$$\xi_{\text{III}} = \frac{1}{8} \left( \frac{\pi}{x} \right)^2 \left( 1 - 1,03 \left( \frac{d_{\text{III}}}{D_{\text{BH}}} \right)^2 \right), \quad (2.139)$$

As can be seen from the above dependencies, for the selection of throttle washers and verification calculations, it is necessary to have expressions for the direct function  $\frac{d_{\text{III}}}{D_{\text{BH}}} = f(x)$ , which is available in graphical form [2], and the inverse function  $x = f\left(\frac{d_{\text{III}}}{D_{\text{BH}}}\right)$ . The interpolation of the graph by the least squares method [22, 23] allows us to obtain the necessary dependencies:

$$\frac{d_{\text{III}}}{D_{\text{BH}}} = e^{6,93147(V-0,56667)}, \quad (2.140)$$

where the formulas for calculating the function  $V$  are given in Table 2.14, here  $U = 1 + 0,1442695 \ln x$ ;



Table 2.14 - Auxiliary function V

$x$	$V$
$10^{-3} \div 2 \cdot 10^{-3}$	$V = 0,030212 + 1,92855 U - 10,446853 U^2 + 8,617785 U^3$
$2 \cdot 10^{-3} \div 2 \cdot 10^{-1}$	$V = 0,0795907 + 0,504093 U$
$2 \cdot 10^{-1} \div 1$	$V = 4,791096 - 15,869364 U + 18,966359 U^2 - 7,336897 U^3$

$$x = e^{6,93147(U-1)}, \quad (2.141)$$

where the formulas for calculating the function U are given in Table 2.15,

here  $V = 0,56667 + 0,1442695 \ln \frac{d_{III}}{D_{BH}} \cdot$

Table 2.15 - Auxiliary function U

$d_{III} / D_{BH}$	$U$
$<0,05$	$U = -0,049978 + 2,429335 V - 30,215311 V^2 + 156,442991 V^3$
$0,05 \div 0,5$	$U = 1,98546 + 0,1592098 V$
$>0,5$	$U = -46,364456 + 277,066081 V - 545,62313 V^2 + 360,710032 V^3$

## 2.6 Design characteristics

The heat flow through pipe surfaces depends on the design parameter of the heat transfer area. To calculate the velocities of the heat transfer fluids in the zones, it is necessary to know the flow areas. The accuracy of this determination has a significant impact on the accuracy of all thermal and hydraulic calculations of heaters. When the feedwater moves in pipes, pipes and collectors, the determination of the flow areas is straightforward. For the external movement of heating steam, the determination of flow areas is a more difficult task, since its flow patterns are

complex and varied. In thermal and hydraulic calculations, it is also important to determine the equivalent diameters and other design values.

For the sake of unambiguity of calculations, the outer surface of a cylindrical pipe is usually taken as the heat transfer area in surface feedwater heaters of power plants:

$$F = \pi d_{\text{об}} L N, \quad (2.142)$$

where  $d_{\text{об}}$  - is the outer diameter of the pipe;

$L$  - length of pipes or coils in the area or zone;

$N$  - number of pipes or coils in the area or zone;

Passage areas for the movement of feedwater in round pipes, pipes or collectors:

$$f_{\text{H}} = \pi \frac{d_{\text{BH}}^2}{4} N_{\text{OD}}, \quad (2.143)$$

where  $d_{\text{BH}}$  - is the internal diameter of one pipe, branch pipe or collector;

$N_{\text{OD}}$  - the number of pipes, nozzles or collectors through which the entire studied flow of coolant flows simultaneously.

When calculating the flow areas for feedwater in the condensate coolers, steam condensation and steam cooling zones,  $N_{\text{OD}}$  - is equal to the total number of pipes or spiral coils in these zones.

The equivalent thermal and hydraulic diameter  $d_{\text{E}}$  - is equal to the internal diameter of the pipe  $d_{\text{BH}}$ .

The passage areas for the movement of steam and condensate in the chambers and casings of the steam cooling, steam condensation and condensate cooling of the tubing during transverse movement in the section are equal to the minimum live section area not occupied by pipes:

$$f_{\Gamma} = l (a - d_{\text{3OB}} n_1) \quad , \quad (2.144)$$

where  $d_{\text{3OB}}$  - is the outer diameter of one tube in the tube bundle;

$a$  - the width inside the casing or the equivalent width of the casing or housing;

$l$  is the distance between the baffles;

$n_1$  - average number of tubes in the direction perpendicular to the direction of steam flow (in one row);

The equivalent thermal and hydraulic diameter  $d_E$  is equal to the outer diameter of one tube  $d_{\text{3OB}}$ .

Schemes of steam cooler shells used in domestic tubing are shown in Fig. 2.3. The design scheme of condensate cooler shells used in domestic tubing is shown in Fig. 2.4.

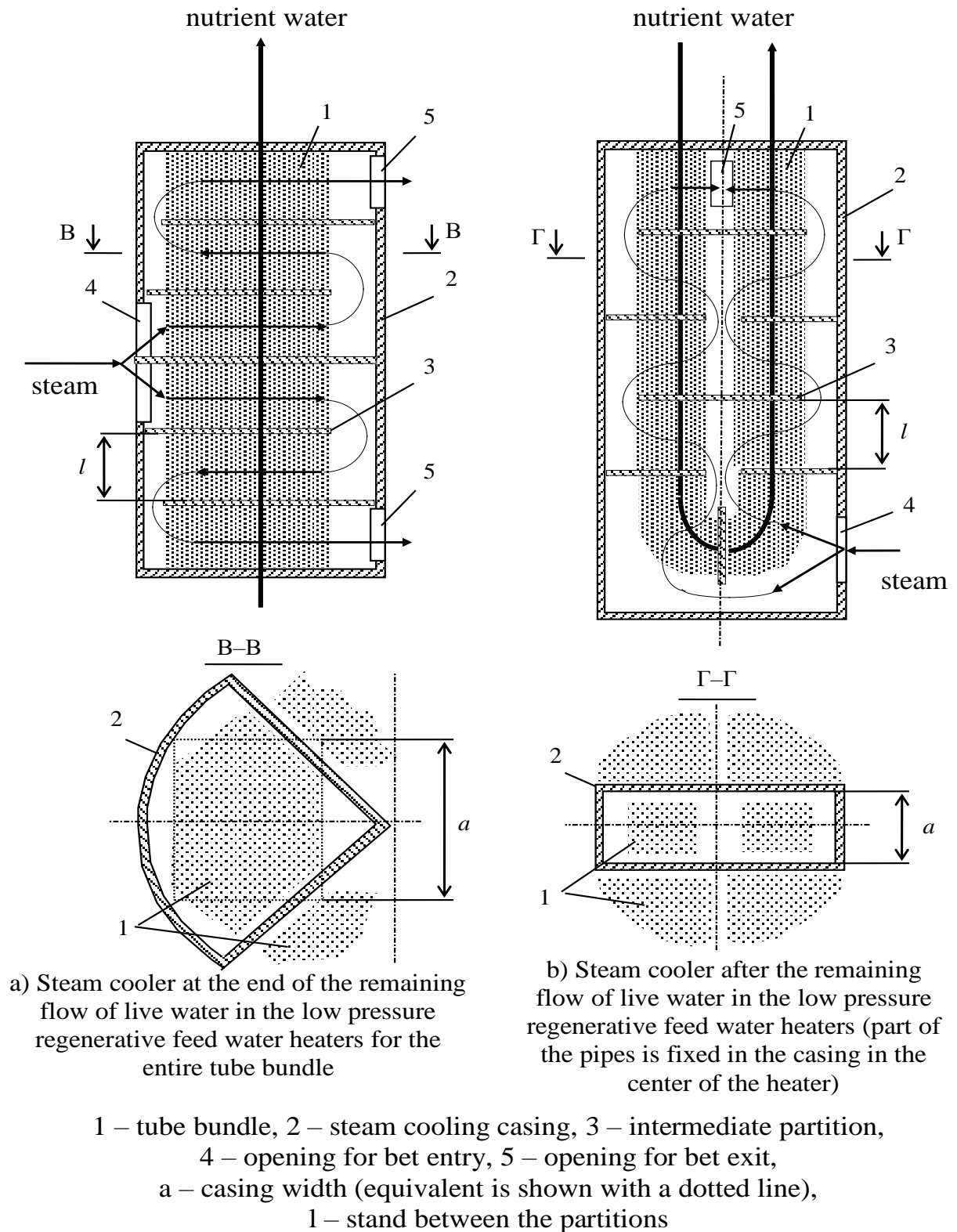
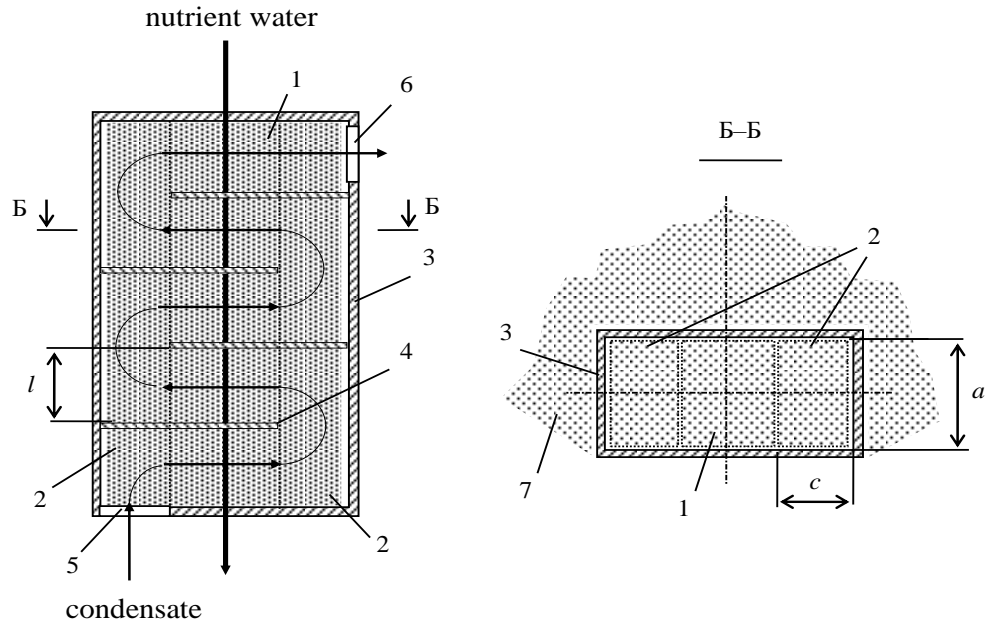


Fig. 2.3 - Diagrams of the main structures of steam cooler shells used in tubing and the flow of coolants in them



- 1 – part of the tube bundle with transverse flow,  
 2 – part of the tube bundle with longitudinal flow,  
 3 – condensate cooler casing,  
 4 – intermediate partition,  
 5 – condensate inlet holes,  
 6 – condensate outlet holes,  
 7 – part of the tube bundle not enclosed in the casing,  
 a – casing width, c – longitudinal flow width,  
 l – distance between partitions

Fig. 2.4 - Schematics of the main structures of condensate cooler shells used in tubing and coolant flows in them

Flow areas for condensate movement in zones or sections of longitudinal flow:

$$f_{\Gamma_{\text{np}}} = a \cdot c - \pi \cdot \frac{d_{\text{3OB}}^2}{4} \cdot \frac{N_{\text{np}}}{2}, \quad (2.145)$$

where  $d_{\text{3OB}}$  - is the outer diameter of one tube in the tube bundle;

$a$  - width of the casing;

$c$  - width of the free space for longitudinal flow from the edge;

$N_{\text{пOB}}$  - total number of longitudinal flow tubes on both edges.

The equivalent thermal and hydraulic diameter  $d_E$  in this case is:

$$d_E = \frac{4f_{\Gamma mp}}{\Pi}, \quad (2.146)$$

where  $\Pi$  - is the wetted perimeter,  $\Pi = a + 2c + \pi d_{30E} \cdot \frac{N_{mp}}{2}$

As a rule, such condensate coolers are designed so that  $f_{\Gamma mp} \approx f_{\Gamma noH}$ . This minimises pressure losses due to sudden constrictions and expansions in the flow.

There is a wide variety of steam flow patterns in the control zone of a CTD. In each case, the vapour flow pattern and chamber design is developed to minimise the surface area required for condensation, good condensate drainage from the pipes and strength considerations. Schemes of chamber designs and the movement of condensing steam in them are shown in Figs. 1.7 -1.9.

The flow areas for steam or condensate in the steam cooling or condensate cooling LDVT casings through the column of coils perpendicular to the plane of their winding are considered as follows:

$$f_{\Gamma} = f_K - f_B - \frac{d_{30E} L_{\Pi \text{ cH}}}{n_{\Pi \Pi}}, \quad (2.147)$$

where  $f_K$  - is the cross-sectional area of the cavity of the casing enclosing the coil column;

$f_B$  - is the cross-sectional area of the displacer installed in the centre of the coils (if any);

$d_{30BH}$  - outer diameter of the pipe from which the spiral coil is made;

$n_{\Pi \Pi}$  - number of planes in one coil;

$L_{\Pi \text{ cH}}$  - total length of the spiral coil.

Passage areas for steam or condensate when flowing in the casings of the steam cooling or condensate cooling LDV through the bypass boxes installed to pass from one column of coils to another:

$$f_{\text{ПЕРЕП}} = a \cdot h \cdot n_{\text{ПОТ}}, \quad (2.148)$$

where  $a$  and  $h$  are the width and height of the bypass.

If the flow areas are to be calculated based on the total steam or condensate flow rate, they must be multiplied by the number of parallel steam or condensate flows  $n_{\text{ПОТ}}$ .

The equivalent thermal and hydraulic diameter  $d_{\text{E}}$  is equal to the outer diameter of the coil pipe  $d_{\text{ЗОВН}}$ .

Schemes of structures and flow of coolants of built-in steam and condensate coolers of modern EFCs on the example of EFCs of turbine unit

K-500-240-2 are shown in Fig. 2.5.

The flow areas for condensation of steam moving from top to bottom in the zone of the IBC control (see Figs. 1.10-1.12) can be estimated as follows:

$$f_{\text{Г}} = \pi \frac{D_{\text{КОРБН}}^2}{4} - \pi \frac{D_{\text{КОЛЗОВ}}^2}{4} N_{\text{КОЛ}} - \pi \frac{D_{\text{ЦТП}}^2}{4} - \frac{d_{\text{НАР}} L_{\text{ПСП}}}{n_{\text{ПЛ}}} N_{\text{КОЛ}}, \quad (2.149)$$

where  $D_{\text{КОРБН}}$  - is the inner diameter of the heater body;

$D_{\text{КОЛЗОВ}}$  - outer diameter of the collectors;

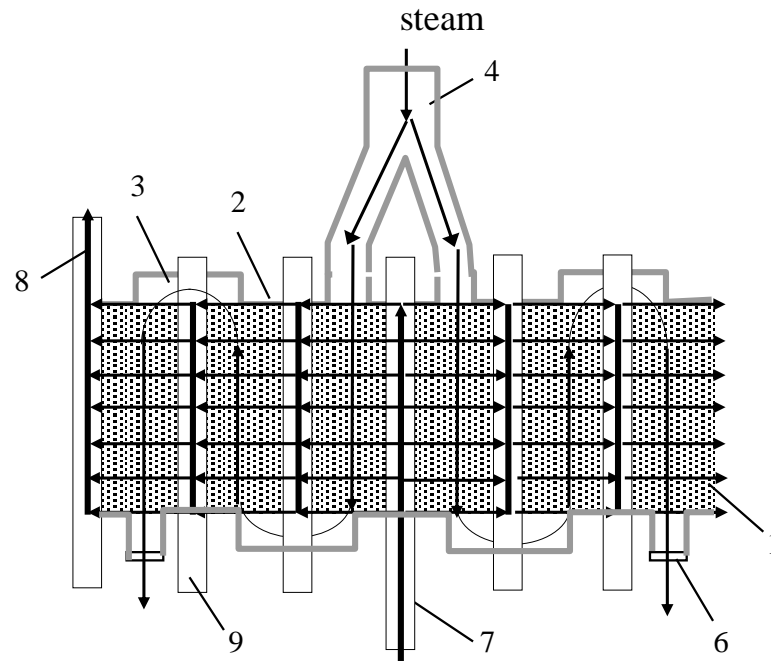
$N_{\text{КОЛ}}$  - number of collectors;

$D_{\text{ЦТП}}$  - outer diameter of the pipeline installed in the centre of the heater (steam pipeline, feedwater collection and discharge pipeline);

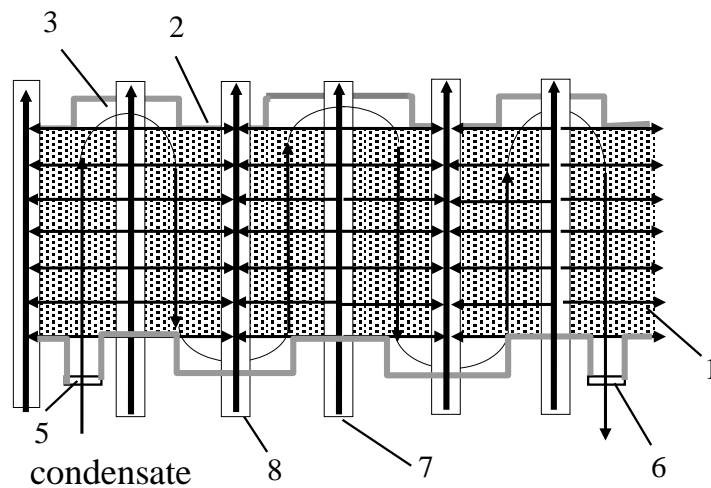
$d_{\text{ЗОВН}}$  - outer diameter of the pipe from which the spiral coil is made;

$n_{\text{ПЛ}}$  - number of planes in one coil;

$L_{\text{ПСП}}$  - total length of the spiral coil.



a) steam cooler



b) condensate cooler

1 – spiral coil units, 2 – casing, 3 – bypass boxes, 4 – steam line, 5 – condensate inlet, 6 – steam (condensate) outlet, 7 – collectors that distribute feed water, 8 – collectors that collect feed water, 9 – intermediate feed water collectors.

Fig. 2.5 - Design of steam and condensate coolers of modern steam turbines and flow patterns of coolants in them



## CHAPTER 3

### EFFICIENCY OF THE SCHEMES OF MUTUAL FLOW OF HEAT CARRIERS IN SURFACE HEAT EXCHANGERS WITH CROSS-CURRENT

One of the steps in the design, verification or optimisation calculations of a surface heat exchanger or its individual zone is to determine the average temperature head. In cross-flow or mixed flow, the average temperature head (or average temperature difference) is determined as the product of the logarithmic mean temperature head in the counterflow by the correction factor  $\Psi$ , which takes into account the peculiarities of the mutual flow of heat transfer fluids. In essence, the coefficient  $\Psi_e$  is the efficiency of the existing current circuit relative to the ideal one - a pure countercurrent. The form of the  $\Psi$  function is usually given in the known literature as graphs (nomograms) [2, 4, 13-20, 26, 32-35]. For computer calculations, the use of such nomograms is very difficult. In addition, the area of determination of dimensionless temperature parameters in these graphs often does not cover the entire range present in the surface heat exchangers of TPP and NPP power plants. For the cross-flow scheme of coolants, some implicit formulas in the form of infinite series are given in the literature [18, 35] or explicit dependencies using indices against accuracy [33]. Moreover, the implicit dependencies [18] are different for each number of cross-flow strokes (up to 6 in total), and the indices against accuracy for cross-flow from [33] only approximately reflect the efficiency of the scheme. As a result, the calculation inaccuracies of the above values can reach tens of percent. For the convenience of calculations of such heat exchangers or their individual zones (sections of the heat exchange surface), analytical dependencies of the correction factors to the logarithmic mean temperature pressure are given below.

For cross-current and mixed current, the correction factor to the logarithmic mean temperature pressure is determined by formula (2.33) as follows:

$$\Psi = \frac{\Delta t_{CP}}{\Delta t_{Л}} . \quad (3.1)$$

The correction factor is usually given in the literature in a graphical form depending on the dimensionless temperature complexes  $P$  and  $R$  (formulas (2.115) and (2.116).

If we represent the formulas as  $\Delta t_{CP} = (t_{H2} - t_{H1}) \cdot f_1(P, R)$ ,  $\Delta t_{JI} = (t_{H2} - t_{H1}) \cdot f_2(P, R)$ , where  $\Delta t_{JI}$  is the countercurrent, and the notations correspond to Fig. 3.1, then using relation (3.1), we can obtain dependences for different types of cross-current.

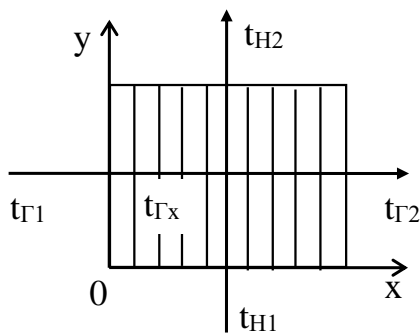
After the transformations using expressions (2.115) and (2.116) and the excellent limits, formula (2.114) with the countercurrent through the complexes  $P$  and  $R$  takes the form:

$$\Delta t_{JI} = (t_{H2} - t_{H1}) \cdot \frac{R-1}{\ln \frac{1-P}{1-PR}} \quad \text{при } R \neq 1 \quad \text{and} \quad \Delta t_{JI} = (t_{H2} - t_{H1}) \cdot \frac{1-P}{P} \quad \text{при } R = 1. \quad (3.2)$$

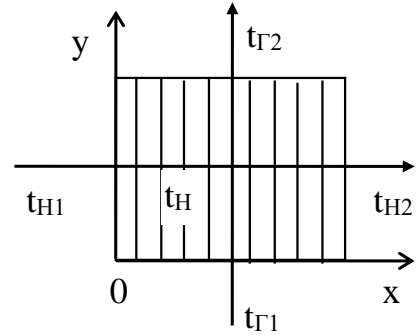
Usually, two extreme states of the coolant are distinguished: mixed and unmixed. Complete mixing implies that all the liquid (gas) in any given plane normal to the flow direction has the same temperature, although this temperature varies in the flow direction. An unmixed flow means that there are temperature differences in the liquid (gas) at least in the direction of one of the normal to the flow direction, but there is no heat flux associated with these temperature differences. It is noted that if one or both of the heat transfer fluids are partially mixed, then the calculation method  $\Delta t_{CP}$  is not available. It is indicated that  $\Delta t_{CP}$  is lower when one of the heat transfer fluids is mixed than when both heat transfer fluids are not mixed [18]. In many real heat exchangers, the actual flow is partially mixed. Fig. 3.1 shows all possible cases of a single cross-current. The conclusions of the formulas are given below for schemes where one of the heat transfer fluids is mixed (Fig. 3.1 a and b) and which are mainly used in surface heat exchangers of power plants of TPPs and NPPs. The scheme of Fig. 3.1, when both heat transfer fluids are not mixed, is often found in other types of heat exchangers, and the scheme of Fig. 3.1 d, when both

coolants are mixed, has not found much practical application [18]. However, in order to summarise the results at the end of the section, we will give the final dependencies for all possible cross-current schemes. In the heat exchanger schemes given in the literature, it is assumed that the number of parallel elements (pipes or rows of pipes, sections, spiral coils, hereinafter referred to as pipes) that cross the mixed and unmixed coolant is infinite (or quite large).

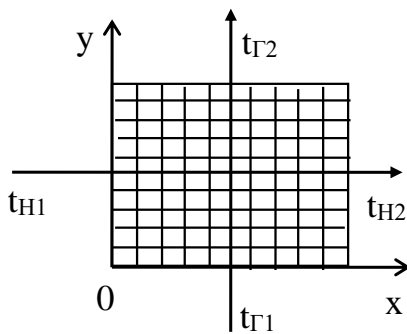
The formulas for average temperature heads for a one-pass (single) cross-current (see Fig. 3.1) are obtained after integrating the temperature heads along the  $0 \leq x \leq 1$  axes:



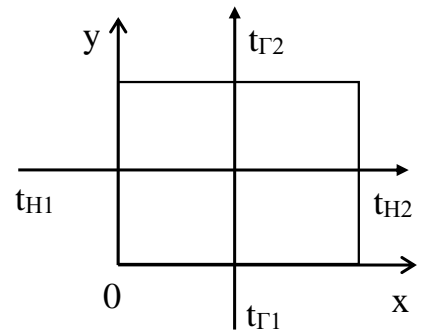
a) the heating coolant is mixed



b) the coolant is mixed and heated



c) both coolants do not mix



d) both coolants are mixed

$t_{\Gamma 1}, t_{\Gamma 2}$  - temperatures of the heating medium at the inlet and outlet

$t_{H1}, t_{H2}$  - temperatures of the heated coolant at the inlet and outlet

Fig. 3.1 - Diagrams of an elementary single cross-current

$$\Delta t_{CP} = -\frac{t_{H2} - t_{H1}}{\ln\left(1 - \frac{t_{H2} - t_{H1}}{t_{\Gamma1} - t_{\Gamma2}} \ln \frac{t_{\Gamma1} - t_{H1}}{t_{\Gamma2} - t_{H1}}\right)} \text{ (diagram of Fig. 3.1 a), } \quad (3.3)$$

$$\Delta t_{CP} = -\frac{t_{\Gamma1} - t_{\Gamma2}}{\ln\left(1 - \frac{t_{\Gamma1} - t_{\Gamma2}}{t_{H2} - t_{H1}} \ln \frac{t_{\Gamma1} - t_{H1}}{t_{\Gamma1} - t_{H2}}\right)} \text{ (diagram of Fig. 3.1 б), } \quad (3.4)$$

$$\Delta t_{CP} = \frac{t_{\Gamma1} - t_{\Gamma2}}{\ln \frac{t_{\Gamma1} - t_{H1}}{t_{\Gamma2} - t_{H1}}} + \frac{t_{H2} - t_{H1}}{\ln \frac{t_{\Gamma1} - t_{H1}}{t_{\Gamma1} - t_{H2}}} - (t_{\Gamma1} - t_{H1}) \text{ (diagram of Fig. 3.1 в), } \quad (3.5)$$

$$\Delta t_{CP} = \frac{t_{\Gamma1} - t_{\Gamma2}}{\ln \frac{t_{\Gamma1} - t_{H2}}{t_{\Gamma2} - t_{H2}}} + \frac{t_{H2} - t_{H1}}{\ln \frac{t_{\Gamma2} - t_{H1}}{t_{\Gamma2} - t_{H2}}} - (t_{\Gamma2} - t_{H2}) \text{ (diagram of Fig. 3.1 г). } \quad (3.6)$$

Using relation (3.1) and formulas (3.2)-(3.6), we obtain the dependences of the correction factors for a single cross-current with an infinite number of parallel unmixed elements:

$$\psi = -\frac{1}{\delta} \frac{1}{\ln\left(1 + \frac{1}{R} \ln(1 - PR)\right)}; \text{ (diagram of Fig. 3.1 a)} \quad (3.7)$$

$$\psi = -\frac{1}{\delta} \frac{R}{\ln(1 + R \ln(1 - P))}; \text{ (diagram of Fig. 3.1 б)} \quad (3.8)$$

$$\psi = -\frac{1}{\delta} \left( \frac{1}{\ln(1 - P)} + \frac{R}{\ln(1 - PR)} + \frac{1}{P} \right); \text{ (diagram of Fig. 3.1 в)} \quad (3.9)$$

$$\psi = \frac{1}{\delta} \left( \frac{R}{\ln \frac{1 - P}{1 - P(R+1)}} + \frac{1}{\ln \frac{1 - PR}{1 - P(R+1)}} - \frac{1 - P(R+1)}{P} \right); \text{ (diagram of Fig. 3.1 г)} \quad (3.10)$$

where  $\delta$  - is a dimensionless parameter:

$$\delta = \frac{R - 1}{\ln \frac{1 - P}{1 - PR}}, \text{ at } R \neq 1 \text{ and } \delta = \frac{1 - P}{P} \text{ at } R = 1. \quad (3.11)$$

The results of calculations using formulas (3.7)-(3.10) are shown in Fig. 3.2 in the form of graphs similar to those given in the literature.

Some expressions for a single cross-current (transformed or implicit) are mentioned in some literature sources [1, 18, 36].

Figs. 3.3, 3.4 show variants of the multi-pass (multiple) cross-current, where one of the coolants is mixed. It is assumed that the flow rates and heat capacities of the coolants, heat transfer coefficients and areas are the same for all passages and the number of pipes is infinite (sufficiently large).

When deriving the dependencies from the example of the current circuit in Fig. 3.3 with the sequential inclusion of the moves of the type shown in Fig. 3.1a, we use a system consisting of the equations of heat balance and heat transfer for the entire heat exchanger and its individual passes, the formula (3. 3) of the average temperature head for a single cross-current in one pass:

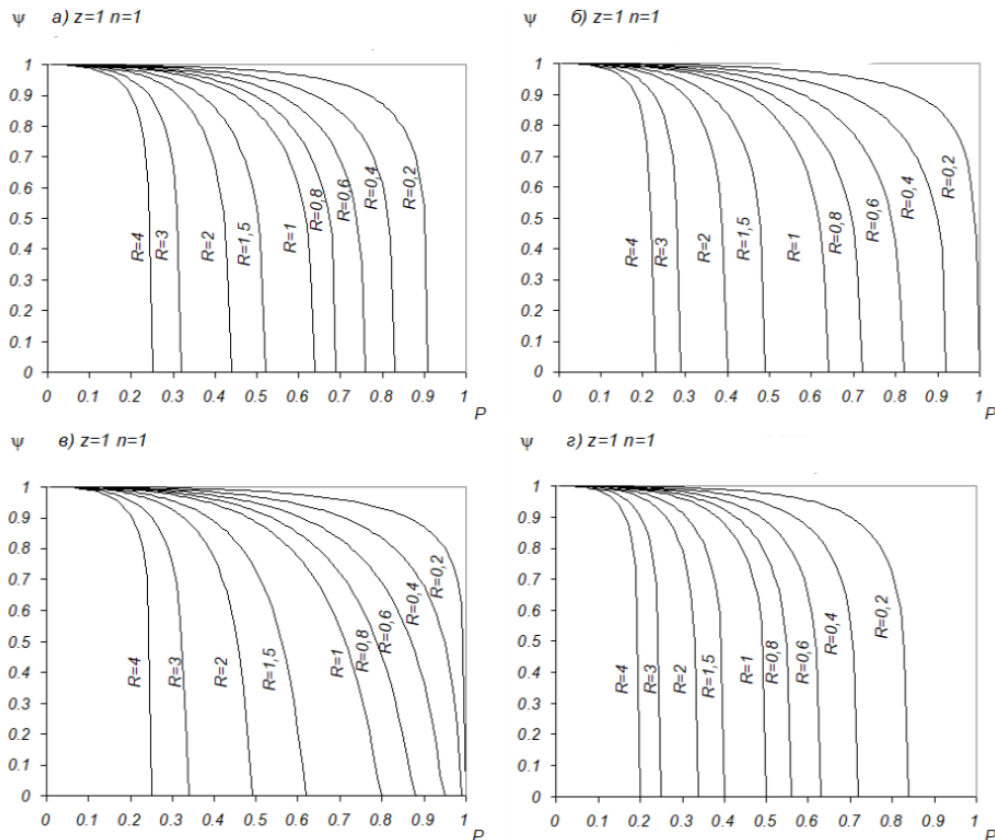


Fig. 3.2 - Graphs of correction factors for a single cross-current for elementary current circuits from Fig. 3.1

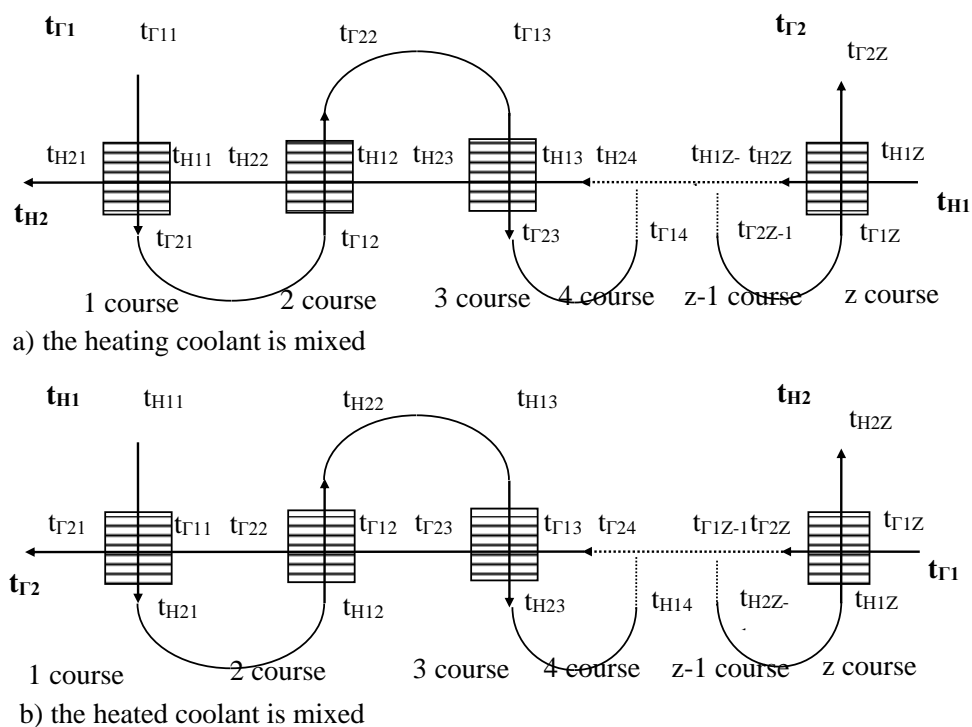


Fig. 3.3 - Diagram of multiple cross-current at countercurrent switching of strokes

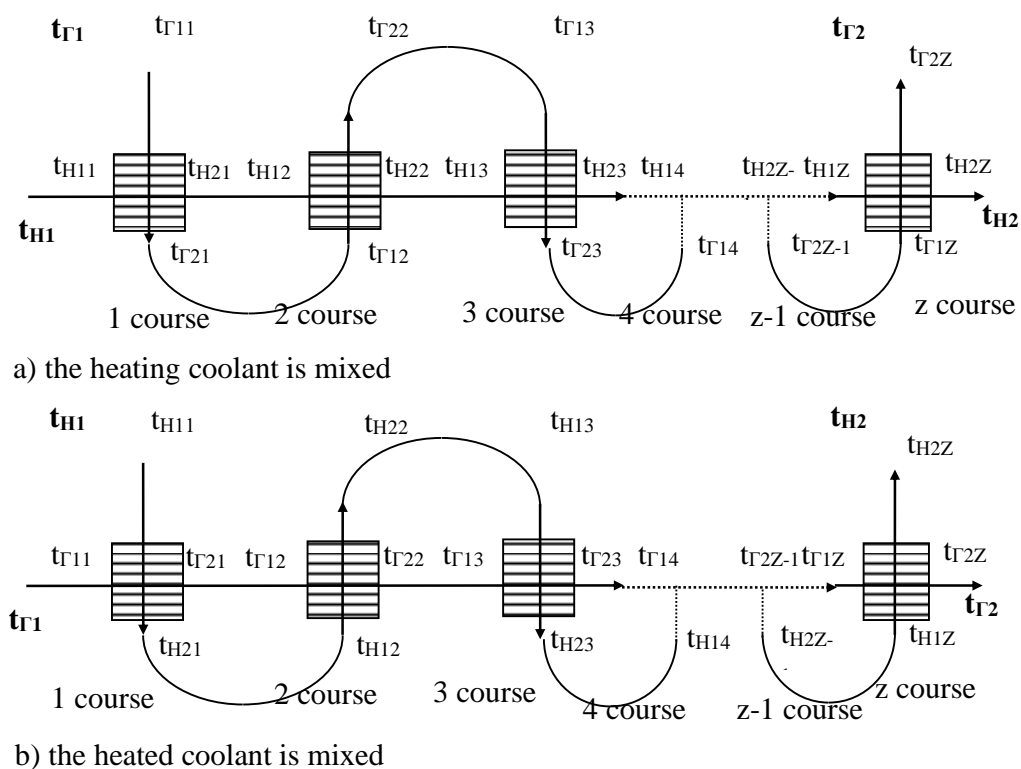


Fig. 3.4 - Diagram of multiple cross-current with direct-flow switching of strokes

$$Q_j = c_{PH} G_H(t_{H2j} - t_{H1j}) = c_{PT} G_T(t_{T1j} - t_{T2j}) = K \Delta t_{CPj} F_j \text{Ta}^{F_j} = \frac{F}{z}; \quad (3.12)$$

$$Q = \sum_{j=1}^z Q_j = c_{PH} G_H(t_{H2} - t_{H1}) = c_{PT} G_T(t_{T1} - t_{T2}) = K \Delta t_{CP} F; \quad (3.13)$$

$$t_{T1j} = t_{T2j-1}, \quad t_{H1j} = t_{H2j+1}; \quad (3.14)$$

$$\Delta t_{CPj} = - \frac{t_{H2j} - t_{H1j}}{\ln \left( 1 - \frac{t_{H2j} - t_{H1j}}{t_{H1j} - t_{H2j}} \ln \frac{t_{H1j} - t_{H1j}}{t_{H2j} - t_{H1j}} \right)}, \quad (3.15)$$

where is the *number* -of moves;

$j$  - is the index of the current move;

equations are written for all current moves  $j$ .

After the transformation, the system of equations (3. 12)-(3.15) has the form:

$$\Delta t_{CP} = - \frac{t_{H2} - t_{H1}}{z} \sum_{j=1}^z \left[ \ln \left( 1 - \frac{t_{H2j} - t_{H1j}}{t_{T1j} - t_{T2j}} \ln \frac{t_{T1j} - t_{H1j}}{t_{T2j} - t_{H1j}} \right) \right]^{-1}, \quad (3.16)$$

$$t_{T1j} = t_{T2j-1}, \quad t_{H1j} = t_{H2j+1} \quad \frac{t_{T1j} - t_{T2j}}{t_{H2j} - t_{H1j}} = \frac{c_{PH} G_H}{c_{PT} G_T} = R = \text{const}, \quad (3.17)$$

$$\ln \left( 1 - \frac{t_{H2j} - t_{H1j}}{t_{T1j} - t_{T2j}} \ln \frac{t_{T1j} - t_{H1j}}{t_{T2j} - t_{H1j}} \right) = - \frac{KF}{z c_{PH} G_H} = \text{const}. \quad (3.18)$$

After the transformation, the system (3. 16)-(3.18) takes a simple form:

$$\frac{t_{T1j} - t_{H1j}}{t_{T2j} - t_{H1j}} = \text{const}, \quad t_{T1j} = t_{T2j-1} \text{ and } t_{H1j} = t_{H2j+1}. \quad (3.19)$$

The system of equations (3. 19) is reduced to a dimensionless form:

$$\frac{t_{T1j} - t_{H1j}}{t_{T2j} - t_{H1j}} = \frac{1 - P + \varphi_j P - \varphi_{j-1} PR}{1 - P + \varphi_j P - \varphi_j PR} = \text{const}. \quad (3.20)$$

where  $\varphi_j$ , is an additional dimensionless parameter introduced equal to the degree of heating of the heating medium heated from the first stroke of the heating medium to the current stroke  $j$  inclusive:

$$\varphi_j = \frac{t_{H2} - t_{H1j}}{t_{H2} - t_{H1}} . \quad (3.21)$$

The system (3.20) is represented as a sequence:

$$\varphi_j + \frac{1-P}{P(1-R)} = \frac{\left( \varphi_{j-1} + \frac{1-P}{P(1-R)} \right)^2}{\varphi_{j-2} + \frac{1-P}{P(1-R)}} . \quad (3.22)$$

As can be seen from the sequence (3.22), the degree of heating in the current stroke  $j$  depends on the two previous values. To solve this system of equations, it is enough to know the degree of heating in the first stroke  $\varphi_1$  (in the zero (inlet)  $\varphi_0 = 0$ , and in the last (outlet)  $\varphi_Z = 1$ ). Writing down the systems of equations (3.20) for one-, two-, and three-pass heat exchangers and using the sequences (3.22), it is possible to obtain the expressions  $\varphi_1$ :

- for a single pass heat exchanger:

$$\varphi_1 = \frac{1-P}{P(1-R)} \left[ \left( \frac{1-PR}{1-P} \right) - 1 \right], \quad (3.23)$$

- for a two-pass heat exchanger:

$$\varphi_1 = \frac{1-P}{P(1-R)} \left[ \left( \frac{1-PR}{1-P} \right)^{\frac{1}{2}} - 1 \right], \quad (3.24)$$

- for a three-pass heat exchanger:

$$\varphi_1 = \frac{1-P}{P(1-R)} \left[ \left( \frac{1-PR}{1-P} \right)^{\frac{1}{3}} - 1 \right]. \quad (3.25)$$



It is obvious that with an arbitrary number of passes  $z$ , the final statements for  $\varphi_1$  using the method of mathematical induction will be:

$$\varphi_1 = \frac{1-P}{P(1-R)} \left[ \left( \frac{1-PR}{1-P} \right)^{\frac{1}{z}} - 1 \right]. \quad (3.26)$$

Similarly, using the sequence (3.22), the values of  $\varphi_0 = 0$  i  $\varphi_1$ , we obtain the values of the current degree of heating of the coolant heated by  $\varphi_j$  from stroke 1 to stroke  $j$  inclusive:

$$\varphi_j = \frac{1-P}{P(1-R)} \left[ \left( \frac{1-PR}{1-P} \right)^{\frac{j}{z}} - 1 \right]. \quad (3.27)$$

After substituting the values of  $\varphi_j$  y into equation (3.20) and then their dependence on  $\Delta t_{CP}$  (3.16), using the relations (3.1) - (3.2) and excellent limits, we obtain the formulas of correction factors for the multiple cross-current of the circuit of Fig. 3.3. a, where the moves (elements) from Fig. 3.1 a are connected in series [37]:

$$\psi = \frac{1}{z} \frac{\frac{1}{R-1} \ln \frac{1-PR}{1-P}}{\ln \left( 1 - \frac{1}{R} \ln \left( \frac{1}{R-1} \left( R \left( \frac{1-PR}{1-P} \right)^{-\frac{1}{z}} - 1 \right) \right) \right)} \quad \text{at } R \neq 1; \quad (3.28)$$

$$\psi = -\frac{1}{z} \frac{\frac{P}{1-P}}{\ln \left( 1 - \ln \left( 1 + \frac{1}{z} \frac{P}{1-P} \right) \right)} \quad \text{at } R = 1. \quad (3.29)$$

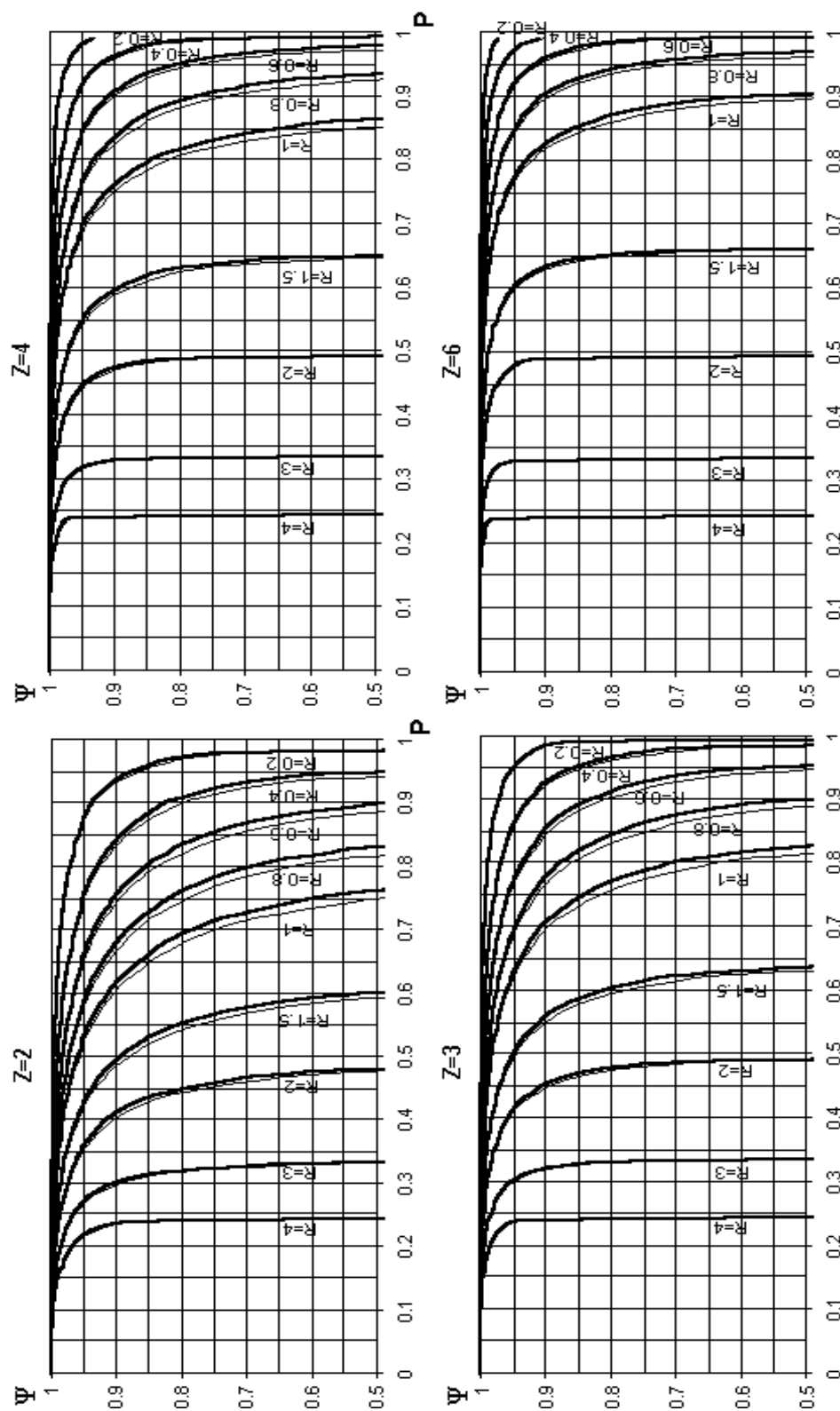
Fig. 3.5 shows the graphs of correction factors for the multiple cross-current circuits of the corresponding Figs. 3.3. a, where the moves (elements) from Fig. 3.1 a are included in series, constructed according to formulas (3.28) and (3.29). For comparison, the results of calculations for the same current circuit according to complex implicit dependencies of the form  $(P=f(P,R, \psi))$  from [18] are

superimposed by thin lines. These dependencies are different for each number of moves  $z$  (up to 6 in total). The solutions to these equations were obtained by the chord method [22 , 23]. The figure shows a good agreement of the results.

Fig. 3.6 shows a diagram of a one-stroke (one-time) cross-current, similar to Figs. 3.1 a and 3.1 b, provided that one of the coolants moves in a cross-current pattern, and the other in pipes or rows (sections) of pipes, spiral coils (hereinafter referred to as pipes). The number of pipes  $n$  is finite.

It is assumed here that the coolant moving in a cross-flow pattern between the pipes is completely mixed (see Fig. 3.6), and that its jets are not mixed when the pipes themselves are washed (which is practically true, especially for spiral coils). The heat transfer fluid flowing inside will be mixed for each individual pipe, and not mixed for the heat exchanger as a whole.

For the heat exchanger as a whole, Fig. 3.6, a corresponds to Fig. 3.1 a, and Fig. 3.6 b corresponds to Fig. 3.1 b for a single cross-current and an infinite (sufficiently large) number of pipes where one of the heat transfer fluids is mixed. For a single pipe, Fig. 3.6, a corresponds to Fig. 3.1 b, and Fig. 3.6 b corresponds to Fig. 3.1 a at a single cross-current and an infinite (sufficiently large) number of pipes where one of the heat carriers is mixed between them. This scheme is similar to the parallel connection of passages.



$z$  - the number of strokes of the heating coolant

Fig. 3.5 - Graphs of correction coefficients for multiple cross flow (Fig. 3.3 a) with an infinite number of pipes

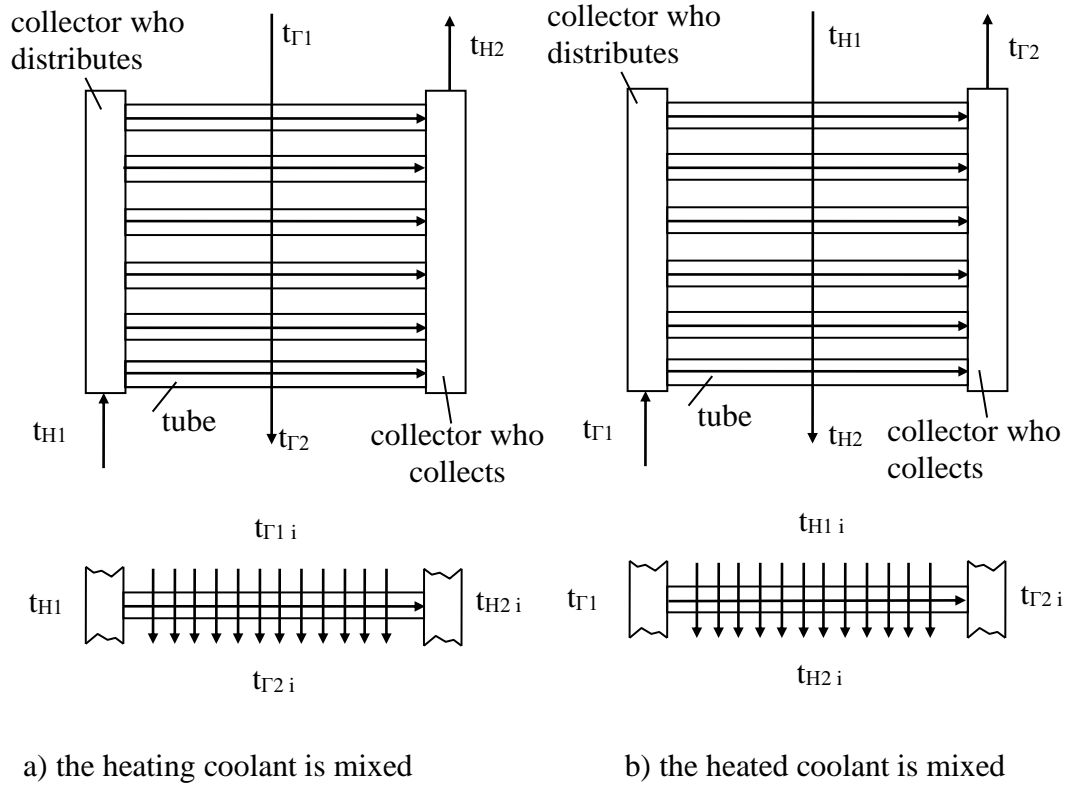


Fig. 3.6 - Diagrams of a single cross-current at a finite number of pipes

When deriving the dependencies for this type of cross-current, a system of heat balance and heat transfer equations for the entire heat exchanger and its individual passages is used, similar to the previously given (3.12)-(3.15). Here, we consider a scheme where the heating medium is mixed between the pipes (passages) (see Fig. 3.6 a). However, the parallel elements (pipes, passages) will be the elements from Fig. 3.1 б:

$$Q_i = c_{PH} G_{Hi} (t_{H2i} - t_{H1}) = c_{PT} G_{Ti} (t_{\Gamma1i} - t_{\Gamma2i}) = K \Delta t_{CPi} F_i; \quad (3.30)$$

$$Q = \sum_{i=1}^n Q_i = c_{PH} G_H (t_{H2} - t_{H1}) = c_{PT} G_T (t_{\Gamma1} - t_{\Gamma2}) = K \Delta t_{CP} F; \quad (3.31)$$

$$G_{Hi} = \frac{G_H}{n}, \quad F_i = \frac{F}{n} \quad t_{\Gamma1i} = t_{\Gamma2i-1}; \quad (3.32)$$

$$\Delta t_{CPi} = - \frac{t_{\Gamma 1i} - t_{\Gamma 2i}}{\ln \left( 1 - \frac{t_{\Gamma 1i} - t_{\Gamma 2i}}{t_{H2i} - t_{H1}} \ln \frac{t_{\Gamma 1i} - t_{H1}}{t_{\Gamma 1i} - t_{H2i}} \right)}, \quad (3.33)$$

where  $n$  - is the number of passages (pipes);

$i$  -is the index of the current stroke (pipe);

equations are written for all current moves (pipes)  $i$ .

After the transformations, this system of equations is given in the form:

$$\Delta t_{CP} = - \frac{t_{\Gamma 1} - t_{\Gamma 2}}{n} \sum_{i=1}^n \left[ \ln \left( 1 - \frac{t_{\Gamma 1i} - t_{\Gamma 2i}}{t_{H2i} - t_{H1}} \ln \frac{t_{\Gamma 1i} - t_{H1}}{t_{\Gamma 1i} - t_{H2i}} \right) \right]^{-1}; \quad (3.34)$$

$$t_{\Gamma 1i} = t_{\Gamma 2i-1} \quad t_{H2} = \frac{1}{n} \sum_{i=1}^n t_{H2i}; \quad (3.35)$$

$$\frac{t_{\Gamma 1i} - t_{\Gamma 2i}}{t_{H2i} - t_{H1}} = \frac{c_{pH} \frac{G_H}{n}}{c_{p\Gamma} G_{\Gamma}} = \frac{R}{n} = \text{const}; \quad (3.36)$$

$$\ln \left( 1 - \frac{t_{\Gamma 1i} - t_{\Gamma 2i}}{t_{H2i} - t_{H1}} \ln \frac{t_{\Gamma 1i} - t_{H1}}{t_{\Gamma 1i} - t_{H2i}} \right) = - \frac{KF}{nc_{p\Gamma} G_{\Gamma}} = \text{const}. \quad (3.37)$$

System (3.34)-(3.37) are reduced to the dimensionless form:

$$\frac{t_{\Gamma 1i} - t_{H1}}{t_{\Gamma 1i} - t_{H2i}} = \frac{1 - PR + \varphi_i PR - (\varphi_i - \varphi_{i-1})nP}{1 - PR + \varphi_i PR} = \text{const}; \quad (3.38)$$

where  $\varphi_i$  - is the degree of cooling of the mixed (heating) coolant from 1 to  $n$  stroke (counting from its outlet):

$$\varphi_i = \frac{t_{\Gamma 1i} - t_{\Gamma 2}}{t_{\Gamma 1} - t_{\Gamma 2}}. \quad (3.39)$$

The systems (3.38), (3.39) are presented in the form of a sequence:

$$\varphi_i + \frac{1-PR}{PR} = \frac{\left(\varphi_{j-1} + \frac{1-PR}{PR}\right)^2}{\varphi_{j-2} + \frac{1-PR}{PR}}. \quad (3.40)$$

The values of  $\varphi_0 = 0$ ,  $\varphi_n = 1$ , and  $\varphi_1$  can be obtained similarly to the conclusions for the multi-pass circuit given above:

$$\varphi_1 = \frac{1-PR}{PR} \left[ (1-PR)^{-\frac{1}{n}} - 1 \right]. \quad (3.41)$$

Using the sequences (3.42) and  $\varphi_0, \varphi_1$ , we find  $\varphi_i$  :

$$\varphi_i = \frac{1-PR}{PR} \left[ (1-PR)^{-\frac{i}{n}} - 1 \right]. \quad (3.42)$$

After substituting the values of  $\varphi_i$  in equation (3.38) and then - their dependence for  $\Delta t_{CP}$  (3.34), using relations (3.1)-(3.2), we obtain the formulas of correction factors for a single cross-current with the number of pipes  $n$  (Fig. 3.6 a, parallel elements from Fig. 3.1 b) [37]:

$$\psi = \frac{1}{n} \frac{\frac{R}{R-1} \ln \frac{1-PR}{1-P}}{\ln \left( 1 + \frac{R}{n} \ln \left( 1 - \frac{n}{R} \left( 1 - (1-PR)^{\frac{1}{n}} \right) \right) \right)} \quad \text{at } R \neq 1, \quad (3.43)$$

$$\psi = -\frac{1}{n} \frac{\frac{P}{1-P}}{\ln \left( 1 + \frac{1}{n} \ln \left( 1 - n \left( 1 - (1-P)^{\frac{1}{n}} \right) \right) \right)} \quad \text{at } R = 1. \quad (3.44)$$

If, depending on (3.43), the number of pipes  $n$  is set to infinity, it is easy to obtain (due to the cumbersome nature of the derivation, it is not shown) that formula

(3.43) turns into (3.7). If we set the number of pipes  $n = 1$ , then formula (3.43) becomes (3.8).

For multiple cross-current with a finite number of pipes  $n$  and the number of passes  $z$ , a system similar to (3.12)-(3.15) is developed. However, here, equation (3.15) for the average temperature head in one pass is replaced by an equation that takes into account the finite number of parallel elements (transformed to the dimensional form of formula (3.43), taking into account (2.115), (2.116) and (3.1):

$$\Delta t_{CPj} = \frac{-\frac{1}{n}(t_{\Gamma 1j} - t_{\Gamma 2j})}{\ln \left[ 1 + \frac{1}{n} \frac{t_{\Gamma 1j} - t_{\Gamma 2j}}{t_{H2j} - t_{H1j}} \ln \left( 1 - n \frac{t_{H2j} - t_{H1j}}{t_{\Gamma 1j} - t_{\Gamma 2j}} \left( 1 - \left( 1 - \frac{t_{\Gamma 1j} - t_{\Gamma 2j}}{t_{\Gamma 1j} - t_{H1j}} \right)^{\frac{1}{n}} \right) \right) \right]}. \quad (3.45)$$

Thus, in the case of a general countercurrent (see Fig. 3.3 a) with the sequential inclusion of the moves from Fig. 3.6 a and parallel inclusion of elements (pipes) from Fig. 3.1 b, the system will consist of equations (3.12)-(3.14) and (3.45). As a result, the generalised dependencies for single and multiple cross-current with the number of passes  $z$  and parallel pipes (rows of pipes, coils)  $n$  in one pass in this case will be:

$$\psi = \frac{\frac{1}{zn} \frac{R}{R-1} \ln \frac{1-PR}{1-P}}{\ln \left[ 1 + \frac{R}{n} \ln \left[ 1 - \frac{n}{R} \ln \left( 1 - \left( \frac{1}{R-1} \left( R \left( \frac{1-PR}{1-P} \right)^{-\frac{1}{z}} - 1 \right) \right)^{\frac{1}{n}} \right) \right] \right]} \quad \text{at } R \neq 1; \quad (3.46)$$

$$\psi = - \frac{\frac{1}{zn} \frac{P}{1-P}}{\ln \left[ 1 + \frac{1}{n} \ln \left[ 1 - n \ln \left( 1 - \left( 1 + \frac{1}{z} \frac{P}{1-P} \right)^{\frac{1}{n}} \right) \right] \right]} \quad \text{at } R = 1. \quad (3.47)$$

From the summarizing dependence (3.46) we can obtain:

a) for a single cross-current, where  $z=1$ :

- for an infinite number of pipes (i.e.  $n \rightarrow \infty$ ) – formula (3.7);
- for a finite number of pipes  $n$  (see the diagram in Fig. 3.6 a) – dependence (3.43);
- b) for a multiple cross-current with the number of strokes  $z$  for an infinite number of pipes (i.e.  $n \rightarrow \infty$ ) – equation (3.28).

It should be noted that if in formula (3. 7), formally swap the heating and cooling fluids, which is equivalent to replacing the parameters  $P$  with  $PR$  and  $R$  with  $1/R$  , we obtain dependence (3.8). Similarly, this is true for dependencies (3.28), (3.43) and (3.46), from which formulas for the cross-current can be obtained in the same way, where the flow of the heating medium rather than the heating fluid is assumed in the unmixed elements (i.e. pipes).

In the above calculations, we consider schemes where elements are involved as parallel (i.e., unmixed), with only one of the heat transfer fluids being mixed, and which are shown in Figs. 3.1 a and b. However, similar conclusions can be drawn initially for other schemes with the main elements shown in Figs. 3.1 and d (i.e. where both heat transfer fluids are mixed or not mixed). As a result, after summarizing all the calculations, the universal dependences on the parameters  $P$  ,  $R$  ,  $z$  and  $n$  for different types of single- and multi-pass cross-current (see the diagram in Fig. 3.7), where the parallel elements can be any of those shown in Fig. 3.1, will be as follows:

- b) the main element – a scheme where only the heated coolant is mixed (pipe, a series of pipes, a spiral coil) (see Fig. 3.1 a):

$$\psi = - \frac{R}{zn\delta} \frac{1}{\ln(1 + R \ln(1 - P_s))}; \quad (3.48)$$

- b) the main element – a scheme where only the heating medium is mixed (pipe, row of pipes, spiral coil) (see Fig. 3.1 b):



$$\psi = -\frac{1}{zn\delta} \frac{1}{\ln\left(1 + \frac{1}{R} \ln(1 - P_3 R)\right)}; \quad (3.49)$$

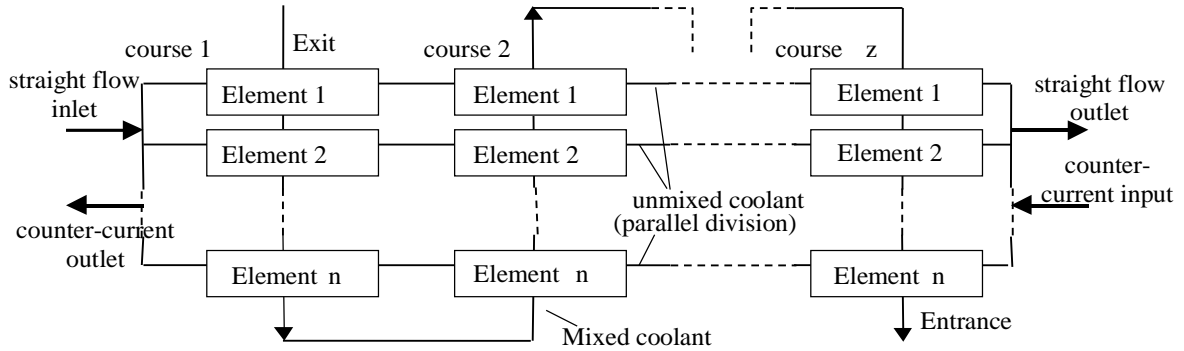


Fig. 3.7 - Generalised diagram of a multi-pass cross-current circuit with parallel element separation:

c) the main element is a circuit (section) where both coolants are not mixed (see Fig. 3.1 c):

$$\psi = -\frac{1}{zn\delta} \left( \frac{1}{\ln(1 - P_E)} + \frac{R}{\ln(1 - P_E R)} + \frac{1}{P_E} \right); \quad (3.50)$$

d) main element - a circuit (section) where both coolants are completely mixed (see Fig. 3.1 d):

$$\psi = \frac{1}{zn\delta} \left( \frac{R}{\ln \frac{1 - P_E}{1 - P_E(R+1)}} + \frac{1}{\ln \frac{1 - P_E R}{1 - P_E(R+1)}} - \frac{1 - P_E(R+1)}{P_E} \right), \quad (3.51)$$

where  $\delta$  - is a dimensionless parameter calculated according to Eq. (3.11);

$P_E$  - is a dimensionless temperature complex  $P$  of a separate heat exchanger element:

a) multiple of  $n$  parallel separation of the elements by the heated coolant:

$$P_E = 1 - \left( 1 - \frac{n}{R} \left( 1 - (1 - P_x R)^{\frac{1}{n}} \right) \right)^{\frac{1}{n}}, \quad (3.52)$$

b) multiple  $n$  parallel separation of elements by the heating medium:

$$P_E = \frac{1}{R} \left( 1 - \left( 1 - nR \left( 1 - (1 - P_x)^{\frac{1}{n}} \right) \right)^{\frac{1}{n}} \right), \quad (3.53)$$

where  $P_x$  is the dimensionless temperature complex  $P$  of a separate heat exchanger stroke:

a) multiple of  $z$  sequential multi-pass cross-flow of the heating or cooling medium in the common countercurrent:

$$P_x = \frac{1 - \left( \frac{1-P}{1-PR} \right)^{\frac{1}{z}}}{1 - R \left( \frac{1-P}{1-PR} \right)^{\frac{1}{z}}} \text{ at } R \neq 1 \text{ and } P_x = \frac{P}{z(1-P) + P} \text{ при } R = 1; \quad (3.54)$$

c) multiple  $z$  sequential multi-pass cross-flow of the heating or heating medium in the common upstream:

$$P_x = \frac{1 - (1 - P(R+1))^{\frac{1}{z}}}{R+1}. \quad (3.55)$$

In the limiting case, where the number of elements in the course tends to infinity ( $n \rightarrow \infty$ ), the following transformations were obtained using the excellent limits:

- formulas (3.50) and (3.51) with parallel distribution of elements in the procession along the heated coolant, as well as formula (3.48), turn into formula (3.49) when  $n = 1$ :

$$\psi = -\frac{1}{z\delta} \frac{1}{\ln \left( 1 + \frac{1}{R} \ln(1 - P_x R) \right)}; \quad (3.56)$$

- formulas (3.50) and (3.51) with parallel distribution of elements in the course along the heating medium, as well as formula (3.49), turn into formula (3.48) when  $n = 1$ :

$$\psi = - \frac{R}{z\delta} \frac{1}{\ln(1 + R \ln(1 - P_x))}, \quad (3.57)$$

where  $P_x$  is calculated according to dependencies (3.54) or (3.55).

From the comparative graphs of single current presented in Fig. 3.8 of the comparative graphs of the single current ( $z = 1$ ), it is clear that already at the number of parallel elements  $n = 10$ , the differences between the main elements of the heat exchanger completely disappear. But with the number of elements  $n = 4$ , the differences, as can be seen from Fig. 3.8 (a, b), are very significant.

In the limit of the multiple scheme, where the number of strokes tends to infinity ( $z \rightarrow \infty$ ), all the formulas for correction factors for countercurrent inclusion of strokes tend to unity (i.e.).

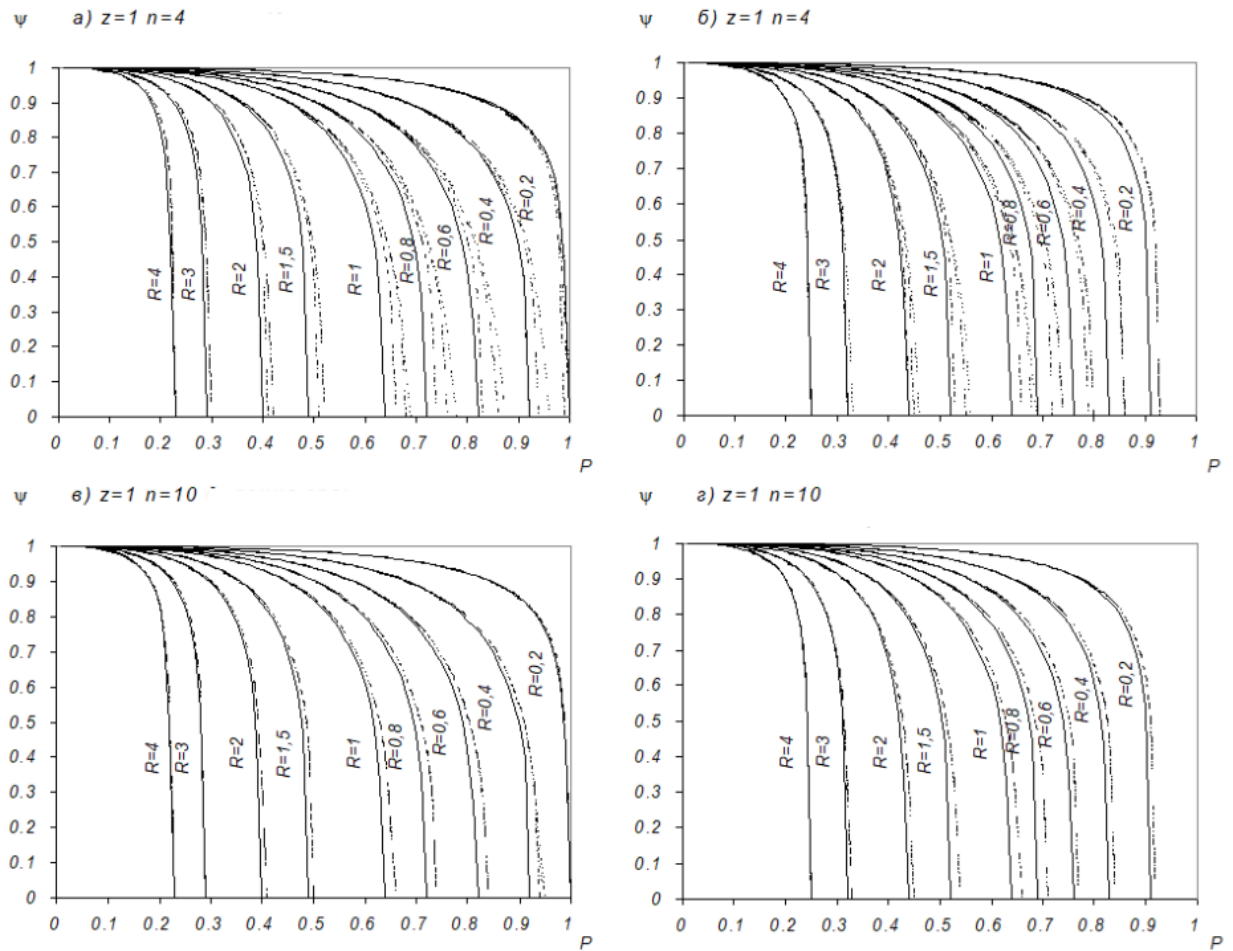


Fig. 3.8 - Graphs of correction factors for a single cross-current consisting of 4 (a, b) and 10 (c, d) parallel main cells. Lines: - element with two unmixed coolants; - element with two mixed coolants; - element with mixing of only the heating coolant (for a and c) and only the heated coolant (for b and d). The solid line shows the limits at  $n \rightarrow \infty$ .

In Fig. 3.9 shows comparative graphs of four times the current ( $z = 4$ ). It can be seen from the graphs that at this number of moves there is practically no difference between the results with the number of parallel elements  $n = 10$  and  $\infty$ . Thus, for current multiples greater than four, simpler dependencies (3.56) and (3.57) can be used. Otherwise, in order to prevent a decrease in the accuracy of calculations, it is recommended to use the generalised dependencies (3.48)-(3.51), since in the range of parameters  $P$  and  $R$  close to asymptotic, the difference in results can be very significant.

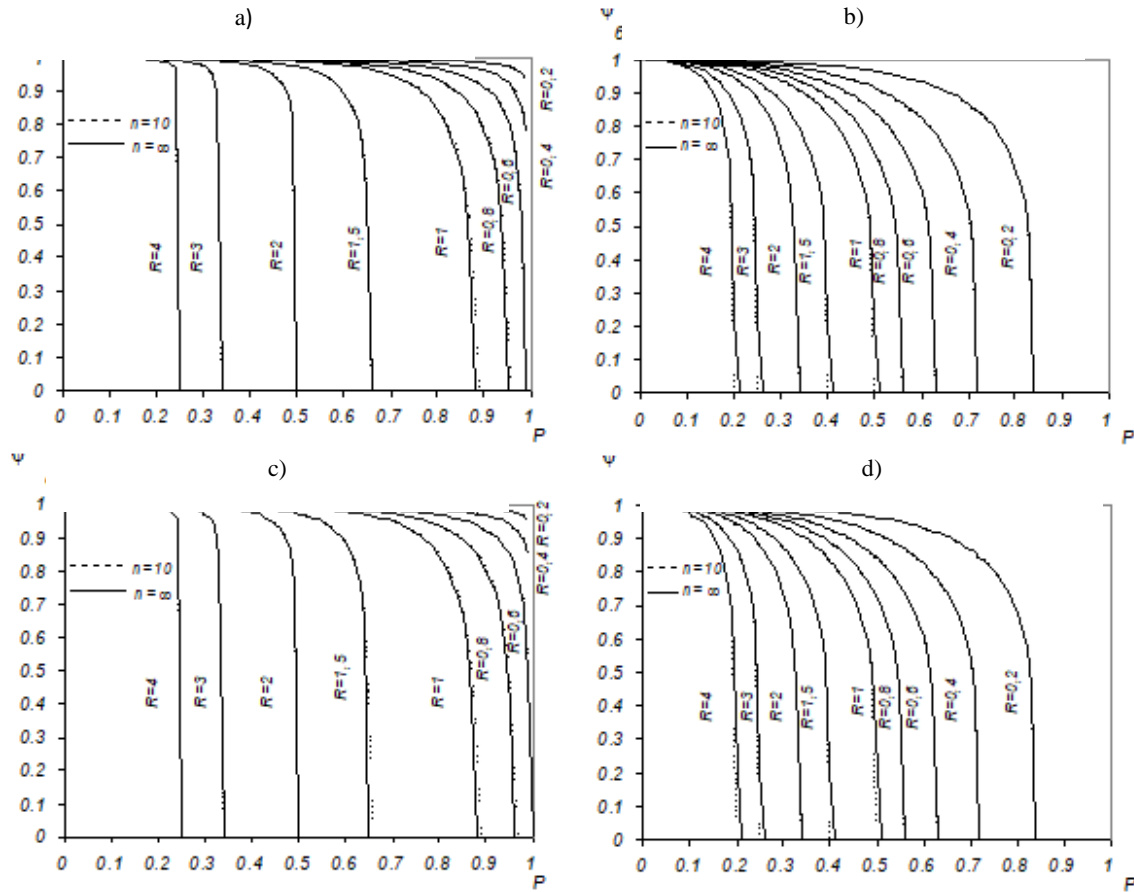


Fig. 3.9 - Graphs of correction factors for a fourfold cross-current ( $z = 4$ ), consisting of  $n = 10$  and  $n \rightarrow \infty$  parallel main elements.

- a) - countercurrent division of the heated coolant;
- b) - direct flow division of the heated coolant;
- c) - countercurrent heating coolant division;
- d) - direct flow heating coolant division.

According to the proposed universal analytical dependencies, it is possible to calculate the average temperature head at arbitrary cross-current multiplicity and the number of parallel cross-wash main elements (pipes, rows of pipes, sections, coils), as well as correctly set temperatures of the apparatus coolants, known from the heat exchanger design. Thus, the analytical dependencies of the correction factors presented in this book take into account both the number of cross-current passes and the number and type of parallel main elements in one pass. These dependencies can be used in design, verification, optimisation and other calculations of any similar cross-flow recuperative heat exchangers.

## **CHAPTER 4**

### **THERMAL AND HYDRAULIC CALCULATIONS FOR HIGH AND LOW PRESSURE SURFACE HEATERS AND THEIR GROUP**

#### **4.1 Design thermal and hydraulic calculation**

The structural thermal-hydraulic calculation of a heat exchanger is to determine the heat transfer surfaces of the apparatus required to transfer a given amount of heat. This calculation assumes predefined flow rates, temperatures (enthalpies) and pressures of the heat transfer fluids both at the inlet and outlet of the apparatus or its characteristic zones (i.e., the steam cooling, steam condensation and condensate coolers). The methodology for this calculation, unlike the verification calculation, is quite simple, since the required parameters are determined immediately without the use of iterative methods. Structural thermal-hydraulic calculation is usually carried out at the design stage of a heat exchanger or to select it from a standard range [3] (nomenclature).

Structural thermal and hydraulic calculation of heaters is preceded by a preliminary design study. This takes into account the design features depending on the location of the devices in the thermal scheme of the power plant (high or low pressure heater (determined by the pressure of feed water or main condensate), vacuum or high pressure (determined by the pressure of the heating steam from the turbine exhaust). The preliminary design includes: selection of the layout of the apparatus (i.e., the location of zones), determination of the mutual direction of flow, and the scheme of washing of pipe bundles or blocks of spiral elements. Both the design and subsequent thermal and hydraulic calculations involve the implementation of restrictions on the coolant velocity to prevent vibrations and corrosion wear of the heating surfaces.

It is recommended to take the steam velocity when flowing around pipe bundles no more than, m/s:

$$W_{\Pi} = 30\sqrt{v_{\Pi}} \text{ [4] and } W_{\Pi} = 45\sqrt{v_{\Pi}} \text{ [1]} - \text{transverse}; \quad (4.1)$$

$$W_{\Pi} = 80\sqrt{v_{\Pi}} \text{ [4] and } W_{\Pi} = 120\sqrt{v_{\Pi}} \text{ [1]} - \text{longitudinally}, \quad (4.2)$$

where  $v_{\Pi}$  - is the specific volume of steam at the inlet to the section,  $\text{m}^3/\text{kg}$ .

The velocity of the vapour-air mixture in the suction pipelines is recommended to be within 10-30 m/s. The cross-section of the air suction devices is determined from the conditions that the amount of the mixture to be sucked out is 0.25 % of the heating steam flow rate. In air suction devices as a perforated pipe, the holes are made with a diameter of 5-8 mm. To ensure uniform suction of the steam-air mixture, it is necessary that the resistance of the pipe is low compared to the resistance of the holes. This is achieved if the total cross-section of the holes is 23 times smaller than the pipe cross-section [2, 4].

The velocity of saturated steam in the nozzles of devices with a pressure above atmospheric pressure is recommended to be 30-50 m/s, with a pressure below atmospheric pressure – 80-100 m/s, superheated steam – 50-60 m/s [4]. To ensure uniform distribution of steam along the tube bundle and to prevent steam flow impacts, steam baffles are installed at the inlet of the tube bundle.

The condensate (drainage) velocity in the drain pipes is assumed to be 1.0-1.5 m/s (depending on the location of the steam trap and local resistance). The condensate velocity in the inter-pipe space of the condensate coolers (drainage) is recommended to be 0.515 m/s to prevent its boiling [1, 2, 4].

The diameters of the feedwater supply and drainage pipes should be calculated at a speed of 2-3 m/s in accordance with the diameters of the supply and drainage pipelines [2, 4].

In order to reduce the uneven distribution of water through the tubes in the chamber heaters and prevent impact erosion, it is recommended to install a removable grid (perforated sheet) 45 mm thick with 10 mm diameter holes in the water chambers at a distance of 100-150 mm from the tube board. On the other side

of the pipe board, a protective partition is installed at a distance of 30 mm from the pipe board to protect against the effects of superheated steam in the inlet area [2, 4].

The distance between the condensate drainage baffles in the chamber apparatus is determined taking into account the prevention of pipe vibrations, their abrasion against each other or the baffle, and ensuring the rigidity of the pipe system. In spiral-snake high pressure regenerative feed water heater, 1-10 spiral elements are usually placed between the condensate drainage baffles [1, 2, 4].

The velocity of water flows in the tubes  $W$  is determined from the conditions of ensuring the greatest heat transfer with restrictions on erosion and corrosion wear of their inlet sections. For the ratio of velocities  $W_{\text{КОЛ}} / W_0 \leq 2$  in steel carbon coils and tubes with a diameter of  $d = 22-24$  mm,  $d = 22-24$  mm  $W_0 \leq 1,7$  m/c, at  $d = 12-16$  mm  $W_0 \leq 2$  m/c; in brass and copper-nickel tubes,  $W_0 \leq 2$  m/c, in stainless steel tubes,  $W_0 \leq 3-4$  m/c [2].

Here,  $W_{\text{КОЛ}}$  та  $W_0$  - are the average velocities in the inlet cross-sections of the collector and outlet pipes of the heat exchange surfaces. The permissible velocity calculated from the nominal cross-section of the pipes should be 10% lower than the calculated  $W_0$ , i.e.  $W \approx 0,9 W_0$  [2].

If it is structurally necessary to have a velocity ratio  $W_{\text{КОЛ}} / W_0 \leq 2-5$ , in the apparatus, then  $W_0 \leq 1,6-1$  m/c [2].

The average water velocity in the collectors of spiral-coil high pressure regenerative feed water heater is taken in the range of 23 m/s, while the maximum velocity in carbon steel pipes should not exceed 5 m/s [2, 4].

The diameter of the tubes is selected from the range of thin-walled tubes, as well as taking into account the experience of designing heaters. For high-pressure regenerative feed water heaters heating surface pipes, it is usually 16 x 1 or 16 x 1.2 mm; for high-pressure regenerative feed water heaters spiral coils, it is 32 x 4, 32 x 5 or 32 x 6 mm [1-4].



It is recommended to design the built-in condensate cooler in high-pressure regenerative feed water heaters (condensate coolers) to pass the entire feedwater flow. This allows to increase the temperature head in the zone and reduce the required heat transfer surface. Such a design of the condensate cooler zone can be used for horizontal and vertical heaters with a lower water chamber [2]. In vertical heaters with *U*- or *P*- shaped tubes with an upper location of the water chamber, such a scheme of the condensate cooler zone is structurally difficult to implement due to the complexity of sealing the lower intermediate partition separating the control zone from the condensate cooler zone and the possible boiling of condensate as it rises. In such heaters, the coolant zone is usually made to the full height of the tube bundle by laying the required part of the feedwater tubes of the first pass into the casing [2]. In this case, the coolant is fed by condensate from the lower cavity of the heater and then, moving upwards, gives off heat to the feedwater. In this zone, as a rule, there is a transverse-longitudinal flow of condensate through the tube bundle. This flow is due to the fact that part of the pipe bundle is enclosed in a casing that forms the cooler, and there is no way to organise empty spaces for condensate to pass from one passage to another. Therefore, longitudinal washing of the outermost pipes of the bundle occurs, through which condensate passes from one run to another.

In chamber high-pressure regenerative feed water heaters, at a given water velocity  $W_{\text{IIB}}$  and a selected dimension  $d$ , the number of *U*- or *P*- shaped pipes installed in the heater tube board is given by [2, 4]:

$$N = \frac{z v_{\text{IIB}} G_{\text{IIB}}}{1,8 \pi d^2 W_{\text{IIB}}}, \quad (4.3)$$

where  $z$  - is the number of water passes in the heater (usually 4);

$v_{\text{IIB}}$  - is the specific volume of water, m<sup>3</sup> / kg;

$G_{\text{IIB}}$  - feed water (main condensate) flow rate of the heater, t/h.

The number of holes in the tube board  $N_{\text{д}}$  will be twice the number of *U*- or *P*-shaped tubes  $N$ . It is recommended to place the tubes in the tube board on the

sides of an equilateral triangle (triangular layout). This results in an equipartite staggered hexagonal layout with the cavities between the body and the hexagon filled (see Figures 1.7-1.9). The spacing  $S_{TP}$  is determined by the condition of maximum heat transfer from the outside of the tube bundle, the strength of the tube board and the fixing of the tubes in it, and is taken to be  $(1.35 - 1.5) \cdot d$ . Taking into account the experience of designing chamber high-pressure regenerative feed water heaters with a tube diameter of 16 mm, the spacing is usually 22 mm [2, 4].

The diameter of the entire tube board, and thus the internal diameter of the heater body, is initially assumed to be as follows [2, 4]:

$$D_{TP} = S_{TP} \sqrt{1,33 \frac{N_{\Delta}}{am} - 1}, \quad (4.4)$$

where  $a$  and  $m$  - are the coefficients that take into account the tubes located in the segments between the circumference of the tube board and the sides of the hexagon inscribed in it, as well as the number of tubes excluded when installing anchorages and inter-passage partitions in the water chamber (see Figs. 1.7 1.9).

The found internal diameter of the heater casing, taking into account the gap between the casing and the pipe system (necessary for removing the pipe system from it) and the casing wall thickness (determined by calculations of the strength of pressure vessels), is compared with the diameters of similar heaters from the nomenclature range [3, 4]. If it turns out that this diameter is significantly larger than the diameters of similar devices or transport dimensions, the length of the pipe system can be increased. However, the length of the pipe system, and therefore the height of the vertical heaters, is limited by the height of the machine room. If all these parameters do not fit the designed apparatus, it is necessary to switch either to a two-stream (two-strand) scheme or to make adjustments to the thermal scheme of the turbine unit [4].

After adjusting the diameter of the tube board  $D_{TP}$ , the number of holes in it (which must be even) is calculated again:

$$N_{\text{Д}} = 0,75(n_{\text{Д}}^2 - 1) + 1, \quad (4.5)$$

where  $n_{\text{Д}}$  - is the number of holes along the main diagonal of the hexagon,

$$n_{\text{Д}} = \frac{D_{\text{TP}}}{S_{\text{TP}}} + 1.$$

Next, the number of holes is adjusted due to the final bending radii of the pipes, filling of segments, installation of dividing walls and anchorages [2, 4].

If, after adjusting the number of holes on the pipe board, the water velocity in the pipes is within the specified permissible interval, the structural thermal calculation can be performed. At the same time, the design study of the pipe system shells, the steam cooling and condensate coolers zones, the steam supply casing and the frame structure of the pipe system is carried out [2, 4].

In spiral-collector high pressure regenerative feed water heater (see Figs. 1.10, 1.12), during the preliminary design study, the number of turns in the spiral is initially set, which is determined by the diameter of the pipes. The experience of designing high-pressure regenerative feed water heaters shows that the acceptable number of turns  $n$  in two-plane pipes ranges from 6 to 10. The smaller number of turns is usually in the steam cooler zone, and the larger number in the condensate coolers zone. The internal (minimum) diameter of a two-plane coil  $D_{\text{BH}}$  - is taken to be 0.19-0.2 m, and that of a single-plane coil - 0.15 m [1, 2, 4].

The winding pitch of spiral coils is usually taken to be  $S = d_{\text{H}} + 0,004 \text{ м}$  [1, 2, 4].

The outer (maximum) diameter of the coil is considered as follows [1, 2, 4]:

- for a single-plane spiral (Fig. 1.11 b):

$$D_{\text{H}} = 2 D_{\text{BH}} + 2 (n_{\text{B}} - 1) S_{\text{B}} \quad (4.6)$$

- for a two-plane helix (Fig. 1.11 a):

$$D_{\text{H}} = D_{\text{BH}} + (2 n_{\text{B}} - 1) S_{\text{B}}, \quad (4.7)$$

Next, the working length of the spiral coils is considered, which includes the part of the coil that is directly involved in the heat transfer process [1, 2, 4]:

- for a single-plane coil (Fig. 1.11 b):

$$l_p = \pi \frac{(D_H + 2D_{BH} - d_H - S_B)(D_H - 2D_{BH} - d_H + 2S_B)}{4S_B} - \pi \frac{2D_{BH} - 3S_B}{4}, \quad (4.8)$$

- for a two-plane helix (Fig. 1.11 a):

$$l_p = \pi \frac{(D_H + D_{BH})(D_H - D_{BH} + S_B)}{2S_B}. \quad (4.9)$$

The blocks of spiral coils of one stroke of a pair of zones of the heating medium and the cooling medium, for organising its flow, are enclosed in a casing, the inner diameter of which will be [1, 2, 4]:

$$D_K = D_H + d_H + \delta, \quad (4.10)$$

where  $\delta$ - is the gap,  $\delta = 10-15$  mm.

The internal diameter of the collectors is calculated based on the restrictions on the velocity of the feedwater in them  $W_{КОЛ}$ :

$$D_{КОЛ} = \sqrt{\frac{v_{ИБ} G_{ИБ}}{0,45\pi n_{КОЛ} W_{КОЛ}}}, \quad (4.11)$$

where  $n_{КОЛ}$  - is the number of collectors in the heater (usually 4 or 6).

The outer diameter of the collectors  $D_{КОЛH}$  is selected from the range of products with observance of the collector strength.

The diameter of the casing of the device body is determined depending on the layout. For a six-collector scheme [1, 4]:

$$D_{КОП} = 3 D_H + 2(\delta_1 + \delta_2), \quad (4.12)$$

$$D_{КОП} = 2(D_H + 2\delta_3) + 3 D_{КОЛH} + 2\delta_1 \quad (4.13)$$

where  $\delta$  - is the gap between the collectors and the housing,  $\delta_1 \geq 20$  mm;

$\delta_1$  - the gap between the coils and the housing,  $\delta_1' \approx 80$  mm;

$\delta_2$  - gap between the coils,  $\delta_{246} \geq \text{mm}$  -;

$\delta_3$  is the gap between the coil and the collector,  $\delta_3 = 15 - 40$  mm.

Of the two calculated values of the internal diameters of the casing, the larger one is accepted.

Taking into account the restrictions on the water velocity in the coils, the required number of coils in the zones is considered to be [1, 2, 4]:

$$N_3 = \frac{v_{\text{ИБ } 3} G_{\text{ИБ } 3}}{0,9 \pi d_3^2 W_{\text{ИБ } 3}}, \quad (4.14)$$

where '3' denotes the zones of steam cooling, steam condensation or condensate coolers;

$G_{\text{ИБ } 3}$  - feed water consumption in the heater zones, t/h.

The installation pitch on the collectors  $S_{\text{КОЛ}}$ , is usually taken for two-plane spirals - 75 -80 mm, single-plane  $\approx 38$  mm [1, 3].

The working height of the collector in the zones is considered as follows:

$$H_{\text{КОЛ } 3} = \left( \frac{N_3 z}{n_{\text{КОЛ}}} - 1 \right) \left( S_{\text{КОЛ}} + \frac{\delta_{\text{ПЕР}}}{n_{\text{ТП}}} \right), \quad (4.15)$$

where  $z$  - is the number of strokes in the zone;

$\delta_{\text{ПЕР}}$  and  $n_{\text{ТП}}$  - are the thickness of the partitions (if any) and the number of pipes between them.

The height of the pipe system is determined by the sum of the working heights of the collectors, as well as additional lengths required for the installation of bypass pipelines, casings, bypass boxes in the shells of the steam cooling and condensate coolers, the height of the upper and lower parts required for the pipelines

for distributing and removing water from the collectors, the height of the steam distribution collector 4].

After the preliminary determination of the geometric dimensions, it is necessary to work out the flow pattern of water and heating steam (condensate) in the heater [1-4].

The following values are usually known for the entire designed apparatus (low-pressure regenerative live water preheater, high pressure regenerative feed water heater or steam cooler) from the thermal diagram of the turbine plant

- feedwater (main condensate) and heating steam (condensate) inlet and outlet pressures;
- flow rate  $G_H$ , enthalpy of feed water (main condensate) at the inlet and outlet and  $i_{H_1}$  and  $i_{H_2}$
- is the flow rate  $G_{II}$  and enthalpy  $i_{II}$  of the heating steam at the inlet;
- flow rate  $G_{KK}$  and enthalpy  $i_{KK}$  of additional condensate from the cascade drain from the heater with higher steam pressure in the shell;
- flow rate  $G_{IIB}$  and enthalpy  $i_{IIB}$  of additional steam from the steam-air mixture (SAM), which is introduced from the heater with a higher steam pressure in the vessel;
- the enthalpy  $i_K$  of condensate (drainage) at the outlet, which flow  $G_K$  is determined from the material balance:

$$G_K = G_{II} + G_{KK} + G_{IIB} ; \quad (4.16)$$

- saturation temperature  $t_s$  at the steam pressure in the chamber of the control zone (for high-pressure regenerative feed water heaters or low pressure regenerative feed water heaters), thermophysical properties of water and water vapour at the saturation line [16, 17, 20, 21, 27, 38, 39] (formulas (2.25)-(2.36);

- flow areas for the movement of coolants (their definition is described in paragraph 2.6).

The structural thermal calculation of the heater begins with the condensate coolers (if it is available in the apparatus).

For this zone of the heat exchanger, the following must be known:

- the inlet and outlet pressures of the heat transfer media;

- the enthalpy  $i_{\Gamma_{1OK}}$  and temperature  $t_{\Gamma_{1OK}}$  of the condensate at the inlet. In this type of calculation, they are usually assumed to be equal to the condensate parameters  $i'$  and  $t_s$  of the saturation line (for high-pressure regenerative feed water heaters or low pressure regenerative feed water heaters);

- The flow rate  $G_{H_{OK}}$  and enthalpy  $i_{H_{1OK}}$  of feed water (main condensate) at the inlet to the SC, which corresponds to the value at the inlet to the heater  $i_{H_1}$ , and the temperature  $t_{H_{1OK}} = t_{H_1}$  is calculated using (2.37) or tables of thermal properties of water [21, 27, 38, 39];

- The enthalpy of condensate (drainage) at the outlet of the SC  $i_{\Gamma_{2OK}} = i_K$ . The temperature  $t_{\Gamma_{2OK}} = t_K$  corresponding to this and the pressure is calculated using (2.37) or tables of thermophysical properties of water [21, 27, 38, 39]. This temperature is usually above  $t_{H_1} 6 - 10^\circ \text{C}$ .

From the heat balance equation, the heat flux to be transferred in the zone,  $Q_{OK}$ :

$$Q_{OK} = G_K (i_{\Gamma_{1OK}} - i_{\Gamma_{2OK}}); \quad (4.17)$$

From the heat balance equation, the enthalpy of the feed water at the outlet of the condensate cooling is calculated:

$$i_{H_{2OK}} = i_{H_{1OK}} + \frac{Q_{OK}}{G_{H_{OK}}}; \quad (4.18)$$

According to the value of enthalpy  $i_{H_{2OK}}$  and pressure according to (2.37) or tables of thermophysical properties of water [21, 27, 38, 39], we determine  $t_{H_{2OK}}$  ;

Using formula (2.113), the average temperature pressure in the condensate cooling  $\Delta t_{CP OK}$  is calculated;

Using dependencies (2.106) - (2.112), the average temperatures of the heat carriers and pipe walls are calculated;

From the continuity equation (2.118), the coolant velocities are determined;

Criterion heat transfer coefficients are calculated (described in Section 2.3);

In accordance with dependence (2.54), the heat transfer coefficient in the condensate cooling  $K_{OK}$  section is determined;

The required heat transfer area in the condensate cooling is considered:

$$F_{OK} = \frac{Q_{OK}}{K_{OK} \cdot \Delta t_{CP OK}} . \quad (4.19)$$

This is usually the end of the design thermal calculation of the condensate cooler (condensate cooling or drainage cooler). The calculation of the condensing zone of the high-pressure regenerative feed water heaters or low pressure regenerative feed water heaters is then carried out. For the heat exchanger's steam condensation zone, the following are known:

- the inlet and outlet pressures of the heat transfer fluids;

- the enthalpy  $i_{\Gamma_{1KII}} = i_{II}$  of the heating steam at the inlet (if there is no steam cooler, i.e., the low pressure regenerative feed water heaters in the apparatus). The temperature  $t_{\Gamma_{1KII}} = t_{II}$  is calculated from the enthalpy and pressure dependence (2.47) or tables of thermal properties of superheated water steam [21, 27, 38, 39];

- the temperature of the heating steam at the inlet  $t_{\Gamma_{1KII}}$  , which is usually taken above the saturation temperature  $t_s$  to avoid droplet erosion of the pipe exterior



due to partial condensation of steam in the low pressure regenerative feed water heaters zone (if there is an low pressure regenerative feed water heaters). The enthalpy of superheated steam  $i_{\Gamma_{1\text{КП}}}$  corresponding to it and pressure is determined by the dependence (2.47) or tables of thermal properties [21, 27, 38, 39];

- enthalpy  $i_{\Gamma_{2\text{КП}}} = i'$  and temperature of condensate at the outlet  $t_{\Gamma_{2\text{КП}}} = t_s$ ;

- enthalpy  $i_{H_{1\text{КП}}}$  and temperature  $t_{H_{1\text{КП}}}$  of feed water (main condensate) at the inlet to the SC (steam condensation ). When connecting the cooler in parallel, or if there is no cooler in the apparatus, the enthalpy and temperature are equal to the values at the inlet to the heater  $i_{H_1}$  and  $t_{H_1}$ , and in the case of a pre-enabled cooler, the enthalpy is calculated by formula (2.17), and the temperature - by (2.37) or tables of thermophysical properties of water [21, 27, 38, 39];

- is the approximate value of the heat transfer area in the zone, since it depends on the determination of the heat transfer coefficient during steam condensation.

From the heat balance equation, the heat flux to be transferred in the zone is calculated,  $Q_{\text{КП}}$  :

$$Q_{\text{КП}} = G_{\Pi} i_{\Gamma_{1\text{КП}}} + G_{\text{КК}} i_{\text{КК}} + G_{\Pi\text{Б}} i_{\Pi\text{Б}} - G_{\text{К}} i_{\Gamma_{2\text{КП}}} ; \quad (4.20)$$

From the heat balance equation, the enthalpy of the feed water at the outlet of the boiler is calculated:

$$i_{H_{2\text{КП}}} = i_{H_{1\text{КП}}} + \frac{Q_{\text{КП}}}{G_{\text{H}}} ; \quad (4.21)$$

According to the enthalpy  $i_{H_{2\text{КП}}}$  and pressure values in accordance with (2.37) or tables of thermophysical properties of water [21, 27, 38, 39], we determine  $t_{H_{2\text{КП}}}$  . Here it is necessary to check that the condition  $t_{H_{2\text{КП}}} < t_s$  is met and the underheating of feed water (main condensate) at the outlet of the boiler to the

saturation temperature does not exceed 1-3 °C. Otherwise, it is necessary to revise the set parameters and repeat the calculation again;

In accordance with (2.113), the average temperature head in the control unit is calculated  $\Delta t_{CP\text{KII}}$ . However, here, the saturation temperature of the heating steam  $t_s$  should be substituted as the input and output temperatures of the heating medium;

Using dependencies (2.106)-(2.112), the average temperatures of the heat carriers and pipe walls are calculated;

The heat carrier velocities are calculated from the continuity equation (2.118);

Criterion heat transfer coefficients are determined (described in Section 2.3);

In accordance with dependence (2.54), the heat transfer coefficient in the control unit is  $K_{\text{KII}}$  calculated;

The required heat transfer area in the control unit is calculated:

$$F_{\text{KII}} = \frac{Q_{\text{KII}}}{K_{\text{KII}} \cdot \Delta t_{CP\text{KII}}} \quad (4.22)$$

The resulting area value is compared with the specified or previous value. If the discrepancy is greater than the permissible value, the zone calculation must be repeated.

At the final stage of the design thermal calculation, the steam cooler in the high pressure regenerative feed water heater and the low-pressure regenerative live water preheater (if any) is considered. For the heat exchanger header zone, the following are known:

- inlet and outlet pressures of the heat transfer fluids;
- enthalpy  $i_{\Gamma_{1\text{KII}}} = i_{II}$  of the inlet heating steam. The temperature  $t_{\Gamma_{20\text{II}}} = t_{\Gamma_{1\text{KII}}}$  is calculated from the enthalpy and pressure dependence (2.47) or tables of thermal properties of superheated water vapour [21, 27, 38, 39];

- enthalpy  $i_{\Gamma_{2O\Pi}} = i_{\Gamma_{1K\Pi}}$  and temperature  $t_{\Gamma_{2O\Pi}} = t_{\Gamma_{1K\Pi}}$  of the heating steam at the outlet;

- Feed water flow rate  $G_{H_{O\Pi}}$ , enthalpy  $i_{H_{1O\Pi}} = i_{H_{2K\Pi}}$  and temperature  $t_{H_{1O\Pi}} = t_{H_{2K\Pi}}$  of feed water (main condensate) at the inlet.

From the heat balance equation, the heat flux to be transferred in the zone is calculated,  $Q_{O\Pi}$ :

$$Q_{O\Pi} = G_{\Pi} (i_{\Gamma_{1O\Pi}} - i_{\Gamma_{2O\Pi}}); \quad (4.23)$$

From the heat balance equation, the enthalpy of the feed water (main condensate) at the outlet of the steam cooler (O\Pi) is calculated:

$$i_{H_{2O\Pi}} = i_{H_{1O\Pi}} + \frac{Q_{O\Pi}}{G_{H_{O\Pi}}}; \quad (4.24)$$

According to the values of enthalpy  $i_{H_{2O\Pi}}$  and pressure according to (2.37) or tables of thermophysical properties of water [21, 27, 38, 39], we calculate  $t_{H_{2O\Pi}}$ ;

According to formula (2.20), the enthalpy of feed water  $i_{H_2}$  at the outlet of the heater after conditional or actual mixing with the flow from the DHU is considered according to the equation of the heat balance of mixing. Based on its value and pressure, depending on (2.37) or tables of thermophysical properties of water [21, 27, 38, 39], the temperature  $t_{H_2}$  is calculated;

According to (2.113), the average temperature pressure in the steam cooling(O\Pi) is calculated  $\Delta t_{CP_{O\Pi}}$ ;

Using dependencies (2.106)-(2.112), the average temperatures of heat carriers and pipe walls are determined;

From the continuity equation (2.118), the coolant velocities are calculated;

Criterion heat transfer coefficients are calculated (described in Section 2.3);

In accordance with dependence (2.54), the heat transfer coefficient in the heat transfer device is determined  $K_{\text{OII}}$ ;

The required heat transfer area in the steam cooler is calculated:

$$F_{\text{OII}} = \frac{Q_{\text{OII}}}{K_{\text{OII}} \cdot \Delta t_{\text{CP OII}}} \quad (4.25)$$

The next design study of the low pressure regenerative feed water heaters or steam cooler is to adjust the pipe bundles based on the calculated areas:

The average working length of the *U*- or *P*- shaped tubes is calculated:

$$l_p = \frac{F}{\pi \cdot d_H \cdot N} \quad (4.26)$$

where  $F$  - is the total calculated heat transfer area of the entire apparatus; (the sum of all calculated areas  $F_{\text{OK}}$ ,  $F_{\text{KII}}$  i  $F_{\text{OII}}$ ) multiplied by a safety factor (usually taken in practice from 1.1 to 1.6) [2, 40];

The full length of the *U*- or *P*- shaped pipes is considered:

$$l_{\text{II}} = 2(h + n_{\text{IIEP}} \delta_{\text{IIEP}}) + l_p \quad (4.27)$$

where  $h$  - is the thickness of the pipe board (determined in the strength calculation);

$n_{\text{IIEP}}$  and  $\delta_{\text{IIEP}}$  are the number and thickness of partitions.

After that, the water chamber and the frame of the pipe system are worked out in detail [2, 4].

In spiral-collector heat exchangers, the number of pipes required to provide the heat transfer surface required by the thermal calculation of the heat transfer surfaces is adjusted:

$$N_3 = \frac{F_3}{\pi \cdot d_{H3} \cdot l_{p3}} \quad (4.26)$$

where '3' denotes the zones of the steam cooling, steam condensation or condensate coolers;

where  $F_3$  - is the calculated heat transfer area of the entire apparatus of the steam cooling, steam condensation or condensate coolers zone multiplied by a safety factor (usually taken in practice from 1.1 to 1.6) [2, 40].

Since the surface of a single pipe is known after determining the length of the coil, the calculated value of the number of coils in the zones, selected from the limitation of water velocity in the coils, is compared with the adjusted number of pipes. Thus, as a result of the thermal calculation, the preliminary design of the apparatus (height of the collectors and number of pipes) is changed. In coiled tubing, some parameters (flow areas, etc.) are usually also changed after the adjustment of the pipe bundles.

After all the flow areas have been adjusted, the hydraulic calculation of the apparatus is carried out by sequentially calculating the resistances and pressure losses of the heat carriers in the process of their movement (described in Section 2.5).

A verification calculation may be required to clarify the thermal characteristics of the heaters and their zones.

#### **4.2. Verification thermal-hydraulic calculation**

In contrast to the design calculation, the verification calculation of the heat exchanger knows in advance the design of the apparatus, all heat transfer areas, as well as operational features (the presence of layers of corrosion products and deposits on the pipe surfaces, air suction in the chamber, etc.) The parameters of the heat carrier are known only at the inlet to the apparatus. The task of the verification calculation is to determine the parameters of the heat transfer fluids at the outlet of the heat exchanger and inside it, as well as to calculate the efficiency (i.e., the efficiency). In addition, sometimes it is necessary to know the parameters and

efficiency of the heat exchanger not only at the design (nominal) operating mode, but also at other modes. Experience and practice show that this type of heat exchanger calculation is much more complicated than a structural thermal calculation. A complex nonlinear system of heat balance and heat transfer equations with all the criteria is usually solved here by successive approximations. It is practically impossible to implement such a calculation by a computer alone.

The algorithm of verification calculation of the high pressure regenerative feed water heater, low-pressure regenerative live water preheater or steam cooler on a computer should include the following main blocks: input and preparation of initial data, verification thermal-hydraulic calculation, preparation and output of results. In addition to the above blocks, the algorithm for the verification calculation of the high pressure regenerative feed water heater includes a block for the hydraulic calculation of the collector system (described in detail in Section 5).

The block for input and preparation of initial data should have the following main points: input of input parameters of heat carriers (pressures, flow rates and enthalpies); input of design characteristics; conversion of these values to the calculation systems used in the methodology; calculation of the required derivatives of design and geometric dimensions; setting the parameters of heat carriers for the initial approximation.

The block of preparation and output of results should include conversion of parameters and values to the technical system of units, if necessary; output of all necessary parameters and properties of heat carriers and pipe materials (at the inlet, outlet by sections and zones) and design characteristics to separate files.

The sequence and features of the algorithm for the verification thermal-hydraulic calculation of the entire heater can be as follows:

- 1) calculation of the condensate cooling zone. In addition to the design characteristics of the zone, the following parameters are set as initial parameters

- the enthalpy of condensate at the inlet  $i_{\Gamma_{1OK}}$  and its flow rate  $G_{KH}$  at the current approximation, which should be equal to that obtained as a result of calculating the condensation of steam in the control zone steam condensation (KП)  $i_{\Gamma_{2KП}}$ . For the drainage cooler, these parameters are set;

- the enthalpy of feed water at the inlet to the condensate coolers (OK)  $i_{H_{1OK}}$ , which is equal to the enthalpy of feed water at the inlet to the heater  $i_{H_1}$  and its flow rate through the zone  $G_{H_{OK}}$ .

As a result of the calculation of the heat balance and heat transfer in the cooler, the algorithm of which is given below, the following are calculated

- the enthalpy of condensate at the outlet of the heater or the condensate cooler:

$$i_K = i_{\Gamma_2} = i_{\Gamma_{2OK}} \quad (4.27)$$

- enthalpy of feed water at the outlet of the cooler condensate coolers  $i_{H_{2OK}}$ .

If there is no cooler, then

$$i_K = i_{\Gamma_2} = i_{\Gamma_{1OK}} = i_{\Gamma_{2KП}}, \quad i_{H_{2OK}} = i_{H_{1OK}} = i_{H_1} \quad (4.28)$$

2) calculation of the control zone. The initial parameters, in addition to the design characteristics of the zone, are set:

- Flow rate  $G_H$  and enthalpy  $i_{H_{1KП}}$  of feed water at the inlet to the control unit. When connecting the cooler in parallel, it is equal to the enthalpy of feed water at the inlet to the heater  $i_{H_1}$ , and when the cooler is switched on, it is calculated by formula (2.17);

- Flow rate  $G_{II}$  and enthalpy  $i_{\Gamma_{1KП}}$  of the heating steam at the inlet to the control unit. If there is a steam cooler in this heater condensate coolers  $i_{\Gamma_{2OП}}$ , it is equal to the enthalpy of steam at the outlet of the steam cooler calculated on the

previous approximation, and if there is no steam cooler, it is equal to the enthalpy of heating steam at the inlet to the heater  $i_{I_1}$ ;

- mass or volume  $\varepsilon_{II}$  content of air in the heating steam;
- flow rate  $G_{KK}$  and enthalpy  $i_{KK}$  of additional condensate from the cascade drain of the heater with a higher steam pressure in the vessel;
- flow rate  $G_{IIB}$  and enthalpy  $i_{IIB}$  of additional SWM steam injected from the heater with a higher steam pressure in the vessel;
- Flow rate  $G_{BB}$  of additional air from the SWM, which is introduced from the heater with a higher vapour pressure in the housing;

The heat balance and heat transfer in the zone are calculated according to the algorithm below.

As a result, at the outlet of the zone, the following are determined:

- enthalpy  $i_{I_{2KII}}$  and condensate flow rate  $G_K$ ;
- the enthalpy  $i_{IO}$  and flow rate  $G_{IO}$  of non-condensable steam, which is discharged from the heater through the air exhaust device to the downstream heater;
- The flow rate of the air  $G_{BO}$  that is discharged from the heater through the air extraction device to the downstream heater;
- enthalpy  $i_{H_{2KII}}$  of feed water at the inlet from the control unit.

This item is not included in the calculation of the steam cooler.

3) Calculation of the heat exchanger zone. As initial parameters, in addition to the design characteristics of the zone, the following are set

- enthalpy of feed water at the inlet to the steam cooling (condensate coolers)  $i_{H_{1OI}}$ , which is equal to the enthalpy of feed water at the outlet of the control unit  $KII$   $i_{H_{2KII}}$ , flow rate  $G_{H_{OI}}$  and pressure  $p_{H_{1OI}}$ ;



- the enthalpy of the heating steam at the inlet to the steam cooling (condensate coolers)  $i_{\Gamma_{10\Pi}}$ , which is equal to the enthalpy of the heating steam at the inlet to the heater  $i_{\Pi} = i_{\Gamma_1}$ , its flow rate  $G_{\Pi}$  and pressure  $p_{\Gamma_{10\Pi}}$ .

The heat balance and heat transfer in the zone are calculated according to the algorithm below.

As a result, the following are determined:

- the enthalpy  $i_{\Gamma_{20\Pi}}$  and pressure  $p_{\Gamma_{20\Pi}}$  of the heating steam at the outlet;
- enthalpy  $i_{H_{20\Pi}}$  and pressure  $p_{H_{20\Pi}}$  of the feed water at the outlet;

If there is no steam cooling, then

$$i_{\Gamma_{20\Pi}} = i_{\Gamma_{10\Pi}} = i_{\Gamma_1} = i_{\Pi}, \quad i_{H_{20\Pi}} = i_{H_{10\Pi}} = i_{H_{2K\Pi}}. \quad (4.29)$$

4) using formula (2.20), the enthalpy of feed water  $i_{H_2}$  at the outlet of the heater after conditional or actual mixing with the flow from the main heater is calculated according to the heat balance equation of mixing. It is determined regardless of whether there is a steam cooler or not;

5) in the low-pressure regenerative live water preheater, the feed water flow rate through the steam cooling (OII)  $G_{H_{0\Pi}}$  is calculated by the method of successive approximations, assuming equality of pressures at the point of mixing the flow from the steam cooling with the main flow. This takes into account the pressure losses of the flows in the water chambers, outlet pipes, throttle washer and pipes of the heating surface of the steam cooling. To accelerate the overall convergence of the calculation, this item can be directly included in the calculation of the steam cooling zone (item 3). If the entire feedwater flow rate is passed through the steam cooler or if it is absent, this item is not involved.

6) heat flows are calculated for the entire heat exchanger:

- a) given off by the heating medium (formula (2.1);

b) received by the heated coolant (formula (2.2);

7) determine the heat imbalance in the control unit as a function of :

$$\varphi_Q = Q_\Gamma - Q_H. \quad (4.30)$$

and the error due to the imbalance:

$$\varepsilon_Q = \frac{|\varphi_Q|}{Q_H} \cdot 100\%. \quad (4.31)$$

If the error value is greater than the permissible value, the calculation returns to step 1.

In the event that the steam flow rate through the air exhaust device  $G$  is less than zero, the material balance in the heater on the steam side is disturbed. Obviously, here part of the surface of the intertubular space (mainly in the lower part of the control zone) will be flooded with condensate. This process will be influenced by surface tension forces and the capillary effect. It is difficult to accurately calculate the heat transfer coefficient for such a process, where the heat transfer will be determined by condensation in the upper part of the vertical or horizontal pipe bundle and convection in the lower part. It is also difficult to say what part of the condensate will accumulate near the condensate drainage baffles and what part will accumulate at the bottom of the heater chamber. Therefore, the heat transfer coefficients for steam condensation in the control room can be corrected for condensate flooding  $\varepsilon_{3AT}$ . Such an integral correction factor can be found by the chord method [22, 23] as a function of zero steam flow through the air exhaust device  $G$ .

Thus, as a result of the calculation, a system of nonlinear equations of the mathematical model describing thermal processes in the heater is solved with a given accuracy with the linkage of the amount of condensate and non-condensable steam in the control unit. As a result, in addition to the drainage cooler, the balance of condensate flow according to formula (2.21) through the condensate coolers or at

the outlet of the heater through the corresponding pipe must be observed with a certain error after reaching the end of the calculation.

It should be noted that successive approximations can be made in a different way and the temperature of feed water or condensate at the outlet can be selected as the varying parameters for thermal calculations of the entire heat exchanger [2] with the refinement of subsequent values for the heat imbalance in one of the zones (condensate cooling, steam condensation or steam cooling) by methods of accelerating the iterative process (chords, tangents, etc. [22, 23]). However, this approach does not immediately determine the mode of operation of the control zone. As the practice of calculations shows, the process of iteration in this case converges very slowly, or even does not converge. The algorithm of this approach will be complicated by conditional transitions and additional procedures that determine the mode of operation of the control zone. In the proposed methodology, the convergence of the iterative process is determined by the heat balance equations for the entire heat exchanger.

In contrast to the thermal calculation algorithm, the hydraulic calculation algorithm is reduced to a sequential calculation for each zone and section of hydraulic and local resistances and pressure losses of heat transfer fluids. For feed water, pressure losses are calculated from the inlet through the inlet pipe, the condensate cooling, steam condensation and steam cooling zones, and the outlet pipe to the outlet. For heating steam (condensate) – from the inlet through the inlet pipe, the steam cooling, steam condensation and condensate cooling zones, the outlet pipe to the outlet. In the low-pressure regenerative live water preheater, where the feedwater flow through the steam cooling is determined by the throttle washer installed in the outlet pipe, the flow and pressure loss in the steam cooling are calculated by the method of successive approximations, taking into account that the feedwater pressure at the mixing point at the outlet of the steam cooling with the main flow flowing through the throttle washer should be equal. In a high pressure regenerative feed water heater, the pressure losses in the feed water path, as well as

its flow rates through individual pipelines, condensate coolers and steam cooling zones, cannot be calculated by a sequential calculation of pressure losses. Here, these parameters are determined by a complex calculation of collector systems, the methodology and algorithm of which are described in Section 5.

Next, we consider the specifics of the calculation algorithms for the characteristic zones of heaters – condensate cooling, steam condensation and steam cooling.

As initial data for the condensate coolers zone, the parameters of the heat carriers at the inlet (pressure  $p_{H_{1OK}}$  and  $p_{\Gamma_{1OK}}$ , enthalpy and  $i_{H_{1OK}}$  i  $i_{\Gamma_{1OK}}$ ), their flow rates  $G_{H_{OK}}$  and  $G_K$  of design characteristics are known. In case of dividing the condensate cooler zone into sections, the calculation is performed during feedwater. The condensate enthalpy at the outlet  $i_{\Gamma_{2OK}}$  is found by the method of successive approximations as a function of the zero heat imbalance in the entire condensate cooler zone (condensate coolers)  $\phi_{OK}$ . As a method of acceleration, it is advisable to choose the chord method [22, 23], for which two initial values are set.

The algorithm for calculating a separate section of the condensate coolers zone is as follows:

As initial parameters, the enthalpy of feed water at the inlet to the section  $i_{H_{1OK_j}} = i_{H_{2OK_{j-1}}}$ , condensate at the outlet of the section  $i_{\Gamma_{2OK_j}} = i_{\Gamma_{1OK_{j-1}}}$  with countercurrent or at the inlet to the section  $i_{\Gamma_{1OK_j}} = i_{\Gamma_{2OK_{j-1}}}$  with forward flow of coolants is known. For the first section, the enthalpy of feed water at the inlet  $i_{H_{1OK_1}} = i_{H_{1OK}}$  of the condensate at the outlet  $i_{\Gamma_{2OK_1}} = i_{\Gamma_{2OK}}$  with countercurrent flow of heat carriers or at the inlet  $i_{\Gamma_{1OK_1}} = i_{\Gamma_{1OK}}$  with direct flow of heat carriers is known. The pressure of the heat transfer fluids at the inlet  $p_{H_{1OK_j}} = p_{H_{2OK_{j-1}}}$  or outlet  $p_{\Gamma_{2OK_j}} = p_{\Gamma_{1OK_{j-1}}}$  of  $p_{\Gamma_{1OK_j}} = p_{\Gamma_{2OK_{j-1}}}$  the section  $p_{\Gamma_{2OK_j}}, p_{H_{2OK_j}}$  is considered to be in the external cycle;

By the method of successive approximations, the enthalpy of the condensate at the inlet  $i_{\Gamma_{1OK_j}}$  with countercurrent or outlet  $i_{\Gamma_{2OK_j}}$  with forward flow is calculated as a function of the zero heat imbalance in the condensate cooling section condensate coolers  $\phi_{OK_j}$ . As a method of acceleration, it is advisable to choose the chord method, for which two initial values of the condensate enthalpy are given;

The heat flux given off by the condensate is calculated:

$$Q_{OK_j} = G_K(i_{\Gamma_{1OK_j}} - i_{\Gamma_{2OK_j}}); \quad (4.32)$$

From the heat balance equation, the enthalpy of the feed water at the outlet is calculated:

$$i_{H_{2OK_j}} = i_{H_{1OK_j}} + \frac{Q_{OK_j}}{G_{HOK}}; \quad (4.33)$$

In accordance with the dependencies (2.37) of thermodynamic properties for underheated water, the inlet and outlet temperatures of feed water and condensate are calculated using known enthalpies and pressures. For the condensate, the saturation line crossing is checked (the enthalpy is compared with the one calculated using formula (2.27), where the saturation temperature is calculated according to the condensate pressure relationship (2.25)) and the degree of dryness is determined;

The average temperature pressure in the area  $\Delta t_{CP_{OK_j}}$  is calculated according to formula (2.113);

Using dependencies (2.106) – (2.112), the average temperatures of the heat carriers in the section and the pipe walls are calculated;

The thermophysical properties of feed water and condensate (dependencies (2.38)-(2.41) for underheated water) in the section (thermal conductivity, specific volume, kinematic or dynamic viscosity, Prandtl's number) are calculated at the average value of its temperature. If the degree of dryness of the condensate at the inlet and/or outlet is different from zero, its thermal properties are calculated as for

a two-phase medium. The thermal conductivity of the pipe material is determined by the average wall temperature (Table 2.9);

The velocities of the heat carrier are calculated from the continuity equation (2.118);

Criterion heat transfer coefficients of heat carriers and their resistances are calculated (given in paragraphs 2.3, 2.5);

In accordance with dependence (2.54), the heat transfer coefficient in the condensate cooling section condensate coolers  $K_{OK_j}$  is determined;

The heat flux transferred by heat transfer in the section of the condensate cooling zone with area  $F_{OK_j}$  is calculated:

$$Q^T_{OK_j} = K_{OK_j} F_{OK_j} \Delta t_{CP_{OK_j}}; \quad (4.34)$$

The heat imbalance in the area and the accuracy in it are considered:

$$\varphi_{OK_j} = Q^T_{OK_j} - Q_{OK_j} \text{ and } \varepsilon_{OK_j} = \frac{|\varphi_{OK_j}|}{Q_{OK_j}} \cdot 100\% . \quad (4.35)$$

If the accuracy value does not meet the acceptable value, the calculation for the area is repeated until an acceptable accuracy is achieved.

Calculation of the heat balance and heat transfer of the condensate cooler section can be accompanied by an external cycle of calculation of heat carrier pressure losses  $\Delta p_{H_{OK_j}}$  (  $\Delta p_{\Gamma_{OK_j}}$  (formula (2.119) with verification of the convergence of the values of these losses. In this case, the pressure of heat carriers at the outlet of the section will be as follows:

$$p_{H_{2OK_j}} = p_{H_{1OK_j}} - \Delta p_{H_{OK_j}} \text{ and } p_{\Gamma_{2OK_j}} = p_{\Gamma_{1OK_j}} - \Delta p_{\Gamma_{OK_j}} . \quad (4.36)$$

The average coolant pressures are calculated according to (2.120).

The heat flux given off by the condensate is calculated for the entire condensate cooler zone:

$$Q_{OK} = G_K (i_{\Gamma_{1OK}} - i_{\Gamma_{2OK}}), \quad (4.37)$$

and transferred by heat transfer:

$$Q^T_{OK} = \sum_{j=1}^n Q^T_{OKj}. \quad (4.38)$$

The heat imbalance in the coolant and its accuracy are considered:

$$\varphi_{OK} = Q^T_{OK} - Q_{OK} \text{ and } \varepsilon_{OK} = \frac{|\varphi_{OK}|}{Q_{OK}} \cdot 100\%. \quad (4.39)$$

If the accuracy value does not meet the acceptable value, the calculation of the entire zone shall be repeated until an acceptable accuracy is achieved.

If the condensate coolers zone is not divided into sections for the purpose of the study or consists of only one characteristic section, the algorithm is carried out according to the above methodology with the number of sections  $n = 1$ .

The initial data of the condensate coolers zone are the parameters of the heat transfer fluids at the inlet (pressure  $p_{H_{1O\Pi}}$  and  $p_{\Gamma_{1O\Pi}}$  and enthalpy  $i_{H_{1O\Pi}}$  and  $i_{\Gamma_{1O\Pi}}$ ), their flow rates  $G_{H_{O\Pi}}$  and  $G_{\Pi}$  for the zone and individual sections, and design characteristics.

The algorithm for calculating the heat transfer and heat balance of a section and the entire steam cooling zone is similar to the algorithm for calculating the condensate coolers zone and its sections, except that superheated steam is used as a heating medium instead of condensate. The thermophysical and thermodynamic properties of superheated steam are calculated according to dependencies (2.42)-(2.53).

As initial data for the control zone, the parameters of the heat carriers at the inlet (pressure  $p_{H_{1K\Pi}}$  and  $p_{\Gamma_{1K\Pi}}$  and enthalpy  $i_{H_{1K\Pi}}$ ,  $i_{\Gamma_{1K\Pi}}$ ,  $i_{KK}$ ,  $i_{\Pi B}$ ), the flow rate of feed water  $G_H$ , heating steam  $G_{\Pi}$ , additional condensate  $G_{KK}$ , steam  $G_{\Pi B}$  and air  $G_{BB}$  of the introduced steam-blower mixture, and design characteristics are known. To take

into account the influence of air content on the steam condensation process in the control unit, the mass or volume content of air in the heating steam can be set  $\varepsilon_{\Pi}$ .

The flow rate of the air present in the heating steam is equal to:

$$G_{\text{BII}} = \varepsilon_{\Pi} G_{\Pi}. \quad (4.40)$$

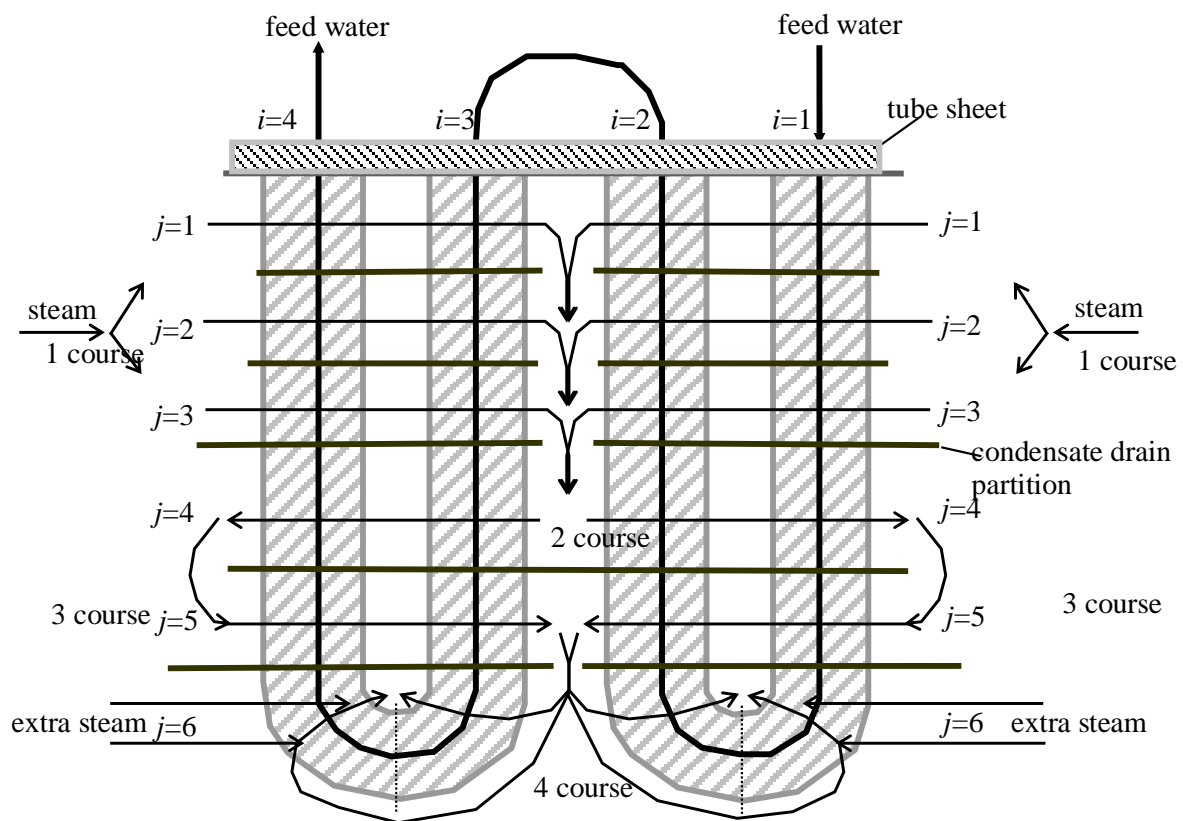
In a high pressure feed water, steam is supplied to the condensing zone evenly to the individual spiral coil blocks and the free space is very large. The feedwater temperature at the inlet to each section is identical. Therefore, it is possible to limit the calculation of steam condensation in one section (spiral coil block) enclosed between two condensate separators. Other sections will work in a similar way. In a coiled tubing system, steam moves in a cross-current pattern in the control chamber, successively washing different pipe bundles and losing considerable speed and pressure along the way (especially in vacuum pipes). The distance between the partitions and, consequently, the passage areas for steam can vary during its movement. The flow patterns of steam and feed water are very diverse. Therefore, it is advisable to divide the condensation zone in the low pressure regenerative feed water heaters into separate sections, which are a bundle of pipes of one feedwater passage enclosed between two condensing baffles. The temperature of the feed water at the inlet to each section will be different. The flow rate, steam pressure at the inlet to each section and the saturation temperature in them will also be different. An example of the formation of an array of design sections of the steam condensation of the low pressure regenerative feed water heaters shown in Fig. 1.8 is given in Fig. 4.1. The sections are calculated sequentially during the feedwater. The algorithm for calculating a separate section of the low pressure regenerative feed water heaters control unit is as follows:

- As initial parameters, the enthalpy of feedwater at the inlet to the section  $i_{\text{H}_{\text{IKII } j}} = i_{\text{H}_{\text{IKII } j-1}}$ , and steam at the inlet to the section are known  $i_{\Gamma_{\text{IKII } j}}$ . For the first section, the enthalpies of feed water and steam at the inlet are known. The heat transfer pressures at the inlet  $p_{\text{H}_{\text{IKII } j}} = p_{\text{H}_{\text{IKII } j-1}}$ ,  $p_{\Gamma_{\text{IKII } j}}$ , and outlet of the section



$p_{\Gamma_{2\text{КП}j}}$ ,  $p_{H_{2\text{КП}j}}$  are considered to be in the external loop. The steam flow rate at the inlet to the section  $G_{\Pi_{1\text{КП}j}}$  is determined by deducting from the steam flow rate in the previous section the condensate flow rate resulting from its condensation and taking into account the steam flow pattern through the heater sections. For the first section, the flow rate is determined minus the moisture content (if any):

$$G_{\Pi_{1\text{КП}j}} = G_{\Pi}^{\Pi} = x_{\Pi} G_{\Pi}; \quad (4.35)$$



$i$  – index of the section for the main condensate (feed water)

$j$  – index of the section for the heating steam

Fig. 4.1 - Scheme of formation of the array of calculation sites of the КП ПИТ ПИИ -400-26-2 -IV

- by the method of successive approximations, the enthalpy of the feed water at the outlet  $i_{H_{2\text{КП}j}}$  is calculated as a function of the zero heat imbalance in the

steam condensation section steam condensation  $\phi_{\text{KП}j}$ . As a method of acceleration, it is advisable to choose the chord method, for which two initial enthalpy values are set;

- the heat flux received by the feed water is calculated:

$$Q_{\text{KП}j} = G_{\text{H}} (i_{\text{H}_{2\text{KП}j}} - i_{\text{H}_{1\text{KП}j}}); \quad (4.36)$$

- according to the dependencies (2.37) of thermodynamic properties for underheated water, the feedwater inlet and outlet temperatures are calculated using known enthalpies and pressures. The saturation temperature of steam  $t_{\text{S}j}$  in the section is calculated by its average pressure in accordance with dependence (2.25). For steam, the transition of the saturation line is checked and the degree of dryness, its inlet and outlet temperatures are calculated according to (2.25) for saturated or (2.47) superheated steam;

The average temperature pressure in the section is calculated  $\Delta t_{\text{CPKП}j}$  according to formula (2.113), where the temperature of the heating medium at the inlet and outlet is the saturation temperature of the steam  $t_{\text{S}j}$ ;

Using dependencies (2.106)-(2.112), the average temperatures of the heat carriers in the section and the pipe walls are calculated.

The thermophysical properties of the feed water (formulas (2.37)-(2.41) for underheated water and (2.27)(2.36) for saturated water and (2.42), (2.51)(2.53) for superheated steam) in the section (thermal conductivity, specific volume, dynamic viscosity, Prandtl's number) are calculated based on the average value of its temperature. If the degree of mass (volume) air content in the mixture is different from zero, the thermal properties of the vapour-air mixture are calculated (2.88), (2.93) (2.96) The thermal conductivity of the pipe material is determined by the average wall temperature (Table 2.9).

From the continuity equation (2.118), the velocities of the feed water of the section are considered;

Criterion heat transfer coefficients of feedwater in pipes and their resistances, as well as heat transfer coefficients for condensation of pure steam or steam-air mixture in pipe sections are calculated (see paragraphs 2.3, 2.5);

In the process of film condensation of steam on pipes with a linear temperature distribution and parabolic distribution of velocities in the film (formulas (2.72) and (2.103), the average temperature of the condensate film in the section will be:

$$t_{K_j} = t_{S_j} - \frac{3}{8}(t_{S_j} - t_{CT_{HAP_{K\Pi_j}}}) ; \quad (4.37)$$

In accordance with the dependencies (2.37) of thermodynamic properties for underheated water, the enthalpy of condensate  $i_{K_j}$  at the outlet of the section is calculated using known values of temperature  $t_{K_j}$  and pressure  $p_{S_j}$

The heat balance equation is used to calculate the condensate flow rate received by the section, taking into account heat losses through the casing insulation:

$$G_{K_j} = \frac{Q_{K\Pi_j} + Q_{\text{ИЗ}_j}}{i_{\Gamma_{IK\Pi_j}} - i_{K_j}} ; \quad (4.38)$$

In accordance with dependence (2.54), the heat transfer coefficient in the control unit section steam condensation  $K_{K\Pi_j}$  is determined;

The heat flux transferred by heat transfer in the area of the control unit zone with area  $F_{K\Pi_j}$  is calculated:

$$Q^T_{K\Pi_j} = K_{K\Pi_j} F_{K\Pi_j} \Delta t_{CP_{K\Pi_j}} ; \quad (4.39)$$

The heat imbalance in the area and its accuracy are taken into account:

$$\varphi_{\text{KП}_j} = Q^{\text{T}}_{\text{KП}_j} - Q_{\text{KП}_j} \text{ and } \varepsilon_{\text{KП}_j} = \frac{|\varphi_{\text{KП}_j}|}{Q_{\text{KП}_j}} \cdot 100\% . \quad (4.40)$$

If the accuracy value does not meet the acceptable value, the calculation for the site is repeated until an acceptable accuracy is achieved.

The total condensate flow rate is defined as the sum of the condensed steam flow rates at all sites:

$$G_{\text{KП}} = \sum_{j=1}^{n_{\text{KП}}} G_{\text{K}_j} + G_{\text{П}}^{\text{K}} , \quad (4.41)$$

where  $G_{\text{П}}^{\text{K}} = (1 - x_{\text{П}})G_{\text{П}}$ .

The resulting enthalpy of condensing steam at all sites, taking into account the mixed condensate flow, which was previously subtracted at the entrance to the control unit from the wet heating steam flow, is determined by the heat balance of their mixing:

$$i_{\text{K}} = \frac{\sum_{j=1}^{n_{\text{KП}}} G_{\text{K}_j} i_{\text{K}_j} + G_{\text{П}}^{\text{K}} i'_{\Gamma_{1\text{KП}}}}{G_{\text{KП}}} . \quad (4.42)$$

The supply of the steam-air mixture and additional condensate from the cascade drain is usually carried out in the lower part of the heater. The steam of the steam-air mixture and steam from the self-boiling of the additional condensate condenses on the lower sections (bends) of the control pipes. The total amount of additional steam from these streams and pure condensate is determined by their dryness degrees, which are calculated by enthalpies at the steam saturation line at the outlet of the last sections  $i''_{2\text{KП}}$  and  $i'_{2\text{KП}}$  according to the lowest steam pressure in the control unit zone (outlet)  $p_{\Gamma_{2\text{KП}}}$ . The flow rates and degrees of dryness of these streams will be:

$$x_{\text{KK}} = \frac{i_{\text{KK}} - i'_{2\text{KП}}}{i''_{2\text{KП}} - i'_{2\text{KП}}} \text{ at } i_{\text{KK}} > i'_{2\text{KП}} , \text{ or } x_{\text{KK}} = 0 , \quad (4.43)$$

$$x_{\text{IIB}} = \frac{i_{\text{IIB}} - i'_{2\text{KII}}}{i''_{2\text{KII}} - i'_{2\text{KII}}} \text{ at } i_{\text{IIB}} < i''_{2\text{KII}}, \text{ or } x_{\text{IIB}} = 1, \quad (4.44)$$

$$G_{\text{KK}}^{\text{II}} = x_{\text{KK}} G_{\text{KK}} \text{ and } G_{\text{KK}}^{\text{K}} = (1 - x_{\text{KK}}) G_{\text{KK}}, \quad (4.45)$$

$$G_{\text{IIB}}^{\text{II}} = x_{\text{IIB}} G_{\text{IIB}} \text{ and } G_{\text{IIB}}^{\text{K}} = (1 - x_{\text{IIB}}) G_{\text{IIB}}; \quad (4.46)$$

The previously determined enthalpy of mixing of condensed steam at the lowest steam pressure in the control unit may fall into the two-phase region (condensate self-evaporates when falling down the heater). Therefore, a check must be made here:

$$x_{\text{K}} = \frac{i_{\text{K}} - i'_{2\text{KII}}}{i''_{2\text{KII}} - i'_{2\text{KII}}}, \text{ at } i_{\text{K}} > i'_{2\text{KII}}, \text{ or } x_{\text{K}} = 0, \quad (4.47)$$

$$G_{\text{KII}}^{\text{II}} = x_{\text{K}} G_{\text{KII}} \text{ and } G_{\text{KII}}^{\text{K}} = (1 - x_{\text{K}}) G_{\text{KII}}, \quad (4.48)$$

If  $x_{\text{K}} > 0$ , then it is assumed that  $i_{\text{K}} = i'_{2\text{KII}}$ ;

The total additional steam flow from all these streams is:

$$G_{\text{IIдоп}} = G_{\text{KK}}^{\text{II}} + G_{\text{IIB}}^{\text{II}} + G_{\text{KII}}^{\text{II}}, \quad (4.49)$$

The enthalpy of this steam is equal to  $i''_{2\text{KII}}$ ;

The total flow rate of additional condensate separated from these streams:

$$G_{\text{Kдоп}} = G_{\text{KK}}^{\text{K}} + G_{\text{IIB}}^{\text{K}}, \quad (4.50)$$

The total flow rate of all condensate leaving the control unit is:

$$G_{\text{K}} = G_{\text{Kдоп}} + G_{\text{KII}}^{\text{K}}, \quad (4.51)$$

The enthalpy of the condensate at the outlet of the control unit zone is equal to:

$$i_{\Gamma_{2\text{КП}}} = \frac{G_{\text{КДОП}} i'_{2\text{КП}} + G_{\text{ККП}}^{\text{К}} i_{\text{К}}}{G_{\text{К}}} . \quad (4.52)$$

The calculation of the heat balance and heat transfer of the control unit area can be accompanied by an external cycle of calculation of feedwater pressure losses  $\Delta p_{H\text{КП}_j}$  (formula (2.119) with verification of the convergence of these losses  $\Delta p_{\Gamma\text{КП}_j}$ . (condensate) The air flow rate in the steam-air mixture remains unchanged.

$$p_{H_{2\text{КП}_j}} = p_{H_{1\text{КП}_j}} - \Delta p_{H\text{КП}_j} \text{ та } p_{\Gamma_{2\text{КП}_j}} = p_{\Gamma_{1\text{КП}_j}} - \Delta p_{\Gamma\text{КП}_j}. \quad (4.53)$$

The heat flux received by the feedwater is calculated for the entire control zone:

$$Q_{\text{КП}} = G_H (i_{H_{2\text{КП}}} - i_{H_{1\text{КП}}}), \quad (4.54)$$

where the enthalpy of the feedwater at the outlet of the control unit steam condensation  $i_{H_{2\text{КП}}}$  is equal to the enthalpy of the feedwater at the outlet of the last section along its movement.

Heat flux transferred by heat transfer:

$$Q^{\text{T}}_{\text{КП}} = \sum_{j=1}^n Q^{\text{T}}_{\text{КП}_j} . \quad (4.55)$$

These two heat fluxes will differ within the tolerance of the error, and the heat imbalance in the zone will be determined by the difference between the amount of heat transferred by the heating medium, taking into account the mass balance, heat losses through the insulation, and the amount received by the feedwater. The value of this imbalance is calculated by the algorithm for the thermal calculation of the entire heater described above.

If the control zone is not divided into sections or consists of only one section for the purpose of the study, the algorithm is carried out according to the above methodology with the number of sections  $n = 1$ .

The flow rate of air exhausted from the heater through the air exhaust device  $G_{BO}$ , will be equal to the sum of the inlet air flows with the heating steam  $G_{BII}$ , heating, and from the upstream apparatus  $G_{BB}$ .

The flow rate of steam discharged from the heater through the air exhaust device  $G$ , will be equal to the total flow rate of steam at the outlet of the last sections along its course. For tubing, these sections are the pipe bends. Thus, the sum of the flow rates of steam  $G_{IIO}$  and air  $G_{BO}$  is the flow rate of the steam-air mixture discharged from the heater.

#### **4.3. Joint verification calculations of heater groups**

The variety of heaters included in the regeneration systems (Figs. 1.1-1.6) imposes its own peculiarities on the construction of algorithms for their verification calculations. For each regeneration system of thermal schemes of steam turbine plants, a different algorithm is developed. The generalised methodology and algorithm for verification calculations of regeneration systems are as follows:

1) Initial data are set:

- design characteristics of each preheater or individual drainage cooler;
- steam parameters at the outlets to each heater (flow rate, pressure and enthalpy);
- feed water parameters at the inlet to the regeneration system (flow rate, pressure and enthalpy);
- Drainage pump heads (if available);
- flow rates and enthalpies of the steam-air mixture (SAM) and cascade drain condensate that may enter the regeneration system from higher pressure units that are not part of the system;

- are estimated for a first approximation of the enthalpy of cascade drain condensate from higher pressure vessels included in the regeneration system. Their steam consumption in the steam-air mixture (SAM) is assumed to be zero;

2) Feedwater sequential calculation of all heaters and devices of the regeneration system (described in paragraph 4.2). In this case, the pressure and enthalpy of the feed water at the inlet of the next heater are assumed to be equal to the outlet of the previous one. If the condensate stream after the drainage pumps (ДН) or a separate drain cooler (ОД) is mixed upstream of the heater, the enthalpy of the feed water inlet is determined taking into account the mixing of these streams. The enthalpy of the condensate after the drainage pumps (ДН) is calculated based on their head. The enthalpy of dry saturated steam and condensate in the expansion tank (ET) is calculated from its pressure, and the flow rate of steam and condensate from it is calculated from the degree of dryness of the wet steam in it. The enthalpy of this wet steam is determined after mixing the condensate flows entering it from higher pressure units;

3) All the obtained enthalpies of the cascade condensate from the units included in this regeneration system are compared with the previous values. If the difference between them is less than the permissible value, the calculation is stopped, otherwise it goes back to step 2.

As a result, after the calculation is complete, all the parameters of interest for each heater can be output to separate files. In this case, the results will be linked to their operation in the regeneration system. The aggregated parameters for the entire regeneration system can be output in a separate file (as thermal diagrams of turbine units). The output data (except for design data) can be generated in separate files for each unit as lists of output parameters for all warranty modes of turbine units. At the same time, in the computer dialogue window, it is possible to provide for the selection of these modes and to calculate regeneration systems for them.



## **CHAPTER 5**

### **FLOW DISTRIBUTION IN THE HYDRAULIC NETWORKS OF HIGH-PRESSURE HEATER MANIFOLD SYSTEMS**

The hydraulic network of the collector system of spiral-coil high-pressure regenerative feed water heaters is a complex system of connecting feedwater pipelines (see Figures 1.10, 1.12). The hydraulic calculation of collector systems of such high-pressure regenerative feed water heaters consists in determining the velocities and flow rates of feedwater in each section of the pipeline (spiral coil, distributing or collecting section of the collector, feedwater supply or discharge pipelines). Only after such a calculation can the feedwater flow rates through the characteristic zones (steam cooling, steam condensation and condensate coolers) of the heater be accurately determined.

When designing a heat exchanger according to known methods [2], in practice, they are limited to finding the unevenness coefficient, which represents the ratio of the maximum and minimum flow rates of the heat carrier through individual coils in a spiral block using simplified and empirical dependencies. In this case, the total flow rate of feedwater through the zones is set, and the throttle washers that regulate it are selected. However, as it is known from the practice of operating this type of water treatment unit, these irregularities significantly affect the reliability and service life of the units, so the accuracy of their determination is very important. To solve this problem, elements of graph theory are used below, which is usually used in the calculation of the entire thermal scheme of a power plant and complex engineering networks of various types (gas, heat, water, ventilation, etc.) [41-47].

## 5.1. System of equations for the hydraulic network of the collector system of high-pressure heaters

The system of pipelines of the collector system of the high-pressure regenerative feed water heaters (network topology) is represented as a graph [41-43] (see an example in Fig. 5.1), where the branches (edges) are spiral coils, sections of the distributing and collecting collectors, between the coil mounts, supply and bypass pipelines, and throttle washers. The junctions (nodal points) of branches are used as nodes (nodal points). The distribution of flow rates across branches and pressures across nodes in such a graph is described by the well-known Kirchhoff laws. The closing equations here are the dependencies for determining the hydraulic, local resistance and pressure drop in each branch, and even the flow equations.

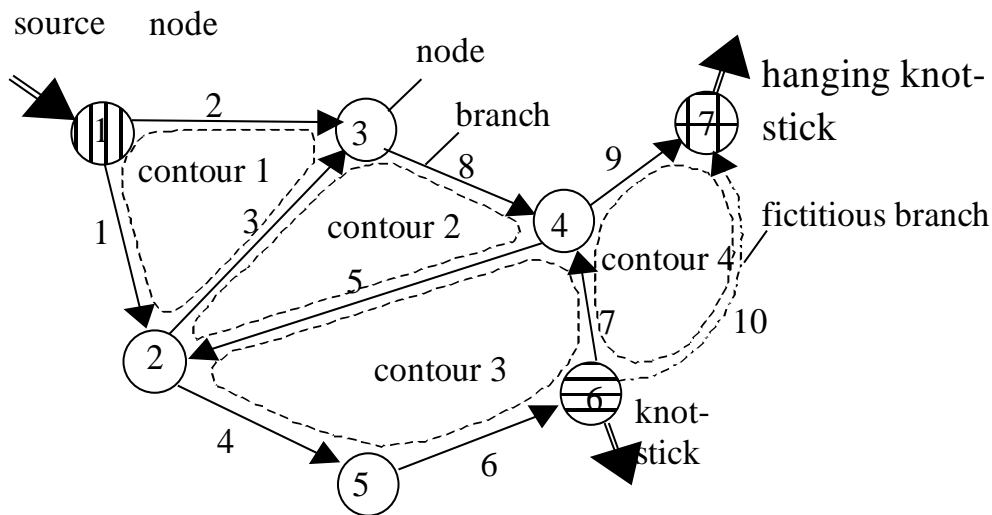


Fig. 5.1 - Example of a complex hydraulic network graph

Kirchhoff's first law for a mathematical model of a graph is as follows:

$$A_{ij}G_j = M_i, \quad (5.1)$$

where  $A_{ij}$  is a matrix of connections (incidents) of size  $m \times n$ , the element of the matrix is equal to -1 if the flow along the branch leaves the node (the initial

node of the branch), 1 if the flow along the branch enters the node (the final node of the branch) and 0 if the node does not belong to the branch;

$m$  and  $n$  are the number of nodes and branches in the graph;

$G_j$  – is a vector of mass flows along branches of size  $n$ , the element has a sign (+) – the direction of the flow coincides with the direction of the branch, (-) the direction of the flow does not coincide with the direction of the branch;

$M_j$  – is a vector of mass sources in nodes of size  $m$ , the element has a sign (+) – source, (-) – sink of mass in the node;

$I$  – index, each  $i$ -th row corresponds to a node;

$j$  – index, each  $j$ -th column corresponds to a branch.

If we introduce a matrix of linearly independent circuits [42 -47], then Kirchhoff's first law can be written in the form:

$$G_j = \sum_{k=1}^S K_{jk}^T G_k, \quad (5.2)$$

where  $K_{jk}^T$  - is the matrix obtained by transposing the matrix of linearly independent contours  $K_{kj}$  of size  $s \times n$ . The matrix element is equal to 1 if the branch enters the contour and its direction coincides with the direction of the contour traversal, -1 if the branch enters the contour and its direction does not coincide with the direction of the contour traversal, and 0 if the branch does not enter the contour;

$s$  – number of contours (root of the graph tree),  $s = n - m + 1$ ;

$G_k$  - is a vector of mass flow rates along the links of the contour of size  $s$ , the element of which is equal to the mass flow rate in one of the branches of the contour (link);

$k$  – index, each  $k$ -th row corresponds to a circuit,

$j$  – index, each  $j$ -th column corresponds to a branch.

Kirchhoff's second law for the mathematical model of a graph is as follows:

$$\sum_{j=1}^n K_{kj} \Delta p_j = 0, \quad (5.3)$$

$K_{kj}$  - is a matrix of linearly independent contours;

where  $\Delta p_j$  - is a vector of pressure drops in branches of size  $n$ .

The closing equations for the pressure drops in each branch are:

$$\Delta p_j = Z_j G_j |G_j| - Y_j, \quad (5.4)$$

where  $Z_j$  - is the vector of branch impedances, with size equal to the number of branches  $n$ ;

$$Z_j = \frac{v_j}{2f_j^2} \sum \xi_j$$

$v_j$  - is a vector of average specific volumes of fluid flow in a section of branches;

$f_j$  - is a vector of flow areas of the branch channels;

$\sum \xi_j$  - Vector of total hydraulic and local resistances of branches,

$$\sum \xi_j = \lambda_{TPj} \frac{L_j}{d_{\ominus j}} + \sum \xi_{Mj};$$

$\lambda_{TPj}$  - a vector of friction coefficients per unit length of the branch channel sections, determined by formulas (2.122)-(2.125);

$L_j$  - is the vector of branch channel lengths;

$d_{Ej}$  - is the vector of equivalent diameters of the branch channels;

$\sum \xi_{Mj}$  - is the vector of total local impedances of the branches;

$Y_j$  – vector of active sources of pressure in the branches (pumps, fans, hydrostatic pressure, etc.).

Equation (5.4) is written in such a way as to take into account the direction of mass flow against the branch direction. If, as a result of the calculation, the sign of the mass flow  $G_j$  in the branch is reversed, then the flow in the channel will be in the other direction.

The elements of the flow velocity vector in the branches are determined from the flow equation (2.118):

$$W_j = \frac{|G_j| v_j}{f_j} . \quad (5.5)$$

The vector of active sources of pressure  $Y_j$  (both with (+) and ( - ) signs in collector high-pressure regenerative feed water heaters systems) is the hydrostatic pressure caused by the difference in the height of the initial and final branch node:

$$Y_j = \Delta p_{\text{ГСТ}j} = -g \frac{A_{ji}^T h_i}{v_j} , \quad (5.6)$$

where  $h_j$  - is a vector of node heights of size  $m$ ; the lowest point of the pipe system is the zero point;

$A_{ji}^T$  - is the matrix obtained by transposing the matrix of connections (incidents)  $A_{ij}$ ;

$g$  - is the acceleration of free fall.

Below are examples of incident matrices  $A_{ij}$  and circuits  $K_{kj}$  for the hydraulic network graph shown in Fig. 5.1 (here: number of nodes  $m = 7$ , branches  $n = 10$ , linearly independent circuits  $s = 4$ ):

$A_{ij}$ $i$	$j$									
	1	2	3	4	5	6	7	8	9	10
1	-1	-1	0	0	0	0	0	0	0	0
2	1	0	-1	-1	1	0	0	0	0	0
3	0	1	1	0	0	0	0	-1	0	0
4	0	0	0	0	-1	0	1	1	-1	0
5	0	0	0	1	0	-1	0	0	0	0
6	0	0	0	0	0	1	-1	0	0	-1
7	0		0	0	0	0	0	0	1	1

$K_k$ $k$	$j$									
	1	2	3	4	5	6	7	8	9	10
1	1	-1	1	0	0	0	0	0	0	0
2	0	0	-1	0	-1	0	0	-1	0	0
3	0	0	0	1	1	1	1	0	0	0
4	0	0	0	0	0	0	-1	0	-1	1

Fig. 5.1- Below are examples of incident matrices  $A_{ij}$  and circuits  $K_{kj}$  for the hydraulic network graph

In practice, there are many variants of hydraulic networks: closed, open and open-closed. In an open network, the boundary conditions prevail in all nodes where the flow enters the network - i.e., sources, or leaves the network - i.e., sinks (see nodes 1, 6 and 7 in Fig. 5.1), the pressure is set (fixed) and the flow rate of the medium passing through the network and its individual branches is determined. In a closed network, flow rates and pressures are set as boundary conditions at the source

nodes, and flow rates and pressures are determined at the sink nodes and along all branches. In open-circuit systems, some sink nodes may have fixed pressures. In this case, there should be two or more sink nodes, and at least one of them should not have a pressure. In the calculations of collector high-pressure regenerative feed water heaters systems, closed and open-loop systems are mostly present (for example, when fixing the pressure at the end of the feedwater outlet pipeline from the steam cooling). It should be noted that in closed or open-loop networks, only the sink nodes are connected to each other by additional ‘dummy’ branches for calculation purposes (see branch 10 in Fig. 5.1). The pressure drop across such branches is considered as the difference in pressure at the source and destination nodes. In open networks, all source and sink nodes are connected by dummy branches for calculation purposes. Additional dummy branches allow you to form the necessary circuits (see circuit 4 in Fig. 5.1), without which the hydraulic network graph will be incomplete. In closed systems, there may be ‘hanging’ branches and nodes that are not included in any circuit and the flow rate in them will be constant.

## **5.2. Calculation of the hydraulic network of the collector system of high-pressure heaters by the method of contour correction flows**

Kirchhoff's laws (5.2), (5.3), the closing dependencies (5.4)-(5.6) and the topological structure of the graph are a complex and cumbersome system of nonlinear equations. There are many ways to solve these systems, which have been tested in the calculation of water supply, heating, ventilation and other complex engineering networks and systems [41-47]. Here, it is proposed to use the iterative method of contour correction flows [45-47] with the calculation of corrections by the Newton method [22, 23]. The advantage of this method is that it operates with a matrix of contours [42-47], which reduces the order of the system compared to the matrix of connections (incidents) and has fast convergence. The disadvantage of this is that it is necessary to clearly specify a cost-balanced initial flow distribution [46].

In this case, there is no such problem for the topological structure of the graph of the high-pressure regenerative feed water heaters collector systems, since the initial flow rates through pipelines and collectors can be easily set without taking into account irregularities.

The calculation algorithm for this method, adapted for the calculation of high-pressure regenerative feed water heaters collector systems, is as follows:

1) Input, initial data and boundary conditions for the network graph are specified:

- geometric and hydraulic characteristics of branches (arrays): vector of flow areas of branch channels  $f_j$ , vector of lengths of branch channels  $L_j$ , vector of equivalent diameters of branch channels  $d_{Ej}$ , vectors of the number of identical parallel connected physical branches (channels)  $n_j$ , which are included in one when replaced by equivalent ones, vector of total local resistances of branches  $\sum \xi_{Mj}$ ;

- vector (array) of heights of nodes  $h_i$  relative to the lowest node;

- topology of the graph (connection matrix)  $A_{ij}$ , which can be represented as an array, the element number of which corresponds to the branch number, and the columns contain the number of the start and end node and the identifier of the branch type (pipe, spiral coil, distributing or collecting collector, throttle washer);

- temperature characteristics necessary for calculating the thermophysical properties of the flow: a vector of flow temperatures in nodes  $t_i$  a vector of average flow temperatures in branches  $t_{CPj}$ ;

- a vector of approximate initial average flow pressures in the branches  $p_{CPj}$ , necessary for calculating the thermophysical properties of the flow. As a result of the calculation, this vector will acquire accurate values according to the balanced flow distribution;



- Boundary conditions: identifier of the closed or open system, flow rates and pressures in the source nodes and, if available, fixed pressure in individual sink nodes for a closed system or pressure in all source nodes and sinks for an open system;

- initial flow distribution in the network: mass flow rates in the branches with the balance of mass flow rates in the nodes in accordance with the first Kirchhoff's law in the form (5.1). In this case, as a result of the calculation, the values of mass flow rates in source or sink nodes for a closed system will be saved, and the flow rates in branches (mass flows) will be specified;

2) a matrix (array) of linearly independent circuits  $K_{kj}$  of size  $s \times n$  is constructed from the matrix of compounds  $A_{ij}$ , which is presented in the form of an array, using a separate algorithm,  $s = n - m + 1 - n_B - m_B$ ,  $n$  is the number of graph branches,  $m$  is the number of graph nodes,  $n_B$  is the number of 'hanging' graph branches including dummy branches,  $m_B$  is the number of 'hanging' graph nodes including dummy branches. From this matrix, another algorithm is used to build a tree for calculating the pressures in the nodes as an array of the order of passage of the branches. In nodes where the pressure is fixed, its value should not be recalculated.

Then, using a computer subroutine, the method of contour correction flows with corrections according to the Newton method is implemented, the algorithm of which looks like this

3) calculation of the thermophysical properties of the medium in each branch, construction of vectors of flow velocities in branches  $W_j$ , impedances of branches  $Z_j$  of active pressure sources in branches  $Y_j$  and vectors of other parameters characterising the flow;

4) using the array of the connection matrix and the array of the pressure calculation tree, the elements of the pressure vector in the nodes are calculated:

$$p_{Kj} = p_{Hj} - \Delta p_j, \quad (5.7)$$

where  $p_{Doj}$  and  $p_{Hj}$  are the pressures at the end and initial nodes of the current branch  $j$  ;

- the vector of average flow pressures in the branches is constructed using the array of the connection matrix:

$$p_{CPj} = \frac{p_{Kj} + p_{Hj}}{2}, \quad (5.8)$$

5) according to the second Kirchhoff's law (formula (5.3), a vector of unbound pressure drops along the contours is calculated and formed, with the size  $s$  :

$$f_l = f_k = \sum_{j=1}^n K_{kj} \Delta p_j, \quad (5.9)$$

where the index symbol  $l$  is used in the implementation of Newton's method;

6) determine the maximum modulo value of the uncoupling from the vector  $f$  and compare it with the permissible value. If this value is less than the permissible value, the calculation is stopped, otherwise it proceeds to the next step;

7) the elements of the Jacobi matrix of size  $s \times s$  are calculated [22, 23]:

$$B_{lk} = \frac{\partial f_l}{\partial G_k} = 2 \sum_{j=1}^n K_{lj} K_{kj} Z_j G_j, \quad (5.10)$$

8) the system of linear equations is solved by the Gauss method [22, 23].

$$B_{lk} \Delta G_k = f_k, \quad (5.11)$$

where  $\Delta G_k$  is a vector of contour correction costs (solution vector) of size  $s$  for the Newton method;

9) according to Kirchhoff's first law (formula (5.2), new values of the costs in the branches are calculated (the cost vector is built) for the next approximation:

$$G_j^{(q+1)} = G_j^{(q)} - \sum_{k=1}^S K_{jk}^T \Delta G_k, \quad (5.12)$$

where  $G_j^{(q+1)}$  и  $G_j^{(q)}$  are the refined mass flow vectors in the branches for the next approximation (iteration)  $q + 1$  and in the current approximation (iteration)  $q$  ;

10) the calculation again goes to step 3 and is repeated until the maximum modulo value of the nonunion from the vector  $f_l$  is less than the permissible value.

The hydraulic network of the collector system for any high-pressure regenerative feed water heaters has a homogeneous structure (collectors - spiral coils) with the inclusion of individual elements specific to certain types of high-pressure regenerative feed water heaters (choke washers, feedwater supply, discharge and bypass pipelines). The formation of collector system graphs and arrays of initial data for the calculation of individual types of high-pressure regenerative feed water heaters can be performed automatically by a computer.

The collector system of the high-pressure regenerative feed water heaters has features that allow simplifying the algorithm and calculation. One of them is that there are columns of spiral coils from different collectors in the high-pressure regenerative feed water heaters chamber, arranged symmetrically and operating in parallel. In this case, some elements can be represented as one equivalent branch of the graph, the flow rate and cross-sectional area of which are equal to the flow rate and cross-sectional area of one physical branch multiplied by their number  $N_j$  , and other parameters will remain unchanged. As an equivalent branch of a spiral coil, it is advisable to take all spiral coils located in the same horizontal plane and operating in parallel. In this case, their number  $N_j$  is equal to the number of collectors in the high-pressure regenerative feed water heaters  $N_{\text{КОЛ}}$ . The equivalent branch of the graph of collecting or distributing collectors will include half of the total number of

collectors in the high-pressure regenerative feed water heaters  $N_{\text{КОЛ}}/2$ . When coils are connected in series through collecting collectors in some steam coolers with one distributing collector and an output from the steam cooler, the equivalent branch of the spiral coil  $N_j$  will be a multiple of the number of spiral blocks in series in the steam cooler  $N_{\text{КОЛ}}/n_{\text{ПОСЛ}}$ . For an equivalent branch supplying the entire flow to the distributing collector and discharging the entire flow from the collecting collector,  $N_j$  will be equal to one. The equivalent branch of intermediate collectors in the steam cooling will include the quantity  $(N_{\text{КОЛ}}-2)/(n_{\text{ПОСЛ}}-1)$ . The equivalent branches of the bypass, supply and discharge pipelines  $N_j$  will include the number of these pipelines operating in parallel. For the equivalent branch of constriction devices (choke washers),  $N_j$  will correspond to the pipelines or collectors in which they are installed.

Equivalent replacement allows to significantly reduce the volume of branches and nodes of the graph (see examples in Figures 5.2 and 5.3) without any noticeable impact on the calculation accuracy. The characteristics of the graphs taking into account the equivalent replacement of the elements of the hydraulic networks of the collector systems of the high-pressure regenerative feed water heaters of 300 and 500 MW turbines are given in Table 5.1.

As a result of the calculation using this method, a balanced flow distribution in the network is obtained with a given accuracy, and there are vectors of all the necessary parameters for branches and nodes that can be displayed in tabular form in separate files. Using this data, you can build various graphs of the distribution of hydraulic parameters and get an idea of the operation of individual components of the apparatus. This data can be used to analyse the erosion and corrosion wear and elastic-plastic state of coils and pipes (see Sections 7 and 8 for the methodology), as well as in the thermal calculation of the machine (Section 4). Examples of the distribution of velocities and pressures of feed water in the graph of the collector system of the apparatus shown in Fig. 5.2 are given in Figs. 5.4, 5.5.

Table 5.1 - Characteristics of the graphs of collector systems of high-pressure regenerative feed water heaters turbines with a capacity of 300 and 500 MW

Type of ПBT	Heating surface area, m <sup>2</sup>	Total number of elements (branches) before equivalent replacement		Graph topology after equivalent replacement		
		coils	all branches	branches	nodes	contours
ПBT group of turbine unit K 300 240 KhTGZ						
ПBT -1	444	324	654	265	177	89
ПBT -2	567	324	654	261	175	87
ПBT -3	444	324	652	244	165	80
ПBT group (1 thread)	1455	972	1960	770	517	256
ПBT group (2 thread)	2910	1944				
ПBT group of turbine unit K 500 2402 KhTGZ						
ПBT -1	2016	1068	2226	646	417	230
ПBT -2	2016	1068	2226	606	397	210
ПBT -3	2052	1068	2184	646	417	230
The entire HST group	6084	3204	6636	1898	1231	670

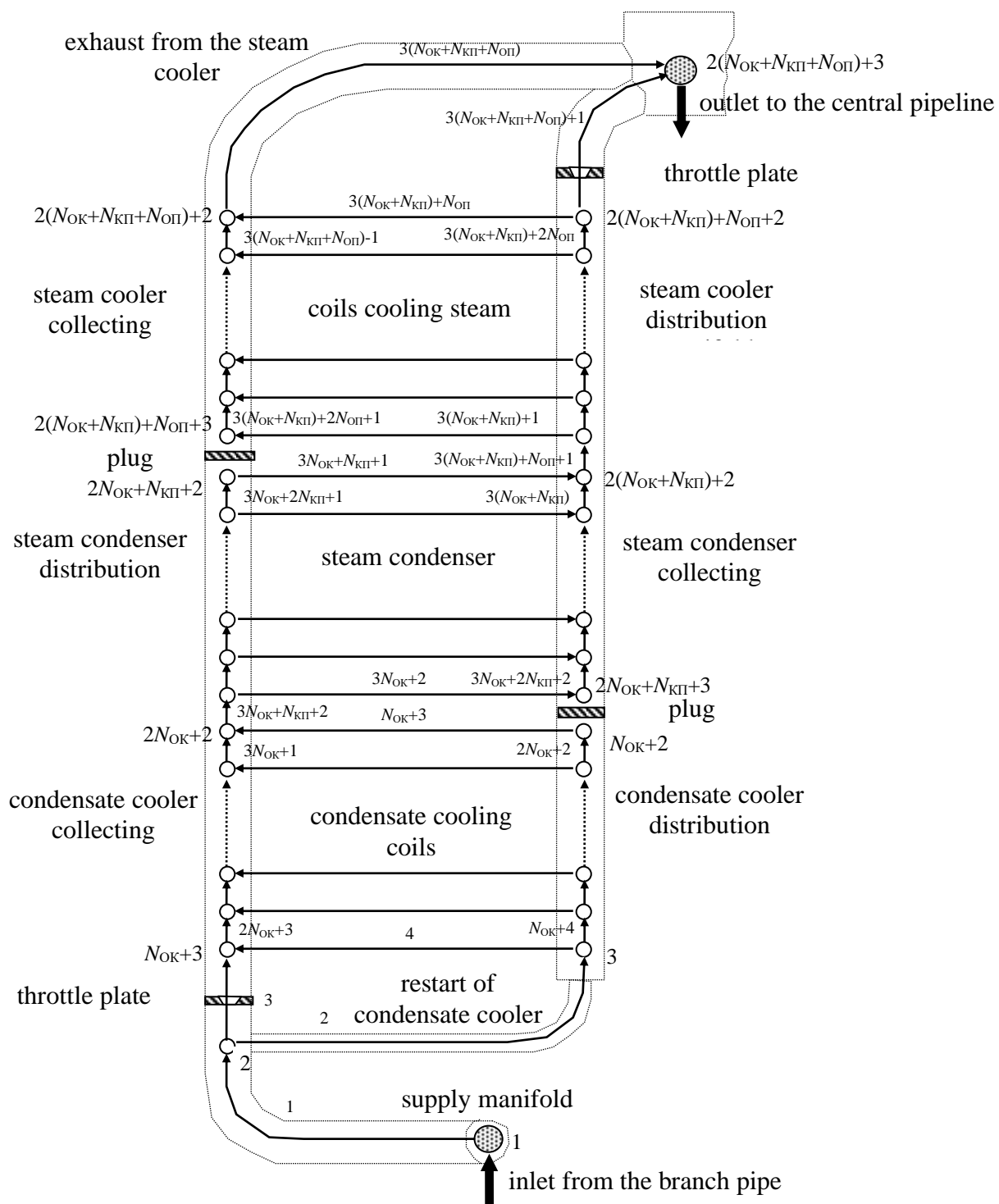


Fig. 5.2 - Graph for the calculation of the collector system of the PIBT-3 turbine unit K 300-240 KhTGZ

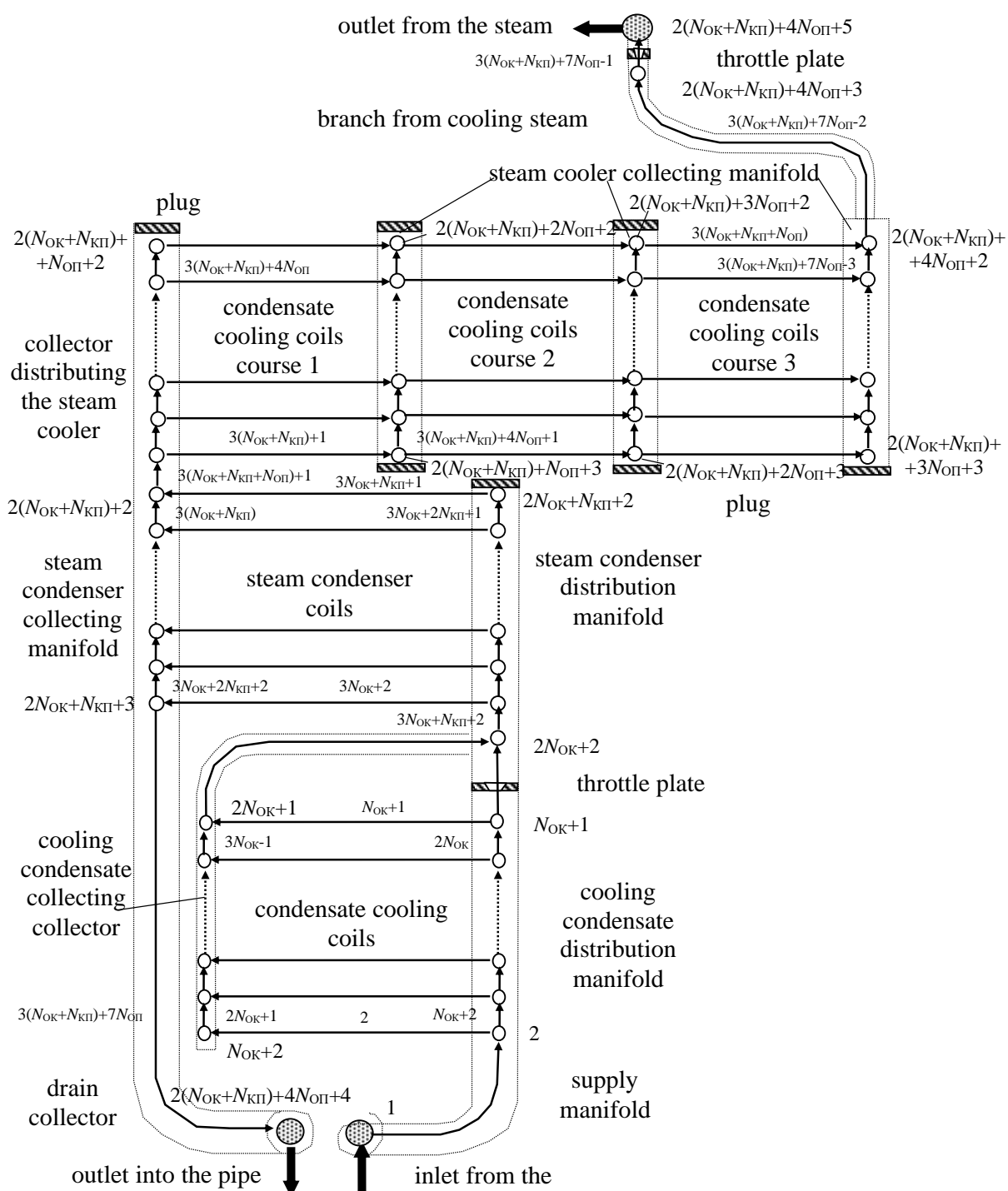


Fig. 5.3 - Diagram for calculation of the collector system of the high-pressure regenerative feed water heaters of the turbine unit K 500-2402 KhTGZ with the steam cooling switched on

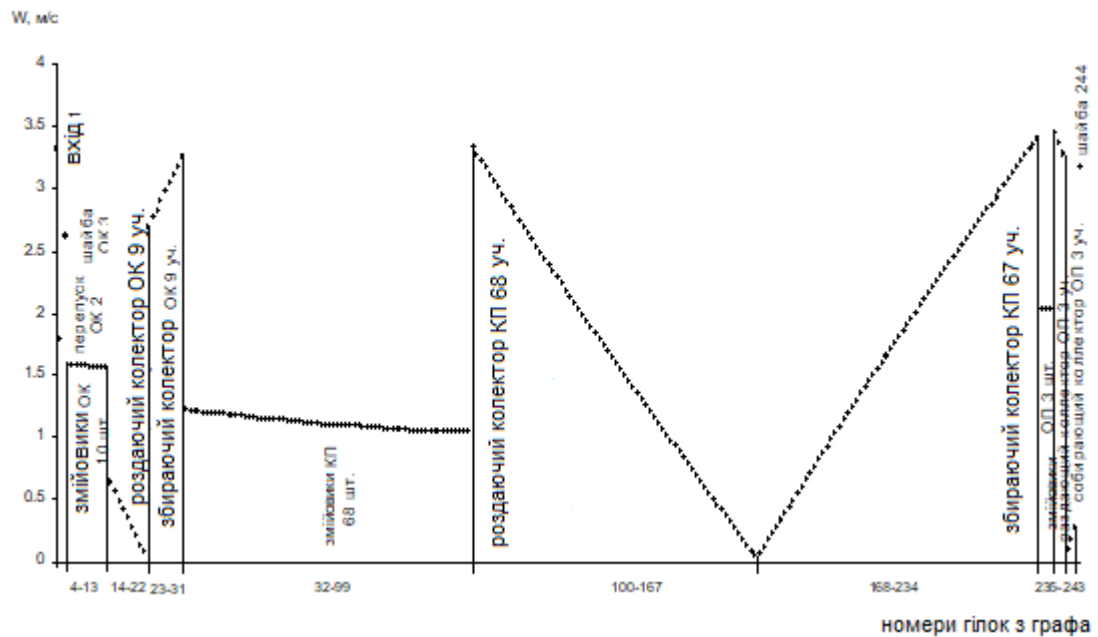


Fig. 5.4 - Distribution of feed water velocities in the collector system of ПБТ-3 of the turbine unit K 300240 KhTGZ at the nominal (see graph in Fig. 5.2)

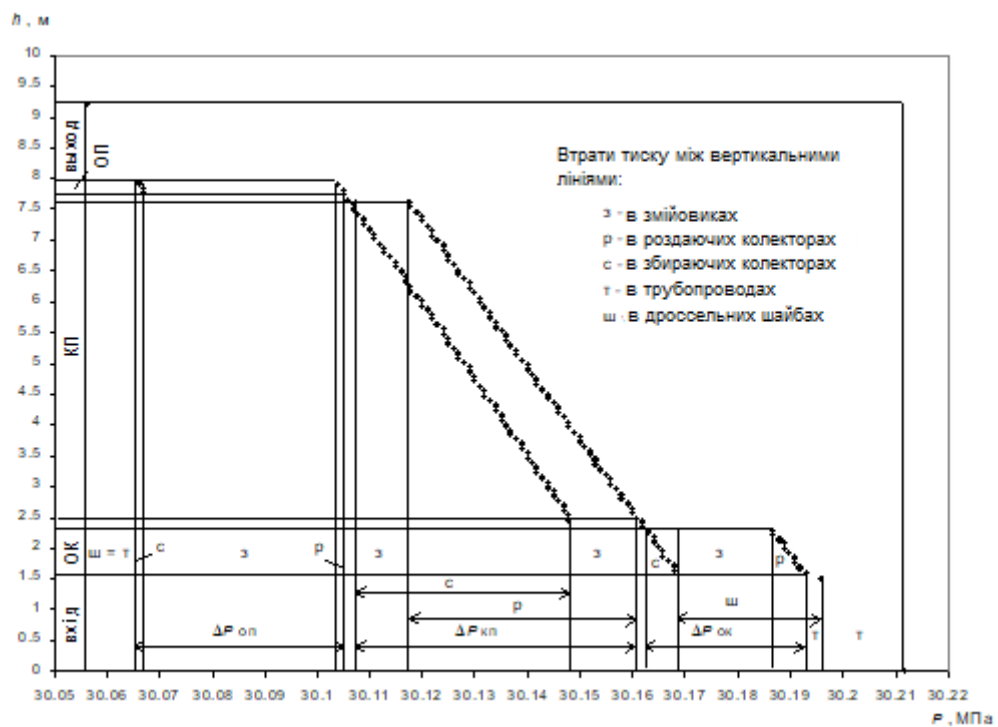


Fig. 5.5 - Nomogram of feedwater pressure distribution by height and zones of the collector system of the ПБТ-3 turbine unit K 300240 KhTGZ at nominal (see graph in Fig. 5.2)



## CHAPTER 6

### DISTRIBUTION OF THERMAL CHARACTERISTICS IN SURFACE HEAT EXCHANGERS FOR POWER PLANTS

When analysing the processes inside surface heat exchangers in power plants, it becomes necessary to determine the local thermal characteristics at a study point at an arbitrary length of one of the pipes that make up the heating surface. In this section, we consider the schemes of cross-current flow of heat transfer fluids, which are typical for surface heat exchangers and heat transfer tubing, and which have already been studied in detail in Section 3. In such schemes (see Fig. 3.7), one of the heat transfer fluids flows inside the elements (pipes or rows of pipes, sections, coils), i.e. it is not mixed, and the other flows outside in a cross-flow pattern, i.e. it is mixed. The main elements in the cross-current schemes of surface high-pressure regenerative feed water heaters and low pressure regenerative feed water heaters are elements with mixing of only one of the heat transfer fluids (see Fig. 3.1 a and b) - i.e., rows of pipes or spiral coils, hereinafter referred to as pipes.

The initial data for the design or verification calculation of a separate section or the entire zone are the temperatures of the heat carriers at the inlet  $t_{\Gamma 1}$ ,  $t_{H1}$  and outlet  $t_{\Gamma 2}$ ,  $t_{H2}$ . For this zone or section, the number of passes (current multiplicity)  $z$  and the number of pipes in one pass  $n$  are also known. At the initial stage, the task is to build four arrays of heat carrier temperatures of size  $n \times z$ : unmixed at the inlet and outlet of each pipe and mixed before and after each pipe.

When deriving the correction factors for the logarithmic mean temperature pressure in Section 3, the dependences of the degree of heating or cooling of  $\varphi$  heat transfer medium, were obtained for a single pipe scheme with the number of pipes  $n$  (Fig. 3.6). When forming an array of coolant temperatures, it is convenient to first calculate the temperatures of the non-mixed coolant at the inlet and outlet of the pipes, and then the temperatures of the mixed coolant in front of and behind each pipe are easily determined. From the degree of heating (cooling) of the heat transfer

fluid, the degree of heating (cooling) of the non-mixed heat transfer fluid in each pipe is easily obtained, since these parameters are interrelated. For the one-time scheme from Fig. 3.6a, the degree of heating of the non-mixed coolant in each pipe will be:

$$\varphi_{Ti} = \frac{n}{PR} (1-PR)^{\frac{i}{n}} \left[ (1-PR)^{-\frac{1}{n}} - 1 \right], \quad (6.1)$$

where  $P$  and  $R$  -are dimensionless parameters calculated by formulas (2.115) and (2.116) from the temperature values  $t_{\Gamma 1}$ ,  $t_{H1}$  i  $t_{\Gamma 2}$ ,  $t_{H2}$ ;

$I$  – is the index of the flow pipe; the countdown of which begins from the inlet of the mixed coolant.

Dependence (6.1) applies only to a single circuit. In order to move to a multiple circuit, it is necessary to multiply formula (6.1) by a coefficient representing the difference in the heating degree of the non-mixed coolant before and after the current and previous stroke inclusive  $\varphi_j - \varphi_{j-1}$ , and in the formula (6.1) itself, take into account the current multiplicity. The desired differences for the current diagram in Fig. 3.3 a, will be:

$$\varphi_{Xj} = \frac{1-P}{P(1-R)} \left( \frac{1-PR}{1-P} \right)^{\frac{j}{z}} \left[ 1 - \left( \frac{1-PR}{1-P} \right)^{-\frac{1}{z}} \right], \quad (6.2)$$

where  $j$  - is the index of the current stroke; the countdown is from the inlet of the mixed coolant.

Taking into account the multiplicity of the current circuit, formula (6.1) for the circuit of Fig. 3.6 a will be as follows:

$$\varphi_{Ti} = \frac{n}{PR} \omega^{\frac{i}{n}} \left[ \omega^{-\frac{1}{n}} - 1 \right], \quad (6.3)$$

where the parameter is considered to depend on

$$\omega = \left( \frac{1}{R-1} \left( R \left( \frac{1-P}{1-PR} \right)^{\frac{1}{z}} - 1 \right) \right)^{-1}.$$

After similar transformations and other current circuits of Figs. 3.3 and 3.4, the generalised dependence of the degree of heating (cooling) of the non-mixed coolant in a particular pipe  $i$  located in the course  $j$  will be as follows:

$$\Phi_{i,j} = \Phi_{T_i} \Phi_{X_j} = \frac{n}{(\beta-1)(1-\omega)} \cdot \beta^{\frac{j}{z}} \cdot \omega^{\frac{k}{n}} \cdot \left( 1 - \beta^{-\frac{1}{z}} \right) \cdot \left( \omega^{-\frac{1}{n}} - 1 \right), \quad (6.4)$$

where  $\beta, \omega$  -are dimensionless parameters:

(a) Schematic of Fig. 3.3 a:

$$\beta = \frac{1-PR}{1-P}, \quad \omega = \frac{R-1}{R\beta^{-\frac{1}{z}}-1} \text{ at } R \neq 1 \text{ and } \omega = 1 + \frac{1}{z} \frac{P}{1-P} \text{ at } R = 1;$$

b) scheme of Fig. 3.3 б:

$$\beta = \frac{1-P}{1-PR}, \quad \omega = \frac{R-1}{\beta^{-\frac{1}{z}}-R} \text{ at } R \neq 1 \text{ and } \omega = 1 + \frac{1}{z} \frac{P}{1-P} \text{ at } R = 1;$$

c) scheme of Fig. 3.4 a:

$$\beta = 1 - P(R+1) \text{ and } \omega = \frac{R\beta^{\frac{1}{z}}+1}{R+1};$$

d) scheme of Fig. 3.4 б:

$$\beta = 1 - P(R+1) \text{ and } \omega = \frac{\beta^{\frac{1}{z}}+R}{R+1},$$

where  $k$  is the index of the current pipe of the number  $n$  in the stroke;  $k=i$  if the parity (oddity) of  $j$  and  $z$  coincide, otherwise  $k=n-i+1$ ; the index  $i$  starts from

the first pipe that meets the path of the coolant mixed in the apparatus, and for all strokes its direction does not change, and the index  $j$  is counted from the first stroke of the coolant mixed.

The array of temperatures of the non-mixed coolant at the inlet to each pipe, depending on the current pattern, will be formed as follows:

$$t_{H1i,j} = t_{H2i,j+1} \text{ and } t_{H1i,z+1} = t_{H1} \text{ ( schemes of Fig.. 3.3 a),} \quad (6.5)$$

$$t_{\Gamma1i,j} = t_{\Gamma2i,j+1} \text{ and } t_{\Gamma1i,z+1} = t_{\Gamma1} \text{ ( schemes of Fig. 3.3 б),} \quad (6.6)$$

$$t_{H1i,j} = t_{H2i,j-1} \text{ and } t_{H1i,0} = t_{H1} \text{ ( schemes of Fig.. 3.4 a),} \quad (6.7)$$

$$t_{\Gamma1i,j} = t_{\Gamma2i,j-1} \text{ and } t_{\Gamma1i,0} = t_{\Gamma1} \text{ ( schemes of Fig. 3.4 б).} \quad (6.8)$$

Together with these temperatures, the temperature of the non-mixed coolant at the outlet is considered for each pipe:

$$t_{H2i,j} = t_{H1i,j} + \varphi_{i,j}(t_{H2} - t_{H1}) \text{ ( schemes of Fig. 3.3 a та 3.4 a),} \quad (6.9)$$

$$t_{\Gamma2i,j} = t_{\Gamma1i,j} - \varphi_{i,j}(t_{\Gamma1} - t_{\Gamma2}), \text{ ( schemes of Fig. 3.3 б i 3.4 б),} \quad (6.10)$$

where  $\varphi_{i,j}$  dependence (6.4) is considered.

Similarly, the array of temperatures of the coolant mixed before each pipe is constructed:

$$t_{\Gamma1k,j} = t_{\Gamma2k-1,j}, \quad t_{\Gamma10,j} = t_{\Gamma2k,j-1} \text{ та } t_{\Gamma11,0} = t_{\Gamma1} \text{ ( schemes of Figs. 3.3 a, 3.4 a),} \quad (6.11)$$

$$t_{H1k,j} = t_{H2k-1,j}, \quad t_{H10,j} = t_{H2k,j-1} \text{ та } t_{H11,0} = t_{H1} \text{ ( schemes of Figs. 3.3 б, 3.4 б),} \quad (6.12)$$

and for each pipe:

$$t_{\Gamma2i,j} = t_{\Gamma1i,j} - \frac{R}{n}(t_{H2i,j} - t_{H1i,j}) \text{ (Fig. 3.3 a, 3.4 a),} \quad (6.13)$$

$$t_{H2i,j} = t_{H1i,j} + Rn(t_{\Gamma1i,j} - t_{\Gamma2i,j}) \text{ (Fig . 3.3 a, 3.4 a).} \quad (6.14)$$

In the sections of the distributing collectors (see Fig. 3.6), the temperatures of the non-mixed coolant will be the same. For collecting or intermediate collectors in

a multi-pass scheme, the enthalpy of this heat carrier in the section after the adjacent pipe or pipes is determined on the basis of the heat balance at the point of mixing of flows from the previous section of the collector and the current pipe. The enthalpy and pressure of the heat carrier are used to calculate its temperature.

For a complete understanding of the thermal processes in the devices, it is necessary to know the temperatures of the heat carriers not only at the ends and outside the pipes, but also their distribution along the length of the pipe. As an object of study, we take an arbitrary pipe of the heating surface of a heat exchanger with a cross-current of heat carriers of length  $L$ , located in the current passage  $j$  and having a number in this passage  $i$ . From the above calculations for this pipe, the temperatures of the heat carriers at the inlet, outlet, upstream and downstream are known. For the current scheme in one stroke (Fig. 3.6 a), the solution of the system written for this pipe, consisting of equations (2.115), (2.116), heat balance and heat transfer, using excellent bounds, gives the distribution of the dimensionless temperature parameter  $P$  along the length:

$$P_{x,i,j} = 1 - e^{\frac{1}{R_{i,j}} \left( (1 + R_{i,j} \ln(1 - P_{i,j}))^{\frac{x}{L}} - 1 \right)} \quad \text{at } R_{i,j} \neq 0, \quad (6.15)$$

where the parameters  $P_{i,j}$  and  $R_{i,j}$  are calculated by formulas (2.115) and (2.116) from the temperature values  $t_{H1,i,j}$ ,  $t_{\Gamma1,i,j}$ ,  $t_{H2,i,j}$ ,  $t_{\Gamma2,i,j}$ ;

$x$  - is the current coordinate on the length of the pipe  $L$  from the coolant inlet.

For the one-stroke current scheme of Fig. 3.6 b, the system of equations is composed similarly to the previous one and is solved similarly:

$$P_{x,i,j} R_{i,j} = 1 - e^{R_{i,j} \left( (1 + \frac{1}{R_{i,j}} \ln(1 - P_{i,j} R_{i,j}))^{\frac{x}{L}} - 1 \right)} \quad \text{at } R_{i,j} \neq 0. \quad (6.16)$$

In the case of condensation of the heating medium (i.e. ) for both schemes:

$$P_{x,i,j} = 1 - (1 - P_{i,j})^{\frac{x}{L}} \text{ at } R_{i,j} = 0. \quad (6.17)$$

The temperature of the non-mixed heat carrier at position  $x$  on the length of the pipe  $L$  is expressed from formulas (2.115), (2.116) and (6.15)-(6.17):

$$t_{Hx,i,j} = t_{H1i,j} + P_{x,i,j}(t_{\Gamma 1i,j} - t_{H1i,j}) \text{ (Scheme of Fig. 3.6 a),} \quad (6.18)$$

$$t_{\Gamma x,i,j} = t_{\Gamma 1i,j} - P_{x,i,j}R_{i,j}(t_{\Gamma 1i,j} - t_{H1i,j}) \text{ (Scheme of Fig. 3.6 б).} \quad (6.19)$$

The temperatures of the inner and outer walls of the pipe in section  $x$  are found from the Newton-Richman equation:

$$t_{CTBH\ x,i,j} = t_{H\ x,i,j} + \frac{d_{3OB}}{d_{BH}} \frac{q_{x,i,j}}{\alpha_{1i,j}} \text{ and } t_{CTHap\ x,i,j} = t_{\Gamma 1\ i,j} - \frac{q_{x,i,j}}{\alpha_{2i,j}}, \quad (6.20)$$

where  $\alpha_{1i,j}$  i  $\alpha_{2i,j}$  -are the heat transfer coefficients from the inside and outside of the pipe;

$d_{3OB}$  Ta  $d_{BH}$  -are the outer and inner diameters of the pipe;

$q_{x,i,j}$  - heat flux density in the intermediate section  $x$ .

The expression for the heat flux density  $q_{x,i,j}$  is obtained taking into account the dependencies (2.115), (2.116) and the heat balance equations by integrating  $E_{qs}$ :

$$q_{x,i,j} = \frac{dQ_{o-x,i,j}}{dF_{x,i,j}} = \frac{1}{\pi d} \frac{dQ_{o-x,i,j}}{dx}, \quad (6.21)$$

where  $Q_{o-x,i,j}$ -is the heat flux given or received by the heat carriers and transferred through the pipe walls in the area from the origin (0) to the coordinate  $x$  ;

a) for the scheme of Fig. 3.6 a:

$$q_{x,i,j} = -\frac{q_{i,j}}{P_{i,j}R_{i,j}} \cdot \ln(1 + R_{i,j} \ln(1 - P_{i,j}))x$$

$$x(1 + R_{i,j} \ln(1 - P_{i,j}))^{\frac{x}{L}} \cdot e^{\frac{1}{R_{i,j}} \left( (1 + R_{i,j} \ln(1 - P_{i,j}))^{\frac{x}{L}} - 1 \right)} \text{ and } R_{i,j} \neq 0; \quad (6.22)$$

b) for the scheme of Fig. 3.6 б:

$$q_{x,i,j} = -\frac{q_{i,j}}{P_{i,j}} \cdot \ln \left( 1 + \frac{1}{R_{i,j}} \ln(1 - P_{i,j} R_{i,j}) \right) x$$

$$x \left( 1 + \frac{1}{R_{i,j}} \ln(1 - P_{i,j} R_{i,j}) \right)^{\frac{x}{L}} \cdot e^{R_{i,j} \left( \left( 1 + \frac{1}{R_{i,j}} \ln(1 - P_{i,j} R_{i,j}) \right)^{\frac{x}{L}} - 1 \right)} \text{ and } R_{i,j} \neq 0, \quad (6.23)$$

where  $q_{i,j}$  - is the average density of the heat flux through the pipe wall.

With formulas  $R_{i,j} = 0$  (6.22) and (6.23), using excellent limits, we convert to the following dependence:

$$q_{x,i,j} = -\frac{q}{P_{i,j}} (1 - P_{i,j})^{\frac{x}{L}} \ln(1 - P_{i,j}) \quad (6.24)$$

At the extreme values of the interval at  $x = 0$  (inlet of the heated coolant) and  $x = L$  (outlet), dependences (6.22) and (6.23) have the following form:

a) for the scheme of Fig. 3.6 а:

$$q_{0,i,j} = -\frac{q_{i,j}}{P_{i,j} R_{i,j}} \cdot \ln(1 + R_{i,j} \ln(1 - P_{i,j})) \quad (6.25)$$

$$q_{L,i,j} = q_{0,i,j} \cdot (1 + R_{i,j} \ln(1 - P_{i,j})) \cdot (1 - P_{i,j}); \quad (6.26)$$

b) for the scheme of Fig. 3.6 б:

$$q_{0,i,j} = -\frac{q_{i,j}}{P_{i,j}} \cdot \ln \left( 1 + \frac{1}{R_{i,j}} \ln(1 - P_{i,j} R_{i,j}) \right), \quad (6.27)$$

$$q_{L,i,j} = q_{0,i,j} \cdot \left( 1 + \frac{1}{R_{i,j}} \ln(1 - P_{i,j} R_{i,j}) \right) \cdot (1 - P_{i,j} R_{i,j}) \quad (6.28)$$

With formulas  $R_{i,j} = 0$  (6.25)-(6.28), using excellent bounds, they take the form:

$$q_{0,i,j} = -\frac{q_{i,j}}{P_{i,j} R_{i,j}} \cdot \ln(1 - P_{i,j}) \text{ and } q_{L,i,j} = q_{0,i,j} \cdot (1 - P_{i,j}). \quad (6.29)$$

All the parameters obtained can be used to determine the temperatures of heat carriers and the thermal regime of the walls in any section of the pipe located in the zone or section of the heat exchanger of the type under study. Examples of the distribution of thermal characteristics in the shell of the steam cooling of a real heat exchanger (see Fig. 6.1), the current circuit of which corresponds to Fig. 3.3 are presented in Figs. 6.2-6.4. The boundary conditions given in Table 6.1 were used here.

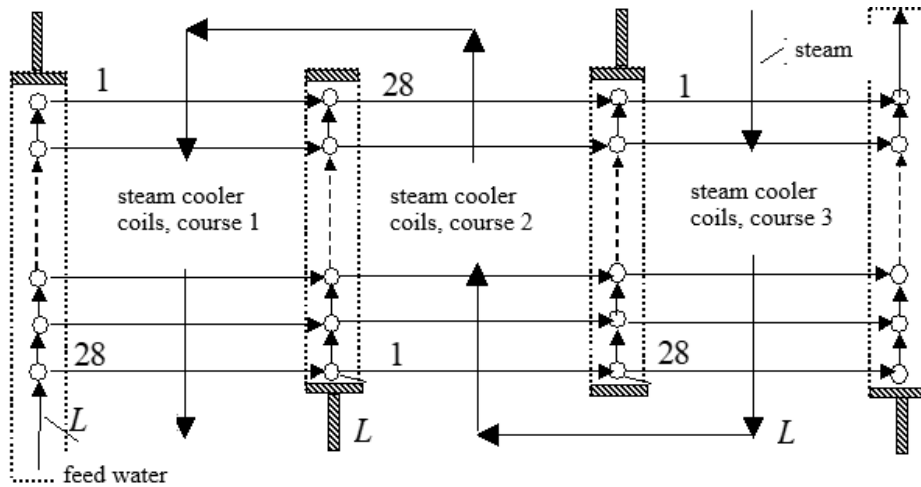


Fig. 6.1 - Diagram of the three-way steam cooler PIBT-1 of the turbine unit K 500-240-2 of KhTGZ (see Figs. 1.10 and 2.5 a, one of the two steam flows)

Table 6.1 - Boundary conditions for a three-pass heat exchanger (see Fig. 6.1)

$t_{H1},$ °C	$t_{H2},$ °C	$t_{\Gamma1},$ °C	$t_{\Gamma2},$ °C	$\alpha_1,$ W/mK	$\alpha_2,$ W/mK	$L,$ m	$z$	$n$	$d_H,$ mm	$d_{BH},$ mm
96,21	300,49	425,00	212,69	13895	768	19,5	3	28	32	20



## **CHAPTER 7**

### **PECULIARITIES OF OPERATION AND MAINTENANCE OF STEAM-WATER HEAT EXCHANGERS OF TES AND NPPS POWER PLANTS**

#### **7.1. Factors Determining the Reliability of Operation of Surface Heat Exchangers for Regeneration Systems of TPP and NPP Turbine Units**

The reliability of heaters largely determines the costs of their manufacture and operation. The heat exchangers of turbine units of TPP and NPP power units are characterised by a period of (2...3) years, during which structural and technological defects are identified and eliminated [48]. This is followed by a period of normal operation and then (after about 5 years) by an increase in malfunctions due to operational wear, which after 10 years become avalanche-like, requiring replacement of the pipe system or complete replacement of the devices. Meanwhile, according to the Polzunov Centre for Chemical Technology, heat exchangers in turbine plants should last 20-30 years. The nature of the damage is as follows: erosion wear of the tubes, corrosion wear leading to fistulae, tube breakage near the tube boards, abrasion in the intermediate partitions, mutual abrasion of the tubes, etc. VTI conducted a survey of block TPPs based on questionnaires on the damage to the fuel assembly, their operating conditions, including data on the water-chemical regime [49]. The data obtained from 30 TPPs on 114 fuel assemblies were summarised and an attempt was made to identify the impact of operational factors and design features on damage. The analysis presented in this paper shows that the damage to the coils of the fuel assembly depends on a large number of factors. According to [1], the main factors that affect the reliability of the operation of the water-insulated coil during the operation of a power plant are

a) erosion and corrosion wear (ECW) of the inlet sections of the coils. It is the result of vortex (detachment) cavitation in the inlet section with the imposition of general corrosion and erosion wear on both the inside and outside of the pipe;

b) depressurisation of internal blind partitions (plugs) in the distribution and collection collectors. Leaks are usually the result of poor welding of the baffle, which is installed in the wall of the two parts of the collector in the form of a lining ring and is located in a hard-to-reach area with a high probability of failure and subsequent water erosion of the welds of the baffle and the collector wall. Particularly harmful is the effect of a loose partition between the steam condensation and the steam cooling in single-pass structures, which opens the way for water to enter besides the steam condensation and steam cooling coils;

c) destruction of the weld connecting the distribution manifolds to the glass. This type of failure is a consequence of a poor design of the welding unit. In addition, the rigid connection of the distribution and collecting collectors in the upper crosshead at the temperature difference between the walls of these collectors, which occurs under operating conditions, causes significant thermal stresses in the weld. At present, these rigid connections have been eliminated in modernised and new designs of the high-pressure regenerative feed water heaters;

d) destruction of coils in the first pass of the steam cooling zone located under the steam inlet pipe due to vibrations and coil rubbing against each other under the impact of steam jets entering the steam cooling. Based on the negative operating experience, in the future, in the modernised and new designs of the high-pressure regenerative feed water heaters, an unstressed steam supply is performed;

e) steam breakthroughs through the SC into a lower pressure heater (deaerator), or, conversely, condensate flooding of the lower coils of the steam condensation due to the difficulty of maintaining a normal condensate level of about 50 mm above the SC inlet when supplied from above. Currently, condensate is supplied to the SC from below, which avoids the above problems;

f) increased steam resistance of the steam generator. The reliability of operation here is mainly related to the decrease in the saturation temperature in the control unit due to high pressure losses in the steam cooling. The use of the steam

cooling zone becomes impractical in this case. The flow of steam or condensate in the plane of the coil winding has a high resistance due to the many turns and constrictions (expansions) of the flow. In addition, the flow in the coil winding plane has low heat transfer efficiency. In modern and upgraded designs of high-pressure regenerative feed water heaters, cross-flow of coils by steam (condensate) in the steam cooling and condensate coolers is organised, where the resistance is significantly reduced and the heat transfer efficiency from the heating medium is increased.

According to [48], the main factors that determine the reliability of the operation of the low pressure regenerative feedwater heaters during the operation of a power plant are

a) erosion-corrosion wear (ECW) of the inlet sections of U- or  $\Pi$ -shaped pipes near the pipe boards, similar to the spiral coils in the high-pressure regenerative feed water heaters;

b) abrasion of pipes near intermediate baffles and mutual rubbing of pipes in large spans and in the area of bends caused by vibration. In modern tubing designs, designers try to avoid large unsupported spans. Damping belts are used to reduce vibrations [2]. To ensure unstressed steam supply to the pipe bundle, a steam deflector is installed at the pipe bundle inlet.

As can be seen from the above analysis, most of the factors that reduce the reliability of heaters can and have already been eliminated by developing a more advanced design of components without a significant increase in costs. According to [48], the malfunctions of the high-pressure regenerative feed water heaters occur in most cases due to poor manufacturing quality and the ECW of the coil inlet sections, while the reliability of the tubing is approximately 50% determined by the ECW of the pipe inlet sections and 50% of the malfunctions are caused by violations of the operating conditions. Therefore, further considerations will be directed to the

ECW of the inlet sections of coils and pipes, since this factor of heaters reliability is the most significant and difficult.

## **7.2. Erosion and corrosion wear of the inlet sections of coils and tubes of surface heat exchangers of power plants**

The cause of erosion damage to the inlet areas inside the pipes is the hydromechanical forces arising in the process of vortex (tear-off) cavitation [2]. In this case, local boiling occurs at the sharp inlet edge or in the immediate vicinity of it, where the boundary layer is torn off due to high local velocity and large longitudinal and transverse pressure gradients. As a result, an annular vortex is formed in the centre of which conditions for the appearance of small cavities arise. The presence of vortices in the wall region (separation zone) and high turbulence in the boundary layer contributes to an even higher decrease in local pressure and the development of the cavitation process. This phenomenon is a complex erosion and corrosion process. The intensity of this process is determined by the flow rate in the coils and in the inlet manifold, the temperature of the feed water, the content of oxygen, free carbon dioxide and other impurities in it, electrical conductivity, pH value, stress concentration in the metal of the pipe wall, the quality of the coil (pipe) docking to the manifold or pipe board, etc. [1, 2]. The impact of each of these factors has not been fully studied, but many researchers believe that this type of wear is significantly reduced at feedwater velocities inside pipes of less than 2 m/s and  $\text{pH}=9-9.5$  [1].

Erosion and corrosion wear is observed at a distance of 100-120 mm ( $46 d_{\text{BH}}$ ) from the distributing manifolds or the pipe wrapping in the pipe board [2]. Erosion and corrosion causes more or less uniform sinking of the pipe wall in this area. The unevenness and intensity of wear can be increased by loose installation of the coil or pipe end in the collector socket (pipe board), misalignment of the socket and pipe bore or skewing. ECW of the inlet sections of coils and pipes eventually leads to

pipe rupture or fistula formation. According to the requirements [2], the water velocity in coils and pipes should not exceed 2 m/s. In domestic water transport pipelines designed before 1972, this speed was  $2.5 \div 3.2$  m/s. A lot of work was done to modernise the existing high-pressure regenerative feed water heaters, i.e. to reduce feedwater velocities. The safe feedwater velocities of mass-produced SFAs are foreseen in advance. At some power units, the condition of the coils during the opening of the fuel assemblies is monitored by an ultrasonic thickness gauge 'Кварц-6', but it has insufficient accuracy in the direction of underestimation of the thickness [1]. When replacing the end sections of coils and their overall assembly, there are frequent cases of damage to the sockets in the reservoirs (misalignment of the hole and the socket in the reservoir, taper of the socket end), which leads to loose fit of the coil ends, misalignment and distortion, which intensifies their wear. Such violations also occur during the manufacture of high-pressure regenerative feed water heaters at the factory. Hydraulic irregularities in the velocity distribution along individual coils in the zone lead to accelerated wear of those coils where the velocities are maximum. The average velocity of feedwater in the reservoirs can also affect the wear of the coils' inlet sections, but this effect is insignificant [1].

The inlet sections are subjected to general corrosion wear from both the outer and inner sides, which leads to a total sinking of the coil wall of up to  $1 \div 1.5$  mm for  $80 \div 90$  thousand hours of operation [1]. The reason for this is the lack of conservation of the fuel assemblies during shutdowns. In the zone of the steam cooling, in certain modes, partial condensation of steam on the outer wall of the coils and the transport of droplets by steam may occur. This results in erosion and corrosion wear of the outer surface of the coils in the form of ulcers on the stretched and compressed net coils, reaching 15-20 mm across on the surface and gradually deepening into the metal to the full wall thickness (droplet erosion). Droplet erosion is most pronounced near the coil inlet area, which exacerbates ECW, as the temperature of the coil outer wall is minimal here and, as a result, the probability of partial steam condensation is maximum. More cases of drop-impact erosion of the

outer surface of coils are observed in the high-pressure regenerative feed water heaters of turbine units of NPPs operating on saturated steam. Here, the coils of the control zone located directly under the condensate baffles in the area of holes in them for the passage of steam from the area above the baffle to the area below it are worn out. As a rule, these openings are blocked by coil turns and steam velocities can be very high. The heating steam here is moist and, in addition, captures condensate flowing down the baffle and entrains it into this opening. The areas of the coils directly below the opening are subject to increased droplet erosion. To prevent this erosion, the opening cross-section of the condensate drainage baffles should be increased.

Thus, the main areas of research into the ECW of coil inlet sections can be identified:

a) ECW of the inlet section on the feed water side inside the pipe (coil) at a distance of 100 -120 mm ( $d_{BH}$ ) from the wrapping point (most dangerous area);

б) ECW of the inlet section from the outside of the pipe.

In the condensate coolers and steam condensation zones from the outside and in all heater zones from the inside, the coil (pipe) wall material is subject to ECW in water during operation. In the steam cooling zone, the wall material is exposed to steam and water corrosion from overheated steam and droplet erosion on the outside during operation. The mechanism of corrosion of steel by superheated steam is the chemical oxidation of iron by steam with the release of hydrogen gas and the formation of a dense layer of scale. This process affects the metal evenly at high temperatures (over 400 °C). A graph of mass loss for this process versus temperature is given in [39]. This type of wear is rare in high-pressure regenerative feed water heaters operation, but it can occur in the first high-pressure regenerative feed water heaters feedwater header, where high-temperature steam is supplied after industrial superheating. The mechanism of droplet erosion is complex [50]. It is very difficult to construct experimental mass and depth data for this process. The form of damage

from droplets hitting the pipe wall is local (ulcerative) in nature. However, from the thermal-hydraulic calculations of the high-pressure regenerative feed water heaters system, it is possible to build graphs that can be used to identify those coils that will be subject to droplet erosion. The first coil to form condensate droplets will be located near the intersection of the saturation temperature curve for the heating steam pressure and the graph of the distribution of the minimum temperature of the outer wall of the coils (pipes). Subsequent coils (pipes) along the path of the heating steam will be subject to droplet erosion.

In the process of shutdowns of heaters or the power unit as a whole, the material of pipes (coils) is subjected to standstill corrosion. The mass index of the rate of parking corrosion can be estimated as  $0.05 \text{ g}/(\text{m}^2 \cdot \text{hour})$  [28]. Parking corrosion occurs mainly as a result of prolonged shutdowns without conservation.

The depth rate of erosion-corrosion is related to the mass rate by the following relation:

$$K_{\Gamma} = 10^{-3} \frac{K_M}{\rho_M} \cdot 8760, \quad (7.1)$$

where  $\rho_M$  - is the density of the pipe wall material in  $\text{g}/\text{cm}^3$  of steel 20 –  $\rho_M = 7.85 \text{ g}/\text{cm}^3$  [28], brass Л -68 -  $\rho_M = 8.6 \text{ g}/\text{cm}^3$ , brass ЛО70 -1 -  $\rho_M = 8.68 \text{ g}/\text{cm}^3$  and copper-nickel alloy МНЖ5 -1 -  $\rho_M = 8.7 \text{ g}/\text{cm}^3$  [51];

$K_M$  is the mass index of corrosion rate,  $\text{g}/(\text{m}^2 \cdot \text{hour})$ .

There is a great deal of experimental data and theoretical research on the ECW of steel and other materials in water [39, 49, -59]. All these data refer to certain narrow experimental conditions and chemical composition of water. Often, these studies contradict each other, since the corrosion-erosion rate dependence is multifactorial. Factors affecting metal corrosion in water are divided into external and internal [56]. External factors include the conditions of the environment in which the metal is located: the chemical composition of water, the presence of

suspended solids, temperature, the speed of water movement relative to the metal, etc. The pH value and the content of dissolved oxygen in water significantly affect the corrosion intensity (see the dependence from [39, 56] in Fig. 7.1, where curve 1 corresponds to the maximum solubility of oxygen in water at a given temperature, curve 4 corresponds to the absence of oxygen, and curves 2 and 3 correspond to intermediate values). Analysis of these curves shows that steel is subject to very intense corrosion at  $\text{pH} < 4$ . At  $\text{pH} = 4 \div 8$ , the corrosion rate is pH dependent.

An increase in the concentration of salts dissolved in drinking water contributes to the intensification of electrochemical corrosion due to an increase in the electrical conductivity of water [56]. Free carbon dioxide causes a decrease in the pH of water. The presence of a significant amount of free carbon dioxide in water prevents the formation of protective films, which become loose and easily carried away by the water flow. The active participation of free carbon dioxide in iron corrosion is a circular process with the release of new amounts of free carbon dioxide as a result of chemical reactions. Therefore, its presence significantly intensifies the process of steel corrosion. Hydrogen sulphide, chlorides, hydrosulphites and sulphates also significantly intensify the corrosion rate. The composition and quality of feed water and condensate at power plants is regulated by the Technical Operation Rules for Power Plants and Networks (PTE). There are several types of water and chemical regimes at power plants. While the peculiarity of the hydrazine-ammonia water regime (HAW) is the suppression of corrosive aggressiveness of water towards structural materials during the operation of power units by increasing the pH of water and almost complete removal and binding of dissolved oxygen, the effectiveness of the neutral-oxide regime (NOR) is based on inhibition of metal corrosion by limiting the access of corrosive agents to the surface by creating a protective film on it [28]. The quality standards for nutrient water in the NOCR differ from the HAR in the absence of additives that correct the pH and oxygen concentration. The dosage of the latter in the amount of  $50\text{--}200\text{ }\mu\text{g/kg}$  ensures the creation of protective films on the surfaces of the condensate-feeding tract at



temperatures above 80 °C. A prerequisite for the use of NPC is deep desalination of condensate and feed water; the electrical conductivity of water should not exceed  $0.15 \div 0.25 \mu \text{ cm/cm}$  to avoid intensification of pitting corrosion of carbon and low-alloy steels, as well as corrosion cracking of austenitic steels.

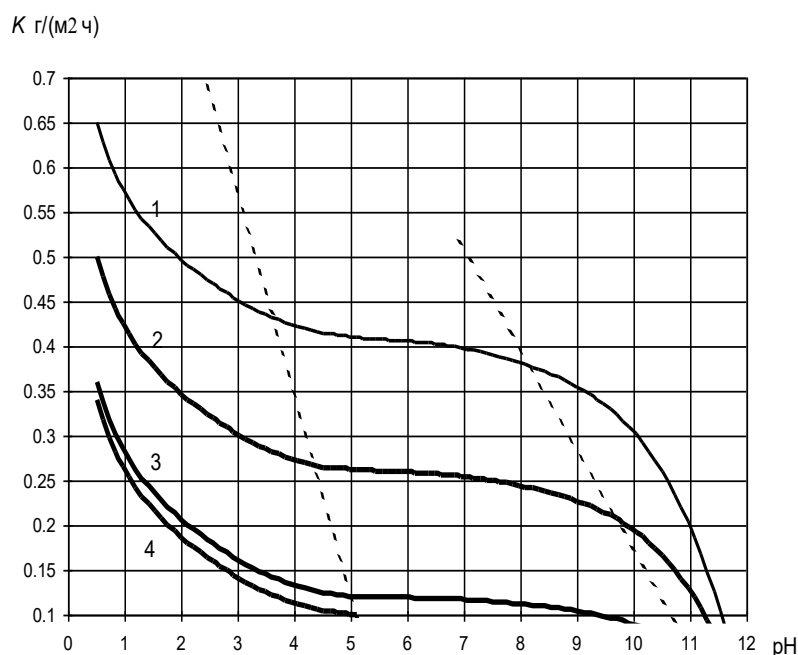


Fig. 7.1 - Dependence of steel corrosion rate in water on pH in the presence of oxygen

The pH value should be maintained at a level close to the neutral point, for which in some cases it is practiced to add small amounts of ammonia to the feed water, which provides a pH value of up to 7.8. The neutral-oxide regime can be used on those units where stainless or carbon steels are used in the tubular system ÷ of the tubular system instead of copper-containing alloys. An additional condition for using this mode is thorough purification of the make-up and feed water from organic impurities, the thermolysis of which can lead to a dangerous decrease in the pH of the medium and an increase in the specific electrical conductivity. Feedwater quality standards for supercritical pressure boilers (SCB) are regulated not only by PTE but also by PTM 108.030.12-82. At TPPs with CKД boilers, it is allowed to use GAR or combined oxidation mode (COM). The latter differs from the neutral-oxidising

mode by dosing ammonia in an amount that ensures the maintenance of the pH of the medium at the level of 7.58. The areas of predominant application of the BCR are power units with a capacity of 250 and 300 MW. It should be noted that, as follows from the analysis conducted in [49, 60], the quality of feedwater and condensate from power plants often deviates from the standards regulated by the PTE and other documents. The pH value in the condensate-feedwater path lies in the range of  $5 \div 9,5$  (see the results of the study [60] in Fig. 7.2). For the heating steam, it will be close to the pH of the feedwater. Experimental dependences of the steel corrosion rate on the concentration of dissolved oxygen are reported in [39, 52]. These dependences are close to linear. Therefore, at intermediate oxygen concentrations in the range of  $\text{pH}=5 \div 8$ , the corrosion rate is directly proportional to the oxygen concentration. The proportionality coefficient  $\gamma_t$  at temperature  $t$  will be the ratio of the true oxygen concentration  $x_t$  to the limiting one  $x_{\text{II}P_t}$ :

$$\gamma_t = \frac{x_t}{x_{\text{II}P_t}}, \quad (7.2)$$

The solubility of oxygen in water is governed by the well-known Henry's law:

$$p = E \cdot x, \quad (7.3)$$

where  $p$  - is the partial pressure of oxygen above the liquid;

$E$  - is Henry's coefficient, the unit of which corresponds to the unit of pressure;

$x$  -is the molar concentration of dissolved oxygen in water.

In dilute solutions, the Henry's coefficient depends only on temperature. The graph of this dependence [52] is shown in Fig. 7.3.

The known value of the corrosion rate at temperature  $t_0$  can be taken as a starting point. Then the dependence of the steel corrosion rate at temperature  $t$ , taking into account Fig. 7.1 and Henry's law (7.3), the conditions of equality of true

concentrations and partial pressures of oxygen at temperatures  $t$  and  $t_0$  and formula (7.2) can be given as follows:

$$K_t = \varepsilon_0 K_{\text{III}} \frac{E_t}{E_0}, \quad (7.4)$$

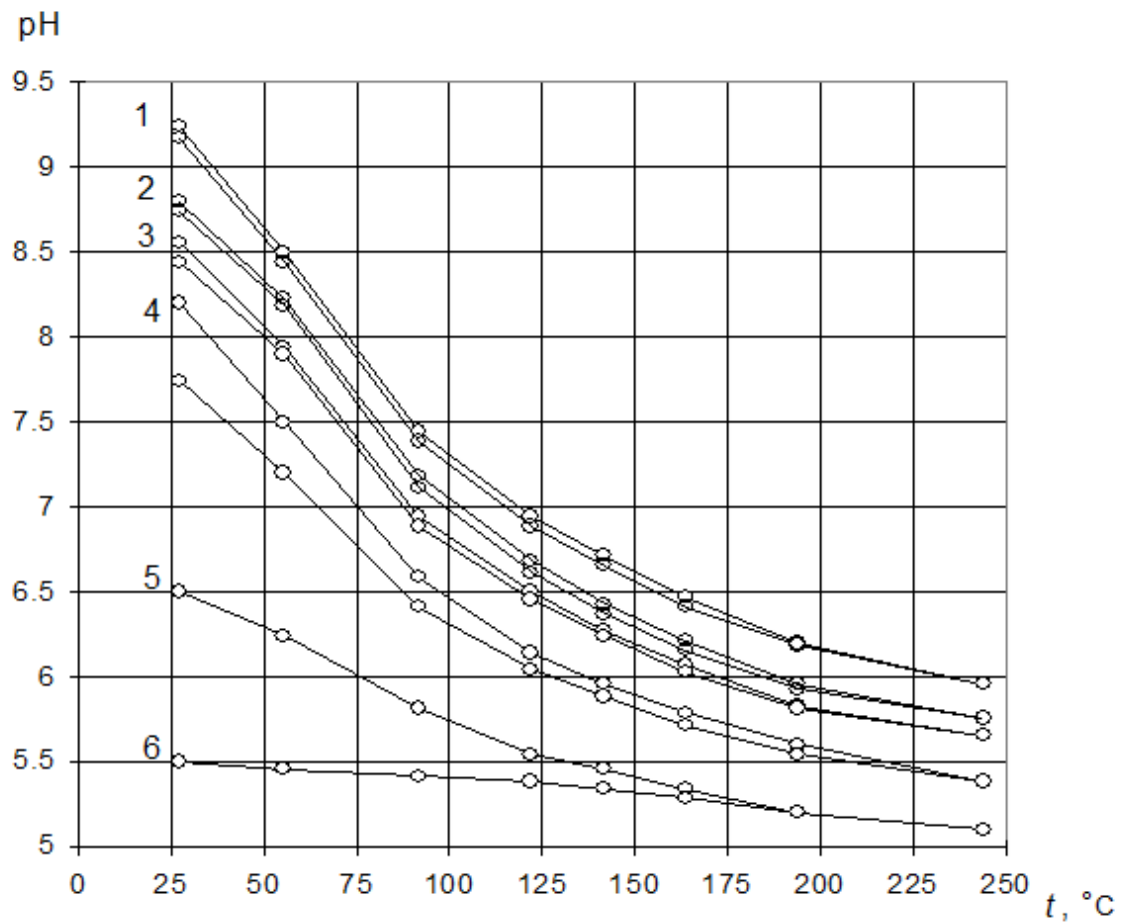


Fig. 7.2 - pH values along the length of the condensate-feed path depending on the concentrations of ammonia and carbon dioxide.

- 1 – ammonia concentration - 1530  $\mu\text{g/l}$ ;
- 2 – ammonia concentration – 510  $\mu\text{g/l}$ ;
- 3 – ammonia concentration – 340  $\mu\text{g/l}$ ;
- 4 – ammonia concentration – 170  $\mu\text{g/l}$ ;
- 5 – clean water;
- 6 – carbon dioxide solution – 88  $\mu\text{g/l}$

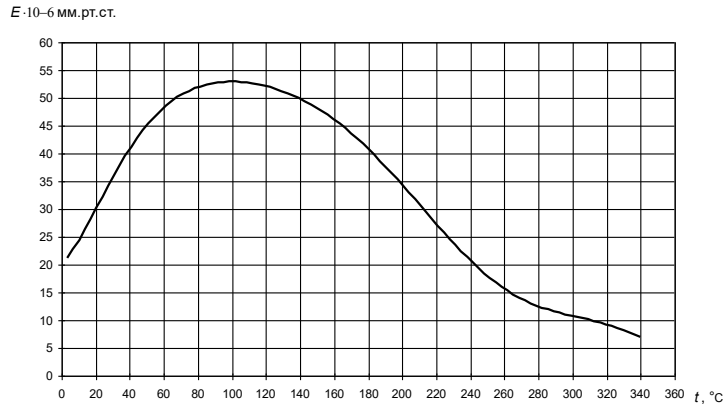


Fig. 7.3 - Henry's coefficient values for determining the solubility of oxygen in drinking water depending on temperature

where  $\varepsilon_0$  - is a correction factor for the maximum corrosion rate, depending on the concentration of dissolved oxygen and other factors at an initial temperature  $t_0$ , which can be determined by experience or expert opinion;

$K_{\text{HP}}$  - corrosion rate at the maximum oxygen concentration (curve 1 in Fig. 7.1);

$E_t, E_0$  - Henry's coefficients at a given temperature  $t$  and initial  $t_0$ .

Studies on the effect of temperature on erosion-corrosion of unalloyed steels are presented in [49, 57]. It is stated here that the peak of erosion-corrosion is observed at a temperature of 160 -180 °C, i.e., under the conditions of operation of the BF-1 (the first after the deaerator). With increasing temperature, the erosion-corrosion rate decreases. The decrease in the erosion-corrosion rate with increasing temperature is explained by the intensification of the formation of protective films. It is advisable to take the feed water temperature in the deaerator (164.2 °C) as the zero reference temperature, since it is constant in all operating modes of the turbine unit. The analysis of dependence (7.4) shows that as the feedwater temperature increases relative to the deaerator temperature, the corrosion rate should also decrease, since the Henry's coefficient  $E_t$  decreases with increasing temperature.

Therefore, if the ammonia and carbon dioxide content of the water is known, it is possible to use Fig. 7.2 to determine the pH value. The pH value is used to determine the maximum corrosion rate  $K_{\text{IP}}$  according to Fig. 7.1 (line 1). Then, based on the known oxygen content and taking into account other factors, the correction factor  $\varepsilon_0$  is set at the initial temperature  $t_0$ . Depending on Fig. 7.3, the Henry's coefficients for the solubility of oxygen at the initial and true water temperatures  $E_0$  and  $E_t$  are calculated. The calculated values are used to determine the corrosion rate of steel (formula (7.4)).

The main difficulty in calculating the corrosion rate according to the above algorithm is the determination of the expert proportionality coefficient  $\varepsilon_0$ . The corrosion rate dependence (Fig. 7.1) is constructed without taking into account the erosion component. As mentioned above, outside the inlet areas (where the erosion component can be neglected), the total depth corrosion rate on the inside and outside of the coils is  $11.5 \pm \text{mm}$  for  $8090 \pm \text{thousand. h}$  of operation. If we choose the maximum of these values, taking into account formula (7.1), the mass corrosion rate  $K$  on one side of the pipe will be equal to  $0.0736 \text{ g}/(\text{m}^2 \cdot \text{hour})$ .

For example, the value of the maximum corrosion rate  $K_0$  at a concentration of ammonia in the feed water of  $510 \mu\text{g/l}$  and carbon dioxide of  $88 \mu\text{g/l}$  (lower line 2 in Fig. 7.2) and a temperature  $164,2 \text{ C}^\circ$  will be  $0.405 \text{ g}/(\text{m}^2 \cdot \text{hour})$ . Based on these initial data, the value of the correction factor  $\varepsilon_0$  can be taken as 0.182.

The study of the corrosion-erosion rate of brass pipes and pipes made of copper-nickel alloy MHЖ5 -1 used in capacitors and tubing. The average service life of a smooth pipe made of Л-68 brass is 7-10 years. The paper presents the results of laboratory and semi-industrial tests for smooth and shaped tubes under conditions as close to realistic as possible. Water was circulated through the  $19 \times 1 \text{ mm}$  test pipes at a speed of  $1 \text{ m/s}$  and a temperature of  $50 \text{ }^\circ\text{C}$ . The results of the steady-state corrosion rate of smooth pipes [58, 59] are given in Table 7.1.

Table 7.1 - Steady-state corrosion rate of copper-containing pipe materials at a water velocity of 1 m/s, g/(m<sup>2</sup> · h)

Material of pipes		
brass Л-68	brass ЛО70-1	alloy МНЖ5-1
0,11	0,0565	0,0343

Paper [54] investigates the corrosion of stainless steel. According to the results of the analysis, stainless steels have high corrosion resistance under conditions of heat transfer up to 2200 kcal/(cm<sup>2</sup> · h) in waters with a specific electrical conductivity of 0.125 ÷ 1 μ cm/cm. However, the presence of chlorine ions Cl<sup>-</sup> - (deterioration of feed water and condensate quality) leads to a sharp increase in corrosion cracking of austenitic stainless steels.

Fig. 7.4 shows the dependence of the results of semi-industrial bench tests from [58] on the erosion-corrosion rate of a pipe sample with an internal diameter of 33 mm made of brass ЛАММ 77-2-0.05 on the water flow rate in the pipe.

It follows from the dependences that at a flow rate of up to 1 m/s, the erosion-corrosion rate is directly proportional to the flow rate, then at a flow rate of 1 m/s to 2 m/s, the erosion-corrosion rate increases slightly, with an increase in the flow rate to 3 m/s, it doubles compared to 2 m/s and then practically stabilises. The described features of the behaviour of the erosion-corrosion rate are typical for both brass pipes and carbon steel pipes [1, 55, 56]. The initial increase in the corrosion rate is associated with an increase in the flow of oxygen to the metal, which increases the depolarisation of the cathodic areas of corroded elements [56]. A further increase in water velocity reduces the intensity of the corrosion rate due to passivation of the metal and the formation of strong oxide protective films under the energetic influx of oxygen. A significant increase in the corrosion rate with a further increase in water velocity is due to the partial or complete destruction of protective films (including the erosion component)

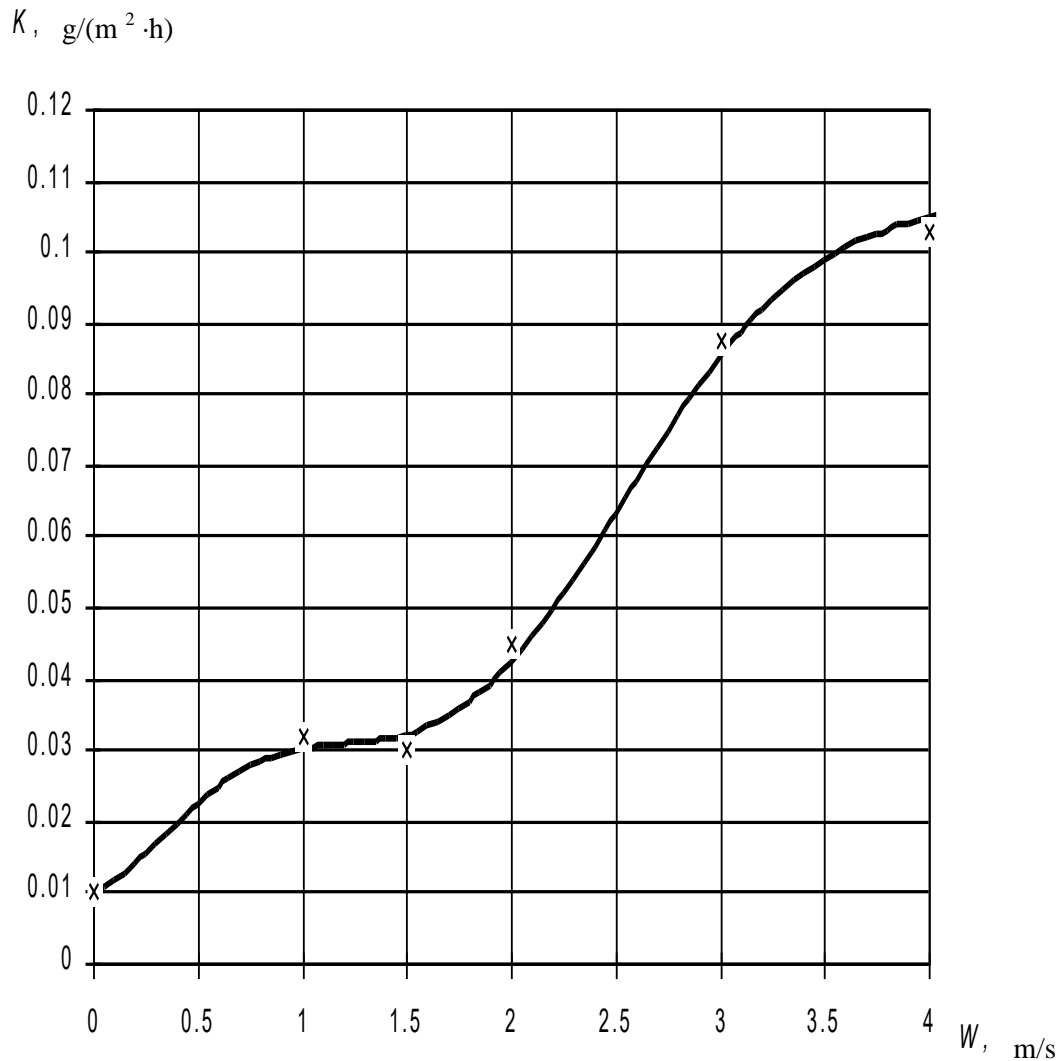


Fig. 7.4 - Effect of water velocity on the rate of erosion-corrosion of brass JAMIII 77-2-0.05.

Thus, the effect of water flow rate on metal erosion-corrosion is explained by the hydrodynamics of the flow and the corrosion properties of the metal itself. For other grades of brass and carbon steel materials, it is proposed to take into account the effect of water flow rate using a dimensionless correction factor  $\varepsilon_W$ :

$$\varepsilon_W = \frac{K_W}{K_{W_0}}, \quad (7.5)$$

where  $K_W$  and  $K_{W_0}$  is the corrosion rate of the sample of JAMIII 77 material -20.05 (Fig. 7.4) at the studied water flow rate  $W$  and water flow rate  $W_0$  in

laboratory and other tests of samples of the studied materials from other grades of brass or carbon steel.

The nature of the resulting dependence of the ECW rate of brass and steel 20 is shown in Fig. 7.5. For steel, the type of dependence on temperature is similar to that given in [49, 57] in the range of the studied temperatures of the high-pressure regenerative feed water heaters feedwater.

To analyse the erosion and corrosion wear of the tubes of the heating surfaces of the heaters, the water-chemical regime established for the power unit is taken as the initial data, where the concentrations of impurities in the feed water (ammonia, oxygen, carbon dioxide, etc.) should be set. In accordance with the methods and algorithms for determining thermal and hydraulic characteristics, the required parameters of the coolants in all pipes of heating surfaces (temperature, pressure, feedwater and steam or condensate velocity) are considered during the warranty period to calculate the corrosion-erosion rate of their walls. Calculation of feed water or main condensate temperatures, outer and inner pipe walls, heat flux density at the distance of the inlet section in the most dangerous place is described in Section 6. In low pressure regenerative feed water heaters, the most dangerous distance of the inlet section is assumed to be 100 mm. In high-pressure regenerative feed water heaters, this distance is assumed to be equal to the thickness of the pipe board (the most dangerous place where stress concentrators are concentrated). For the outer surface of pipes of the steam condensation and condensate coolers zones made of 20 steel, the mass corrosion index  $K$  is calculated according to formula (7.4), for copper-containing alloys - according to Table 7.1.



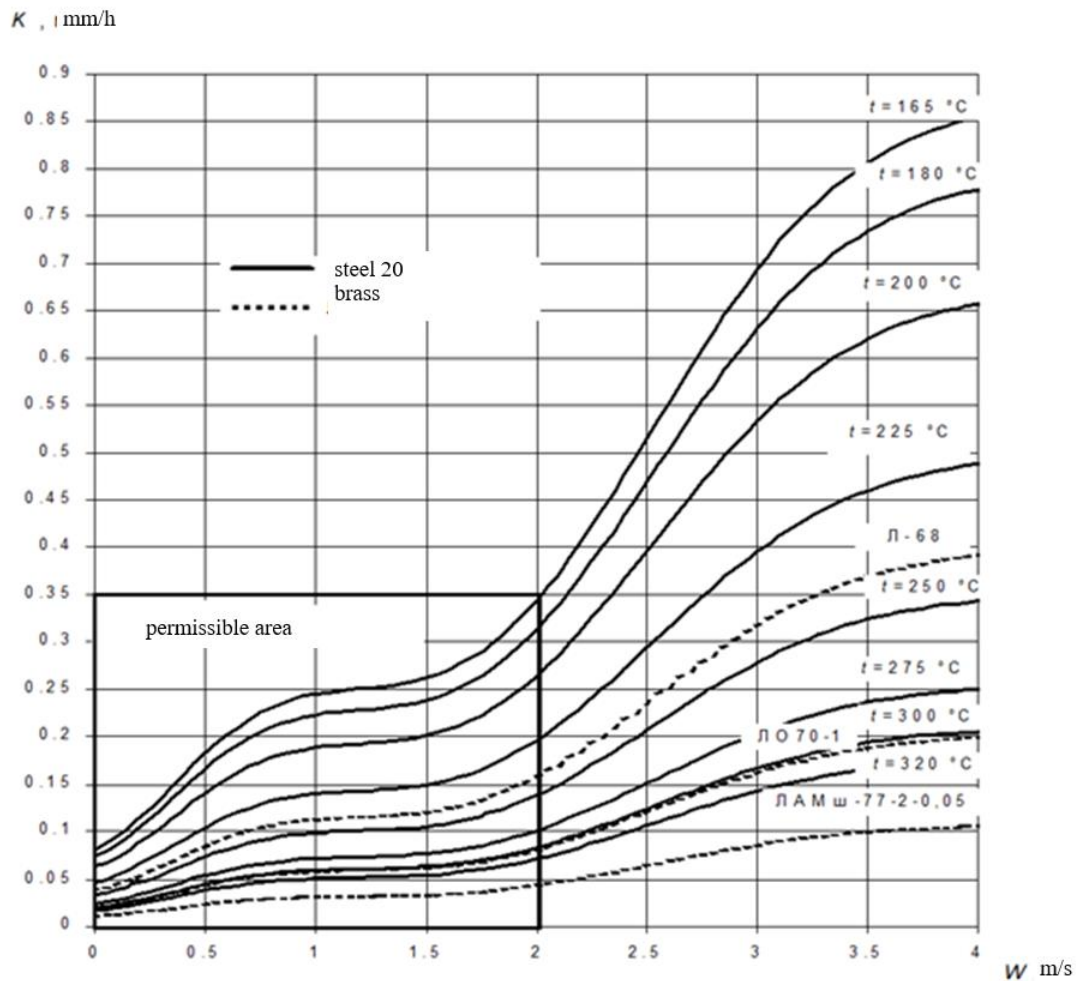


Fig. 7.5 - Resulting depth-based ECR rates

For the inner surface of the pipes, the mass index of the erosion-corrosion rate  $K$  is calculated by formula (7.4) or Table 7.1, corrected for the flow rate according to formula (7.5). The velocity  $W_0$  for steel 20 is assumed to be zero, and for alloys containing copper, it is equal to 1 m/s. There is no mass index of corrosion rate during operation for the outer surface of the steam cooling pipes, except for coils and pipes subject to droplet erosion or high-temperature steam exposure to steel. It is assumed that as a result of droplet erosion, pipe surface areas are subsequently subjected to corrosion, the rate of which is calculated using formula (7.4). The mass index of the corrosion rate on the inside and outside, in accordance with dependence (7.1), is considered to be the depth index. It should be noted that this algorithm does not yet take into account the parking time. The calculation of the corrosion rate in a

calendar period should be based on the weighted average of the operating time in each mode and the idle time. According to these data, the load factor of one of the 300 MW power units (see Table 7.2) is 84% of the rated capacity. The share of idle time is 25%. The number of hours of installed capacity utilisation is 5520 hours. With this load distribution, taking into account the statistical data from [1] on electricity generation in the power system, it is possible to accept the load distribution under guarantee modes for this power unit (see Table 7.3).

Table 7.2 - Load schedule for a 300 MW power unit

Workload	Months											
	01	02	03	04	05	06	07	08	09	10	11	12
Number of hours	744	551	440	719	654	720	744	169	0	364	720	744
% of num.	88,3	82,7	85,3	77,2	88	83	86	79	0	82,7	88,1	80

Table 7.3 - Time distribution by warranty modes of the turbine unit

Workload	Guarantee modes					
% of num.	100	85,2	64,7	52,1	49	42,7
% of hours	40	32	18	5	4	1

## CHAPTER 8

### ESTIMATION OF THE SERVICE LIFE OF SURFACE HEAT EXCHANGERS OF TES AND NPP POWER PLANTS

It follows from the discussion in Section 7 that the reliability and serviceability of surface heat exchangers of regenerative schemes of TPPs and NPPs is largely determined by the intensity of erosion and corrosion damage to the inlet sections of the heating surface pipes.

To simplify the estimated calculations of the time of destruction of a coil or pipe subjected to erosion and corrosion wear (ECW), it is assumed that erosion and corrosion damage is uniform in the inlet section, both from the outside and inside, local stress concentrators, temperature deformations. Internal and external pressure is taken as an influence. The inlet section of the coil (pipe) is a long thick-walled cylinder. It is assumed that the destruction of the coil wall should be expected after the transition of the entire wall thickness to the plastic region due to its sinking during operation. Then, under the influence of pressure, the pipe wall in the inlet section bulges, which leads to an increase in stress and rupture. Under these assumptions, only the estimated service life of a particular coil or pipe can be obtained. The estimated service life of coils and pipes can show the general trend and the locations of the most likely damage.

An approximate solution to the problem of the elastic-plastic state of a thick-walled cylinder under pressure is presented in [61]. The stresses in a long elastic cylinder under internal  $P_a$  and external  $P_b$  pressures are determined by the following formulae of the theory of elasticity [62]:

$$\sigma_r = \frac{P_a a^2 - P_b b^2}{b^2 - a^2} - \frac{(P_a - P_b) a^2 b^2}{(b^2 - a^2) r^2}, \quad (8.1)$$

$$\sigma_\theta = \frac{P_a a^2 - P_b b^2}{b^2 - a^2} + \frac{(P_a - P_b) a^2 b^2}{(b^2 - a^2) r^2}, \quad (8.2)$$

$$\sigma_z = \frac{1}{2}(\sigma_r + \sigma_\theta) = \frac{P_a a^2 - P_b b^2}{b^2 - a^2}, \quad (8.3)$$

where  $\sigma_r$ ,  $\sigma_\theta$ ,  $\sigma_z$  are normal stresses in the radial, tangential and axial directions;

$a$ ,  $b$  and  $r$  are the inner, outer and intermediate radii of the pipe.

The plastic state is determined according to the Mises-Genki condition:

$$(\sigma_r - \sigma_\theta)^2 + (\sigma_\theta - \sigma_z)^2 + (\sigma_z - \sigma_r)^2 = 2\sigma_T^2, \quad (8.4)$$

where  $\sigma_T$  is the yield strength of the pipe wall material.

From this, taking into account formulas (8.1)-(8.3), the plasticity condition is obtained:

$$P_a - P_b = \frac{\sigma_T}{\sqrt{3}} \left( 1 - \left( \frac{a}{b} \right)^2 \right) \quad (\text{for the inner surface}), \quad (8.5)$$

$$P_a - P_b = \frac{\sigma_T}{\sqrt{3}} \left( \left( \frac{b}{a} \right)^2 - 1 \right) \quad (\text{for the inner surface}), \quad (8.6)$$

The stresses in the plastic zone are determined by the equilibrium condition:

$$\frac{d\sigma_r}{dr} + \frac{\sigma_r - \sigma_\theta}{r} = 0, \quad (8.7)$$

and the Mises-Hankey plasticity condition (8.4).

For the case of a thick-walled cylinder, the equilibrium condition will take the form:

$$r \frac{d\sigma_r}{dr} = \frac{2\sigma_T}{\sqrt{3}}, \quad (8.8)$$

The solution of the system of equations (8.1), (8.8) and (8.5) if the plastic zone is formed from the inner to the outer surface at the outer radius  $r=b$  or (8.6) if the plastic zone is formed from the outer to the inner surface at the inner radius  $r=a$  will be the same:

$$P_a - P_b = \frac{2\sigma_T}{\sqrt{3}} \ln \frac{b}{a}. \quad (8.9)$$

Equation (8.9) was obtained at constant wall temperature, hence the yield strength along the cylinder radius. To simplify further calculations in pipes with heating surfaces, we can assume a linear dependence of the wall temperature increase from the inner surface  $t_{CTa}$  to the outer surface  $t_{CTb}$  and a linear dependence of the yield strength  $\sigma_T$  in the area from  $t_{CTa}$  to  $t_{CTb}$ :

$$\sigma_T(r) = \sigma_{Ta} + (\sigma_{Tb} - \sigma_{Ta}) \frac{r-a}{b-a}, \quad (8.10)$$

where  $\sigma_{Ta}$  and  $\sigma_{Tb}$  are the yield strengths at temperatures  $t_{CTa}$  and  $t_{CTb}$ .

As a result of integrating equation (8.8) with regard to dependence (8.10), formulas (8.5), (8.6), and (8.9), respectively, take the form:

$$P_a - P_b = \frac{\sigma_{Ta}}{\sqrt{3}} \left( 1 - \left( \frac{a}{b} \right)^2 \right) \quad (\text{for the inner surface}), \quad (8.11)$$

$$P_a - P_b = \frac{\sigma_{Tb}}{\sqrt{3}} \left( \left( \frac{b}{a} \right)^2 - 1 \right) \quad (\text{for the inner surface}), \quad (8.12)$$

$$P_a - P_b = \frac{2}{\sqrt{3}} \left( \frac{\sigma_{Ta} \frac{b}{a} - \sigma_{Tb}}{\frac{b}{a} - 1} \ln \frac{b}{a} - (\sigma_{Ta} - \sigma_{Tb}) \right). \quad (8.13)$$

In the case of sinking of the pipe wall, the value  $\frac{b}{a}$  can be given in the form:

$$\frac{b}{a} = \frac{d_H - 2z_H}{d_{BH} + 2z_{BH}}, \quad (8.14)$$

where  $d_H$  та  $d_{BH}$  are the nominal outer and inner diameters of the pipe, mm;

$z_H$  and  $z_{BH}$  – absolute value of wall sinking as a result of ECW on the outer and inner sides, mm.

The absolute values of the pipe wall thinning can be expressed as follows:

$$z_H = \frac{K_H \cdot \tau}{8760} \text{ and } z_{BH} = \frac{K_{BH} \cdot \tau}{8760}, \quad (8.15)$$

where  $K_H$  and  $K_{BH}$  are the depth indicators of the erosion-corrosion rate on the outer and inner sides of the pipe wall in the inlet section, mm/year;

$\tau$  - is the operating time of the coil (pipe), including stops, h.

The solution of equations (8.11) or (8.12) and (8.13), taking into account dependencies (8.14), (8.15) gives the time of the beginning of the formation of the plastic deformation zone  $\tau_1$  (8.11) or (8.12) and its completion  $\tau_2$  (8.13). In this case, the smaller of the calculated dependencies (8.11) and (8.12), the value of  $\tau_1$ , will determine on which of the surfaces - internal (8.11) or external (8.12) - the plastic zone begins to form.

The yield strength of soft brasses used to make pipes for heating surfaces of heat exchange equipment is  $\sigma_T = 98$  MPa for Л-68 brass and  $\sigma_T = 159$  MPa for ЛО70-1 brass [51]. For steel 20, the yield strength  $\sigma_T$  in the range of the high-pressure regenerative feed water heaters operation parameters significantly depends on the temperature (see Fig. 8.1 [21]), and with its increase, it decreases almost linearly. Taking this into account, for pipes with heating surfaces where the temperature of the outer wall is higher than the inner wall, the value of time  $\tau_2$ , calculated by Equation (8.13) will be less than that calculated by Equation (8.9), where the wall temperature is constant. Thus, pipes with heating surfaces will deteriorate faster than pipes with a constant wall temperature. In addition, when determining  $\tau_1$ , its value calculated by formula (8.11) is in all cases less than that calculated by (8.12). This indicates the beginning of the plastic zone growth in the pipes of surface heaters mainly from the

inside. Calculation of the estimated service life of coils taking into account the operation of the power unit turbine unit is based on the calculation of the time of the beginning of the formation of the plastic deformation zone  $\tau_{1i}^j$  and its completion  $\tau_{2i}^j$  for each warranty mode  $j$  for a particular coil  $i$  using formulas (8.11)-(8.15).

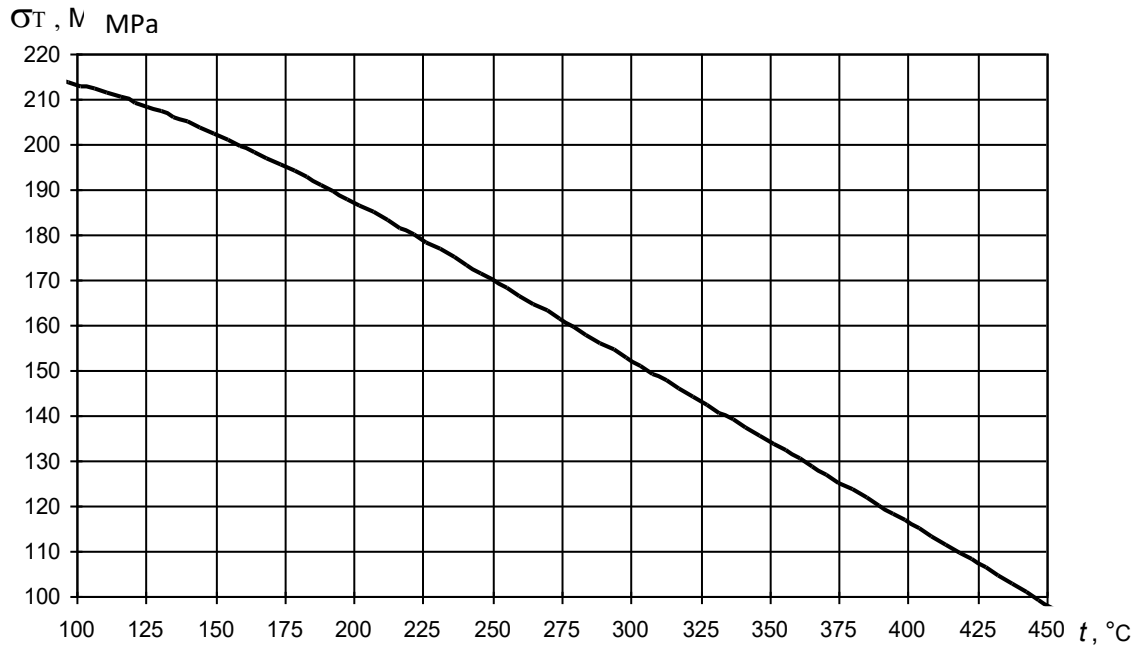


Fig.

### 8.1 - Dependence of yield strength of steel 20 on temperature

From the obtained values  $\tau_{1i}^j$  and  $\tau_{2i}^j$  for coil  $i$ , the minimum values are selected, which indicate at which warranty mode of operation of power unit  $j$  the coil destruction should be expected and after a certain assessment period. The initial data are the values of pressures and temperatures on the inner and outer sides of the pipe walls in the inlet section (Chapters 5 and 6) from the calculations of the high-pressure regenerative feed water heaters or regenerative low-pressure feed water heaters system at the warranty conditions and the depth erosion-corrosion rates taking into account the power unit load (Chapter 7). It is obvious that the most stressful operating mode for coils and tubes of heaters is the maximum or installed power mode (100%). However, as can be seen from the graphs of the estimated service life of coils and tubes of the K 300-240 KhTGZ turbine unit (see Fig. 8.28.5), the erosion-corrosion

indicators of which correspond to Fig. 7.67.10, in some modes of operation of the HF for the coils of the steam cooling the most stressful is the maximum mode with the steam cooling disconnected. Here, the high temperature of the coil walls in the coolant when it is disconnected from the feed water (no cooling and heating with high-temperature steam) affects the yield strength reduction.

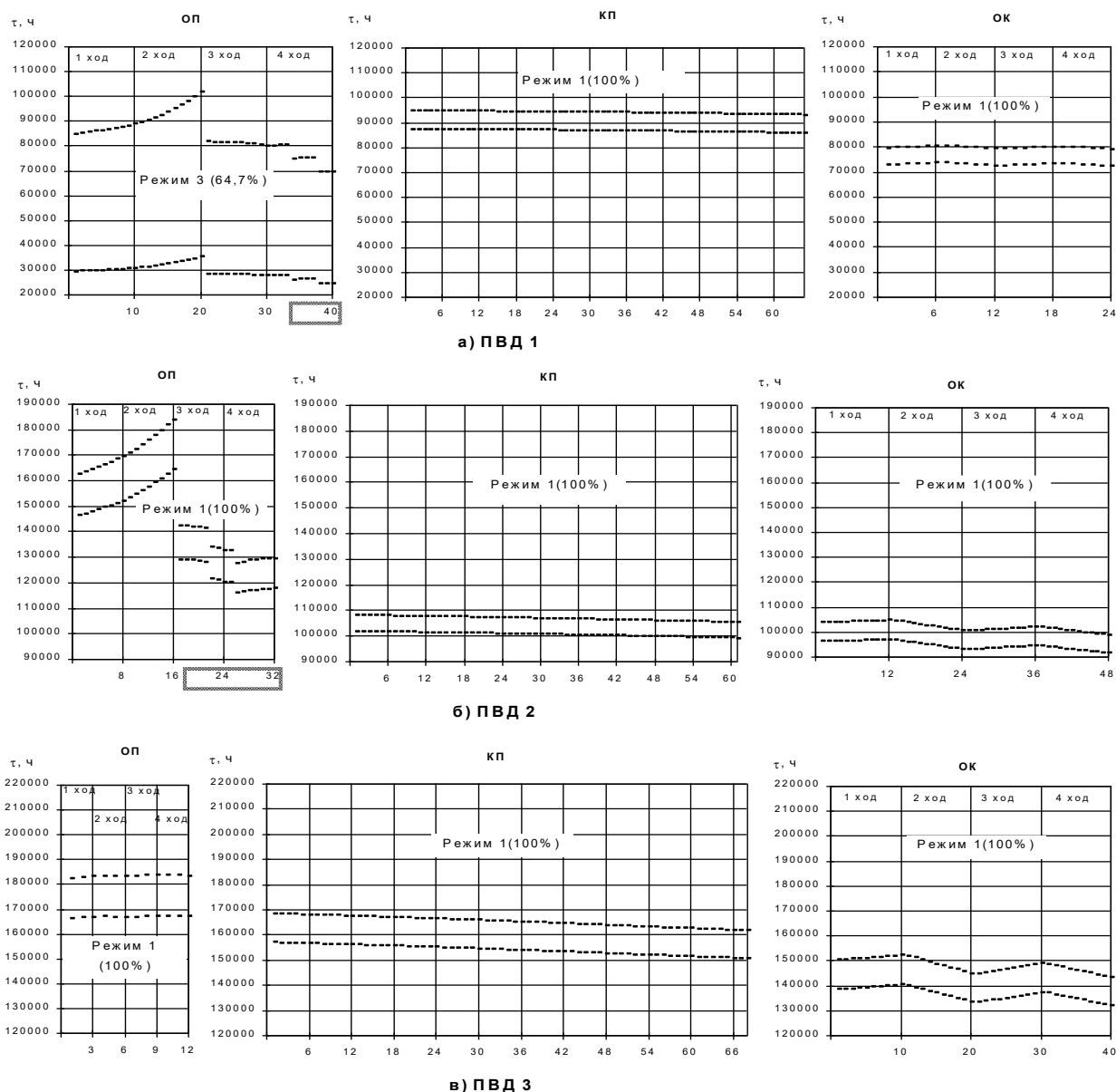


Fig. 8.2 - Time of the beginning of the formation of the plastic deformation region (lower curve) and the transition of the entire wall thickness to the plastic deformation region (upper curve) of the inlet sections of the coils of the ПБТ(ПВД) turbine unit up to 300-240 KhTGZ



(numbering of coils in the course of the heating steam (condensate) flow. The rectangle circles the coils subject to droplet erosion

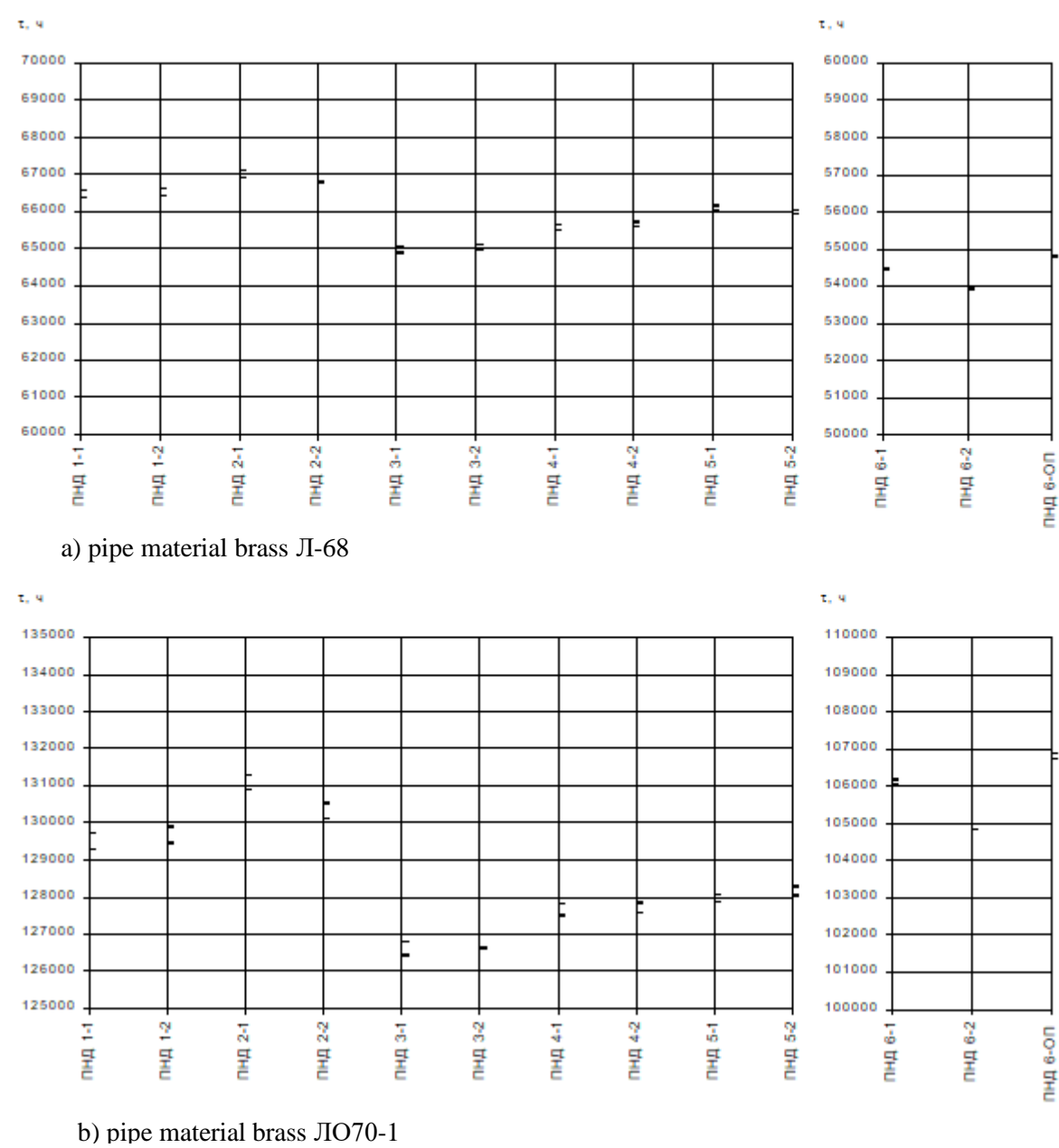


Fig. 8.3 - Time of the beginning of the formation of the plastic deformation region (lower line) and the transition of the entire wall thickness to the plastic deformation region (upper line) of the inlet sections of the tubing of the K 300-240 KhTGZ turbine unit (numbering of pipe bundles along the main condensate flow).

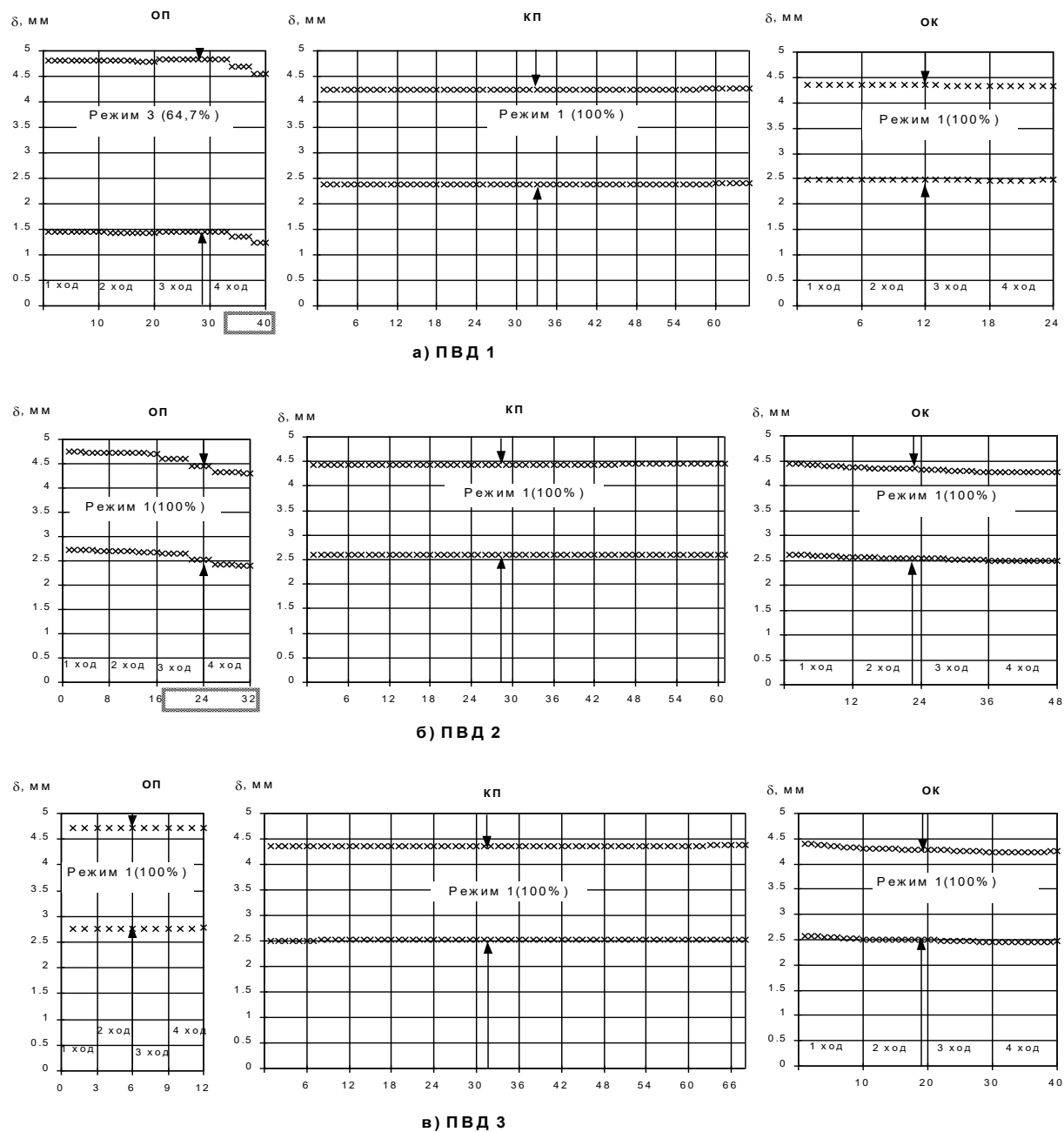
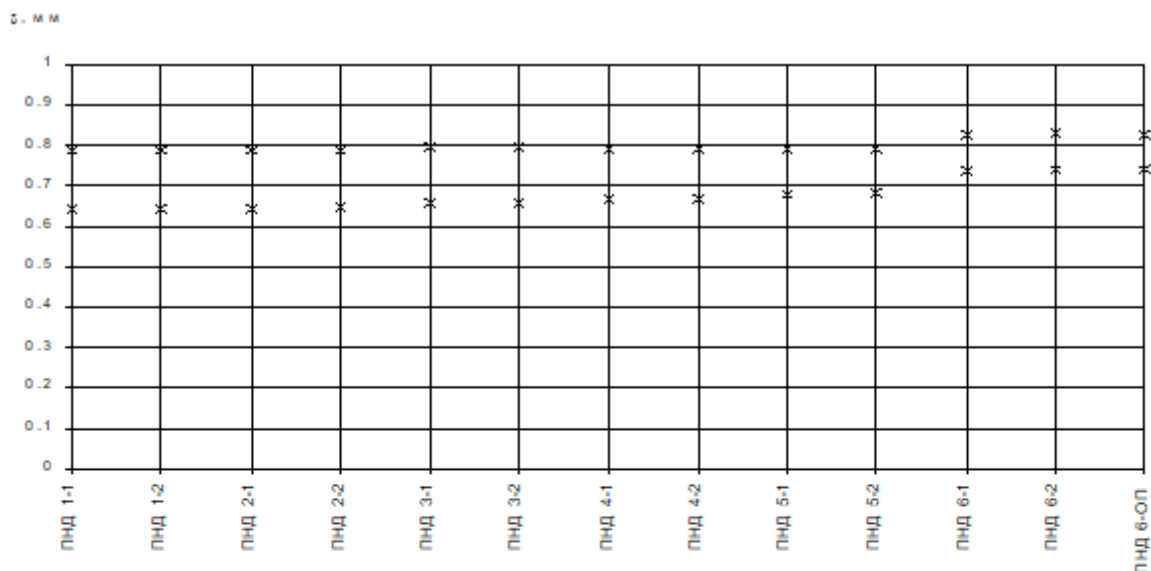
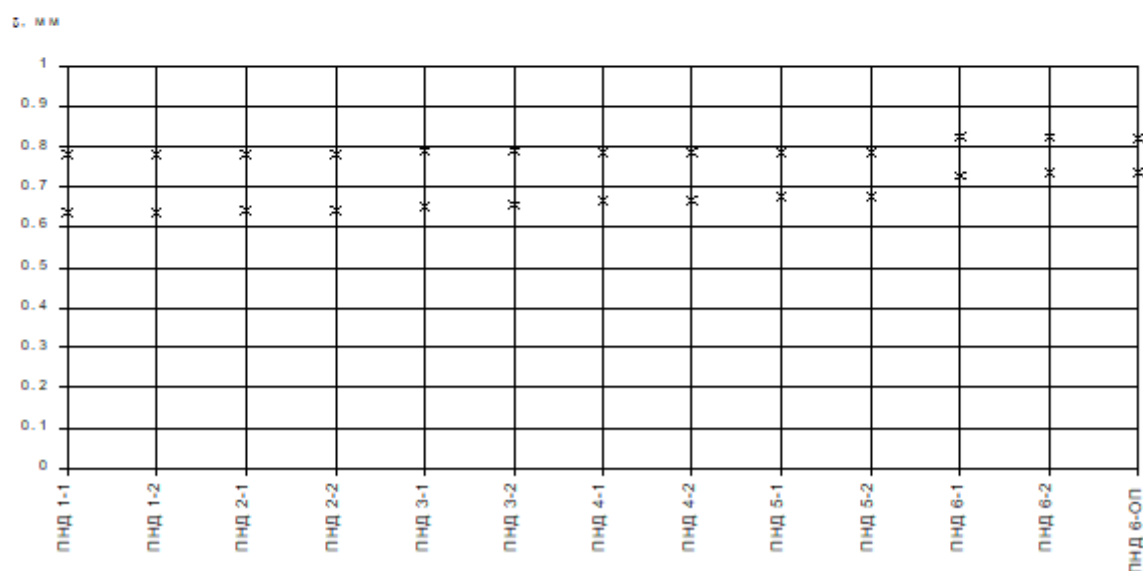


Fig. 8.4 - Boundary wall sinking of the inlet sections of coils (transition of the entire thickness to the region of plastic deformation) of the ПБТ of turbine unit K 300-240 KhTGZ

(numbering of coils in the course of heating steam (condensate) flow, top line - outer wall, bottom line - inner wall, the plotting area along the ordinate axis corresponds to the initial thickness)



a) pipe material brass Л-68



b) pipe material brass ЛО 70-1

Fig. 8.5 - Boundary wall sinking of the inlet pipe sections (transition of the entire thickness to the region of plastic deformation) of the tubing of the turbine unit

K 300-240 KhTGZ

(numbering of pipe bundles along the main condensate flow), top point - outer wall, bottom point - inner wall, the plotting area along the ordinate axis corresponds to the initial thickness)

The most accelerated erosion and corrosion wear (ECW) of coils is observed in the UC ПБТ-1 (see Fig. 8.2), where the temperature of feed water (condensate),

both on the outside and inside, is in the region of maximum ECW (160-180 °C). The feedwater velocity here is about 2 m/s or more, which contributes to an increase in the erosion-corrosion rate. The first (along the distributing collector) coils of the condensate coolers in all the high-pressure regenerative feed water heaters are most rapidly subjected to ECW. The acceleration of wear is imposed by the condition of maximum feedwater pressure and minimum condensate pressure in this zone. Wear of the steam cooling coils subjected to droplet erosion is at the level of the SC coils, and may be higher. The service life of the coils in a separate heater increases from the first condensate cooling coil to the steam cooling coils that are not subject to droplet erosion, and increases from ПІBT-1 to ПІBT-3. The intensity of ECW is also affected by the uneven distribution of feedwater velocities in the coils. In the steam cooling of all the high-pressure regenerative feed water heaters, except for ПІBT-3 of turbine unit K 300-240 KhTGZ, coils subject to droplet erosion are observed (see Figs. 7.6, 7.7, 8.2, 8.4). This indicates an imperfect design of the steam coolers in these heaters. In order to avoid droplet erosion in the ECW, it is necessary to reduce the heat transfer area in them by reducing the length of the coils while maintaining their number so as not to increase the ECW on the inside. The most dangerous zone in low pressure regenerative feedwater heaters is manifested in the pipes of the ПІHT-6 pipeline (see Figs. 7.9, 7.10, 8.3, 8.5), where the feedwater velocities are maximum. ПІHT-1 pipes can also be dangerous. Although the corrosion-erosion rates are low, the steam velocities are high, which significantly increases the vibration component of wear. It is better to use ЛІO70-1 brass, MHЖ5-1 alloy, or stainless steels with increased corrosion resistance for tubing.

Paper [49] presents the results of the analysis of the ECW of coils of block TPPs conducted by VTI in 1988-1989 on the basis of questionnaires on damage to the low pressure regenerative feed water heaters, operating conditions, and water-chemical regime. The data obtained from 30 TPPs with 300 MW power units and 114 fuel assemblies [49] are shown in the diagram of coil damage (Fig. 8.6). Comparison of the data on the estimated life of coils (Fig. 8.2) and damage data (Fig. 8.6) shows

that the calculated data are close to the operational (experimental) values. The general trend of the calculated and experimental data corresponds to each other. The fastest deterioration is observed for coils ПІВТ-1 and/or ПІВТ-2, while coils ПІВТ-3 are less susceptible to wear. As is evident from the operational data in Fig. 8.6, the intensity of wear is significantly affected by the quality of feed water and turbine condensate. The greatest intensity of destruction of the coils of the ПІВТ (1 or 2) is determined by operational characteristics, especially the power unit load schedules. When the load decreases, the wear intensity of the ПІВТ-1 coils decreases, and vice versa, the wear intensity of the ПІВТ-2 coils increases. The picture is different for Karmanivska TPP. Here, the first place in terms of destruction is occupied by coils of ПІВТ2, and the least destruction is experienced by coils of ПІВТ1. This can be explained by a possible difference in the design, manufacturing quality and operating characteristics of the OHVs at this plant from the others shown in Fig. 8.6.

The analysis of the research results (see Figs. 8.2, 8.3) shows that plastic deformations fill the walls of the high-pressure regenerative feed water heaters coils most susceptible to ECW in 70-130 thousand hours (8-15 years), and brass tubing of the high-pressure regenerative feed water heaters coils in 55 105 thousand hours (6-12 years). This determines the safe service life of the heaters: about 8 years for ПІВТ-1, 15 years for ПІВТ-3, 6 years for brass tubing (ЛІ-68) and 12 years for brass tubing (ЛІО70-1). Further accumulation of plastic deformations leads to the formation of cracks (fistulas) in the pipes and failure of the heat exchanger. It is very difficult to determine how long this additional time will be.

The production of a safe service life and its possible reserves can be shown by measuring the wall thicknesses of the pipes subjected to ECW, for example, by ultrasonic method during scheduled or any other long equipment shutdowns. Knowing the measured values, annual wear depths and thicknesses determined by the safe life, it is easy to determine the life reserves in the watch  $\tau_p$  using the formula:

$$\tau_p = 8760 \cdot \frac{\delta_{нз} - \delta_{нп}}{K}, \quad (8.16)$$

Reftinskaya SDPP:  $\chi_{П.В.} = 0.15$  (0.19),  $\chi_{Т.К.} = 0.3$  (0.4; Trypillia DRES:  $\chi_{П.В.} = 0.2$  (0.3),  $\chi_{Т.К.} = 0.4$  (0.5); Iriklinskaya DRES:  $\chi_{П.В.} = 0.2$ ,  $\chi_{Т.К.} = 0.3$  (0.5); Karmanivska DRES:

$\chi_{П.В.} = 0.17$  (0.22),  $\chi_{Т.К.} = 0.35$  (0.5)

$\chi_{П.В.}$  and  $\chi_{Т.К.}$  - average electrical conductivity of feedwater and turbine condensate,  $\mu\text{S}/\text{cm}$ ; maximum values in brackets

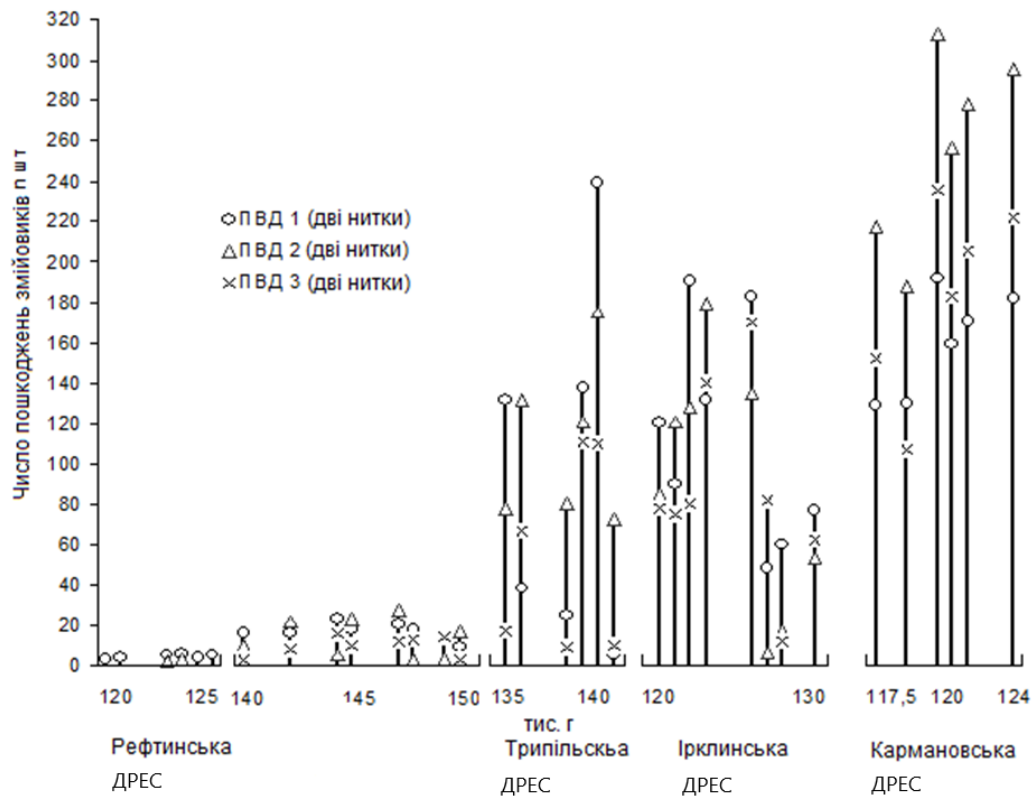


Fig. 8.6 - Number of damages of the ПБТ coils (two-strand) for a number of 300 MW TPPs (data for 114 heaters)

where  $\delta_3$  - is the measured wall thickness of the coil or pipe during equipment shutdown, mm;

$\delta_{ПР}$  - is the maximum permissible wall thickness determined by the safe service life, mm;  $\delta_{ПР} = 0,5 \cdot (d_H - d_{ВН}) - (z_H + z_{ВН})$ ;

$K$  - is the total depth index of annual wear, mm/year,  $K = K_H + K_{BH}$ .

The above data of the calculation studies are in satisfactory agreement with the VTI data on failures of fuel assemblies of 300 MW power units [49], shown in Fig. 8.6 (failures after 100-150 thousand hours), and high-pressure regenerative feed water heaters with brass pipes, systematised by the UTI [48, 58, 59] (failures after 7-10 years). Comparison of these data shows that failures occurred in the aforementioned additional period of time, when the accumulation of plastic deformations exceeded the permissible limit (defined by the safe service life) and led to the formation of cracks (fistulas).

The calculation studies also revealed the lower limit (safe life) of the operation of ПНТ-1 and 2 (7090 thousand hours, 8-10 years), after which, according to [48], an avalanche-like failure of heat exchangers often begins. Thus, the assessment of the service life according to simple dependencies (8.11) (8.15) gives acceptable reliable results.

A more thorough approach to determining the service life and assessing the reliability of the apparatus as a whole requires a detailed solution of two-dimensional axisymmetric (or even three-dimensional) problems of the stress-strain elastic-plastic state in the studied assembly, the geometry of which is constantly changing in time under the influence of ECW. Here, the locality of the process (the finite length of wall scour) must be taken into account. All loads should be applied as boundary conditions: power (pressure, etc.), vibration, cavitation, etc., taking into account their concentration (including stress concentration), and the determination of vibration, cavitation, etc. is a very difficult task in itself. It is possible to take them into account in the form of influence coefficients (coefficients of vibration and cavitation loads, stress concentration, etc.) when solving the task only with the addition of well-known power loads (pressure loads, etc.).

When determining the service life of the entire apparatus, it is necessary to take into account that with an increase in the number of openings and the number of

replacements of the same coils, the sockets in the collectors and tube boards are destroyed, which makes the entire heater unserviceable.

The presented methodology makes a certain contribution to solving such problems by providing in-depth information on the geometry of the area under study and the parameters of the processes taking place here (thermal-hydraulic, corrosion-erosion, etc.), without which a reliable solution is not possible at all. In the end, the above simplified methodology for life assessment allows:

- Identify coils and pipes that are most intensively exposed to erosion and corrosion wear and estimate the service life of each coil. Strength calculations with vibration analysis can be used here;
- develop recommendations on the timing of current and overhaul repairs of heaters or their complete replacement and the optimal sequence of personnel actions during repairs;
- make recommendations for improving the design of heaters. The optimal design is one where all coils have the same service life. This reduces the number of forced shutdowns;
- Estimate the service life of the entire heater.



## REFERENCE LIST

1. Марушкін В. М., Іващенко С. С., Вакуленко Б. Ф. Подогреватели высокого давления турбоустановок ТЭС и АЭС. Москва : Энергоатомиздат, 1985. 136 с.
2. Расчет и проектирование поверхностных подогревателей высокого и низкого давления : РТМ 108.271.23-84. Москва : МЭМ, 1984. 216 с.
3. Каталог 18-2-76. Теплообменное оборудование / НИИЭинформэнергмаш. Москва, 1977. 203 с.
4. Ільченко О. Т. Тепло- і масообмінні апарати ТЕС і АЕС. Київ : Вища школа, 1992. 207 с.
5. Переверзев Д. А., Лебедев А. Г., Ганжа А. Н. Моделирование, алгоритмизация і програмування вирішення повіркових задач пароводяних теплообмінників. Проблеми машинобудування. 1999. № 2. Т. 2. С. 21–26.
6. Ганжа А. Н. Проектно-дослідницьке моделювання підігрівачів паротурбінних установок та аналіз їх сумісної роботи за різних режимів. Механіка і машинобудування. 1999. С. 200–204.
7. Переверзев Д. А., Лебедев А. Г., Ганжа А. Н. Дослідження роботи підігрівачів високого і низького тиску... Харків : ППМаш НАН України, 2000. С. 35–38.
8. Сепаратори-пароперегрівники турбін АЕС : РТМ 108.020.107-84. Москва : МЭМ, 1984. 125 с.
9. Процеси в перспективних дизелях / за ред. А. Ф. Шеховцова. Харків : Основа, 1992. 352 с.
10. Вукалович М. П., Зубарев В. Н., Сергеева Л. В. Рівняння стану перегрітого водяного пару... Теплоэнергетика. 1967. № 5. С. 60–65.
11. Юза Я. Рівняння для термодинамічних властивостей води і пари. Теплоэнергетика. 1969. № 2. С. 80–86.
12. Майоров В. В., Горячев А. А. Формули для визначення теплофізичних властивостей повітря і води. Вопросы радиоэлектроники. 1981. Вип. 3. С. 105–107.

13. Методика і залежності для теоретичного розрахунку теплообміну... : РТМ 24.031.05-72. Москва : МТЕ і ТМ, 1974. 125 с.
14. Ісаченко В. Н., Осипова В. А., Сукомел А. С. Теплопередача. Москва : Енергія, 1975. 488 с.
15. Кутателадзе С. С. Основи теорії теплообміну. Москва : Атоміздат, 1979. 416 с.
16. Кутателадзе С. С., Боришанський В. М. Довідник з теплопередачі. Москва–Ленінград : Госенергоиздат, 1959. 414 с.
17. Кириллов П. Л., Юр'єв Ю. С., Бобков В. П. Довідник з теплогідрравлічних розрахунків... Москва : Енергоатомиздат, 1990. 360 с.
18. Довідник з теплообмінників : пер. з англ. У 2 т. / за ред. Б. С. Петухова, В. К. Шикова. Москва : Енергоатомиздат, 1987. Т. 1. 560 с.
19. Ликов А. В. Теплообмін : довідник. Москва : Енергія, 1978. 480 с.
20. Міхєєв М. А. Основи теплопередачі. Москва : Енергія, 1973. 320 с.
21. Короткий фізико-технічний довідник / за ред. К. П. Яковлєва. Москва : ФІЗМАТГІЗ, 1962. Т. 3. 686 с.
22. Хеммінг Р. В. Чисельні методи. Москва : Наука, 1972. 400 с.
23. Демідович Б. П., Марон І. А. Основи обчислювальної математики. Москва : Физматиздат, 1963. 659 с.
24. Лабунцов Д. А. Узагальнення теорії конденсації Нуссельта... Тр. Моск. енерг. ін-ту. 1965. Вип. 63. С. 79–84.
25. Іващенко С. С. Середньологарифмічні значення температур... Київ : Наук. думка, 1978. С. 233–237.
26. Клименко А. П., Каневець Г. Є. Розрахунок теплообмінних апаратів на ЕОМ. Москва–Ленінград : Енергія, 1966. 271 с.
27. Довідник з теплообмінників : пер. з англ. У 2 т. / за ред. О. Г. Мартиненко та ін. Москва : Енергоатомиздат, 1987. Т. 2. 352 с.
28. Кемельман Д. Н., Ескін Н. Б. Налагодження котельних установок : довідник. Москва : Енергоатомиздат, 1989. 320 с.

29. Галин Н. М., Кириллов П. Л. Тепломасообмін у ядерній енергетиці. Москва : Енергоатомиздат, 1987. 376 с.
30. Кулінченко В. Р. Довідник з теплообмінних розрахунків. Київ : Техніка, 1990. 165 с.
31. Ідельчик І. Є. Довідник з гідравлічних опорів. Москва : Машинобудування, 1975. 559 с.
32. Якоб М. Питання теплопередачі. Москва : Вид-во іноземної літератури, 1960. 520 с.
33. Каневець Г. Є. Узагальнені методи розрахунку теплообмінників. Київ : Наук. думка, 1979. 352 с.
34. Керн Д., Краус А. Розвинуті поверхні теплообміну : пер. з англ. Москва : Енергія, 1977. 462 с.
35. Тепловий розрахунок котельних агрегатів : нормативний метод / за ред. Н. В. Кузнєцова. Москва, 1973. 269 с.
36. Іванова Н. В. Проектний і повірковий розрахунок теплообмінних апаратів... Київ : Наук. думка, 1978. С. 219–224.
37. Переверзєв Д. А., Ганжа А. Н. Математичне моделювання поправочних коефіцієнтів... Харків : ХАІ, 1999. Вип. 9. С. 99–102.
38. Варгафтік Н. Б. Теплофізичні властивості речовин : довідник. Москва–Ленінград : Госенергоиздат, 1956. 368 с.
39. Теплотехнічний довідник. У 2 т. / за ред. В. Н. Юренєва, П. Д. Лебедева. Москва : Енергія, 1975. Т. 1. 744 с.
40. Сімаков С. М., Єгоров А. Д. Оптимізація і уніфікація обладнання теплових схем ТЕС і АЕС. Енергетичне машинобудування. 1986. Вип. 9. 35 с.
41. Палагін А. А. Автоматизація проектування теплових схем турбоустановок. Київ : Наук. думка, 1983. 160 с.
42. Берж К. Теорія графів і її застосування. Москва : ІЛ, 1962. 319 с.
43. Методи й алгоритми розрахунку теплових мереж / В. Н. Хасілев, А. П. Меренков, Б. М. Качанович та ін. Москва : Енергія, 1978. 175 с.

44. Євдокимов А. Г. Оптимізаційні задачі на інженерних мережах. Харків : Вища школа, 1976. 152 с.
45. Євдокимов А. Г., Яловкін Б. Д. Аналіз методів дискретного моделювання... Гірничий журнал. 1966. № 3. С. 101–108.
46. Аврух В. Ю., Дугінов Л. А. Теплогідравлічні процеси в турбо- та гідрогенераторах. Москва : Енергоатомиздат, 1991. 209 с.
47. Блінков В. Н., Горбенко Г. А., Брус Н. А. та ін. Математичне моделювання інтегрованих... М. : Центр НТІ "Пошук", 1992. С. 10–21.
48. Плотніков П. Н., Купцов В. І., Анісімова О. С. Підвищення надійності теплообмінників... Харків, 1997. С. 397–402.
49. Богаєв А. Ф. Аналіз пошкоджуваності підігрівачів високого тиску... Теплоенергетика. 1991. № 7. С. 14–18.
50. Шубенко А. Л., Ковальський А. Е., Стрельников І. С., Шевякова І. М. Оцінка впливу... Проблеми машинобудування. 1998. № 3–4. Т. 1. С. 9–16.
51. Конструкційні матеріали : довідник / за ред. Б. Н. Арзамасова. Москва : Машинобудування, 1990. 688 с.
52. Акользін П. А., Герасимов В. В. Корозія конструкційних матеріалів... Москва : Вища школа, 1963. 376 с.
53. Корольова Т. І., Караваєва А. П., Маршаков І. К., Мазо А. А. Вплив кисню... 1971. Вип. 6. С. 97–99.
54. Караваєва А. П., Корольова Т. І., Маршаков І. К. Корозія міді... 1971. Вип. 6. С. 100–102.
55. Лучина М. А., Ногінов Ю. М., Петров Ю. С. та ін. Захист обладнання ГЕС... Москва : Енергія, 1981. 152 с.
56. Кучеренко Д. І., Гладков В. А. Оборотно-водопостачання. Москва : Стройиздат, 1980. 168 с.
57. Keller H. Erosionskorrosion an Nassdampfturbinen. VGB Kraftwerkstechnik. 1974. № 5. S. 292–295.
58. Анісімова О. С., Бродов Ю. М., Юдіна Є. А. Порівняльне дослідження корозійної стійкості... Теплоенергетика. 1982. № 8. С. 68–69.

59. Бродов Ю. М., Юдіна Є. А. Корозійна стійкість труб конденсаторів. Теплоенергетика. 1984. № 8. С. 57–58.
60. Кострикін Ю. М., Сітнікова Є. Є., Валуєва І. В. Вплив рН на тракти живлення. Теплоенергетика. 1984. № 8. С. 57.
61. Бурлаков А. В. Основи теорії пластичності та повзучості. Харків : Вид-во ХНУ, 1968. 156 с.
62. Іцкович Г. М., Мінін Л. С., Винокуров А. І. Керівництво до розв'язання задач з опору матеріалів. Москва : Вища школа, 2001. 592 с.

Наукове видання

ГАНЖА Антон Миколайович  
КУНДЕНКО Микола Петрович  
ЄГОРОВА Ольга Юріївна

Пароводяні теплообмінники енергоустановок ТЕС та АЕС

Монографія

Англійською мовою

В авторській редакції

---

Видавничий центр НТУ «ХПІ», 61002, Харків, вул. Кирпичова, 2  
Свідоцтво про державну реєстрацію ДК № 5478 від 21.08.2017 р.

---

Електронне видання